COLD-FORMED STEEL RESEARCH CONSORTIUM

Characterizing the load-deformation behavior of steel deck diaphragms using past test data

P. O'Brien, M.R. Eatherton, W.S. Easterling

June 2017

COLD-FORMED STEEL RESEARCH CONSORTIUM
REPORT SERIES
CFSRC R-2017-02

SDII
Steel Diaphragm Innovation Initiative

About the authors

P. O'Brien was a Masters student at Virginia Polytechnic Institute and State University (Virginia Tech) and the primary author of this report. Associate Professor M.R. Eatherton and Professor W.S. Easterling also of Virginia Tech University served as co-advisors on the research.

CFSRC Information

The Cold-Formed Steel Research Consortium (CFSRC) is a multi-institute consortium of university researchers dedicated to providing world-leading research that enables structural engineers and manufacturers to realize the full potential of structures utilizing cold-formed steel. More information can be found at www.cfsrc.org. All CFSRC reports are hosted permanently by the Johns Hopkins University library in the DSpace collection: https://jscholarship.library.jhu.edu/handle/1774.2/40427.

SDII Information

The Steel Diaphragm Innovation Initiative (SDII) is a multi-year industry-academic partnership to advance the seismic performance of steel floor and roof diaphragms utilized in steel buildings through better understanding of diaphragm-structure interaction, new design approaches, and new three-dimensional modeling tools that provided enhanced capabilities to designers utilizing steel diaphragms in their building systems. SDII was created through collaboration between the American Iron and Steel Institute and the American Institute of Steel Construction with contributions from the Steel Deck Institute, the Metal Building Manufacturers Association, and the Steel Joist Institute in partnership with the Cold-Formed Steel Research Consortium; including, researchers from Johns Hopkins University, Virginia Tech, Northeastern University, and Walter P Moore.

Abstract

Recent research has identified that current code level seismic demands used for diaphragm design are considerably lower than demands in real structures during a seismic event. However, historical data has shown that steel deck diaphragms, common to steel framed buildings, perform exceptionally well during earthquake events. A new alternative diaphragm design procedure in ASCE 7-16 increases diaphragm seismic demand to better represent expected demands. The resulting elastic design forces from this method are reduced by a diaphragm design force reduction factor, R_s, to account for the ductility of the diaphragm system. Currently, there exist no provisions for R_s factors for steel deck diaphragms. This research was therefore initiated to understand inelastic steel deck diaphragm behavior and calculate R_s factors.

A review of the literature showed that a large number of experimental programs have been performed to obtain the in-plane load-deformation behavior of steel deck diaphragms. To unify review of these diaphragm tests and their relevant results, a database of over 750 tested specimens was created. A subset of 108 specimens with post-peak, inelastic behavior was identified for the characterization of diaphragm behavior and ductility. A new recommended method for predicting shear strength and stiffness for steel deck diaphragms with structural concrete fill is proposed along with an appropriate resistance factor. Diaphragm system level ductility and overstrength are estimated based on subassemblage test results and R_s factors are then calculated based on these parameters. The effects of certain variables such as deck thickness and fastener spacing on diaphragm ductility are explored.

Acknowledgements

This work is part of the Steel Diaphragm Innovation Initiative which is managed by the Cold-Formed Steel Research Consortium and funded by industry: American Institute of Steel Construction, American Iron and Steel Institute, Steel Deck Institute, Steel Joist Institute, Metal Building Manufacturers Association and government: National Science Foundation. This material is based upon work supported by the National Science Foundation under Grant No. CMMI-1562669: NEESR-CR: Transforming Building Structural Resilience through Innovation in Steel Diaphragms. Any opinions, findings, and conclusions or recommendations expressed in this material are those of the authors and do not necessarily reflect the views of the National Science Foundation or other sponsors.

Input from SDII investigators Ben Schafer (Johns Hopkins University) and Jerry Hajjar (Northeastern University) was instrumental in shaping this work. Other members of the SDII team that contributed include Cris Moen (NBM Technologies), Rafael Sabelli (Walter P. Moore), David Padilla-Llano (Northeastern University), Shahab Torabian (Johns Hopkins University), Guanbo Bian (Johns Hopkins University), Astrid Winther Fischer (Johns Hopkins University), Shaoning Li (Northeastern University), and Basit Qayyum (Virgnia Tech University). Several people helped substantially by contributing reports and data from past tests for use in the diaphragm testing database and/or by giving advice. These people include Larry Luttrell (West Virginia University), Bill Gould (ICC-ES), Hermann Beck (Hilti), Chris Gill (Hilti), Jeff Martin (Verco Decking), John Mattingly (Consultant, Steel Deck Institute), Colin Rogers (McGill University), Robert Tremblay (Polytechnique Montreal), Patrick Bodwell (Verco Decking), Bob Paul (Steel Deck Institute), and Thomas Sputo (Steel Deck Institute).

TABLE OF CONTENTS

LIST OF FIGURES

LIST OF TABLES

1 INTRODUCTION

1.1 Background

Floor and roof systems in a building play several key roles that contribute to a structure's ability to resist both gravity and lateral loads, as shown in Figure 1-1. When considering lateral loads, these systems function as critical force transfer elements that allow for continuous load path to the vertical elements of a building's lateral force resisting system (LFRS), and are referred to as diaphragms.

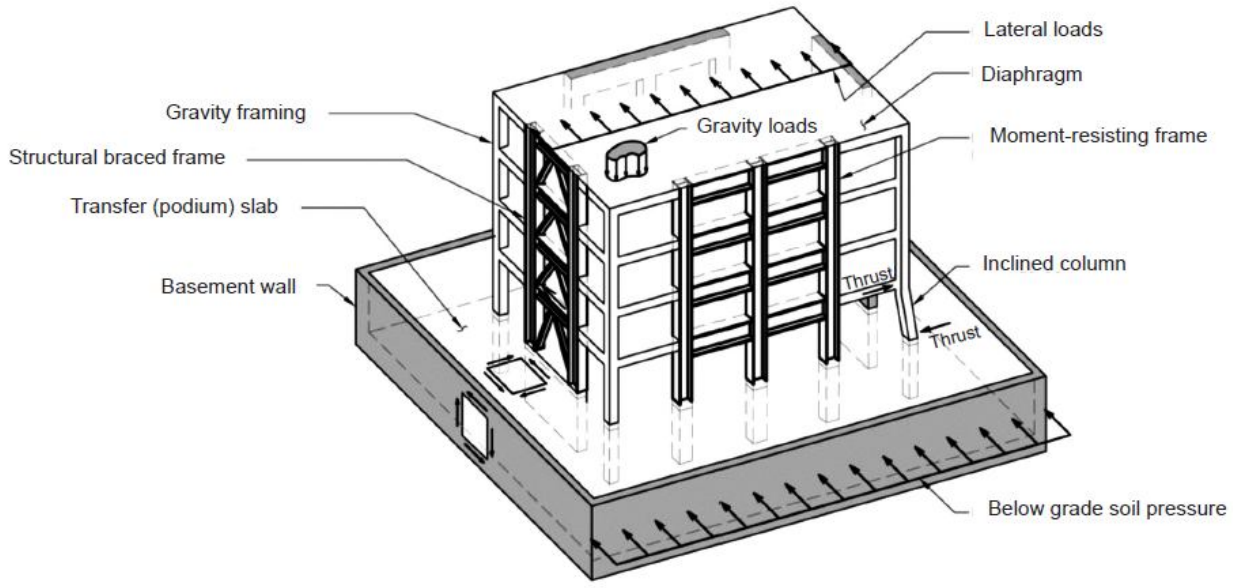

Figure 1-1 Roles of Floor and Roof Systems [from Sabelli et al. (2010)]

Steel deck diaphragms, with or without concrete fill, are the most common for roof and floor systems in structural steel buildings. Steel deck roof diaphragms consist of corrugated sheets, which when fastened to each other and the structural building frame, are able to resist significant in-plane forces. When concrete fill is placed on the steel deck for flooring systems, lateral load resistance considerably increases. Since the 1960's, there has been a substantial amount of research

investigating steel deck diaphragm behavior. Initial steel deck diaphragm research focused on characterizing diaphragm strength and stiffness, with the intent of the diaphragm to be utilized as a force transfer element. Recent earthquake reconnaissance, experimental and analytical research provide strong evidence that diaphragms designed for current design seismic diaphragm loads prescribed by U.S. building codes (ASCE, 2010) will experience inelastic deformations. As a result, experimental programs began to shift focus to characterizing the inelastic, post-peak behavior of diaphragms and their ability to dissipate energy.

During the 1994 Northridge Earthquake, the collapse of concrete parking garages due to poorly confined gravity columns were linked to significant precast concrete diaphragm inelastic deformations (EERI, 1996). Shake table tests and analytical investigations further demonstrated that diaphragm demands developed during real seismic events may be larger than code level forces (Rodriguez et al., 2007; Fleishcman and Farrow, 2001).

Despite observations that seismic design loads may not accurately represent actual elastic diaphragm demands during real events, the majority of steel deck diaphragm systems have a history of exceptional performance (i.e. almost no reports of damage during earthquakes). This is likely due to a steel deck diaphragm's available reserve capacity with respect to either strength or inelastic deformations. Some researchers believe that the balance between diaphragm demand and capacity is adequate and no major modifications to the ASCE 7 provisions are needed (NEHRP, 2015). Others suggest adjustments to increase the seismic demands, but utilize the ductility and reserve strengths of diaphragms through a diaphragm design force reduction factor, R_s (NEHRP, 2015). These R_s factors are analogous to response modification factors, R, used in ASCE 7-10 and are further elaborated on in Section 2.1.

1.2 Research Motivation

The behavior of real three-dimensional buildings during earthquakes is complex, especially if the vertical LFRS and the horizontal LFRS (diaphragms) are both experiencing inelastic deformations. To understand the seismic performance of buildings including the interaction of vertical LFRS and horizontal LFRS inelasticities, it is crucial to have a clear understanding and characterization of diaphragm behavior. As a result, an academic-industry partnership, known as the Steel Deck Innovation Initiative (SDII), was formed between researchers at Johns Hopkins University, Virginia Tech, Northeastern University and Walter P Moore, as well as several industry sponsors. SDII's objective is to advance building performance in steel framed buildings with steel deck floor and roof diaphragms through better understanding of diaphragm-structure interaction, new design approaches, and three-dimensional modeling tools, with a primary focus on seismic design applications (Schafer, 2016).

As part of SDII, the objective for this study concentrates on the evaluation of steel deck diaphragm system inelastic behavior and the calculation of diaphragm design force reduction factors based on previous test results. There currently exist no diaphragm design force reduction factors available for steel deck diaphragms in the alternate diaphragm design provisions of ASCE 7-16 (ASCE, 2016). Because no failures in steel deck diaphragms have been observed in past earthquake events, an effort to understand the successful seismic performance of this system is needed. To calculate R_s factors for steel deck diaphragms, both the inelastic deformation capacity and reserve strength capacity of a diaphragm must be considered. An extensive review of tested diaphragm specimens, with special attention to post peak-strength behavior, is therefore warranted.

1.3 Scope and Objective

A substantial amount of data exists from previous experimental programs. While initial programs typically only include load-deformation data up to the ultimate strength of a test specimen, post-peak data is available from more recent research programs. Valuable information about diaphragm ductility and post-peak behavior is extracted from these resources and evaluated in an effort to characterize steel deck diaphragm behavior. The objective of this research is to improve understanding of steel deck diaphragm behavior, with an emphasis on post-peak inelastic behavior which is not yet well understood, through analysis of previously tested steel deck diaphragm subassemblage experiments. Furthermore, this research recommends new design provisions for steel deck diaphragms with structural concrete fill and ultimately calculates diaphragm design force reduction factors, R_s, for application in seismic design. In pursuit of this mission, the current research specifically does the following:

1) Investigates previous steel deck diaphragm experimental programs and consolidates their relevant experimental data, such as test setup variables, test results, calculated values and more into a comprehensive database
2) Examines the ductility and post-peak behavior of previously tested diaphragms
3) Evaluates current equations and proposes new equations for strength, resistance factors, and stiffness of steel deck diaphragms with concrete fill. The proposed equations are shown to better agree with available test data than the prediction equations described in the Steel Deck Institute Diaphragm Design Manual, 4th edition
4) Characterizes the inelastic behavior of steel deck diaphragms by examining the influence of several test variables on ductility
5) Classifies diaphragm system ductility and calculates R_s factors for different steel deck diaphragm configurations

1.4 Organization of Thesis

This thesis document is organized in the following manner:

- Chapter 1 – introduces motivation for this research and defines the scope of this work
- Chapter 2 – reviews fundamental earthquake engineering principles for the development of force modification factors and explores literature on past experimental programs
- Chapter 3 – discusses information logged into an experimental diaphragm database
- Chapter 4 – presents methodology used for the calculation of diaphragm force modification factors, R_s
- Chapter 5 – discusses current strength and stiffness prediction methods for steel deck diaphragms with and without concrete fill, as well as recommends new strength and stiffness prediction equations for steel deck diaphragms with structural concrete fill
- Chapter 6 – discusses results of experimental tests and characterizes steel deck diaphragm behavior
- Chapter 7 – summarizes the conclusions reached throughout in this research and recommends future work

2 LITERATURE REVIEW

2.1 Force Modification Factors

A fundamental concept in seismic design involves the reduction of elastic design forces to account for a structural system's ability to deform in a ductile manner. In ASCE 7-10, the reduction of elastic forces is implemented through the use of a system dependent response modification coefficient, R. Elastic response spectra are developed for a site based on seismic hazard analysis and represent anticipated elastic earthquake forces for the design basis earthquake level (ASCE, 2010).

In earthquake engineering, designing for these elastic forces, F_e, is highly uneconomical and inefficient for strong ground motions. Instead, ductile behavior is relied upon to dissipate seismic energy and accommodate earthquake displacement demands. Through proper detailing of the LFRS, ductile behavior can be achieved and accounted for using a design force, F_d, equal to the elastic force divided by the response modification coefficient, R. The prescribed R factor assumes that forces less than the design force, F_d, exhibit elastic behavior on the LFRS (See Figure 2-1). At increasing deformations, strain hardening of plasticized sections result in higher strengths (NEHRP, 2015). The maximum strength, F_{max}, is related to the design force through an overstrength factor, Ω_0. Maximum inelastic deflection, δ_{in}, is considered by the inelastic amplification factor, C_d (ASCE, 2010). Figure 2-1 demonstrates the applications of R, Ω_0, and C_d on a LFRS's elastic and inelastic design curves.

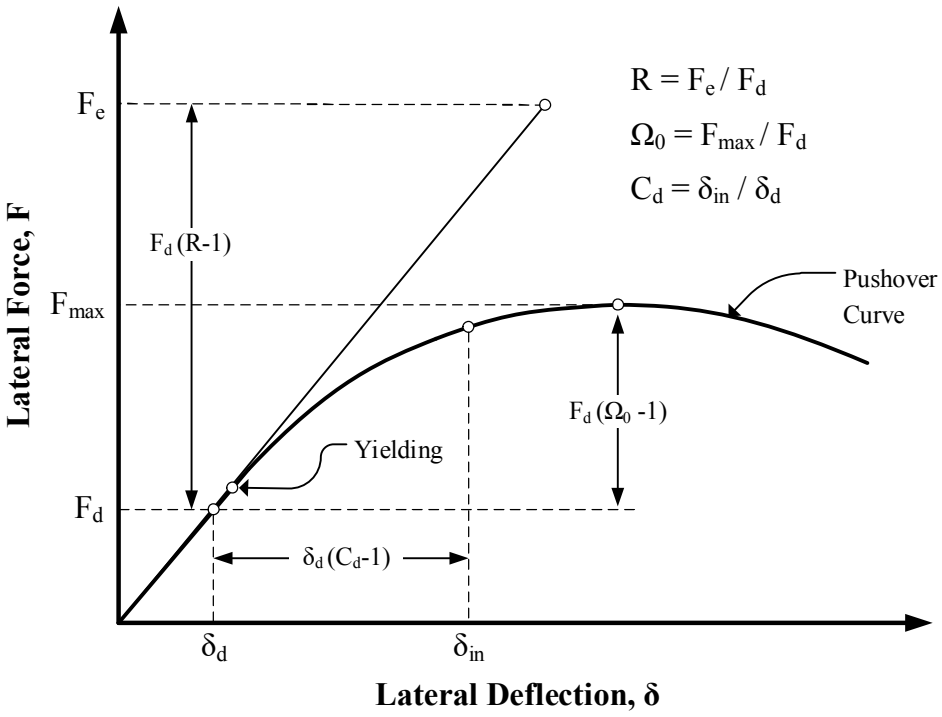

Figure 2-1 Load-Deformation Relationship for Seismic Performance Factors

Codified response modification coefficients, *R*, for different seismic resisting systems are available for seismic design in ASCE 7-10, along with overstrength factors Ω_0, and inelastic deflection amplification factors, C_d. All available design coefficients and factors apply only to vertical LFRSs. This means that design forces, which are dependent on *R* factors that have been specifically calibrated to the vertical LFRS, do not represent the ductility or overstrength that the diaphragm may exhibit.

Currently, ASCE 7-10 prescribes a method to calculate seismic diaphragm demands. However, several research programs indicate that code level diaphragm demands grossly underestimate elastic or near elastic diaphragm demands experienced in real earthquake events (NEHRP, 2015). Rodriguez et al. (2007) measured diaphragm accelerations for four small scale reinforced concrete structures through shake table tests, and concluded that building code

diaphragm loads for rigid diaphragms were non-conservative. This conclusion can be extrapolated to other building types (Rodriguez et al., 2007). Computational simulations for flexible diaphragms performed in Fleischman and Farrow (2001) produced similar conclusions that diaphragm demand predictive procedures are non-conservative and require revision. For a very limited number of diaphragm systems (e.g. precast concrete diaphragms), catastrophic failures such as collapse were observed during the 1994, Northridge Earthquake (EERI, 1996). These revelations about diaphragm demands catalyzed research efforts to better understand diaphragm behavior, such as the Diaphragm Seismic Design Methodology Project (Fleischman et al., 2005; Schoettler et al., 2009), a joint effort to investigate precast concrete diaphragm behavior from research teams at University of Arizona, University of California, San Diego, Lehigh University and a panel of precast, prestressed concrete industry experts. For the vast majority of diaphragm systems, earthquake performance was exceptional, recognizing a diaphragm system's reserve capacity through either overstrength, ductile behavior or both. This prompted a division in the research community – whether to continue to implement the current standards for diaphragm design which have largely proven adequate, or to take a more rational design approach that acknowledges the likelihood that seismic diaphragm forces will exceed current code level demands.

NEHRPS's 2015 Seismic Provisions presents an alternative method for diaphragm design that is mandated for structural systems that exhibited poor performance in past earthquake events, but recommended for all diaphragm systems, assuming adequate research is completed to characterize behavior for that specific diaphragm system. This alternative method will increase demands to be representative of real earthquake events, but will utilize diaphragm inelastic behavior through a diaphragm design force reduction factor, R_s, analogous to the response modification coefficient, R, used in ASCE 7-10 for the vertical LFRS.

Currently, there exist several methods to develop seismic force reduction factors. An approach consistent with the procedures outlined in NEHRP's 2015 Seismic Provisions Commentary, as used in this research to develop R_s factors for steel deck diaphragms, is ATC-19 (Applied Technology Council, 1995). ATC-19 is an empirically based, test dependent method and is further described in detail in Section 4.1. However, several other methods are available for developing seismic performance factors such as R, Ω_0, and C_d. One such methodology becoming increasingly used, due to its rigorous statistical approach to controlling collapse probability, is FEMA P695 (FEMA, 2009) .

Prior to the ATC-19, a shortcoming commonly noted in the development of system dependent seismic performance factors is that past, commonly used methodologies relied upon limited experimental data, linear analysis procedures and comparisons to similar systems using engineering judgement (Kircher and Heintz, 2008). ATC-19 offered a viable method for developing R factors when a sizable population of test data is available. ATC-19 presents some challenges however, namely that subassemblage performance does not always directly translate into performance of the full scale building (e.g. interaction between diaphragm and vertical LFRS not available from subassemblage tests, ductility of subassemblage tests not always indicative of diaphragm system ductility, failure of subassemblage test may not translate to system collapse).

FEMA P695 offers a robust alternative that attempts to directly investigate collapse. The primary goal of the FEMA P695 method is to limit probability of collapse at the maximum considered earthquake level. To do so, a series of steps are outlined by this probabilistic method. A detailed design procedure, specific to the type of LFRS, is developed and applied to a series of archetypical structural models intended to encompass the variety of building types and sizes commonly found in the field. R, Ω_0, and C_d values are assumed for design. Nonlinear time history analyses for the archetype building models is conducted for a specific ground motion. The ground

motion is scaled up until collapse occurs. This analysis, known as incremental dynamic analysis (IDA), is performed for a suite of ground motions for the group of archetype buildings. Ground motion intensity measures (e.g. spectral acceleration, S_a) for each IDA are scaled up until 50% of the ground motions cause collapse. A collapse margin ratio (CMR) is defined as the median ground motion intensity measure that causes collapse divided by the maximum considered earthquake ground motion intensity measure (Kircher and Heintz, 2008).

The CMR is compared to a specified acceptable probability of collapse. If the CMR does not pass the prescribed limit, then new R, Ω_0, and C_d factors are selected for the LFRS type and the entire process is performed again. A FEMA P695 type of analysis is being conducted by others on the SDII team for the development of seismic performance factors for steel deck diaphragms. The goal of this study is to leverage existing test data to characterize steel deck diaphragm behavior. FEMA P695 does not provide a method for calculating R factors based solely on test data. However, the ATC-19 method does, and is therefore used in this work. While several methods are recognized for the calculation of R factors, it is outside the scope of this work to scientifically compare the reliability of each method, nor endorse one method over another. The ATC-19 method used in this research for developing diaphragm design force reduction factors is further described in Section 4.1.

2.2 Diaphragm Components

Due to the reliance on available test data in this study, and in an effort to understand the complex behavior of steel deck diaphragms, a steel deck diaphragm database of past experimental tests was compiled. Prior to examining previous diaphragm experimental programs, it is necessary to recognize the basic structural components that comprise a steel deck diaphragm and the common

mechanics simplification for idealized behavior. These components are shown in Figure 2-2 as part of the diaphragm system in a one story, braced frame building. For practical analysis, diaphragms are often idealized as a horizontal deep beam, with tension and compression chords acting as the flanges resisting flexural forces, and the diaphragm field (e.g. steel deck or composite slab) acting as the web to transfer shear loads either to collector beams or directly to the vertical LFRS. Collector beams drag the horizontal force into the vertical LFRSs when the LFRS does not extend the full frame.

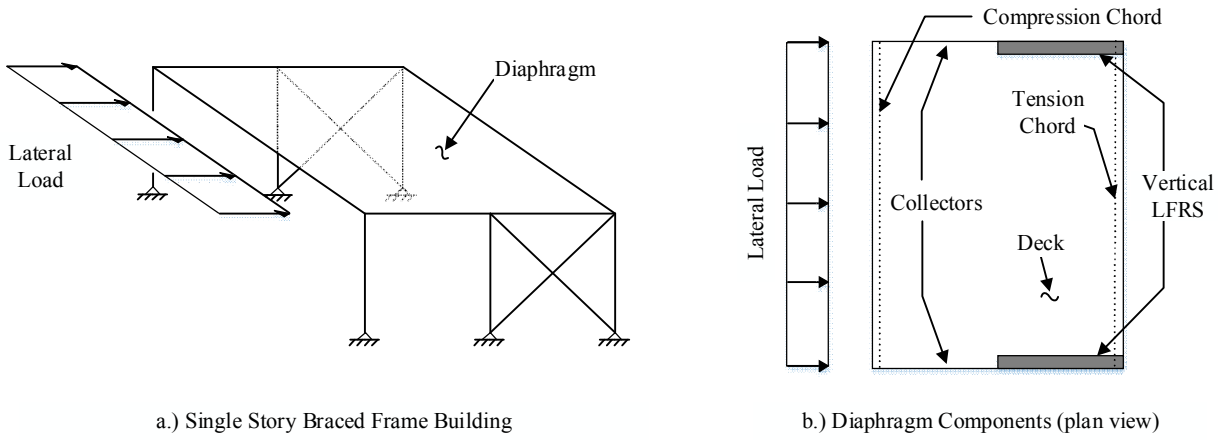

a.) Single Story Braced Frame Building

b.) Diaphragm Components (plan view)

Figure 2-2 Diaphragm Components

To obtain sufficient shear resistance in a steel deck diaphragm, the deck must be adequately fastened to the structural framing. Various fastener types and structural components of a typical floor diaphragm in a steel framed building are shown in Figure 2-3. Steel deck panels are corrugated to their flexural resistance to vertical loads and are fastened to the steel framing at the bottom of their corrugations using welds, power actuated fasteners, self-drilling screws and when concrete fill is placed on the deck, steel headed stud anchors, hereby referred to as shear studs. These deck to structural steel frame fasteners will hereby be referenced as structural fasteners.

Steel deck panels are fastened to the adjacent, overlapping panels through sidelap fastening. Sidelap fastener types include welds, screws and mechanical crimping. Mechanical crimping (e.g. button punching) is common when the steel deck panel used has a standing seam sidelap condition. Diaphragms typically require interior supports to shorten the span lengths of the deck. Steel deck panel ends can either be butted against each other or overlapped to cover longer lengths. For the overlapped condition (commonly referred to as an endlap), fasteners are applied through both sheets and into the structural frame.

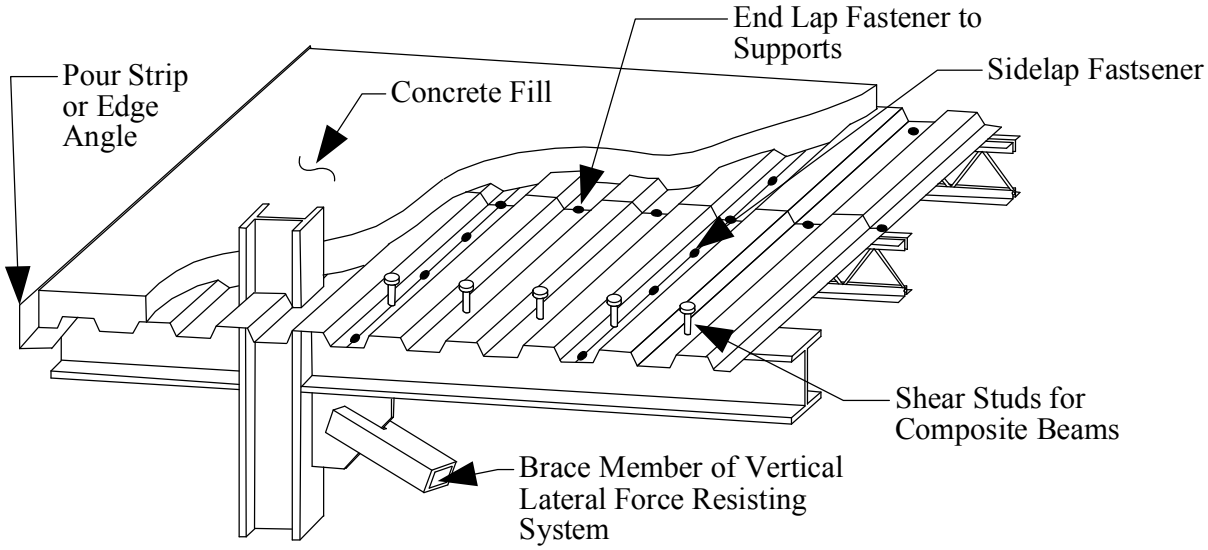

Figure 2-3 Concrete Filled Diaphragm Components

2.3 Experimental Programs

2.3.1 General

A large portion of the historical testing of diaphragms were conducted by and/or sponsored directly by deck manufacturers. Due to the proprietary nature of these tests, not all data was published and made available to the public. Only major experimental programs with significant

findings are discussed in this section. For a more comprehensive list of previous programs included in the diaphragm database, see Table 3-1. It is also noted that earlier research programs described in this section focused on characterizing strength and stiffness, and thus only obtained behavior up to the tested ultimate strength. Later programs interested in diaphragm energy dissipation analyzed post peak-strength load-deformation behavior and included a more complete range of deformations.

The findings of several of these research programs led to the development of design guides as used in this research for calculating diaphragm design strength. The Steel Deck Institute's Diaphragm Design Manual, 4th edition (Luttrell et al., 2015), widely considered as the principal document for diaphragm design in North America and hereby referred to as DDM04. The Seismic Design for Buildings Manual, commonly referred to as the Tri-Services Manual, is a less utilized design guide that also incorporates findings from earlier experimental research (Army, Navy and Air Force, 1982). The American Iron and Steel Institute (AISI) produced a consensus document summarizing these design recommendations into AISI S310-16, North American Standard for the Design of Profiled Steel Diaphragm Panels (AISI, 2016b), hereby referred to as AISI S310.

2.3.2 Steel Deck Diaphragms with no Concrete Fill

There exists a substantial amount of diaphragm research on light gauge steel decking, dating back to the 1950's. Steel deck is largely used for its many advantages, including light weight, low cost, and ease of installation, among others. The initial use of steel deck was to resist vertical loads. In doing so, fasteners were designed to secure the deck to the frame and resist uplift when necessary. Researchers noted that the deck and fasteners could be designed for in-plane shear loads, reducing the need for lateral bracing elsewhere in the structural system (Nilson, 1960).

The first widely recognized experimental research program was led by Arthur Nilson at Cornell University under the administration of George Winter (Nilson, 1960). From 1955 to 1960, approximately 40 static shear diaphragm tests were conducted. Welding techniques that allowed for adequate shear transfer from light gauge deck to structural steel framing were investigated and soon were established as standard industry practice. Only welded structural fastener types were investigated, as mechanical fasteners such as powder actuated fasteners and self-drilling screws were not yet commonly used in diaphragm construction.

Nilson's experimental test setup included a simply supported diaphragm specimen loaded at third points. Due to the high cost of these large experiments, a second phase of this research program initiated smaller scale cantilever tests loaded at the free end. Plan dimensions of the cantilever tests were equivalent to the shear span dimensions of the larger tests (i.e. dimension between the end and loading point). Nilson concluded that cantilever tests yielded extraordinarily similar results as the larger, simply supported tests. Shear deformations in diaphragm testing typically dominate over flexural deformations. For the simply supported tests, the span between third point loads will experience moment but negligible shear, and thus negligible deformations, while diaphragm shear spans experienced constant shear loads. Nilson concluded that a cantilever test setup can effectively reproduce strength and stiffness test results of a similar test specimen in a simply supported configuration.

While this method is reliable for capturing diaphragm strength and stiffness, it does not represent the distributed inertial loading expected in real diaphragms subjected to earthquakes. Cantilever tests have uniform shear throughout the diaphragm and will have inelasticities spread throughout the diaphragm. Conversely, a diaphragm with a uniform load along its span will have highest shear demands at its ends and lowest near midspan, with inelasticities localizing at span ends. This creates a challenge in using cantilever test data to characterize inelastic diaphragm

behavior, as further elaborated on in Section 4.3.2. Nonetheless, the cantilevered diaphragm test method was deemed adequate to determine strength and stiffness, and became the standard for shear diaphragm testing in North American (AISI, 2013a).

Luttrell followed Nilson's work at Cornell, and characterized the effects of different diaphragm structural components on the load-deformation behavior through a series of several tests (Luttrell and Winter, 1965; Luttrell, 1967). Types of fasteners implemented in these tests included welds, screws, lock rivets, and backed-up fasteners. Panels of different shapes were fastened to a "heavy" and "light" structural frame. Luttrell concluded that the flexural resistance of the test frame has a moderate influence on the ultimate strength of a diaphragm – a 98% decrease in the weak axis moment of inertia for the structural members of the test frame developed a 17% reduction of ultimate strength (Luttrell, 1967). Material strength was also observed to have moderate influence in diaphragm behavior. Luttrell noted that a 40% increase in yield strength of the deck provided approximately 10% increase in strength and stiffness (Luttrell, 1967). Luttrell also observed that cyclic and reversed cyclic loading protocols contributed to ultimate strength degradations as high as 30% when compared to diaphragms subject to monotonic loading protocols. Strength degradation of like diaphragms subject to cyclic and monotonic loading protocols was dependent on number of cycles and whether the loading direction was reversed or not.

A major finding from this series of tests was the panel length's influence on a diaphragm's shear stiffness. Luttrell observed that as the panel length of a diaphragm increased, the ultimate strength of that diaphragm remained relatively unchanged. The in-plane stiffness, however, was highly sensitive to the length of the panel. This is because only a finite length of a steel deck panel's corrugations at panel ends is vulnerable to warping distortions (accordion like warping and lateral racking) when the deck is subjected to shear which effectively decreases the stiffness.

Therefore, a single, continuous steel deck panel (i.e. no endlaps) with larger length had a smaller percentage of diaphragm area subject to warping and resulted in increased stiffness. Fasteners at panel ends also significantly restrained the deck and increased stiffness. This warping effect and panel length influence is discussed in detail in SDI's Diaphragm Design Manual 1st Edition (Luttrell, 1981a).

Under the direction of Luttrell, a major experimental program with over 100 full-scale experimental tests was initiated at West Virginia University (Ellifritt and Luttrell, 1971). Narrow rib, intermediate rib and wide rib panel corrugations with panel widths of 18 in., 24 in., 30 in. and 36 in. and a 1.5 in. depth were investigated, as they were determined to be popular in construction. Wide rib profiles resulted in higher shear strength than the other two deck types. Panel width influence was not conclusively assessed, but the experimental data suggested that increasing the panel width increased the strength and stiffness, a finding consistent with Luttrell's work at Cornell (Luttrell, 1967). The increase in strength and stiffness from increased panel widths was likely due to the reduction of fasteners needed for a given diaphragm area.

Major variables affecting diaphragm shear strength were fastener type and spacing, interior member/purlin spacing and deck thickness, as identified by Ellifritt and Luttrell (1971). The relationship between deck thickness and shear strength was conservatively assumed to be linear. A reduction of purlin spacing further restrained out of plane deformations, and subsequently increased the strength and stiffness of the diaphragm. Ellifritt's findings were used to produce a semi-empirical design procedure, including generic design tables for common fastener configurations, deck profiles and deck thicknesses examined in this investigation.

Pinkham (1999), of S.B. Barnes and Associates, tested a series of 20 cantilevered specimens that were identified as having relevant post-peak load-deformation behavior. This marks the first set of test data for steel deck diaphragms without concrete fill used in this work for

characterizing inelastic diaphragm behavior and calculating R_s factors, as shown in Chapter 6. All 20 tests included Wheeling high strength deck with welded structural fasteners. Fastener spacing for both sidelap and structural fasteners were varied. Different sidelap connection types were also investigated (i.e. button punch, top seam weld, filled weld and screw). Ductility values were the lowest for specimens including button punch sidelaps. Shear strengths reported were as high as 6.68 kip/ft, with the majority of specimens resulting in strength between 1.50 to 3.50 kip/ft.

Twenty diaphragm tests with deck depths ranging from 3 in. to 7.5 in. with or without a flat sheet attached to the bottom of the panels were reported in (Bagwell and Easterling, 2008). Deep decks are utilized for longer span lengths, while decks with flat plates attached to the panels (commonly referred to as cellular deck) can significantly increase in-plane stiffness. Bagwell concluded that SDI shear strength prediction equations in the Diaphragm Design Manual, 3rd Edition (Luttrell et al., 2006) produced larger values than experimental strengths. Shear limitations placed on fastener strengths were recommended. Stiffness for non-cellular, deep deck diaphragms were much lower than more typical 1.5 in. deep deck. SDI stiffness predictions and experimental stiffness comparisons were inconclusive.

A multi-phase research program from researchers at McGill University and École Polytechnique de Montréal investigated behavior of roof deck diaphragms, with a focus on energy dissipation and ductility characteristics in correlation with different fastener types, spacings, deck types and loading protocols. The general objective of this research was to understand seismic behavior of and improve design procedures for steel deck diaphragms including using the diaphragm as the energy-dissipating element in a building, reducing design requirements for the deck as an elastic transfer element, and possibly eliminating ductility requirements for vertical LFRSs. The first phase of tested diaphragms included cantilever specimens subjected to static and dynamic loads with both monotonic and reversed cyclic loading protocols. Essa et al. (2003) tested

18 diaphragm specimens with welds, welds with washer, screws and powder actuated fasteners as structural fasteners in combination with welds, screws or button punch sidelap fasteners. Both monotonic and cyclic loading protocols were used. Welded diaphragms exhibited limited ductility when compared to diaphragms with mechanical fasteners or welds with washers. The most ductile diaphragm configuration included powder actuated structural fasteners and screwed sidelaps (Essa et al., 2003).

Martin (2002) expanded the scope of this program to include dynamic loads typical to one story buildings in different Canadian geographic regions with the objective being to simulate real seismic events. Deck profiles and fastener configurations were similar to those used in Essa et al. (2003). Findings were consistent with Essa et al. (2003), where behavior was dictated by the fastener combination type of structural fasteners and sidelap fasteners. Diaphragm tests with welded structural fasteners and button-punched sidelaps exhibited poor ductility. The powder actuated structural fastener and screwed sidelap configuration demonstrated a ductile, but pinched, hysteretic response, due to screw tilting at sidelaps and deck slotting at the nails (Martin, 2002). No mass was added to the relatively light-weight experimental diaphragms, and load was introduced to the system through the cantilever test frame at the free end using a displacement history through an actuator with dynamic capability. Since mass was not added to the diaphragm, inertial forces primarily originated from the mass of the supporting test frame. While these tests captured fast loading and related strain-rate effects, inertial forces were not truly represented of seismic loads since the test was cantilevered (uniform shear throughout the diaphragm) and no mass was added to the diaphragm to account for additional sources of seismic weight.

Yang (2003) investigated the influence of longitudinal overlap of panels at panel ends, or end laps, and non-structural components of diaphragms such as roofing membranes and gypsum boards through a series of 12 tests. End laps had negligible effects on diaphragm strength, but

decreased the stiffness due to the potential for warping at panel ends. Nonstructural components, particularly the gypsum board, increased diaphragm strength by as high as 24%, and should be explicitly considered when designing roof deck diaphragms as the ductile element of a LFRS (Yang, 2003).

The second phase of research included a larger, simply supported diaphragm test setup with displacement histories introduced at each end of the diaphragm to simulate dynamic loads from ground motions (Franquet, 2009). Since roof diaphragms are proposed as a ductile fuse, Franquet investigated repair strategies for diaphragms through the testing of 12 specimens. Mass was added to the steel deck to drive deformations into the inelastic range. Franquet concluded that 22 gauge deck using mechanical fasteners demonstrated satisfactory ductile behavior, while thicker gauge deck and weld with button punch configurations did not (Franquet, 2009).

Massarelli (2010) complimented Franquet's work with a series of 9 dynamically tested specimens. Each underwent ambient vibrations, medium and large amplitude displacement cycles to cover a range of loading conditions. Repair and retrofit strategies were implemented for 8 of the 9 specimens. SDI stiffness predictions showed good agreement with experimental results for diaphragms tested only at low level, elastic displacements. However, stiffness at displacements corresponding to 40% of ultimate strength exhibited only 67% of the stiffness predicted using SDI's method (Massarelli, 2010). Ductility assessment for the different test configurations proved consistent with Franquet's conclusions.

Ongoing research sponsored by Hilti further examines diaphragm behavior with mechanical fasteners. Through 9 tests, the method of end lap fastening (screws vs. powder actuated fasteners) for typical 22 gauge deck was determined to have very little effect on diaphragm performance (Beck, 2008). Foster (2008) tested a series of 62 full scale cantilever specimens to further investigate diaphragm strength and stiffness when using Hilti fasteners. All specimens used

Hilti structural fasteners and sidelap screws with typical 1.5 B steel deck. Verco and Vulcraft decking included nominal 33 ksi yield material, while high strength Wheeling Deck specified a nominal 80 ksi yield strength. Post-peak behavior for the specimens in this reference is available. However, the SDII team recently received this proprietary data, and therefore was not able to include it in the analyses for this document in quantifying ductile diaphragm behavior. Further research conducted by the SDII group will consider this data in future work.

Researchers at Hilti then tested 6 mechanically fastened diaphragms to prove that adequate ductility is achievable for mechanically fastened steel deck diaphragms with thicker decks of up to 16 gauge (Beck, 2013a). Hilti developed a powder actuated fastener, X-HSN 24, with a knurled point to better resist tension pullout, which proved to increase the ductility of diaphragms, especially for thicker decks at the endlap/sidelap intersections where the nail must penetrate through four layers of deck and the support member. Four tests were run on 18 and 20 gauge deck, with high ductility for 18 gauge Grade 33 deck. 20 gauge deck, however, experienced brittle fracture of the deck at panel ends which was attributed to the high strength Grade 80 deck and not the fastener type (Beck, 2013b).

2.3.3 Steel Deck Diaphragms with Concrete Fill

Floor systems in steel framed buildings often have steel deck diaphragms with concrete fill placed on top for the floor slab. Initial use of steel deck in concrete slab systems was primarily as economical permanent formwork, with reinforcing steel added for flexural resistance where necessary. Steel deck's mechanical bond through the deck-concrete interface, in combination with headed shear studs, allows for a composite system, with the deck acting as flexural tension reinforcement, negating the need for reinforcing bars. Research initially focused on this system

with respect to vertical loads before examining the in-plane resistance these diaphragms may exhibit. Due to the proprietary nature of diaphragm testing and the extensive cost and time needed to construct, disassemble, and reconstruct concrete filled steel deck diaphragms, only a very limited amount of experimental research is available on this type of system.

A series of proprietary diaphragm tests that included structural concrete fill was performed by S. B. Barnes and Associates in the 1950s and 1960s (S. B. Barnes and Associates 1957, 1961, 1962, 1966, 1967). These static, monotonic tests were conducted in the simply supported condition with applied loads at third points and did not include shear studs. The S.B. Barnes and Associates test data, not available in the public domain, represents a significant portion of the experimental research on this type of system.

A series of 11 monotonic cantilever tests, nine with insulating concrete fill utilizing welded structural fasteners, was carried out by Luttrell (1971) to investigate the effects of insulting concrete fill on steel deck. Concrete compressive strengths ranged from 110 – 171 psi. The concrete fill notably increased diaphragm stiffness due to the steel deck panels being restrained from out-of-plane movements. Ultimate experimental shear strengths ranged from 0.6 – 2.11 kip/ft with shear stiffness values ranging from 38 – 1056 kip/in. for the nine specimens with concrete fill.

Four full scale, monotonic, cantilever tests were performed by Davies and Fisher (1979) on steel deck diaphragms with structural concrete fills. Three of these specimens incorporated re-entrant profile steel deck types, with the final specimen using the more traditional trapezoidal steel deck profile. Structural fasteners were self-drilling, self-tapping screws. The nominal 28-day compressive strength of the concrete fill was approximately 3600 psi. Failure modes for three of the four tests were due to failure of the structural fasteners. The failure mode for the remaining test

was concluded to be non-representative of real diaphragm systems and therefore not practical for design considerations. Ultimate diaphragm shear strengths ranged from approximately 1 – 2 kip/ft.

A series of 14 diaphragm tests were performed by ABK (1981). Of the 14 specimens, only three used typical steel deck on structural steel frame. Furthermore, one of these three specimens included structural concrete fill, with a nominal 28-day concrete compressive strength of 3000 psi. The specimen was tested in a three span, simply supported condition with welded structural supports and subjected to displacement histories at a dynamic rate. The specimen, however, was not loaded to failure; the maximum recorded shear strength was 2.85 kip/ft.

Fukuda et al. (1991) investigated the effects of bottomless trench ducts through a series of 6 cantilever tests. These bottomless trench ducts, or large sections of the diaphragm where no concrete fill is present, were present in 2 of 6 tests. Two diaphragm specimens were constructed without bottomless trench ducts, while the remaining 2 diaphragm specimens did not include concrete fill. Cellular deck was used for the 4 specimens with concrete fill. Specimens ranged from approximately 9 ft x 10 ft to 9 ft x 7 ft in plan dimensions and were subjected to static, reversed cyclic loading. No shear studs were used and the non-conventional failure modes of the deck and concrete debonding or concrete cracking parallel to panel corrugations were observed.

All previously mentioned programs that investigated the effects of concrete on steel deck diaphragms included conditions that dismissed further evaluation by this research for strength, stiffness, or ductility characterization. These conditions include:

1. Data being private and proprietary (S.B. Barnes and Associates 1957, 1961, 1962, 1966, 1967),
2. Use of insulating concrete fill with low compressive strengths (Luttrell, 1971),
3. Irregular deck types and structural fasteners (Davies and Fisher, 1979)
4. Specimen not loaded to failure (ABK, 1981)

5. Absence of concrete fill over large portions of specimen plan dimensions (Fukuda et al., 1991)

2.3.4 Iowa State Testing Program

A landmark study on steel deck diaphragms with concrete fill was performed at Iowa State University (ISU) in the 1970s and 1980s. This experimental research program is used to evaluate current strength and stiffness prediction equations and calibrate new prediction equations, as recommended by this research, as described further in Chapter 5. The ISU program is described in detail in this section.

A series of 32 full scale steel deck diaphragm with structural concrete fill specimens, hereby referred to as "SDDCF" specimens, were tested at Iowa State University's (ISU) Structural Engineering Research Laboratory as reported in numerous research documents (Porter and Greimann, 1980; Porter and Greimann, 1982; Neilson, 1984; Easterling, 1987; Easterling and Porter 1988; Porter and Easterling 1988; Easterling and Porter, 1994a; Easterling and Porter, 1994b; Prins, 1985).

This research program consisted of two phases. The first phase tested specimens 1 – 9, reported by Porter and Greimann (1980), and identified a need for further testing. The second phase included specimens 10 – 32 and are reported in Porter and Easterling (1988). Figure 2-4 shows a schematic of the diaphragm test frame setup. Table 2-1 gives general information about each test specimen. Six specimens in the second phase included a combination of in-plane and vertical loads. All specimens were cantilever specimens subjected to a reversed cyclic loading protocol applied at a static rate. Plan dimensions of specimens 1 - 21 were 15 ft x 15 ft. Specimens 22 – 32 plan dimensions were 12 ft x 15 ft. The 12 ft dimension was the span dimension, oriented

perpendicular to the applied load. For the fixed reaction support of the cantilever diaphragm test setup, a reinforced concrete reaction block, post-tensioned with anchor rods to the strong floor, was constructed. To fasten the steel deck to the test frame, a steel plate was embedded in the concrete reaction block. Shored construction negated the need for intermediate support test frame members. All specimens used arc spot welds, shear studs, or a combination of both as structural fasteners. Normal weight structural concrete fill was placed on top of steel deck for all specimens except specimen 26, which used lightweight concrete. Measured compressive strengths ranged from 2400 psi to 6200 psi. Steel deck profile dimension details for the different deck types can be found in Porter and Easterling (1988).

The reversed cyclic loading protocol specified increasing displacement steps after a minimum of three cycles. Due to cyclic strength degradation, loads at a specific displacement step dropped for successive cycles. A second criteria for progressing to the next displacement step was for the peak load of a cycles to stabilize within a 5% difference from the previous cycle. The test results and research conclusions from this program are used in the recommended strength and stiffness equations proposed in this research, as well as for quantifying SDDCF ductility and are discussed in detail in Chapters 5 and 6.

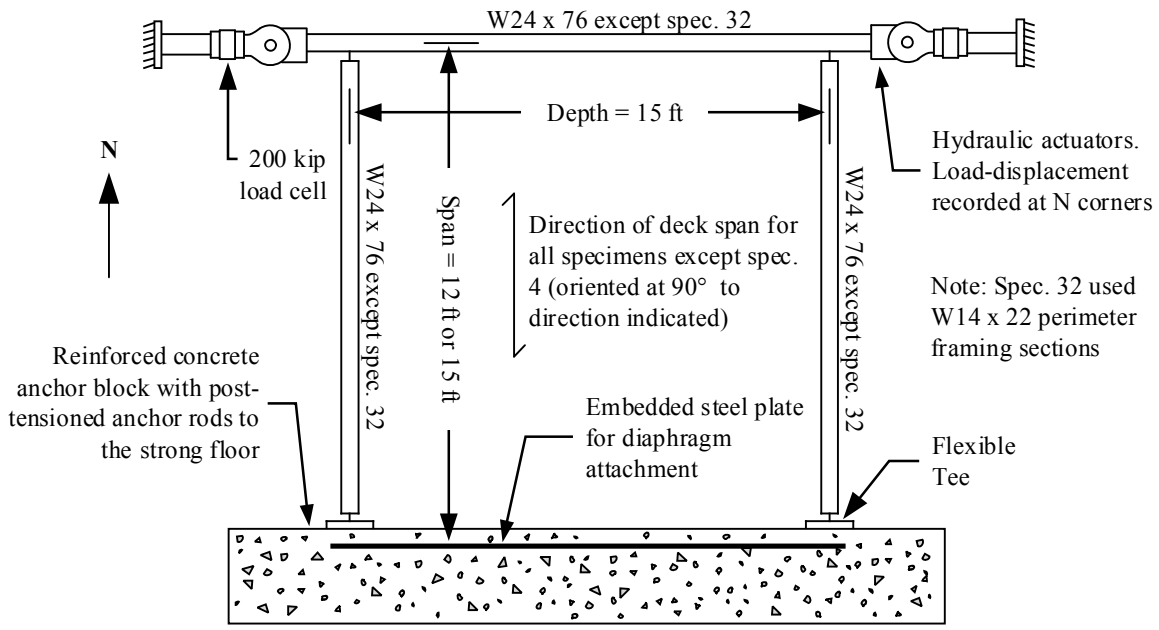

Figure 2-4 Test Frame for Iowa State University Test Program [adapted from Porter and Easterling (1988)]

Table 2-1 Iowa State University Test Setup Variables [from Porter and Easterling (1988)]

Spec. ID	Measured Steel Deck Properties			Measured Conc. Properties		Connections per side
	Thickness (in)	F_y (ksi)	F_u (ksi)	Thickness[1] (in)	f'_c (psi)	
1	0.034	41.7	53.4	5.38	5634	30 studs
2	0.034	41.7	53.4	5.50	5250	30 studs
3	0.034	41.7	53.4	5.65	4068	60 welds
4	0.034	41.7	53.4	5.28	3849	60 welds
5	0.062	48.2	60.7	3.53	2966	30 welds
6	0.062	48.2	60.7	7.44	4549	60 welds
7	0.058	49.7	61.1	5.40	5435	60 welds
8	0.035	41.7	53.4	5.47	3345	4 studs (N,S) 6 studs (E,W)
9[2]	0.058/0.057	51.8/52.4	63.2/64.9	5.48	5412	60 welds
10	0.062	40.4	53.2	5.53	3311	60 welds
11	0.047	89.7	93.7	5.72	3533	60 welds
12[3]	0.062	40.4	53.2	5.59	3412	60 welds
13[2,3]	0.058	51.8/52.4	63.2/64.9	5.53	6187	60 welds
14[3]	0.062	40.4	53.4	8.20	3699	60 welds
15	0.047	89.7	93.6	4.21	2844	60 welds
16[3]	0.047	89.7	93.6	4.18	2952	60 welds
17[3]	0.062	46.0	54.4	7.44	4261	60 welds
18[3]	0.062	40.4	53.4	5.55	3052	60 welds
19	0.062	49.4	55.5	5.75	2681	60 welds
20	0.037	48.6	56.2	5.55	3973	40 welds
21	0.062	40.4	53.4	5.67	3638	15 welds
22	0.062	40.4	53.4	5.68	3301	60 welds (N,S) 48 welds (E,W)
23	0.037	48.6	56.2	5.75	3496	40 welds (N,S) 34 welds (E,W)
24	0.062	49.4	55.5	5.63	4047	48 welds
25	0.062	40.4	53.4	5.69	4672	16 studs (N,S) 8 studs (E,W)
26	0.036	92.8	93.6	4.72	3462	8 studs 15 welds (N,S) 7 studs (W) 11 studs (E)
27	0.037	48.6	56.2	5.66	2883	8 studs 15 welds (N,S) 9 welds (E,W)
28	0.037	48.6	56.2	5.60	3611	8 studs 15 welds (N,S) 6 studs (E,W)
29	0.035	86.9	89.8	5.55	2887	16 studs (N,S) 11 studs (E,W)
30	0.035	86.9	89.8	5.68	3565	12 studs 4 welds (N,S) 7 studs (E,W)
31	0.035	86.9	89.8	5.75	3336	23 welds (N,S) 13 welds (E,W)
32	0.035	86.9	89.8	5.66	2452	30 welds (N,S) 23 welds (E,W)

[1] = thickness measured from top of concrete fill to bottom of steel deck panel

[2] = cellular deck; steel deck properties reported for flat sheet / corrugated sheet

[3] = combination of gravity and in-plane loads

3 DIAPHRAGM DATABASE

An effort was made to consolidate all relevant and available test information from all available sources into a single, comprehensive experimental diaphragm database. Information about a specimen or testing program was deemed relevant if it was considered to influence a diaphragm's load-deformation behavior. The objective of this database is to allow for comparisons of different diaphragm test groups across several experimental research programs, rather than analyzing specimens individually within the scope of a single program. The following sections provide:

1. An overview of the experimental research programs included in the diaphragm database
2. A discussion of critical experimental parameters logged in the diaphragm database

Due to the large amount of information captured in the database, only a list of each specimen and a list of the different database fields is reproduced (see Tables 3-2 and 3-3, respectively). Data for each record and field is available in the database itself.

3.1 Overview of Experimental Research Programs

An extensive number of steel deck diaphragm experimental research programs were identified and cataloged into the diaphragm database. The information recorded in the database is diverse and includes several international programs to. A total of 753 specimens from 47 primary references across 14 research programs currently populate the database, as summarized in Table 3-1. Table 3-2 lists each specimen included in the database. To understand and characterize the ductile behavior of steel deck diaphragms, test specimens that included post peak-strength behavior were identified. Of the 753 specimens, a total of 108 were identified to have complete load-deformation behavior, all of which were tested in a cantilevered fashion. This subset of data,

used for diaphragm ductility and inelastic behavior characterization, is described further in Chapter 6. Additionally, several of these 108 specimens included test setup and results that are outside the scope of this work (e.g. cellular deck, irregular fastener configurations and non-conventional failure modes). The resulting subset of widely applicable configurations and complete inelastic load-deformation data comprised of 95 total specimens, and are discussed in detail in Chapter 6.

Table 3-1 Overview of Experimental Research Programs

Testing Program	Primary Reference	Number of Specimens
Cornell University	Nilson 1960, Nilson 1969	40
S. B. Barnes and Associates	S. B. Barnes and Associates 1957, 1961, 1962, 1966	38
West Virginia University	Luttrell 1967, Ellifritt and Luttrell 1971, Luttrell 1971, Luttrell 1979a, Luttrell 1979b, Luttrell 1981a, Luttrell 1981b, Luttrell 1984, Luttrell 1985, Ameen 1989	246
Development Laboratory of Inland Ryerson Co.	Lacap 1971	1
University of Salford	Bryan 1975, Davies and Fisher 1979	5
ABK, A Joint Venture	ABK 1981	3
Iowa State University	Porter and Greimann 1980, Porter and Easterling 1988, Easterling and Porter 1994a, Easterling and Porter 1994b	32
Virginia Tech	Earls and Murray 1991, Pugh and Murray 1991, Hankins et al. 1992, Rodkey and Murray 1993, Bagwell and Easterling 2008	67
Technical Research Laboratory, Kobe, Japan	Fukuda et al. 1991	6
Nucor – Vulcraft/Verco Group	Pinkham 1997, Pinkham 1999, Pinkham 2008a, Pinkham 2008b	120
University of Montreal, McGill University	Martin 2002, Essa et al. 2003, Yang 2003, Franquet 2009, Masseralli 2010	82
Tongji University	Liu et al. 2007	6
Hilti Corporation	Beck 2008, Foster 2008, Beck 2013a, Beck 2013b, Foster 2013, Foster 2014	92
Tokyo Institute of Tech.	Shimizu et al. 2013	15
	Total =	**753**

Table 3-2 Database Test Specimens

Index No.	Reference	Specimen ID	Index No.	Reference	Specimen ID
1	S. B. Barnes and Assoc. 1957	1	67	S.B. Barnes and Assoc. 1962	A4(II)P
2	S. B. Barnes and Assoc. 1957	2	68	S.B. Barnes and Assoc. 1962	B1(II)P
3	S. B. Barnes and Assoc. 1957	3	69	S.B. Barnes and Assoc. 1962	B2(II)P
4	S. B. Barnes and Assoc. 1957	4	70	S.B. Barnes and Assoc. 1962	B3(II)P
5	S. B. Barnes and Assoc. 1957	5	71	S.B. Barnes and Assoc. 1962	A2(III)P
6	S. B. Barnes and Assoc. 1957	6	72	S.B. Barnes and Assoc. 1962	A2(III)V
7	S. B. Barnes and Assoc. 1957	7	73	S.B. Barnes and Assoc. 1962	A3(III)P
8	S. B. Barnes and Assoc. 1957	8	74	S.B. Barnes and Assoc. 1962	A3(III)V
9	S. B. Barnes and Assoc. 1957	9	75	S.B. Barnes and Assoc. 1966	H-1
10	S. B. Barnes and Assoc. 1957	10	76	S.B. Barnes and Assoc. 1966	H-2
11	S. B. Barnes and Assoc. 1957	11	77	S.B. Barnes and Assoc. 1966	66-2
12	Nilson, A., 1960	2a	78	Luttrell, L., 1967	1
13	Nilson, A., 1960	57-3	79	Luttrell, L., 1967	2
14	Nilson, A., 1960	57-5	80	Luttrell, L., 1967	1-B
15	Nilson, A., 1960	5	81	Luttrell, L., 1967	2-B
16	Nilson, A., 1960	58-3	82	Luttrell, L., 1967	A3
17	Nilson, A., 1960	11	83	Luttrell, L., 1967	A4
18	Nilson, A., 1960	59-5	84	Luttrell, L., 1967	A5
19	Nilson, A., 1960	58-7	85	Luttrell, L., 1967	A6
20	Nilson, A., 1960	59-3	86	Luttrell, L., 1967	A7
21	Nilson, A., 1960	59-1	87	Luttrell, L., 1967	A8
22	Nilson, A., 1960	1c	88	Luttrell, L., 1967	A9
23	Nilson, A., 1960	57-2	89	Luttrell, L., 1967	A10
24	Nilson, A., 1960	58-8	90	Luttrell, L., 1967	A11
25	Nilson, A., 1960	58-5	91	Luttrell, L., 1967	A12
26	Nilson, A., 1960	58-6	92	Luttrell, L., 1967	A13
27	Nilson, A., 1960	59-4	93	Luttrell, L., 1967	A15
28	Nilson, A., 1960	58-4	94	Luttrell, L., 1967	A16
29	Nilson, A., 1960	58-2	95	Luttrell, L., 1967	A17
30	Nilson, A., 1960	5802a	96	Luttrell, L., 1967	4B
31	Nilson, A., 1960	9	97	Luttrell, L., 1967	5
32	Nilson, A., 1960	59-2	98	Luttrell, L., 1967	4P
33	Nilson, A., 1960	4c	99	Luttrell, L., 1967	4R
34	Nilson, A., 1960	3d	100	Luttrell, L., 1967	4R-2
35	Nilson, A., 1960	12	101	Luttrell, L., 1967	4AP
36	Nilson, A., 1960	10	102	Luttrell, L., 1967	4AP2
37	Nilson, A., 1960	58-1	103	Luttrell, L., 1967	4AP3
38	Nilson, A., 1960	5802	104	Luttrell, L., 1967	5P
39	Nilson, A., 1960	58-3	105	Luttrell, L., 1967	5Z
40	Nilson, A., 1960	58-4	106	Luttrell, L., 1967	5R
41	Nilson, A., 1960	58-5b	107	Luttrell, L., 1967	5R2
42	Nilson, A., 1960	58-5c	108	Luttrell, L., 1967	5R3
43	Nilson, A., 1960	59-6	109	Luttrell, L., 1967	5R4
44	Nilson, A., 1960	59-7	110	Luttrell, L., 1967	5R5
45	Nilson, A., 1960	59-8	111	Luttrell, L., 1967	5R6
46	Nilson, A., 1960	59-10	112	Luttrell, L., 1967	5PA
47	Nilson, A., 1960	59-11	113	Luttrell, L., 1967	5PAR
48	Nilson, A., 1960	59-9a	114	Luttrell, L., 1967	4A
49	Nilson, A., 1960	59-12	115	Luttrell, L., 1967	28
50	Nilson, A., 1960	59-13	116	Luttrell, L., 1967	28R
51	S. B. Barnes and Assoc. 1961	4	117	Luttrell, L., 1967	30
52	S. B. Barnes and Assoc. 1961	R1	118	Luttrell, L., 1967	30R
53	S. B. Barnes and Assoc. 1961	R2	119	Luttrell, L., 1967	6AP
54	S. B. Barnes and Assoc. 1961	R3	120	Luttrell, L., 1967	6AP2
55	S. B. Barnes and Assoc. 1961	R4	121	Luttrell, L., 1967	SC1
56	S. B. Barnes and Assoc. 1961	R7	122	Luttrell, L., 1967	SC2
57	S. B. Barnes and Assoc. 1962	A1(I)V	123	Luttrell, L., 1967	SC3
58	S. B. Barnes and Assoc. 1962	A2(I)V	124	Luttrell, L., 1967	7A
59	S. B. Barnes and Assoc. 1962	A3(I)V	125	Luttrell, L., 1967	8
60	S. B. Barnes and Assoc. 1962	A4(I)V	126	Luttrell, L., 1967	7P
61	S. B. Barnes and Assoc. 1962	B1(I)V	127	Luttrell, L., 1967	7R
62	S. B. Barnes and Assoc. 1962	B2(I)V	128	Luttrell, L., 1967	7R2
63	S. B. Barnes and Assoc. 1962	B3(I)V	129	Luttrell, L., 1967	8P
64	S. B. Barnes and Assoc. 1962	A1(II)P	130	Luttrell, L., 1967	8R
65	S. B. Barnes and Assoc. 1962	A2(II)P	131	Luttrell, L., 1967	3
66	S. B. Barnes and Assoc. 1962	A3(II)P	132	Luttrell, L., 1967	3A

Table 3-2 (b) Database Test Specimens

Index No.	Reference	Specimen ID	Index No.	Reference	Specimen ID
133	Luttrell, L., 1967	24	199	Ellifritt and Luttrell, 1971	WB - 11
134	Luttrell, L., 1967	24R	200	Ellifritt and Luttrell, 1971	WB - 12
135	Luttrell, L., 1967	26	201	Ellifritt and Luttrell, 1971	WB - 13
136	Luttrell, L., 1967	26R	202	Ellifritt and Luttrell, 1971	WB - 14
137	Luttrell, L., 1967	9	203	Ellifritt and Luttrell, 1971	WB - 15
138	Luttrell, L., 1967	10	204	Ellifritt and Luttrell, 1971	WB - 16
139	Luttrell, L., 1967	13	205	Ellifritt and Luttrell, 1971	WB - 17
140	Luttrell, L., 1967	14	206	Ellifritt and Luttrell, 1971	WB - 18
141	Luttrell, L., 1967	20	207	Ellifritt and Luttrell, 1971	WB - 19
142	Luttrell, L., 1967	20R	208	Ellifritt and Luttrell, 1971	WB - 20
143	Luttrell, L., 1967	22	209	Ellifritt and Luttrell, 1971	WB - 21
144	Luttrell, L., 1967	22R	210	Ellifritt and Luttrell, 1971	WB - 22
145	Luttrell, L., 1967	11	211	Ellifritt and Luttrell, 1971	WB - 23
146	Luttrell, L., 1967	12	212	Ellifritt and Luttrell, 1971	WB - 24
147	Luttrell, L., 1967	11P	213	Ellifritt and Luttrell, 1971	WB - 25
148	Luttrell, L., 1967	11L	214	Ellifritt and Luttrell, 1971	WB - 26
149	Luttrell, L., 1967	12L	215	Ellifritt and Luttrell, 1971	WB - 27
150	Luttrell, L., 1967	12P	216	Ellifritt and Luttrell, 1971	WB - 28
151	Luttrell, L., 1967	12R	217	Ellifritt and Luttrell, 1971	WB - 29
152	Luttrell, L., 1967	3B01	218	Ellifritt and Luttrell, 1971	WB - 30
153	Luttrell, L., 1967	3B02	219	Ellifritt and Luttrell, 1971	WB - 31
154	Luttrell, L., 1967	3B11	220	Ellifritt and Luttrell, 1971	WB - 32
155	Luttrell, L., 1967	2B01	221	Ellifritt and Luttrell, 1971	WB - 33
156	Luttrell, L., 1967	2B11	222	Ellifritt and Luttrell, 1971	WB - 34
157	Luttrell, L., 1967	1B01	223	Ellifritt and Luttrell, 1971	WB - 35
158	Luttrell, L., 1967	1B11	224	Ellifritt and Luttrell, 1971	WB - 36
159	Luttrell, L., 1967	3C01	225	Ellifritt and Luttrell, 1971	WB - 37
160	Luttrell, L., 1967	3C02	226	Ellifritt and Luttrell, 1971	WB - 38
161	Luttrell, L., 1967	3C11	227	Ellifritt and Luttrell, 1971	WB - 39
162	Luttrell, L., 1967	2C01	228	Ellifritt and Luttrell, 1971	WB - 40
163	Luttrell, L., 1967	2C11	229	Ellifritt and Luttrell, 1971	WB - 41
164	Luttrell, L., 1967	1C01	230	Ellifritt and Luttrell, 1971	A-1
165	Luttrell, L., 1967	1C11	231	Ellifritt and Luttrell, 1971	A-2
166	Nilson, A., 1969	69-2	232	Ellifritt and Luttrell, 1971	A-3
167	Ellifritt and Luttrell, 1971	W-1	233	Ellifritt and Luttrell, 1971	A-4
168	Ellifritt and Luttrell, 1971	W-2	234	Ellifritt and Luttrell, 1971	A-5
169	Ellifritt and Luttrell, 1971	W-3	235	Ellifritt and Luttrell, 1971	A-6
170	Ellifritt and Luttrell, 1971	W-4	236	Ellifritt and Luttrell, 1971	A-7
171	Ellifritt and Luttrell, 1971	W-5	237	Ellifritt and Luttrell, 1971	A-8
172	Ellifritt and Luttrell, 1971	W-6	238	Ellifritt and Luttrell, 1971	A-9
173	Ellifritt and Luttrell, 1971	W-7	239	Ellifritt and Luttrell, 1971	A-10
174	Ellifritt and Luttrell, 1971	W-8	240	Ellifritt and Luttrell, 1971	A-11
175	Ellifritt and Luttrell, 1971	W-9	241	Ellifritt and Luttrell, 1971	A-12
176	Ellifritt and Luttrell, 1971	W-10	242	Ellifritt and Luttrell, 1971	A-13
177	Ellifritt and Luttrell, 1971	W-11	243	Ellifritt and Luttrell, 1971	A-14
178	Ellifritt and Luttrell, 1971	W-12	244	Ellifritt and Luttrell, 1971	A-15
179	Ellifritt and Luttrell, 1971	W-13	245	Ellifritt and Luttrell, 1971	A-16
180	Ellifritt and Luttrell, 1971	W-14	246	Ellifritt and Luttrell, 1971	A-17
181	Ellifritt and Luttrell, 1971	W-15	247	Ellifritt and Luttrell, 1971	A-18
182	Ellifritt and Luttrell, 1971	W-16	248	Ellifritt and Luttrell, 1971	A-19
183	Ellifritt and Luttrell, 1971	W-17	249	Ellifritt and Luttrell, 1971	A-20
184	Ellifritt and Luttrell, 1971	W-18	250	Ellifritt and Luttrell, 1971	A-21
185	Ellifritt and Luttrell, 1971	W-19	251	Ellifritt and Luttrell, 1971	A-22
186	Ellifritt and Luttrell, 1971	W-20	252	Ellifritt and Luttrell, 1971	A-23
187	Ellifritt and Luttrell, 1971	W-21	253	Ellifritt and Luttrell, 1971	A-24
188	Ellifritt and Luttrell, 1971	W-22	254	Ellifritt and Luttrell, 1971	A-25
189	Ellifritt and Luttrell, 1971	WB - 1	255	Ellifritt and Luttrell, 1971	A-26
190	Ellifritt and Luttrell, 1971	WB - 2	256	Ellifritt and Luttrell, 1971	A-27
191	Ellifritt and Luttrell, 1971	WB - 3	257	Ellifritt and Luttrell, 1971	A-28
192	Ellifritt and Luttrell, 1971	WB - 4	258	Ellifritt and Luttrell, 1971	A-29
193	Ellifritt and Luttrell, 1971	WB - 5	259	Ellifritt and Luttrell, 1971	A-30
194	Ellifritt and Luttrell, 1971	WB - 6	260	Ellifritt and Luttrell, 1971	A-31
195	Ellifritt and Luttrell, 1971	WB - 7	261	Ellifritt and Luttrell, 1971	A-32
196	Ellifritt and Luttrell, 1971	WB - 8	262	Ellifritt and Luttrell, 1971	A-33
197	Ellifritt and Luttrell, 1971	WB - 9	263	Ellifritt and Luttrell, 1971	I-1
198	Ellifritt and Luttrell, 1971	WB - 10	264	Ellifritt and Luttrell, 1971	I-2

Table 3-2 (c) Database Test Specimens

Index No.	Reference	Specimen ID	Index No.	Reference	Specimen ID
265	Ellifritt and Luttrell, 1971	I-3	331	Porter and Easterling, 1988	3
266	Ellifritt and Luttrell, 1971	I-4	332	Porter and Easterling, 1988	4
267	Ellifritt and Luttrell, 1971	I-5	333	Porter and Easterling, 1988	5
268	Ellifritt and Luttrell, 1971	I-6	334	Porter and Easterling, 1988	6
269	Ellifritt and Luttrell, 1971	I-7	335	Porter and Easterling, 1988	7
270	Ellifritt and Luttrell, 1971	I-8	336	Porter and Easterling, 1988	8
271	Ellifritt and Luttrell, 1971	I-9	337	Porter and Easterling, 1988	9
272	Ellifritt and Luttrell, 1971	I-10	338	Porter and Easterling, 1988	10
273	Ellifritt and Luttrell, 1971	1	339	Porter and Easterling, 1988	11
274	Ellifritt and Luttrell, 1971	2	340	Porter and Easterling, 1988	12
275	Ellifritt and Luttrell, 1971	3	341	Porter and Easterling, 1988	13
276	Lacap, D., 1971	1	342	Porter and Easterling, 1988	14
277	Luttrell, L., 1971	C1-1	343	Porter and Easterling, 1988	15
278	Luttrell, L., 1971	C3-2	344	Porter and Easterling, 1988	16
279	Luttrell, L., 1971	P1-1	345	Porter and Easterling, 1988	17
280	Luttrell, L., 1971	P3-2	346	Porter and Easterling, 1988	18
281	Luttrell, L., 1971	P3-3	347	Porter and Easterling, 1988	19
282	Luttrell, L., 1971	P3-4	348	Porter and Easterling, 1988	20
283	Luttrell, L., 1971	P3-5	349	Porter and Easterling, 1988	21
284	Luttrell, L., 1971	P3-6	350	Porter and Easterling, 1988	22
285	Luttrell, L., 1971	P3-7	351	Porter and Easterling, 1988	23
286	Luttrell, L., 1971	C1-1A	352	Porter and Easterling, 1988	24
287	Luttrell, L., 1971	C3-2A	353	Porter and Easterling, 1988	25
288	Bryan, E., 1975	1	354	Porter and Easterling, 1988	26
289	Luttrell, L., 1979a	2-1	355	Porter and Easterling, 1988	27
290	Luttrell, L., 1979a	2-2	356	Porter and Easterling, 1988	28
291	Luttrell, L., 1979a	2-3	357	Porter and Easterling, 1988	29
292	Luttrell, L., 1979b	1	358	Porter and Easterling, 1988	30
293	Luttrell, L., 1979b	2	359	Porter and Easterling, 1988	31
294	Luttrell, L., 1979b	3	360	Porter and Easterling, 1988	32
295	Luttrell, L., 1979b	4	361	Ameen, A., 1989	1
296	Luttrell, L., 1979b	5	362	Ameen, A., 1989	2
297	Luttrell, L., 1979b	6	363	Ameen, A., 1989	3
298	Luttrell, L., 1979b	7	364	Ameen, A., 1989	4
299	Luttrell, L., 1979b	8	365	Ameen, A., 1989	5
300	Luttrell, L., 1979b	9	366	Earls and Murray, 1991	B-1
301	Luttrell, L., 1979b	10	367	Earls and Murray, 1991	B-2
302	Luttrell, L., 1979b	11	368	Earls and Murray, 1991	B-3
303	Luttrell, L., 1979b	12	369	Earls and Murray, 1991	C-1
304	Luttrell, L., 1979b	13	370	Earls and Murray, 1991	C-2
305	Luttrell, L., 1979b	14	371	Earls and Murray, 1991	C-3
306	Davies and Fisher, 1979	1	372	Earls and Murray, 1991	D-1
307	Davies and Fisher, 1979	2	373	Earls and Murray, 1991	D-2
308	Davies and Fisher, 1979	3	374	Earls and Murray, 1991	E-1
309	Davies. and Fisher, 1979	4	375	Earls and Murray, 1991	E-2
310	ABK, A Joint Venture, 1981	Q	376	Earls and Murray, 1991	E-3
311	ABK, A Joint Venture, 1981	R	377	Earls and Murray, 1991	F-1
312	ABK, A Joint Venture, 1981	S	378	Earls and Murray, 1991	F-2
313	Luttrell, L., 1981a	1	379	Earls and Murray, 1991	F-3
314	Luttrell, L., 1981a	2	380	Fukuda et al., 1991	CD-1
315	Luttrell, L., 1981a	3	381	Fukuda et al., 1991	CD-2
316	Luttrell, L., 1981a	4	382	Fukuda et al., 1991	C-1
317	Luttrell, L., 1981a	5	383	Fukuda et al., 1991	C-2
318	Luttrell, L., 1981b	1	384	Fukuda et al., 1991	S-1
319	Luttrell, L., 1984	1	385	Fukuda et al., 1991	S-2
320	Luttrell, L., 1984	2	386	Pugh and Murray, 1991	B-1
321	Luttrell, L., 1984	3	387	Pugh and Murray, 1991	B-2
322	Luttrell, L., 1984	4	388	Pugh and Murray, 1991	B-3
323	Luttrell, L., 1984	5	389	Pugh and Murray, 1991	C-1
324	Luttrell, L., 1984	6	390	Pugh and Murray, 1991	C-2
325	Luttrell, L., 1984	7	391	Pugh and Murray, 1991	C-3
326	Luttrell, L., 1985	1	392	Pugh and Murray, 1991	D-1
327	Luttrell, L., 1985	2	393	Pugh and Murray, 1991	D-2
328	Luttrell, L., 1985	3	394	Pugh and Murray, 1991	D-3
329	Porter and Easterling, 1988	1	395	Hankins et al., 1992	1
330	Porter and Easterling, 1988	2	396	Hankins et al., 1992	2

Table 3-2 (d) Database Test Specimens

Index No.	Reference	Specimen ID	Index No.	Reference	Specimen ID
397	Hankins et al., 1992	3	463	Pinkham C., 1999	98-51
398	Hankins et al., 1992	4	464	Pinkham C., 1999	98-52
399	Hankins et al., 1992	5	465	Pinkham C., 1999	98-53
400	Hankins et al., 1992	6	466	Pinkham C., 1999	98-54
401	Hankins et al., 1992	7	467	Pinkham C., 1999	R98-54
402	Hankins et al., 1992	8	468	Pinkham C., 1999	99-1
403	Hankins et al., 1992	9	469	Pinkham C., 1999	99-2A
404	Hankins et al., 1992	10	470	Pinkham C., 1999	99-2B
405	Hankins et al., 1992	11	471	Pinkham C., 1999	99-3
406	Hankins et al., 1992	12	472	Pinkham C., 1999	99-4
407	Hankins et al., 1992	13	473	Pinkham C., 1999	99-5
408	Hankins et al., 1992	14	474	Pinkham C., 1999	99-6
409	Hankins et al., 1992	15	475	Pinkham C., 1999	99-7
410	Hankins et al., 1992	16	476	Pinkham C., 1999	99-8
411	Hankins et al., 1992	17	477	Pinkham C., 1999	99-9
412	Hankins et al., 1992	18	478	Pinkham C., 1999	99-10
413	Rodkey and Murray, 1993	1	479	Pinkham C., 1999	99-11
414	Rodkey and Murray, 1993	2	480	Pinkham C., 1999	99-12
415	Rodkey and Murray, 1993	3	481	Martin, E., 2002	19
416	Rodkey and Murray, 1993	4	482	Martin, E., 2002	20
417	Rodkey and Murray, 1993	5	483	Martin, E., 2002	21
418	Rodkey and Murray, 1993	6	484	Martin, E., 2002	22
419	Pinkham C., 1997	Hilti 97-5	485	Martin, E., 2002	23
420	Pinkham C., 1997	Hilti 98-19	486	Martin, E., 2002	24
421	Pinkham C., 1997	Hilti 98-20	487	Martin, E., 2002	25
422	Pinkham C., 1997	Hilti 98-21	488	Martin, E., 2002	26
423	Pinkham C., 1997	Hilti 98-21A	489	Martin, E., 2002	27
424	Pinkham C., 1997	Hilti 98-22	490	Martin, E., 2002	28
425	Pinkham C., 1997	Hilti 98-23	491	Martin, E., 2002	29
426	Pinkham C., 1997	Hilti 98-24	492	Martin, E., 2002	30
427	Pinkham C., 1997	Hilti 98-25	493	Martin, E., 2002	31
428	Pinkham C., 1997	Hilti 98-26	494	Martin, E., 2002	32
429	Pinkham C., 1997	Hilti 98-27	495	Martin, E., 2002	33
430	Pinkham C., 1997	Hilti 98-28	496	Martin, E., 2002	34
431	Pinkham C., 1997	Hilti 98-29	497	Martin, E., 2002	35
432	Pinkham C., 1997	Hilti 98-29A	498	Martin, E., 2002	36
433	Pinkham C., 1997	Hilti 98-30	499	Martin, E., 2002	37
434	Pinkham C., 1997	Hilti 98-30A	500	Essa et al., 2003	1
435	Pinkham C., 1997	Hilti 99-1	501	Essa et al., 2003	2
436	Pinkham C., 1997	Hilti 99-2	502	Essa et al., 2003	3
437	Pinkham C., 1997	Hilti 99-5	503	Essa et al., 2003	4
438	Pinkham C., 1997	Hilti 99-6	504	Essa et al., 2003	5
439	Pinkham C., 1997	Hilti 99-7	505	Essa et al., 2003	6
440	Pinkham C., 1997	Hilti 99-8	506	Essa et al., 2003	7
441	Pinkham C., 1997	Hilti 00-8	507	Essa et al., 2003	8
442	Pinkham C., 1997	Hilti 00-9	508	Essa et al., 2003	9
443	Pinkham C., 1997	Hilti 00-10	509	Essa et al., 2003	10
444	Pinkham C., 1997	Hilti 00-11	510	Essa et al., 2003	11
445	Pinkham C., 1997	Hilti 00-12	511	Essa et al., 2003	12
446	Pinkham C., 1997	Hilti 00-13	512	Essa et al., 2003	13
447	Pinkham C., 1997	Hilti 00-14	513	Essa et al., 2003	14
448	Pinkham C., 1999	98-31	514	Essa et al., 2003	15
449	Pinkham C., 1999	98-32	515	Essa et al., 2003	16
450	Pinkham C., 1999	98-33	516	Essa et al., 2003	17
451	Pinkham C., 1999	98-34	517	Essa et al., 2003	18
452	Pinkham C., 1999	98-35	518	Yang, W., 2003	38
453	Pinkham C., 1999	98-36	519	Yang, W., 2003	39
454	Pinkham C., 1999	98-37	520	Yang, W., 2003	40
455	Pinkham C., 1999	98-38	521	Yang, W., 2003	41
456	Pinkham C., 1999	98-39	522	Yang, W., 2003	42
457	Pinkham C., 1999	98-40	523	Yang, W., 2003	43
458	Pinkham C., 1999	98-41	524	Yang, W., 2003	44
459	Pinkham C., 1999	98-42	525	Yang, W., 2003	47
460	Pinkham C., 1999	98-43	526	Yang, W., 2003	48
461	Pinkham C., 1999	98-44	527	Yang, W., 2003	49
462	Pinkham C., 1999	98-50	528	Bagwell and Easterling, 2008	1

Table 3-2 (e) Database Test Specimens

Index No.	Reference	Specimen ID	Index No.	Reference	Specimen ID
529	Bagwell and Easterling, 2008	2	595	Foster, T., 2008	33
530	Bagwell and Easterling, 2008	3	596	Foster, T., 2008	34
531	Bagwell and Easterling, 2008	4	597	Foster, T., 2008	35
532	Bagwell and Easterling, 2008	5	598	Foster, T., 2008	36
533	Bagwell and Easterling, 2008	6	599	Foster, T., 2008	37
534	Bagwell and Easterling, 2008	7	600	Foster, T., 2008	38
535	Bagwell and Easterling, 2008	8	601	Foster, T., 2008	39
536	Bagwell and Easterling, 2008	9	602	Foster, T., 2008	40
537	Bagwell and Easterling, 2008	10	603	Foster, T., 2008	41
538	Bagwell and Easterling, 2008	11	604	Foster, T., 2008	42
539	Bagwell and Easterling, 2008	12	605	Foster, T., 2008	43
540	Bagwell and Easterling, 2008	13	606	Foster, T., 2008	44
541	Bagwell and Easterling, 2008	14	607	Foster, T., 2008	45
542	Bagwell and Easterling, 2008	15	608	Foster, T., 2008	46
543	Bagwell and Easterling, 2008	16	609	Foster, T., 2008	47
544	Bagwell and Easterling, 2008	17	610	Foster, T., 2008	48
545	Bagwell and Easterling, 2008	18	611	Foster, T., 2008	49
546	Bagwell and Easterling, 2008	19	612	Foster, T., 2008	50
547	Bagwell and Easterling, 2008	20	613	Foster, T., 2008	51
548	Liu et al., 2007	SJ1-1	614	Foster, T., 2008	52
549	Liu et al., 2007	SJ1-2	615	Foster, T., 2008	53
550	Liu et al., 2007	SJ2	616	Foster, T., 2008	54
551	Liu et al., 2007	SJ3-1	617	Foster, T., 2008	55
552	Liu et al., 2007	SJ3-2	618	Foster, T., 2008	56
553	Liu et al., 2007	SJ-4	619	Foster, T., 2008	57
554	Beck, H., 2008	S 03	620	Foster, T., 2008	58
555	Beck, H., 2008	S 04	621	Foster, T., 2008	59
556	Beck, H., 2008	S 05	622	Foster, T., 2008	60
557	Beck, H., 2008	S 06	623	Foster, T., 2008	61
558	Beck, H., 2008	S 07	624	Foster, T., 2008	62
559	Beck, H., 2008	S 08	625	Pinkham C., 2008a	06-1
560	Beck, H., 2008	63	626	Pinkham C., 2008a	06-2
561	Beck, H., 2008	64	627	Pinkham C., 2008a	06-3
562	Beck, H., 2008	65	628	Pinkham C., 2008a	06-4
563	Foster, T., 2008	1	629	Pinkham C., 2008a	06-5
564	Foster, T., 2008	2	630	Pinkham C., 2008a	06-5
565	Foster, T., 2008	3	631	Pinkham C., 2008a	06-6
566	Foster, T., 2008	4	632	Pinkham C., 2008a	06-7
567	Foster, T., 2008	5	633	Pinkham C., 2008a	06-8
568	Foster, T., 2008	6	634	Pinkham C., 2008a	06-9
569	Foster, T., 2008	7	635	Pinkham C., 2008a	06-11
570	Foster, T., 2008	8	636	Pinkham C., 2008a	06-13
571	Foster, T., 2008	9	637	Pinkham C., 2008a	06-14
572	Foster, T., 2008	10	638	Pinkham C., 2008a	06-15
573	Foster, T., 2008	11	639	Pinkham C., 2008a	06-16
574	Foster, T., 2008	12	640	Pinkham C., 2008a	06-17
575	Foster, T., 2008	13	641	Pinkham C., 2008a	06-18
576	Foster, T., 2008	14	642	Pinkham C., 2008a	06-19
577	Foster, T., 2008	15	643	Pinkham C., 2008a	06-20
578	Foster, T., 2008	16	644	Pinkham C., 2008a	06-21
579	Foster, T., 2008	17	645	Pinkham C., 2008a	06-22
580	Foster, T., 2008	18	646	Pinkham C., 2008a	06-23
581	Foster, T., 2008	19	647	Pinkham C., 2008a	06-24
582	Foster, T., 2008	20	648	Pinkham C., 2008a	06-25
583	Foster, T., 2008	21	649	Pinkham C., 2008a	06-26
584	Foster, T., 2008	22	650	Pinkham C., 2008a	06-27
585	Foster, T., 2008	23	651	Pinkham C., 2008a	06-28
586	Foster, T., 2008	24	652	Pinkham C., 2008b	06-29
587	Foster, T., 2008	25	653	Pinkham C., 2008b	06-30
588	Foster, T., 2008	26	654	Pinkham C., 2008b	06-31
589	Foster, T., 2008	27	655	Pinkham C., 2008b	06-32
590	Foster, T., 2008	28	656	Pinkham C., 2008b	06-33
591	Foster, T., 2008	29	657	Pinkham C., 2008b	06-34
592	Foster, T., 2008	30	658	Pinkham C., 2008b	06-35
593	Foster, T., 2008	31	659	Pinkham C., 2008b	06-36
594	Foster, T., 2008	32	660	Pinkham C., 2008b	06-37

Table 3-2 (f) Database Test Specimens

Index No.	Reference	Specimen ID
661	Pinkham C., 2008b	06-38
662	Pinkham C., 2008b	06-29b
663	Pinkham C., 2008b	06-30b
664	Pinkham C., 2008b	06-31b
665	Pinkham C., 2008b	06-32b
666	Pinkham C., 2008b	06-32bb
667	Pinkham C., 2008b	06-33b
668	Pinkham C., 2008b	06-33bb
669	Pinkham C., 2008b	06-34b
670	Pinkham C., 2008b	06-35b
671	Pinkham C., 2008b	06-36b
672	Pinkham C., 2008b	06-37b
673	Pinkham C., 2008b	06-39b
674	Pinkham C., 2008b	06-29c
675	Pinkham C., 2008b	06-30c
676	Pinkham C., 2008b	06-31c
677	Pinkham C., 2008b	06-32c
678	Pinkham C., 2008b	06-33c
679	Pinkham C., 2008b	06-34c
680	Pinkham C., 2008b	06-35c
681	Pinkham C., 2008b	06-36c
682	Pinkham C., 2008b	06-37c
683	Franquet, J., 2009	DIA-1
684	Franquet, J., 2009	DIA-1R
685	Franquet, J., 2009	DIA-2
686	Franquet, J., 2009	DIA-3
687	Franquet, J., 2009	DIA-3R
688	Franquet, J., 2009	DIA-4
689	Franquet, J., 2009	DIA-4R
690	Franquet, J., 2009	DIA-5
691	Franquet, J., 2009	DIA-5R
692	Franquet, J., 2009	DIA-6
693	Franquet, J., 2009	DIA-6R
694	Franquet, J., 2009	DIA-7
695	Franquet, J., 2009	DIA-7R
696	Franquet, J., 2009	DIA-8
697	Franquet, J., 2009	DIA-8R
698	Franquet, J., 2009	DIA-9
699	Franquet, J., 2009	DIA-9R
700	Franquet, J., 2009	DIA-10
701	Franquet, J., 2009	DIA-10R
702	Massarelli, R., 2010	DIA-11
703	Massarelli, R., 2010	DIA-12
704	Massarelli, R., 2010	DIA-12R
705	Massarelli, R., 2010	DIA-13
706	Massarelli, R., 2010	DIA-13R
707	Massarelli, R., 2010	DIA-14
708	Massarelli, R., 2010	DIA-15
709	Massarelli, R., 2010	DIA-15R
710	Massarelli, R., 2010	DIA16
711	Massarelli, R., 2010	DIA-16R
712	Massarelli, R., 2010	DIA-17
713	Massarelli, R., 2010	DIA-17R
714	Massarelli, R., 2010	DIA-18
715	Massarelli, R., 2010	DIA-18R
716	Massarelli, R., 2010	DIA-19
717	Massarelli, R., 2010	DIA-19R
718	Beck, H., 2013a	M 01
719	Beck, H., 2013a	C 01
720	Beck, H., 2013a	M 02
721	Beck, H., 2013a	C 02
722	Beck, H., 2013a	M 03
723	Beck, H., 2013a	C 03
724	Beck, H., 2013b	S-02
725	Beck, H., 2013b	S-02-cycl
726	Beck, H., 2013b	S-03
727	Beck, H., 2013b	S-03-cycl
728	Foster, T., 2013	E-01
729	Foster, T., 2013	E-02
730	Foster, T., 2013	E-03
731	Foster, T., 2013	E-04
732	Foster, T., 2013	E-05
733	Foster, T., 2013	E-06
734	Foster, T., 2013	E-07
735	Shimizu et al., 2013	t04 - h20 - f40
736	Shimizu et al., 2013	t04 - h20 - f25
737	Shimizu et al., 2013	t04 - h20 - f15
738	Shimizu et al., 2013	t04 - h20 - f0
739	Shimizu et al., 2013	t04 - h30 - f25
740	Shimizu et al., 2013	t04 - h40 - f25
741	Shimizu et al., 2013	t06 - h20 - f25
742	Shimizu et al., 2013	t08 - h20 - f25
743	Shimizu et al., 2013	t04 - h20 - f32
744	Shimizu et al., 2013	t04 - h20 - f32J
745	Shimizu et al., 2013	t06 - h20 - f40 - M
746	Shimizu et al., 2013	t06 - h20 - f40 - C
747	Shimizu et al., 2013	t06 - h20 - f25 - M
748	Shimizu et al., 2013	t06 - h20 - f25 - C
749	Shimizu et al., 2013	t06 - h15 - f40 - C
750	Foster, T., 2014	S-01
751	Foster, T., 2014	S-04
752	Foster, T., 2014	S-05
753	Foster, T., 2014	S-06

3.2 Test Setup Experimental Parameters

Several variables were identified as having the potential to influence test results. In many cases, incomplete data was published, and the database contains only the available information. For some programs, test variables were concluded to have negligible effect on experimental results. In other programs, that same variable may have played a significant role in the diaphragm behavior. For completeness, database fields identified to have influence in only a few programs were logged for all programs. Different test setup fields, test result fields, and calculated fields included in the database are summarized in Table 3-3. Note that currently, only the test setup fields for all 753 specimens are included in the database. Test result fields and calculated fields are currently only included for the specimens analyzed for ductility with post-peak load-deformation data available.

Table 3-3 Database Test Fields

Test Setup Fields	Load Type Load protocol Setup configuration (cantilever vs simply supported) Plan dimensions Span dimension Depth dimension Deck span direction (with respect to direction of loading) Deck span length Test frame support member sizes Test frame interior support member sizes Steel deck profile dimensions Steel deck manufacturer	Steel deck thickness Measured deck yield strength Measured deck percent elongation Type of structural fastener Size of structural fastener Spacing of structural fastener Type of sidelap fastener Size of sidelap fastener Spacing of Sidelap Fastener Endlap location Concrete unit weight Measured concrete fill thickness 28 day concrete compressive strength Type of concrete reinforcement
Test Result Fields	Ultimate shear strength Shear stiffness	Shear angle at 80% strength degradation Load-deformation data points
Calculated Fields	Predicted structural support fastener strength Predicted sidelap fastener strength Predicted diaphragm strength Predicted structural support fastener flexibility Predicted sidelap fastener flexibility Predicted diaphragm stiffness	Strength Factors, R_Ω Subassemblage Ductility System Ductility Ductility Factor (medium and long period), R_μ Diaphragm Design Force Reduction Factor (medium and long period), R_s

An example of test setup fields playing a role in only a select number of programs was the framing members used to support deck connections. In many cases, large test framing members were utilized. Since these framing members may not be representative of real steel-framed buildings, lighter sections were often connected to the frame to provide a more typical connection between steel deck and structural support. In the majority of the test programs, prior to placement of steel decking, the structural frame was displaced with relatively negligible force, and deemed to have little to no impact on the test results. Regardless of influence, section sizes of the structural frame are included in the database along with overall plan dimensions of the frame.

Loading protocol also has a significant impact in the testing results. Diaphragm subassemblies may be subject to either monotonic or reversed cyclic displacement protocols. Cyclic tests generally result in lower strengths at certain displacements due to the effects of cyclic degradation, especially in the inelastic range when compared to their monotonically tested counterpart. Of the 753 specimens currently included in the database, 609 were subjected to monotonic loading with the remaining 104 subjected to cyclic loads. Loading rates are identified as either static or dynamic. Dynamic load rates are more representative of seismic ground motions and may influence diaphragm behavior through strain rate effects and were thus recorded. Fifty-five monotonic curves and 53 cyclic hystereses were digitized. Backbone curves for cyclic tests were traced from one peak cycle to the next. For loading protocols with large displacement steps between cycles, a backbone envelope rather than the traditional peak to peak backbone curve was identified to better capture the load-deformation behavior as shown in Figure 3-1 and therefore used for subsequent analyses.

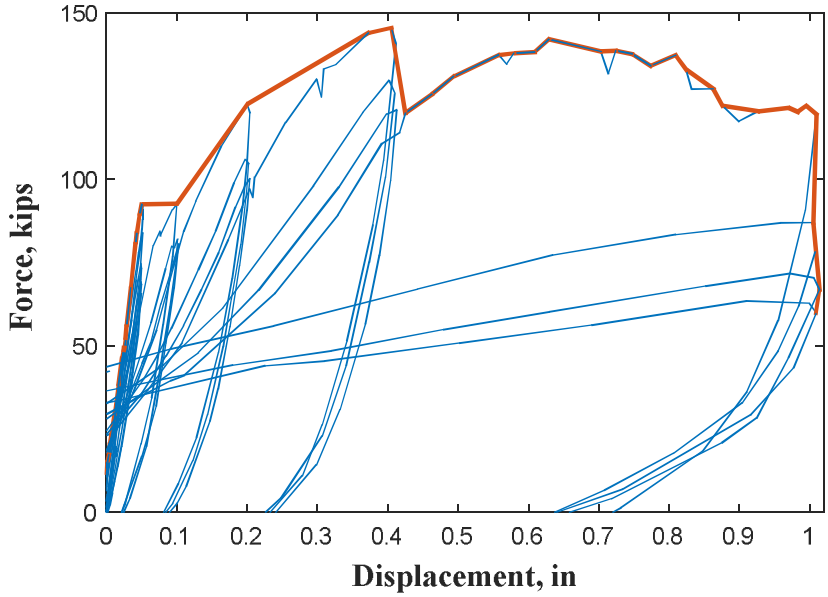

Figure 3-1 Example of Obtaining a Cyclic Envelope

Diaphragms with steel deck depths greater than 3 in., or deep deck diaphragms, are utilized for their increased ability to resist vertical loads for longer deck spans. However, deep deck diaphragms without concrete fill are more prone to warping, resulting in decreased stiffnesses and strengths than decks with depths of 3 in. or less. Steel panel profile geometry for every type of deck tested in the database is therefore documented. Deck thickness ranged from 16 gauge to 26 gauge steel. Deck panel widths range from 12 inches to 40 inches, with depths ranging from 1 in. to 7.5 in. Steel deck material properties, such as nominal and measured yield strengths and ultimate strengths have been shown to impact the performance of a diaphragm, and were thus recorded. Two general types of steel material were identified: 1.) normal yield/ultimate strength steel with nominal values of 33/45 ksi respectively and 2.) high strength steel with nominal yield and ultimate strength values greater than 50 ksi. While high strength steel decks developed larger values for strength and stiffness, energy dissipating capabilities were sometimes compromised (Beck,

2013b). For experimental tests with concrete fill, material properties such as unit weight and compressive strength were recorded.

Historically, diaphragm tests have two basic setup configurations. The first is a simply supported system, consisting of a single bay or multiple bays. This system has considerable advantages, including a more comparable construction setup to diaphragms in the field and a realistic shear demand distribution for dynamically tested specimens with added mass. However, the majority of diaphragm tests have been tested through a cantilevered setup, since it is more economical than a simply supported test setup and still results in reliable strength and stiffness values (Nilson, 1960). Whether a diaphragm test was simply supported or cantilevered is identified for each specimen in the database. Figure 3-2 shows a schematic for a typical cantilevered steel deck diaphragm test setup often idealized as a cantilever deep beam, with the free end on the North side of the diaphragm.

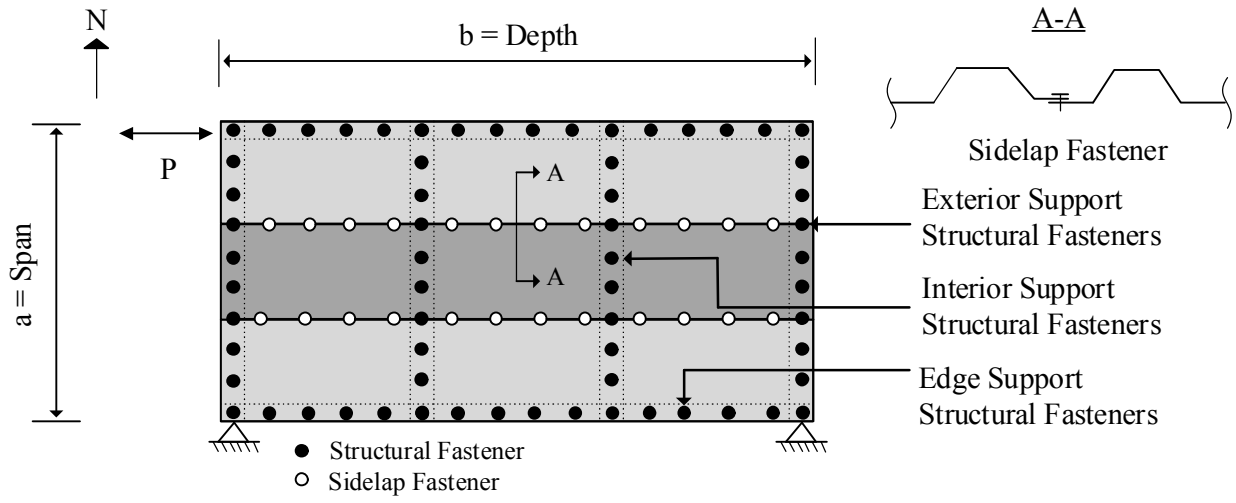

Figure 3-2 Cantilevered Diaphragm Test Setup

The method of fastening the deck to the structural frame plays a crucial role in the tested diaphragm behavior, since different fastener types exhibit different failure modes. The two major categories of fastener location types identified are structural fasteners (deck to support) and sidelap fasteners (panel to panel connections). The database further subcategorizes structural fasteners into whether they are on the perimeter framing members, or whether they are along interior members. Locations of structural fasteners and sidelap fasteners are demonstrated in Figure 3-2.

Four main structural fasteners in the diaphragm database: Power actuated fasteners, self-drilling screws, welds and headed shear studs. Power actuated fasteners, hereby referred to as PAFs, are fasteners that utilize either a pneumatic tool (typically compressed air) or an explosive powder to fire off a hardened steel nail through steel deck and into a structural steel support. The latter is more common (referred to as powder actuated fasteners) since no air compressor is necessary and the fastening system works independently from other equipment. Self-drilling screws include a screw bit (prior to threads and screw head) and do not require a drilled hole before installation. PAFs and self-drilling screws are often referred to as mechanical fasteners. Advantages of mechanical fasteners include ease of use, light mechanical equipment, fast construction time and low variability in strength values. Figure 3-3 shows Hilti PAF fastener X-ENP-19 L15 pre and post installation and Hilti's PAF stand up fastening tool DX 860-ENP.

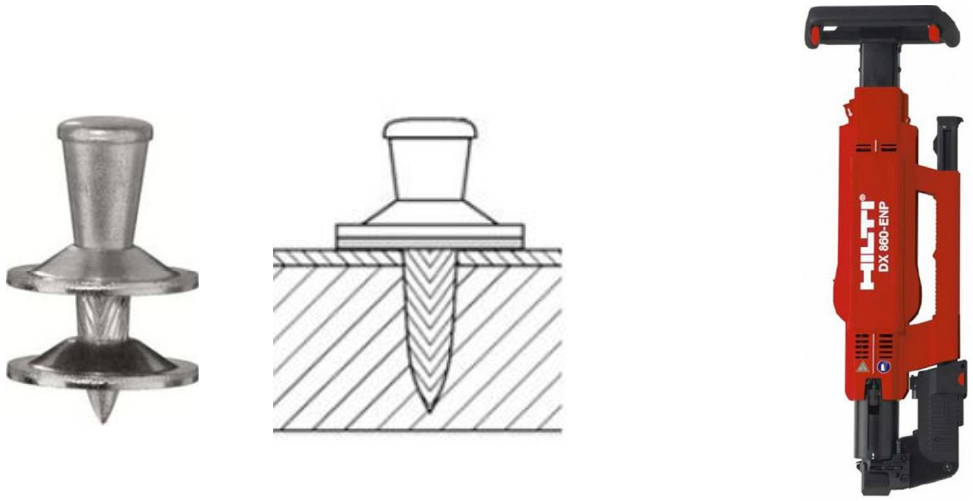

a.) Hilti PAF Before & After Installation b.) Hilti PAF Fastening Tool

Figure 3-3 Hilti PAF and Fastening Tool [from Beck (2013a)]

Arc spot welds in steel deck diaphragms simultaneously burn a hole through the deck and fuse the deck to the support with weld wire material in a single process. Although these welds are detailed as circular with a nominal diameter, it is common to see welds that vary in size and shape. Since no two welds are identical, size and shape inconsistencies should be considered in the design process. AISI S310 specifies arc spot welds to have an effective diameter relative to the visible diameter and sheet thickness, as shown in Figure 3-4 . This effective diameter gives an area of the weld in the maximum shear transfer plane that is active in resisting shear forces (see Figure 3-4). Arc spot weld diameters recorded in the database correspond to specified nominal visible diameters. Arc spot weld diameters for a few testing programs, particularly those from the West Coast of the United States (i.e. references from Pinkham 1997, 1999, 2008a, 2008b), used specified American Welding Society procedures that at the time allowed for visible diameters to be less than effective diameters (Martin, 2017). The diameters recorded in the database for these specimens are visible diameters that would correspond to an effective diameter as currently specified by AISI

S310 and shown in Figure 3-4 where d_e = effective diameter, d = visible diameter, and t = sheet(s) thickness.

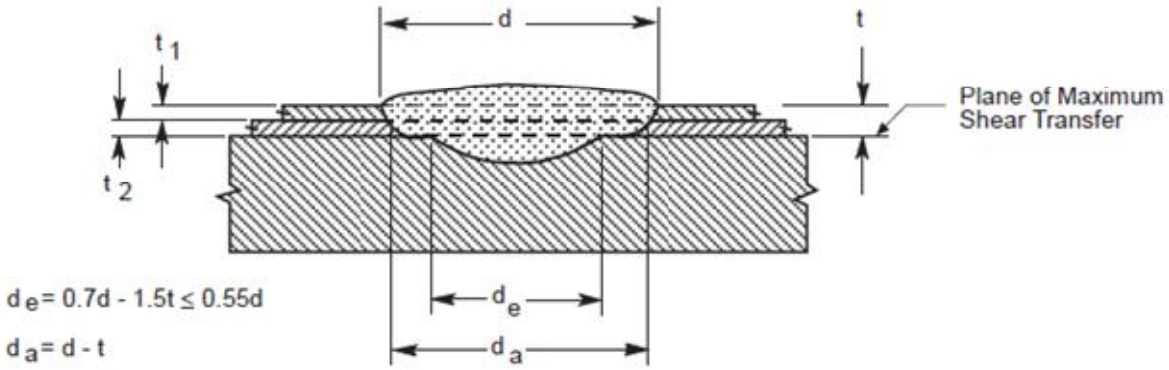

Figure 3-4 Arc Spot Weld Diameters [from AISI (2016a)]

When a steel deck diaphragm has concrete fill placed on top, methods to fasten the deck to support often utilize headed shear studs. These studs protrude into the concrete slab and allow the structural steel support, steel deck and concrete slab to act as a composite system.

Sidelap fasteners may also be welded, although it is difficult to obtain a reliable weld through two light gauge metal sheets without burning through both layers. Sidelap screws offer a more reliable alternative and are constructed similar to self-drilling structural screws. Mechanical crimping devices can join two adjacent decks that have standing edges. The most common sidelap mechanical crimping method is called button punch, although other crimping methods are available. The main advantage of a button punch sidelap connection is that no fastener is necessary. However, button punch connections primarily rely on friction forces and do not offer a significant amount of strength. Strength of button punches are subject to the crimping device and force exerted by the construction worker and offer less reliability than screws. Each type and size of structural and sidelap fastener is recorded in the diaphragm database. Table 3-4 lists the frequency of the

different types of structural or sidelap fasteners for each tested specimen in the database. Note that a large number of diaphragms had incomplete information or alternative fastener types outside the scope of this research.

Table 3-4 Number of Experimental Tests with Fastener Types

Deck to Frame Fasteners		Sidelap Fasteners	
Welds	339	Welds	112
Screws	92	Screws	115
PAF	240	BP	282
Studs	9	Other/Unavailable	244
Other/Unavailable	73		

The spacing of structural and sidelap fasteners may also dictate diaphragm behavior. Fasteners with an excessive amount of fasteners may have the steel deck failure mechanism control, rather than the fastener failure mode control. This will exhibit different behavior than if few fasteners are used and the fastener failure mode controlled. The spacing and location of structural and sidelap fasteners are therefore recorded in the database.

A diaphragm's behavior may be characterized by several test result fields. Test result were recorded only for the subset of data that included post peak-strength load-deformation behavior and used to support diaphragm ductility and behavior characterization. Recorded results in the database include shear stiffness, peak load, yield deformation, deformations at post-peak loads and more. Failure modes that initiated yielding, strength degradation and other notable changes in the load-deformation behavior are described in the database. A detailed discussion of these experimental results and differing failure modes are discussed in Chapters 5 and 6.

4 DIAPHRAGM DESIGN FORCE REDUCTION FACTORS

This chapter describes the methodology used in this research to develop diaphragm design force reduction factors, R_s. These factors are intended for use in diaphragm design when rational lateral demands representative of real earthquake events have been calculated, for instance in accordance with NEHRP's 2015 Seismic Provisions, *Section 12.10.3 - Alternative Provisions for Diaphragms Including Chords and Collectors* (NEHRP, 2015). The diaphragm design force reduction factor derivation used in this research largely follows the procedure established in Applied Technology Council 19 (ATC-19), an accepted method utilizing force displacement response of structural systems to develop seismic performance factors (Applied Technology Council, 1995). A FEMA P695 analysis for steel deck diaphragms in steel framed buildings does not provide a method for calculating *R* factors based solely on test data, and is therefore outside the scope of this work. This type of study will be performed by others. This research does not aim to comment on the accuracy or reliability of the different methods for calculating *R* factors, neither does it endorse one method over another. Please see Section 2.1 for more details on these different methods.

4.1 Applied Technology Council - 19 Approach

ATC-19 calculates R_s as the product of four variables (Eq. 4.1) defined by a system's load – deformation response (Applied Technology Council, 1995). Note that the symbols denoting each variable may have been changed to stay consistent with this text.

$$R_s = R_\Omega R_\mu R_R R_\xi \quad \text{(Eq. 4.1)}$$

$$R_\Omega = Strength\ Factor$$

$$R_\mu = Ductility\ Factor$$

$R_R = Redundancy\ Factor$

$R_\xi = Damping\ factor$

The redundancy factor, R_R is accounted for in seismic design through ASCE 7-10's redundancy factor, ρ (ASCE, 2010). The damping factor, R_ξ, accounts for a building's viscous damping devices and is not applicable to the development of R_s factors for the experimental subassembly tests examined in this research. Thus, the resulting force modification factor is the product of the strength and ductility factors (Eq. 4.2):

$$R_s = R_\Omega R_\mu \quad \text{(Eq. 4.2)}$$

$$R_\Omega = \frac{S_{max}}{S_d} \quad \text{(Eq. 4.3)}$$

The strength factor, R_Ω, is a measure of maximum tested strength, S_{max}, to calculated design strength using nominal geometric and material properties, S_d (Eq. 4.3). The ductility factor, R_μ, is dependent on the system ductility, μ, and period, T, of the system. The ductility for a system is defined as an ultimate deformation, Δ_{ult}, divided by the yield deformation, Δ_y, (Eq. 4.6). Newmark and Rosenbleuth (1971) performed time history analyses on elastic perfectly plastic and elastic systems and established the following "equal energy" and "equal displacements" rules. These rules allowed for the development of ductility factors in relation to building period and ductility (Figure 4-1b) and are used in ATC - 19.

1. Equal displacements rule - R_μ for long period structures (T > 1.0 sec) is equivalent to the ductility of that system

   $R_\mu = \mu\ for\ T > 1.0\,\text{sec}\ \ (long\ period)$ (Eq. 4.4)

2. Equal energy rule - R_μ for medium period structures (0.12 sec < T < 0.5 sec) is a square root function of the ductility

$$R_\mu = \sqrt{2\mu - 1} \; for \; 0.12\,\text{sec} < T < 0.5\,\text{sec} \; (medium\; period) \qquad \text{(Eq. 4.5)}$$

3. R_μ for short period structures (T < 0.03 sec) is equal to 1.0 (this is not used in the ATC-19 methodology and is included only for completeness)

$$\mu = \frac{\Delta_{ult}}{\Delta_y} \qquad \text{(Eq. 4.6)}$$

Figure 4-1 graphically demonstrates ATC-19's method to develop factors necessary for R_s calculations. Strength and deformation parameters in relation to steel deck diaphragms used in R_Ω and R_μ calculations are further defined in Sections 4.2 and 4.3.

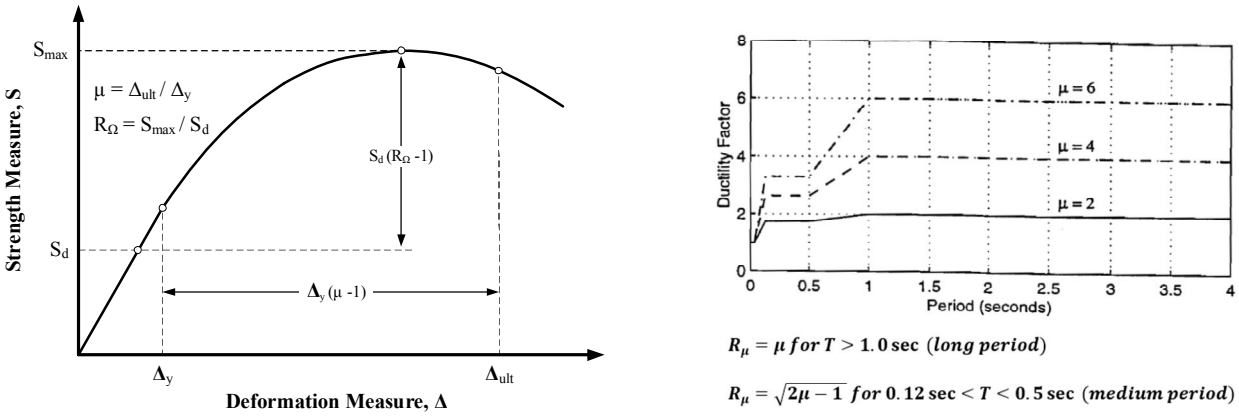

a.) LFRS Experimental Load-Deformation Response

b.) R_μ , T, μ Relationship from ATC (1995)

Figure 4-1 ATC-19 Methodology for R_μ and R_Ω Factors

4.2 Diaphragm Strength Factor, R_Ω

To calculate the strength factor, R_Ω, for the 95 experimental test specimens with relevant post peak-strength data available, a design strength must be calculated. The method used to calculate the predicted design strength for these 95 specimens conforms to the widely accepted design procedure set in SDI's Diaphragm Design Manual 4th edition, or DDM04 (Luttrell et al.,

2015) and AISI's North American Standard for the Design of Profiled Steel Diaphragm Panels, or AISI S310 (AISI, 2016b). The procedure for calculating the design strength of these tested specimens depends on whether or not concrete fill is placed on top of the steel deck, among other factors. The design process used in DDM04 and AISI S310 for steel deck diaphragms both with and without concrete fill is outlined in the Chapter 5. A proposed equation for predicting the shear strengths of steel deck diaphragms with concrete fill is also discussed in the following chapter and used in calculating the strength factor where applicable. Furthermore, strength factor calculations with and without resistance factors for predicted design strengths are included in the results of this study.

4.3 Ductility Factor, R_μ

The ductility factor, R_μ, in (Eq. 4.2), is dependent on a diaphragm system's ductility, μ, which is a measure of an ultimate deformation to a yield deformation (Eq. 4.6). A diaphragm, when idealized as a simply supported deep beam subject to uniform shear along its span, will have a ductility equivalent to the ratio of midspan ultimate to yield displacements, as later defined by this research. The data used in this research derives from past subassemblage cantilevered test specimens with shear demands that are not representative of full diaphragm systems undergoing seismic loading. A methodology is presented to derive full diaphragm system ductility from cantilevered diaphragm ductility in Section 4.3.2. The relevant experimental parameters from the subassemblage cantilever tests necessary for R_μ calculations is discussed in Section 4.3.1.

4.3.1 Subassemblage Ductility, μ_{sub}

The test specimens used in calculating diaphragm design force reduction factors were all tested in a cantilever test configuration. The load-deformation parameters of cantilevered subassemblage tests are shown in Figure 4-2. The demands for these diaphragms were introduced as point loads at the diaphragm's free end, creating uniform shear throughout the entire diaphragm span. This loading condition results in a uniform shear angle, assuming negligible flexural deformations from the chords. The shear angle, γ, gives the slope of the deflected shape and is defined as the diaphragm's displacement, δ, at the free end divided by the span of the diaphragm, a. Shear angle calculations assume small angles. The unit strength of the diaphragm is the applied load, P, divided by the diaphragm depth dimension, b, with the maximum strength, S_{max}, corresponding to the maximum applied load. Experimental shear stiffness, G', is defined as the secant stiffness through the first load-deformation data point at 40% S_{max}. The yield shear angle, γ_y, is then defined as S_{max} / G'. The subassemblage ductility, μ_{sub}, is the ratio between the ultimate shear angle, γ_{ult}, defined as the shear angle when the specimen strength degrades to 80% of S_{max}, to the yield shear angle. FEMA P695 describes non-linear static analysis procedures where a

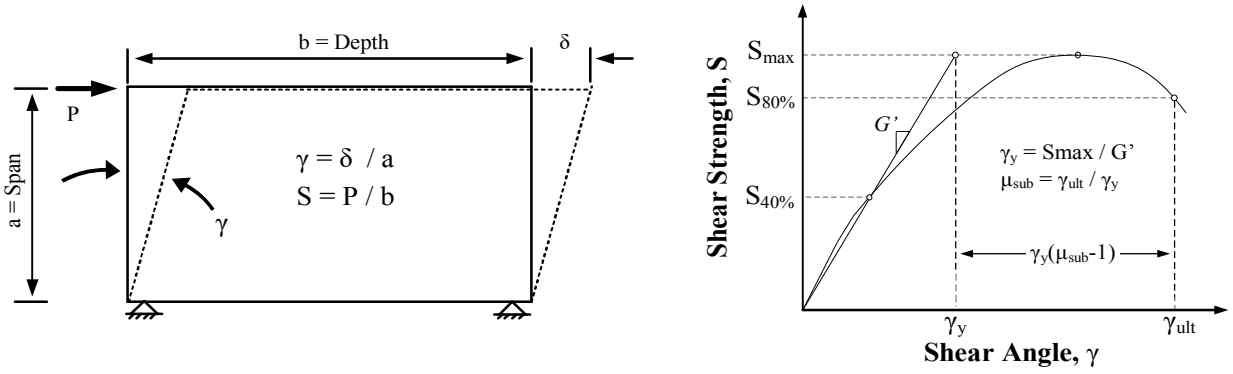

a.) Subassemblage Test Schematic

b.) Load-deformation data

Figure 4-2 Cantilever Test Shear Strength and Shear Angle

system's ultimate deformation is defined at 20% strength loss from ultimate strength (FEMA, 2009), consistent with the definition for γ_{ult} defined in this work. This ultimate deformation value is considered a conservative estimate of the ultimate deformation capacity (FEMA, 2009).

4.3.2 Converting Subassemblage Ductility to System Level Diaphragm Ductility

Diaphragms subject to seismic loading, as idealized by a uniformly distributed load along the span of a diaphragm, will have greatest shear demands at its ends. As a result, inelastic deformations tend to localize at diaphragm ends (Tremblay et al., 2004). Cantilevered subassemblage diaphragms as discussed in Section 4.3.1 are assumed to have a constant shear angle with inelastic behavior spread throughout the entire specimen. Subassemblage ductility values, μ_{sub}, are therefore not indicative of full-scale diaphragm system ductility, μ. Figure 4-3 illustrates the inconsistencies in shear demands between a cantilevered diaphragm and simply supported diaphragm. Diaphragm system ductility is defined in this research as the ratio of midspan ultimate to yield displacements. The process used and assumptions made to arrive at these two displacement steps are described in this section.

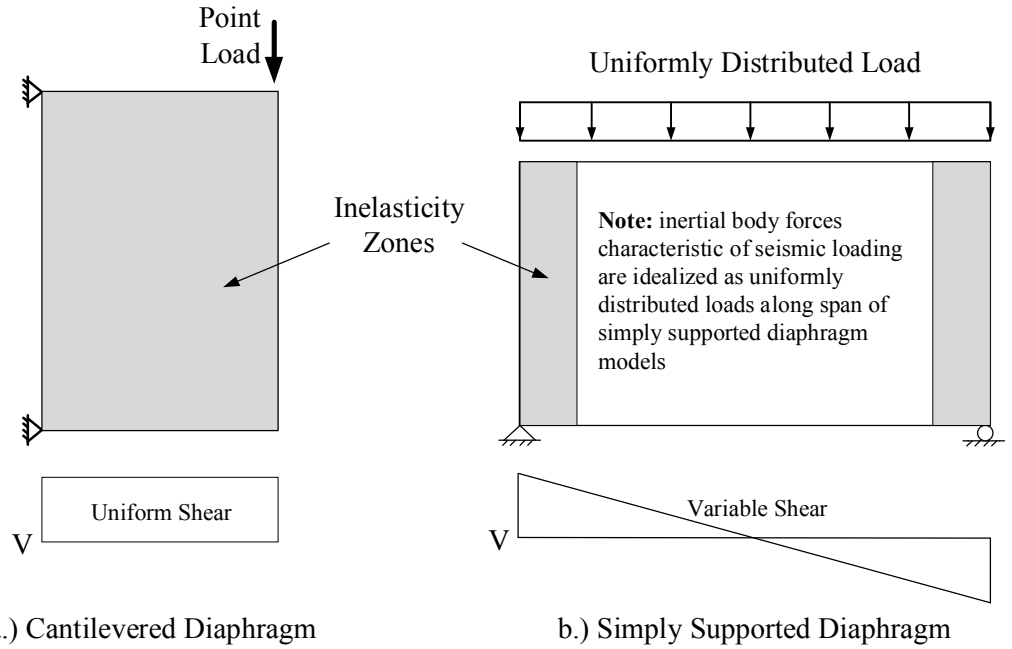

Figure 4-3 Cantilevered vs. Simply Supported Diaphragm Inelasticity

To get the elastic midspan deflection of a diaphragm, δ_{el}, shear and strength expressions along a diaphragms span are necessary (Eq. 4.8). Figure 4-4 shows a simply supported diaphragm's deflected shape due to either elastic or inelastic deformations. Noting the relationship between strength, shear stiffness, and shear angle, and acknowledging that shear angle is the slope of a diaphragm's deflected shape (Figure 4-4), an integral expression is derived to calculate elastic diaphragm displacement along a diaphragm's length (Eq. 4.9). An expression for midspan yield displacement is shown in (Eq. 4.10).This expression, however, has not yet identified the shear load, q, associated with the diaphragm shear strength. From the subassemblage cantilever tests, we are able to correlate the yield shear angle and maximum strength through the diaphragm shear stiffness, G' (see Figure 4-2). S_{max} is therefore used to define the yield shear load, q (Eq. 4.11). Combining (Eq. 4.10) and (Eq. 4.11) gives an expression for elastic displacement at a simply supported diaphragm's midspan (Eq. 4.12) for a given length, L.

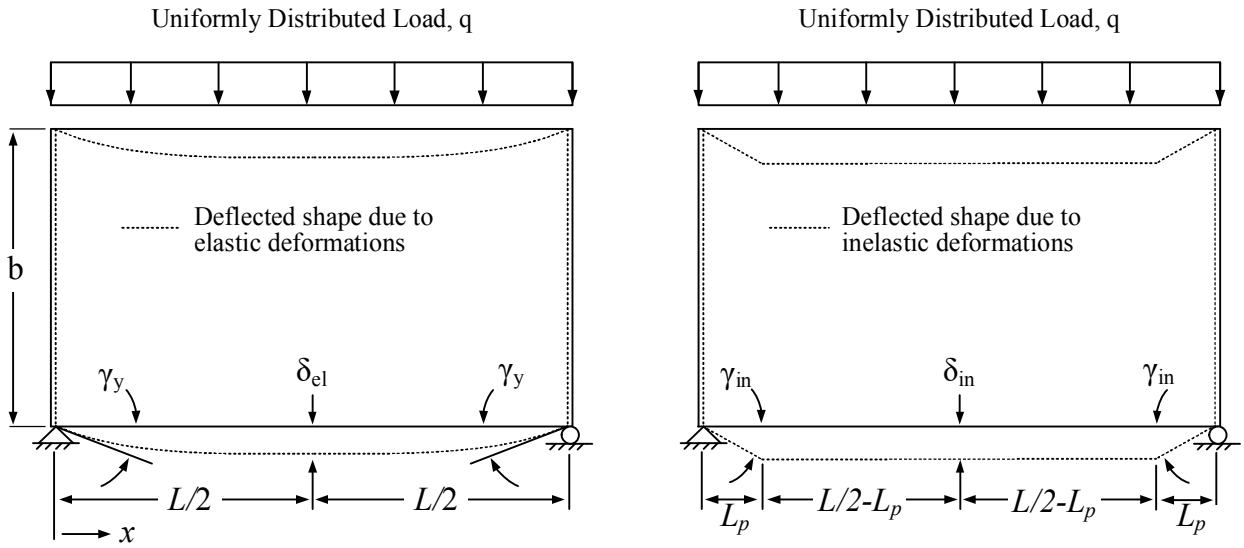

Figure 4-4 Diaphragm System Deflections

$$V_x = \frac{qL}{2} - qx \qquad \text{(Eq. 4.7)}$$

$$S_x = \frac{V_x}{b} = \frac{q}{b}\left(\frac{L}{2} - x\right) \qquad \text{(Eq. 4.8)}$$

$$\delta = \int_{x_1}^{x_2} \gamma_x dx = \int_{x_1}^{x_2} \frac{S_x}{G'} dx \qquad \text{(Eq. 4.9)}$$

$$\delta_{el} = \int_0^{L/2} \frac{q}{G'b}\left(\frac{L}{2} - x\right) dx = \frac{qL^2}{8G'b} \qquad \text{(Eq. 4.10)}$$

$$S_{max} = \frac{qL/2}{b} \rightarrow q = \frac{2S_{max}b}{L} \qquad \text{(Eq. 4.11)}$$

$$\delta_{el} = \frac{S_{max}L}{4G'} = \frac{\gamma_y L}{4} \qquad \text{(Eq. 4.12)}$$

To calculate inelastic midspan deflections of a diaphragm, δ_{in}, a constant inelastic shear angle, γ_{in}, is assumed over a fixed length, L_p, at diaphragm ends. The inelastic shear angle, as obtained from subassemblage tests, is the difference between the ultimate shear angle at 80% strength degradation, γ_{ult}, and the yield shear angle. The total inelastic deflection is the product of the length of this zone of inelasticity, L_p, and the inelastic shear angle, γ_{in} (Eq. 4.14). A notable assumption is that the inelastic shear angle is presumed constant along L_p, regardless of cantilever test specimen size. Also note that the inelastic shear angle is solely dependent on subassemblage cantilever test data, and assumed to be independent of the simply supported diaphragm's span, L.

$$\gamma_{in} = \gamma_y(\mu_{sub} - 1) \quad \text{from cantilevered tests, see Figure 4-2} \tag{Eq. 4.13}$$

$$\delta_{in} = \gamma_{in} L_p \tag{Eq. 4.14}$$

Expressions for the ultimate mid span displacement and diaphragm system ductility are given in Eq. 4.15 and 4.16, respectively. The ductility of a simply supported diaphragm includes variables γ_y and γ_{in} which are available from cantilever test data (Eq. 4.16). The ratio, L_p / L, will be explored in the following paragraphs.

$$\delta_{ult} = \delta_{el} + \delta_{in} = \frac{\gamma_y L}{4} + \gamma_{in} L_p \tag{Eq. 4.15}$$

$$\mu = \frac{\delta_{ult}}{\delta_{el}} = 1 + \frac{4\gamma_{in}}{\gamma_y}\left(\frac{L_p}{L}\right) \tag{Eq. 4.16}$$

Because the cantilevered test setup for diaphragm testing has been prevalent in past experimental research where inelastic behavior spreads throughout the diaphragm span, limited experimental data on the distribution of inelastic deformations for a simply supported diaphragm exists. Often, diaphragms that were tested in a simply supported setup introduced lateral loads at third points along the diaphragm span rather than having a uniformly distributed load, giving shear

demands not representative of seismic demands. This makes the determination of the L_p / L ratio directly from experimental data difficult to assess.

One such data point that is available comes from Franquet (2009). Franquet tested 22 gauge 1.5 B deck diaphragms without concrete fill using mechanical fasteners (PAF structural fasteners and screwed sidelap fasteners) with added mass subjected to dynamic loads, as described in Chapter 2. The added mass, when subjected to accelerations from ground displacements from actuators at diaphragm ends (see Figure 4-6), induced inertial forces on the diaphragm. These forces provided a distributed load along the diaphragm span representative of seismic loading. The span, L, was 69 ft. Fasteners that failed, as determined through post-test visual inspection, were reported to concentrate at extreme thirds of the diaphragm span. However, the distribution of failed fasteners along a diaphragm span was dependent on the type of fastener inspected. Sidelap fasteners proved to consistently fail with approximate $L_p = L/3$. The distribution of failed structural fasteners, however, varied dependent on fastener spacing. Fastener spacings are shown in Figure 4-5. Figure 4-6 shows the distribution of failed fasteners along a joist line for diaphragms 1 (top left), 4 (top right) and 5 (bottom), which had different fastener spacings. Joist lines are perpendicular to the diaphragm span with 12 equal spacings of 5.75 ft. It is observed for the heavier fastener patterns (36/9 and 36/7), the majority of failed structural fasteners accumulate within joist lines 0, 1, 11, and 12, where L_p = 11.5 ft or L / 6. For the light fastener pattern (36/4), this distribution is approximately L / 3 for both structural and sidelap fasteners.

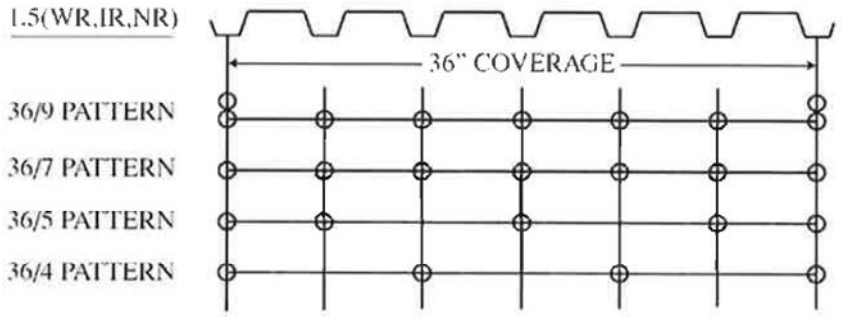

Figure 4-5 Fastener Spacing Patterns [from Luttrell et al. (2015)]

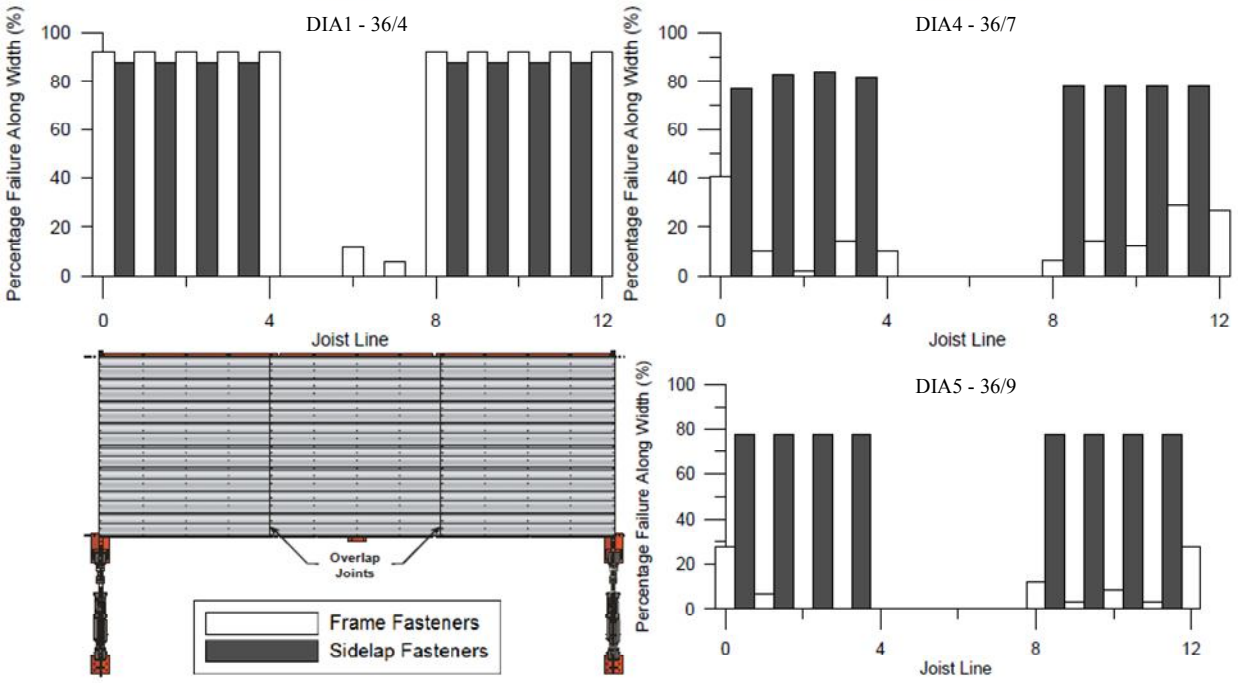

Figure 4-6 Distribution of Failed Fasteners along Diaphragm Span [from Franquet (2009)]

To investigate the effects of deck orientation on roof diaphragm inelastic behavior, 9 specimens were dynamically tested, similar to Franquet (2009) and on the same test frame as previously shown in Figure 4-6 (Massarelli, 2010; Massarelli et al., 2012). Massarelli (2010) reports locations of fasteners failing for each specimen. Figure 4-7 gives the percentage of fasteners that experienced failure along the depth of the diaphragm with respect to the diaphragm

span. All specimens shown in Figure 4-7 used PAF structural fasteners and sidelap screws as connectors for typical 1.5 B deck. DIA 12 and DIA 16 used a 36/7 structural fastener spacing configuration, while DIA 14 and DIA 17 used 36/9 (see Figure 4-5). The most notable effect on the distribution of fasteners failing along a diaphragm span (i.e. L_p / L) was the direction of deck. DIA 12 and DIA 14 had the steel deck oriented perpendicular to the loading, and resulted in lower ductility and a shorter percentage of diaphragm span ends exhibiting damage. In contrasts, DIA 16 and DIA 17, which had deck oriented parallel to loading, experienced higher ductility and percentage of fasteners failing. Damage at diaphragm ends were not symmetric and, with the exception of DIA 12 which was symmetric, the left end consistently experienced more damage than the right end. This may have been the result of torsion, added mass dislodging during the induced ground motions, and more. The majority of damage reported was consistently within 10% and 20% of the diaphragm span at diaphragm ends, giving valuable insight for L_p / L ratios.

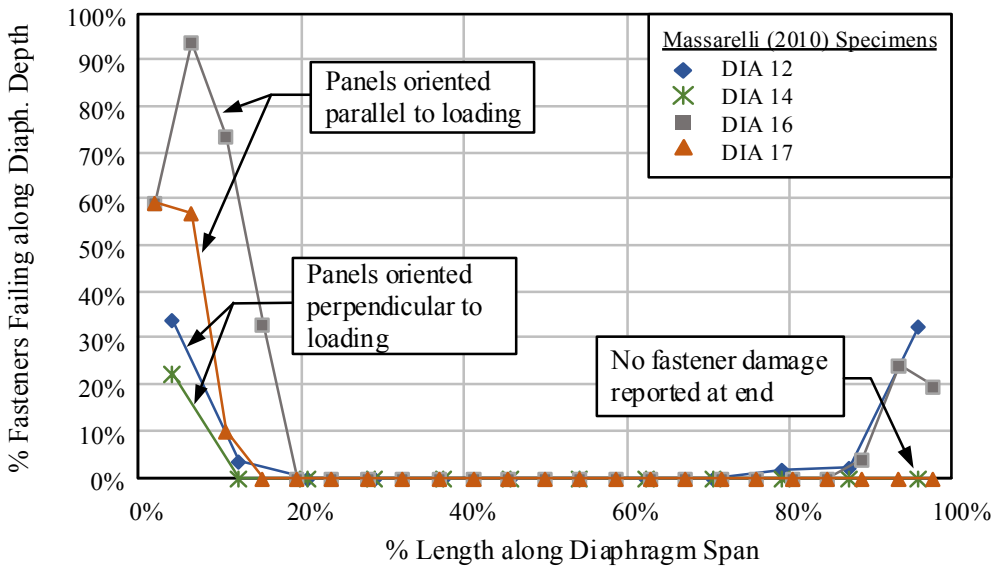

Figure 4-7 Distribution of Failed Fasteners along Diaphragm Span [adapted from Massarelli (2010)]

Cohen et al. (2004) conducted shake table tests on two half-scale low rise reinforced masonry buildings, only one of which included steel deck attached to steel supports. Tests were conducted on the Tri-axial Earthquake and Shock Simulator (TESS) at the United States Army Construction Engineering Research Laboratory in Champaign, Illinois. No mass was added to the system due to cost inefficiencies. Instead, the large accelerations from TESS were assumed to induce damage to the specimens similar to what they would withstand if mass were added. The diaphragm was 22 ft in length and 4 ft in depth. A combination of a 12 in. wide and 36 in. wide Vulcraft 1.5 B deck was used to cover the 4 ft dimension, as shown in Figure 4-8. Welded structural fasteners were used in a 36/3 fastener configuration for the 36 in. wide panel (i.e. 18 in. fastener spacing o.c.). The progression of weld fractures with respect to increasing diaphragm drift ratios (DDR) and their location is reported in Figure 4-8. The diaphragm drift ratio is the in-plane diaphragm displacement divided by midspan length. Similar to Franquet (2009) and Massarelli (2010), it is observed that the majority of damage observed occurred in the outermost quarters of the diaphragm span. Note that a diaphragm drift ratio of approximately 1% corresponds to the ultimate induced force on the diaphragm. Therefore, damage reported for DDR = 1.52% and 2.27% as shown in Figure 4-8 correspond to post-peak deformations.

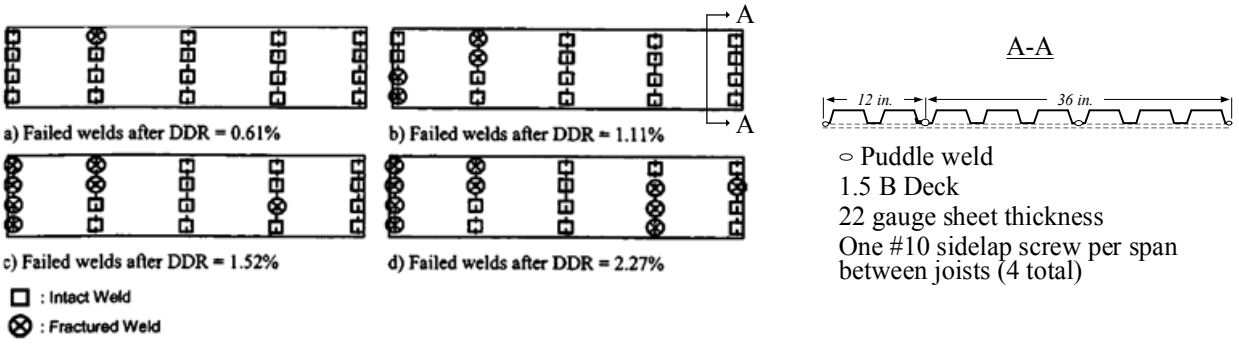

Figure 4-8 Distribution of Failed Fasteners along Diaphragm Span [adapted from Cohen et al. (2004)]

A limitation of using this observed data for determining L_p / L ratios is that the L_p used for the inelastic midspan displacement equation (Eq. 4.14) corresponds to deformations at a post-peak strength degradation of 80% of the ultimate diaphragm strength. However, the damage distribution L_p from Franquet (2009) and Massarelli (2010) is observed after the tests are concluded, where deformations likely exceeded this post-peak limit, resulting in a higher observed L_p. Cohen et al. (2004) addresses this concern by reporting damage with respect to increasing diaphragm displacements.

Due to the limited data for this type of test available in the literature, another method for determining L_p from cantilever test data is described below. The available strength vs. shear angle relationship of a cantilevered diaphragm test is idealized as bilinear (see Figure 4-9). The first line will follow G' up to an approximated yield point at a force equal to αS_{max}. The second line continues from this point to the intersection of γ_u and S_{max}. Variables γ_u, S_{max} and G' are all defined in the previous Section 4.3.1. This bilinear curve is then used to find L_p / L for a simply supported diaphragm model as shown in Figure 4-10 and (Eq. 4.17).

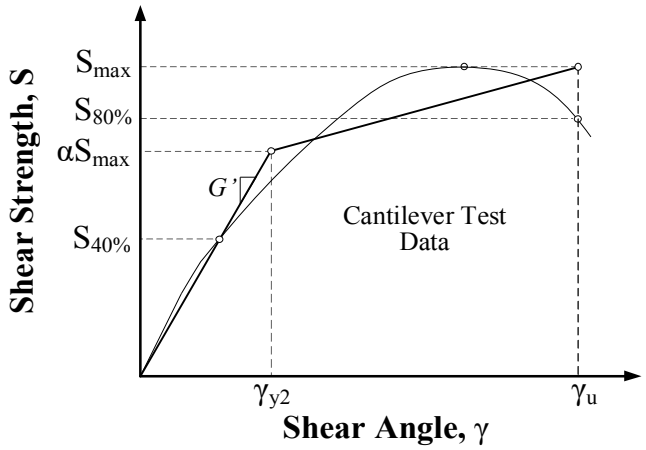

Figure 4-9 Bilinear Curve Approximation of Cantilever Test Data

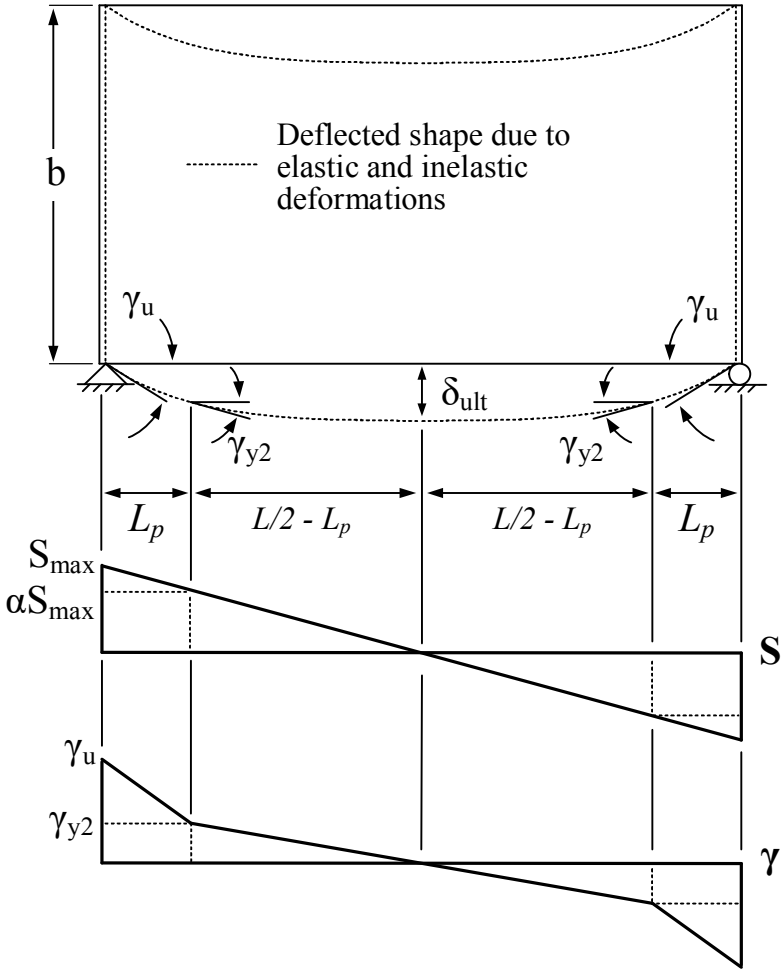

Figure 4-10 Simply Supported Diaphragm Model using Approximated Bilinear Curve

Based on equivalent triangles for the strength distribution along the diaphragm span shown in Figure 4-10, an expression is derived for the L_p / L ratio as given in (Eq. 4.17).

$$\frac{S_{max}}{L/2} = \frac{\alpha S_{max}}{L/2 - L_p} \rightarrow \frac{L_p}{L} = \frac{1-\alpha}{2} \quad \text{(Eq. 4.17)}$$

The approximation of α allows for a direct calculation of the L_p / L ratio, as shown in the derivation above. Using lower values for α will give larger L_p / L ratios and subsequently higher diaphragm ductilities: α = 0.7 gives L_p / L = 0.15; α = 0.9 gives L_p / L = 0.05. The experimental cantilever test data for all 108 specimens with post peak data were reviewed and an approximated, upper bound, and thus conservative α = 0.85 and α = 0.75 for steel deck diaphragms with and without concrete fill, respectively, was deemed most appropriate. The corresponding value of L_p / L is 0.10. Calibration techniques for αS_{max} are offered as future work in Chapter 7.

It is also worth noting that diaphragms designed in practice can include zones with variables fastener spacing along diaphragm spans, meaning lighter fastener spacing configurations can be used towards the diaphragm midspan, where the shear demand is less, and heavier spacing configurations can be used towards diaphragm ends, where shear demand is greatest. This can cause increased inelastic deformation distributions along the diaphragm span giving a larger L_p and diaphragm ductility. Fastener spacings for this model are conservatively assumed constant along the diaphragm span.

All variables for the system ductility calculation are now defined (Eq. 4.16), and diaphragm system ductility, μ, and period dependent ductility factors, R_μ, using (Eq. 4.4) and (Eq. 4.5), are calculated for each of the 95 specimens. These values are made available in Chapter 6.

4.4 Summary

A method for calculating diaphragm design force reduction factors, R_s, using the ATC-19 method was described in this chapter. Equation 4.2 gives R_s as the product of a strength factor, R_Ω, and a ductility factor, R_μ. The strength factor, R_Ω, is calculated as the maximum experimental strength divided by a calculated design strength (Eq. 4.3). DDM04 and AISI S310 give design procedures used for the calculation of diaphragm design strength.

A method to convert subassemblage ductility, μ_{sub}, available from past cantilever tests, to system ductility, μ, for simply supported diaphragm models is described in Section 4.3.2. An equation for diaphragm system ductility was derived and is given in (Eq. 4.16). Diaphragm system ductility was shown to be dependent on variables defined from cantilever testing and the ratio of the length of inelastic deformation distributions, L_p, to diaphragm span, L (see Figure 4-4). Considering both past experimental research (Cohen et al. 2004, Franquet 2009, Massarelli 2010) and a bilinear approximation method, L_p / L was determined to be 10% for steel deck diaphragms with and without concrete fill. Thus, equations for system ductility, ductility factors (Eqs. 4.5 and 4.6), and subsequently diaphragm design force reduction factors (Eq. 4.2) are completely defined. Chapter 6 reports these values for the 95 specimens identified with inelastic post-peak load-deformation data available.

5 DIAPHRAGM STRENGTH AND STIFFNESS PREDICTIONS

Strength prediction equations available in DDM04 and AISI S310 necessary for the calculation of strength factors and subsequently diaphragm design force reduction factors are described in this chapter. A strength prediction equation for steel deck diaphragms with concrete fill, as proposed by Porter and Easterling (1988), is described in this chapter and recommended for future use. An alternative stiffness equation to the current DDM04 equation for steel deck diaphragms with concrete fill is also proposed. The DDM04 and proposed equations are compared to experimental results from an extensive experimental research program executed in the 1970s and 1980s at Iowa State University, as discussed in Section 2.3.4. Diaphragm design resistance and safety factors are also presented in this chapter. Although stiffness prediction equations are not necessary for the calculation of R_s factors, they are included in this chapter nonetheless for completeness.

5.1 Steel Deck Diaphragms without Concrete Fill – Shear Strength

DDM04 identifies four limit states for steel deck diaphragms without concrete fill subject to in-plane shear loads: edge fastener limit, interior panel fastener limit, corner fastener limit, and stability limit. The first three of these limit states are controlled by either the deck bearing against the fastener (e.g. yielding or slotting) or fastener failure (e.g. shear rupture or pull out). The less common fourth limit state (stability limit) applies when plate-like shear buckling behavior occurs. The minimum of these limit states is taken as a diaphragm's nominal shear strength, expressed in force/unit length. Note that shear strength limit expressions in DDM04 are identical to those found in AISI S310-13, despite slightly different notation. These limit states and nominal fastener capacities are discussed in this section.

5.1.1 Shear Strength Limit States

The *edge fastener limit state* described in DDM04 refers to the steel deck diaphragm edge panels, that is, the panel parallel and adjacent to a diaphragm's perimeter framing members along the span (i.e. length) of the steel deck panel. Edge panels will have structural fasteners along its length on one edge of the panel and sidelap fasteners along its other edge. Structural fasteners are also used at the ends of the panel. By taking a section of the edge most half of the edge panel, a statics-based expression for nominal edge panel diaphragm strength per unit length dependent on fastener strength and location, S_{ne}, is derived as shown in Figure 5-1.

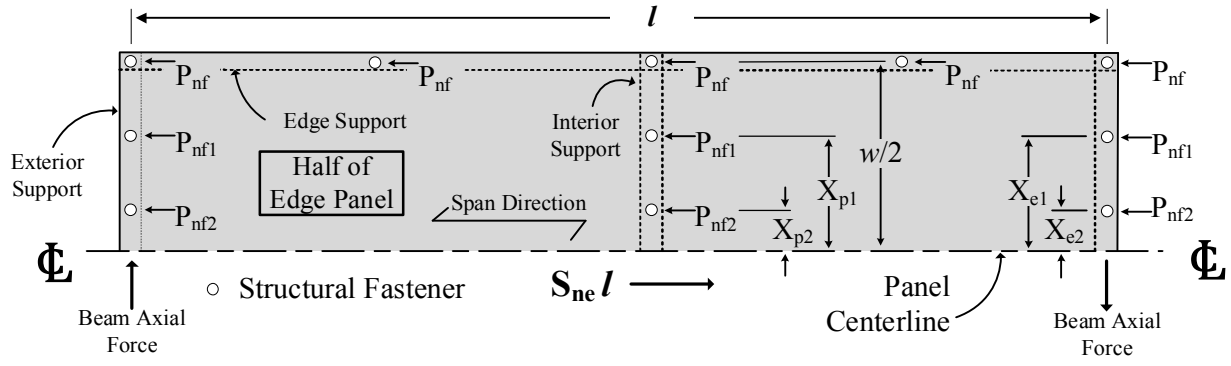

Figure 5-1 Edge Panel Limit State Forces

$$S_{ne} = (2\alpha_1 + n_p\alpha_2 + n_e)\frac{P_{nf}}{l} \qquad \text{(Eq. 5.1)}$$

$\alpha_1 = \frac{\sum x_e}{w}$, summation across entire panel width

x_e = distance from structural fastener at exterior support to panel centerline

w = panel width

n_p = number of interior supports between panel ends

$\alpha_2 = \frac{\Sigma x_p}{w}$, summation across entire panel width

x_p = distance from structural fastener at interior supports to panel centerline

n_e = number of structural fasteners along panel edge not into interior or exterior supports

P_{nf} = structural fastener shear strength

l = panel length (parallel to panel span between adjacent exterior supports)

Brittle behavior is assumed for diaphragm strength equations and the strength contribution in the fasteners towards the panel centerline is scaled down proportional to the distance between the fastener and the panel centerline (i.e. $P_{nfl} = P_{nf}[X_{e1}/(w/2)]$ in Figure 5-1). DDM04 and AISI S310 does however acknowledge that the progression of yielding for a panel in shear, assuming adequate ductility, can allow for fasteners towards the panel width centerline to approach their full capacity, P_{nf}. Distribution scale factors, α_1 and α_2, apply the scaled force assumption to the structural fasteners along interior and exterior supports, respectively.

The *interior panel fastener limit state*, expressed as a nominal shear strength per unit length, S_{ni}, considers the nominal shear strength of an interior panel or edge panel controlled by sidelap fastener nominal strengths. Figure 5-2 shows a free body diagram of an interior panel subjected to shear forces. For the edge panel to control over the interior panel, the structural fasteners at a panel's longitudinal edge must have a total shear strength capacity less than that of the sidelap fasteners. Because this condition rarely controls and is not indicative of common construction practice, this limit state will be examined within the context of interior panels, and not edge panels. By taking rotational equilibrium about the panel centerline, (Eq. 5.2) is derived.

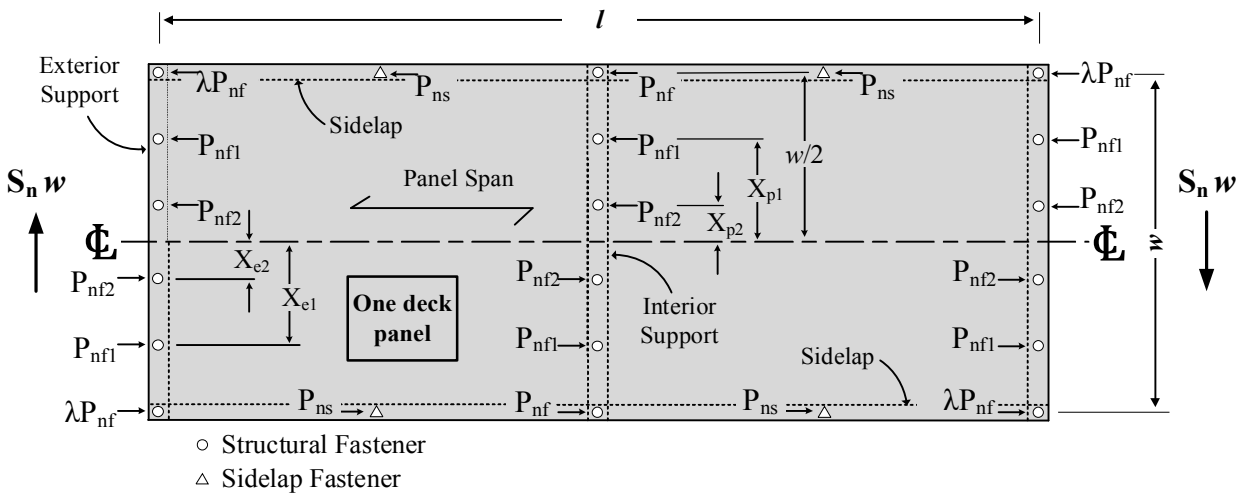

Figure 5-2 Interior Panel Limit State Forces

$$S_{ni} = \beta \frac{P_{nf}}{l} \qquad \text{(Eq. 5.2)}$$

$$\beta = n_s \alpha_s + 2 n_p {\alpha_2}^2 + 4 {\alpha_1}^2$$

n_s = number of sidelap connections along panel span not into interior or exterior supports along one edge of panel for length of panel, l

$$\alpha_s = \frac{P_{ns}}{P_{nf}}$$

P_{ns} = sidelap connection shear strength

The term β, is a factor that considers a total number of equivalent structural fasteners that are effectively resisting shear force. Because of the tendency for a steel deck to locally buckle at the panel's corner fasteners, a corner fastener strength reduction factor, λ, is applied as shown in Figure 5-2. A further developed interior panel fastener shear strength per unit length expression is then available:

$$S_{ni} = [2A(\lambda - 1) + \beta] \frac{P_{nf}}{l} \qquad \textit{(Eq. 5.3)}$$

$A =$ number of fasteners in a single corrugation at a panel's edge and into an exterior support

$\lambda = 1 - \frac{D_d L_v}{240\sqrt{t}} \geq 0.7$

$D_d =$ panel depth, in., see Figure 5-3

$L_v =$ deck panel span between supports, ft. ($L_v = l$ for spans with no interior supports)

$t =$ deck thickness, in.

The *corner fastener limit state* considers shear forces in two, orthogonal directions at the edge of an interior or edge panel at the panel's end. Note that the corner fastener strength reduction factor used in the interior panel fastener limit state addresses local buckling dependent on deck geometries, and is separate from this corner fastener limit state. Instead, this limit state develops an expression for the resultant force of a corner fastener undergoing shear load in two directions, and allows for that resultant force to approach the corner fastener's nominal strength. The resulting expression yields (Eq. 5.4).

$$S_{nc} = P_{nf}\sqrt{\frac{N^2\beta^2}{l^2N^2 + \beta^2}} \quad \text{(Eq. 5.4)}$$

$N =$ number of structural fasteners per unit width at a panel's end

A *stability limit* defines the maximum shear strength a panel can obtain before undergoing out of plane, flat plate-like shear buckling. This behavior mostly occurs when a panel with long spans, L_v, shallow depth, D_d, and deck thickness, t, of gauges 26 and higher, using closely spaced fasteners are used (Luttrell et al., 2015). Since this behavior only occurs for such specific conditions atypical to most diaphragm construction, the stability limit generally represents an upper bound steel deck strength capacity that rarely governs.

$$S_{nb} = \frac{7890}{{L_v}^2}\left(\frac{I^3 t^3 d}{s}\right)^{0.25} \text{, kip/ft} \qquad \text{(Eq. 5.5)}$$

L_v , t as previously defined, ft.

I = panel moment of inertia per unit width, in.^{4}/ft.

d = panel corrugation pitch, in. (see Figure 5-3)

s = panel corrugation developed width, in. (see Figure 5-3)

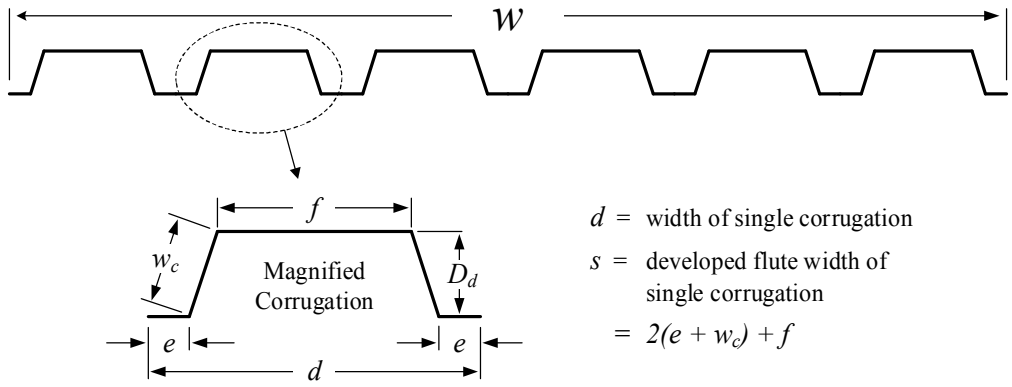

Figure 5-3 Panel Profile with Corrugation Dimensions

It is worth noting that the condition of overlapping panels at panel ends (i.e. endlap), is not considered in these limit states. No distinction is made in DDM04 between fasteners going through multiple sheets at exterior supports due to endlaps. Instead, a negligible difference between nominal structural fastener capacity with or without the endlap condition is assumed for diaphragm strength calculations.

5.1.2 Fastener Shear Strengths

AISI S310 provides several equations for nominal fastener strengths for many different types of structural and sidelap fasteners and also includes a provision that allows for empirical expressions developed from significant testing to govern fastener strength predictions. As such, DDM04 offers several alternative equations to AISI S310's fastener strength equations. Since SDI's several editions of Diaphragm Design Manuals have been widely adopted and used prior to the development of AISI S310, and because DDM04 conforms to AISI S310 (AISI, 2013b), a judgment was made to utilize the alternative fastener strength equations in DDM04 where available for diaphragm strength predictions used herein for R_s analyses. This section provides fastener strength equations for the major types of structural fasteners (weld, weld with washer and power actuated fastener) and sidelap fasteners (weld, screw, and button punch) used in the calculation of predicted diaphragm strengths for the 95 diaphragm specimens of interest with post peak behavior.

Arc spot welds as structural fasteners can be limited by the strength of either the sheet or the deck. AISI S310 offers equations for the several different conditions that may control nominal fastener strength for arc spot welds. The weld strength will not govern for welds with visible nominal diameters of less than half an inch (assuming 60 ksi electrode strength classification), or with sheet thicknesses outside of 24 guage to 16 gauge. Instead, sheet failure will govern. This condition applies to the vast majority of welds used in steel deck diaphragms and all of the welds included in diaphragm design within this research. The resulting governing equation for nominal weld shear strength is (Eq. 5.6):

Structural fastener - arc spot weld:

$$P_{nf} = 2.2tF_u(d - t) \quad \text{(Eq. 5.6)}$$

$t =$ base metal thickness (2*sheet thickness for overlapped sheets)

$d =$ visisble diameter of weld

$F_u =$ tensile strength of sheet

Welds with washers can be used as structural fasteners, especially when burning through thinner sheets without properly attaching the deck to the steel support is of concern. AISI S310 specifies welds with washers to not be permitted as sidelap faster type. Nominal strength predictions for welds with washers as structural fasteners is presented below.

Structural fastener – weld with washer:

$$P_{nf} = 99t(1.33d_0 + 0.3F_{xx}t) \quad \text{(Eq. 5.7)}$$

$t =$ base metal thickness (2*sheet thickness for overlapped sheets), in.

$d_0 =$ washer inner hole diameter, in.

$F_{xx} =$ weld tensile strength electrode classification, ksi

Power actuated fasteners offer several considerable construction and performance benefits in comparisons to welds, as described in Section 3.2 and are only used as structural fasteners. Because PAF strengths are dependent on the manufacturer's fastener designs, there exists a multitude of nominal PAF shear strength equations as outlined in DDM04. The most common PAF types used in diaphragm design for this research were the Hilti X-EDNK-22 and Hilti X-ENP-19 L15 fasteners. The empirical expressions for these fasteners are (Eq. 5.8) and (Eq. 5.9), respectively, with thickness *t* in in.

Structural fasteners – PAF:

For support steel thickness between 1/8 in. and 3/8 in:

$$P_{nf} = 52t(1 - t) \text{ , kip; for Hilti X-EDNK-22 fastener} \quad \text{(Eq. 5.8)}$$

For support thickness > ¼ in. and sheet thickness, *t*, between 0.028 in. and 0.060 in.:

$$P_{nf} = 56t(1 - t) \text{ , kip; for Hilti X-ENP-19 L15 fastener} \quad \text{(Eq. 5.9)}$$

Sidelap screws are often used in conjunction with PAFs. This combination allows for a diaphragm fastener system to be entirely comprised of mechanical fasteners, a desirable construction feature for ease of labor and production speed. Because sidelap screws are often self-drilling, no pre-drilled hole is necessary (this fastener type is often referred to as a self-tapping, self-drilling screw). Softening behavior of sidelap screws occurs as the screw approaches its capacity, and the overlapped sheets begin to separate as the screw starts to tilt. Sheet failure and shear fracture of sidelap screws for thicker sheets is possible. AISI S310 captures these different limits in a series of capacity equations. DDM04 offers a simplified, empirical alternative equation (Eq. 5.10) to AISI S310. While welds may offer higher strength, mechanical fasteners are desirable for ease of construction purposes, and higher confidence in shear capacity. Button punches are possible when panels include an interlocking geometry and are also implemented for their ease of construction, but offer very limited strength as given in (Eq. 5.11). In fact, DDM04 supports the conservative assumption to neglect a button punch's shear strength.

Sidelap fastener – screw:

$P_{ns} = 115dt$, kip (Eq. 5.10)

$d =$ screw diameter, in.

$t =$ base metal thickness of a single sheet, in.

Sidelap connection – button punch:

$P_{nf} = 240t^2$, kip (Eq. 5.11)

$t =$ base metal thickness of a single sheet, in.

5.2 Steel Deck Diaphragms with Concrete Fill – Shear Strength

The information presented in Section 5.1 provided the basis for diaphragm strength design of steel deck diaphragms without concrete fill, typical to roofing systems in steel framed buildings. Limit states and strength prediction equations prescribed by AISI S310 and DDM04 for steel deck diaphragms with concrete fill (SDDCFs), characteristic of floor systems found in steel framed buildings, are described in this section. Current assumptions made in predicting SDDCF shear strength, a proposed alternative design method, and comparisons of predicted strengths to experimental strengths are also discussed here. The experimental strength values are available from the landmark Iowa State University testing program on SDDCFs (Porter and Easterling, 1988).

5.2.1 Shear Strength Limit States

When concrete is placed on top of a steel deck diaphragm, a number of positive influences affect shear strength. Namely, steel deck out of plane deformations are restrained and diaphragm strength capacity dramatically increases due to the concrete's strength contribution, often times by an order of magnitude. For this reason, the stability limit and the corner fastener strength reduction factor, λ, in the interior panel fastener limit state are no longer relevant. Instead, three major failure mechanisms characterizing SDDCF strength are identified: diagonal tension failure, perimeter fastener failure and shear transfer failure (Porter and Easterling, 1988).

Shear transfer failure is the least probable of the three limit states, as a set of unusual construction conditions must apply. Shear transfer failure describes the failure of a SDDCF due to separation of the concrete from steel deck. To create strong composite action, embossments are rolled into the steel deck. Additionally, shear studs are the standard fasteners used in this system,

and allow for a direct load path between the structural frame and concrete, promoting composite behavior at composite beam locations. Aside from these mechanical bonds, the chemical bond between the concrete and deck allows for additional shear transfer strength.

For this failure mode to occur, an unusually large amount of structural fasteners must be used without any shear studs, or other structural fasteners that allow for a direct mechanical connection between steel frame and concrete fill (e.g. standoff screws). This ensures a strong connection between deck and frame, but a weaker connection between deck and concrete. Test setup configurations likely to exhibit this failure mode included specimens with 13 welds/m. Specimens also subjected to gravity loads were less likely to fail in this fashion, due to normal loads imposing additional shear resistance from increased deck-concrete friction (Neilsen, 1984). Although this failure mode was investigated in the ISU program, it does not represent practical construction and is excluded from the limit state equations of a SDDCF further examined in this paper.

Perimeter fastener failure occurs when there is a fracture of structural fasteners that transfer forces between the structural frame and the deck-concrete system. This failure results in relative motion between the steel deck-concrete and the supporting steel beams. Steel deck sidelap connection strength is of little importance since the majority of the shear is transferred through the concrete and the deck-concrete bond prevents slip at sidelaps. The ISU program identifies a diaphragm 'edge zone' over which shear forces are transferred to and from the steel frame (Porter and Easterling, 1988). Structural fasteners to intermediate beams oriented perpendicular to collectors can lie within this edge zone and contribute to the collector's perimeter fastener shear strength. The effects of connector force distributions at SDDCF perimeters are further analyzed in Widjaja (1993). For the ISU program, which did not employ intermediate supports, perimeter

fastener limit shear strength is calculated by summing the total strength of the structural fasteners in both the depth and span dimension of the SDDCF, with the lesser value controlling.

Diagonal tension failure of a SDDCF occurs when the concrete placed on the steel deck behaves as a deep concrete beam and fails through shear cracking. Adequate concrete cover must be be provided to eliminate possible longitudinal cracks. Fire ratings typically govern the minimum depth of the concrete and provide enough concrete cover to alleviate this concern. Failure of the concrete will occur at a 45° angle to the diaphragm edge, initiating a diagonal crack. This behavior is analogous to shear failure of concrete beams. Although steel reinforcement (e.g. welded wire fabric for shrinkage and thermal effects) in the slab may impact shear strength, it is not explicitly considered in strength predictions for SDDCFs.

5.2.2 Current Strength Equation

AISI S310 and DDM04 provide a strength equation for SDDCFs, as shown in (Eq. 5.12). The diaphragm shear strength, S_{n_DDM04}, is the summation of a steel deck connector contribution and concrete fill contribution.

$$S_{n\_DDM04} = \frac{\beta P_{nf}}{L} + \frac{kbd_c\sqrt{f'_c}}{1000} \text{ , kip/ft.} \quad \text{(Eq. 5.12)}$$

β = as previously defined in interior panel fastener limit state (Section 5.1.1)

P_{nf} = shear strength of structural fastener, kip

L = panel length (between exterior supports), ft.

$k = \frac{w^{1.5}}{585}$, concrete strength factor

w = concrete unit weight, pcf

b = unit width, 12 in.

d_c = thickness of concrete slab above top deck corrugation, in.

f'_c = concrete compressive strength, psi

The first term on the right hand side of (Eq. 5.12) represents the strength contribution from the steel deck, as discussed for (Eq. 5.2), and is limited to 25% of the total strength. AISI S310's commentary mentions "a rational limit of 25%" is applied to account for concrete's semi-brittle failure which can limit deck strength contribution and avoid overstating the steel deck contribution of SDDCF strength (AISI, 2013b). The second term gives the concrete's strength contribution above the top flute of the deck. The product of unit width, *b,* and concrete cover, d_c, represents the concrete cross sectional area per unit width subject to shear, with specified concrete compressive strength, f'_c. The structural concrete strength factor, *k*, is dependent on the unit weight of the concrete mix. A second limit is described in DDM04 that ensures acceptable available shear strength from perimeter structural fasteners to develop the full strength, S_{n_DDM04}, as discussed in the perimeter fastener failure mode. AISI S310 includes a user note that if headed shear studs are used, then structural fastener strength, P_{nf}, used in (Eq. 5.12) is to be calculated as an arc spot weld. When checking the second limit of perimeter fastener failure, the shear strength of headed shear studs is to be calculated as prescribed by AISC 360 (AISC, 2010).

5.2.3 Proposed Shear Strength Equation

The method described in Section 5.2.2 uses the same approach to calculate diaphragm strength for SDDCFs as bare deck diaphragms. However, this implies assumptions that don't accurately represent the mechanics of shear load resistance in a SDDCF. The strength contribution from the deck for a SDDCF is dependent on the deck thickness and interfacial deck-concrete area

available for shear transfer, and is not dependent on fastener strength. Thus, fastener strengths need only to be calculated when checking the perimeter fastener failure mode. The concrete strength contribution in (Eq. 5.12) characterizes the shear strength of the concrete placed *above* the top flute. However, diagonal tensions cracks can pass through the concrete in the flutes therefore contributing towards diaphragm strength, especially when deeper panels with gradual changes in panel profile dimensions between top and bottom flutes are used.

To address these issues, a method for predicting SDDCF strength limited by diagonal tension failure, as proposed in Porter and Easterling (1988), is recommended here. ACI 318-14 (Section 22.5.5.1; ACI,2014) defines a range of concrete shear strengths for beams without axial force, as shown in (Eq. 5.13). The product of beam width, b_w, and depth, d, in (Eq. 5.13) represents the beam cross sectional shear area, with λ serving as a lightweight concrete factor.

$$V_{c\_ACI\ 318} = \frac{\lambda k b_w d\sqrt{f'_c}}{1000}, \text{kip} \qquad \text{(Eq. 5.13)}$$

$k =$ concrete strength factor, ranging from 2 to 3.5

$\lambda =$ lightweight concrete factor

$f'_c =$ as previously defined in (Eq. 5.12)

$b_w =$ beam width, in.

$d =$ distance between compression face and centroid of reinforcing steel, in.

Porter and Easterling (1988) take a similar approach by idealizing a SDDCF as a deep, horizontal beam and calculating an equivalent cross sectional shear area. The proposed SDDCF shear strength equation, as reported by Porter and Easterling (1988), is given below (Eq. 5.14). A semi-empirical value of 3.2 is given for the concrete strength factor, k (Porter and Easterling, 1988). The product of the average concrete thickness, t_e, and diaphragm width, b, represents the

cross sectional area of the SDDCF subject to shear forces, as defined in the following. Note that using a unit width (i.e. b = 12 in.) will result in SDDCF shear strength per unit length.

$$S_{n\_Proposed} = \frac{\lambda k t_e b \sqrt{f'_c}}{1000}\text{, kip/ft.} \quad \text{(Eq. 5.14)}$$

$k =$ concrete strength factor, 3.2

$t_e = t_c + t_{dt}$, equivalent total transformed thickness of concrete, in.

$t_c = {}^{D_d}/_{2} + d_c$, average concrete thickness (see Figure 5-4) with D_d and d_c previously defined, in.

$t_{dt} = n_{sc} t_{cd} \frac{d}{s}$, transformed thickness of composite deck with d and s as previously defined in (Eq. 5.5), in.

$n_{sc} = \frac{E_s}{E_c}$, shear modular ratio of steel deck to concrete

$E_s =$ elastic modulus of composite steel deck

$E_c =$ elastic modulus of concrete fill

$t_{cd} =$ thickness of composite deck, in.

$b,\ f'_c$ as previously defined in (Eq. 5.12)

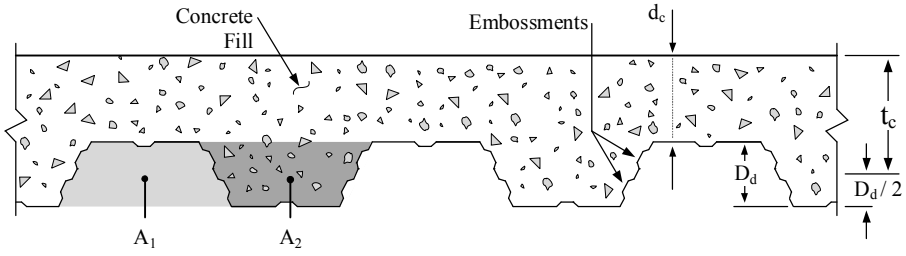

Note: average concrete fill thickness, t_c, assumes area of concrete fill in flute is equal to area in adjacent 'empty' corrugation such that $A_1 = A_2$

Figure 5-4 Steel Deck Panel Profile with Concrete Fill

An equivalent average concrete thickness, t_e, is defined as the summation of the average depth of concrete, t_c (as shown in Figure 5-4), and an equivalent transformed concrete thickness, t_{dt}, for the steel deck. The steel deck's shear strength contribution is accounted for by converting the composite steel deck thickness, t_{cd}, into an equivalent concrete thickness through a shear modular ratio, n_{sc}. The d / s term is a ratio that reduces the shear strength of a panel the more its profile geometry diverges from its equivalent flat plate-like condition. Note that the $S_{n\_Proposed}$ is completely independent of fastener strengths.

5.2.4 Test to Predicted Comparisons

SDDCF predicted and experimental shear strengths for the specimens tested in the ISU testing program that failed in diagonal tension cracking are evaluated in this section. Table 5-1 compares test and predicted strength values for the ISU SDDCF specimens that failed in diagonal tensions cracking using the DDM04 equation (Eq. 5.12) and proposed equation (Eq. 5.14). Test-to-predicted ratios are calculated by dividing the maximum experimental shear strength by the predicted strength and are also given in Table 5-1 for both equations. Specimens are grouped by whether studs were included. Average values are given for both groups individually, and a total average for all specimens, regardless of fastener type, is presented at the bottom of Table 5-1. Tabulated test and predicted strengths are graphically presented in Figure 5-5.

Table 5-1 Test and Predicted Shear Strengths for ISU SDDCF Specimens with Diagonal Tension Cracking Failure

Spec. ID	S_{Test} (kip/ft)	Predicted (kip/ft)		Test / Predicted	
		S_{n_DDM04}	$S_{n\_Proposed}$	S_{n_DDM04}	$S_{n\_Proposed}$
Welded					
5	7.73	5.28	6.72	1.46	1.15
9	14.7	8.71	13.2	1.68	1.11
10	10.7	6.13	9.45	1.75	1.14
12	12.0	6.39	9.71	1.88	1.24
13	16.7	9.50	14.2	1.75	1.18
16	8.27	6.95	7.84	1.19	1.05
18	10.7	5.94	9.15	1.81	1.17
19	9.80	6.80	9.35	1.44	1.05
22	11.3	6.53	9.76	1.73	1.15
24	11.2	7.99	11.0	1.40	1.02
Average	11.3	7.02	10.0	1.61	1.13
Std. dev	2.56	1.25	2.14	0.21	0.06
Welds with Headed Shear Studs					
1	11.2	8.28	11.7	1.35	0.96
2	12.4	8.37	11.6	1.48	1.07
25	12.0	7.80	11.5	1.54	1.05
26[1]	5.80	4.60	7.19	1.26	0.81
29	9.13	6.54	8.9	1.40	1.03
Avg.	10.1	7.12	10.2	1.41	0.98
Std. Dev.	2.43	1.42	1.83	0.10	0.09
Avg. Total	10.9	7.05	10.1	1.54	1.08
Std. Dev. Total	2.58	1.31	2.04	0.20	0.10

[1] *Prediction calculated using lightweight concrete reduction factor of* $\lambda = 0.75$

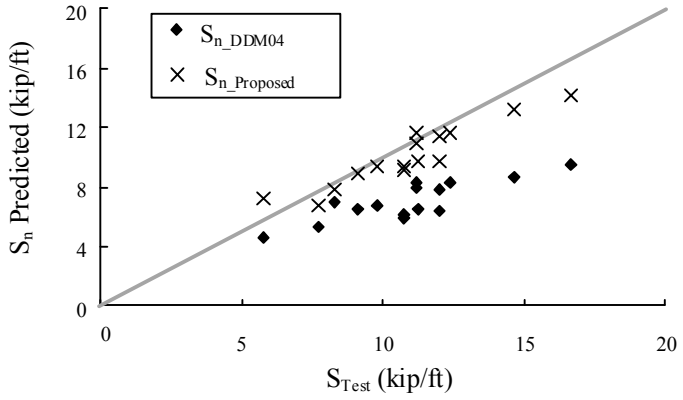

Figure 5-5 Test and Predicted Strengths for ISU SDDCF Specimens with Diagonal Tension Cracking Failure

Strength predictions for SDDCFs using DDM04 equations can give overly conservative values, as shown in Table 5-1. Average test to predicted ratios for specimens without and with studs using the DDM04 method yield values of 1.61 and 1.41 respectively. In contrast, these average ratios reduce to more accurate values of 1.13 and 0.98 respectively, if $S_{n\_Proposed}$ is used for prediction calculations. DDM04 prediction equations can give overly conservative values, as shown by an average test to predicted ratio for of 1.54 for all specimens. This ratio reduces to a more accurate value of 1.08 when using eq. (6), marking a 46% improvement over the DDM04 prediction methods. It is also worth noting the standard deviation drops from 0.20 to 0.10 for all specimens when using the proposed equation over the DDM04 equation. Test to predicted ratios approaching unity in combination with lower standard deviations indicate a more reliable prediction method than DDM04's procedure. It is worth noting that the proposed equation is validated for SDDCF's with concrete compressive strengths ranging from 2400 to 6200 psi, with the majority of specimens testing around 3800 psi.

5.3 Steel Deck Diaphragms without Concrete Fill – Shear Stiffness

The shear stiffness term, *G'*, of a steel deck diaphragm is an indicator of how much in-plane deflection occurs when shear forces are applied. A process to predict shear stiffness of a steel deck diaphragm is presented in both AISI S310 and DDM04. These documents introduce three major sources of flexibility in a diaphragm: in-plane shear, warping of deck, and slip of fasteners as represented by the first, second and third terms in (Eq. 5.15)'s denominator, respectively. Note that the different sources of flexibility are assumed to be independent of each other - an assumption not truly representative of the interdependent behavior of flexibility sources exhibited in real steel deck shear deformation. This interdependency is being investigated by the SDII Group and is outside the scope of this work.

$$G' = \frac{Et}{2(1+\upsilon)\frac{s}{d} + D_n + C} \qquad \text{(Eq. 5.15)}$$

E = Modulus of elasticity

t = sheet thickness

υ = Poisson's ratio

d = pitch of a single panel corrugation

s = developed flute width of a single panel corrugation

D_n = warping coefficient

C = fastener slip coefficient

Flat plate shear stiffness with a uniform thickness is defined by the classical mechanics equation (Eq. 5.16) and expressed in force per unit displacement. Because a steel deck diaphragm is not a continuous flat plate, (Eq. 5.16) must be modified. Steel deck diaphragm shear stiffness is often an order of magnitude less than of continuous flat plates with the same thickness (Luttrell et al., 2015). DDM04 introduces the factor *d / s* (corrugation pitch divided by developed flute width

as previously defined) that reduces the shear stiffness of a corrugated panel. If the deck has rigid fasteners and only pure shear deformations are imposed (i.e. no deck warping), shear stiffness can be expressed as (Eq. 5.17).

$$G' = \frac{Et}{2(1+\upsilon)} \quad \text{(Eq. 5.16)}$$

$$G' = \frac{Et}{2(1+\upsilon)}\frac{d}{s} \quad \text{(Eq. 5.17)}$$

E, t, υ, d, s = As defined in (Eq. 5.15)

The warping coefficient, D_n, reflects a steel deck panel's tendency to relax in shear and distort at panel ends. The warping action occurs through lateral displacement of a panel's upper flat (corresponding to dimension *f* in Figure 5-3) and is referred to as lateral racking. When a panel is not securely fastened at every corrugation, a panel can also undergo accordion like warping, where the panel's bottom flats no longer stay in-plane. The warping coefficient was developed by Luttrell and included in the Steel Deck Institute's Diaphragm Design Manual 1st Edition (DDM01) (Luttrell, 1981). The warping factor, D_n, is related to *D* as shown in (Eq. 5.18) and is the result of a fourth order differential equation accounting for the several possible degrees of freedom at a panel's end when subject to shear warping. The warping factor calculation is dependent on panel profile geometry and the restraint conditions from the panel end structural fasteners. Because warping assumes a fixed length of a panel's end, longer deck panels will have less of a warping contribution in the shear stiffness equation than its shorter equivalent panel as demonstrated by (Eq. 5.18). Note that the warping constant has no units and requires that *D* and *L* be in the same units. The support factor, ρ, accounts for the additional warping restraint that interior supports may provide, effectively reducing the warping contribution accordingly. DDM04 provides tables for ρ and *D* for common panel types and fastening configurations. When unique fastener configurations

or deck panels were used in the tested steel deck diaphragms used in this research, warping constants were calculated as described in AISI S310 Appendix 1 (AISI, 2016b).

$$D_n = \frac{\rho D}{L} \quad \text{(Eq. 5.18)}$$

$\rho =$ support factor

$D =$ warping factor

$L =$ total panel length (i.e. between exterior supports)

The slip coefficient, *C*, introduces another source of flexibility and reflects the stiffness contributions of imperfect structural and sidelap fasteners. When a steel deck panel undergoes shear, slip at sidelap fasteners or structural fasteners between the deck and supporting steel frame can occur. The flexibility of the sidelap fasteners, S_s, and structural fasteners, S_f, is mostly dependent on the fastener type and sheet thickness (flexibility for top arc seam side-lap welds includes an additional term, L_w, to account for the length of the weld). AISI S310 provides flexibility calculations for common fastener types, while DDM04 provides flexibility calculations for common proprietary fasteners.

$$C = \left(\frac{Et}{w}\right)\left(\frac{2L}{2\alpha_1 + \mathrm{n_p}\alpha_2 + 2\mathrm{n_s}\frac{S_f}{S_s}}\right)S_f \quad \text{(Eq. 5.19)}$$

$w =$ panel width

$S_f =$ structural fastener flexibility

$S_s =$ sidelap fastener flexibility

$L =$ total panel length (i.e. between exterior supports)

E, t as described in (Eq. 5.15)

$\alpha_1, \alpha_2, \mathrm{n}_p, n_\mathrm{s}$ as described in (Eq. 5.1)

5.4 Steel Deck Diaphragms with Concrete Fill – Shear Stiffness

5.4.1 Current Shear Stiffness Equation

Similar to DDM04's SDDCF strength equation, AISI S310's shear stiffness equation is the summation of a steel deck term and concrete term, as shown in (Eq. 5.20). Although DDM04 directs its readers to AISI S310 for this equation, to stay consistent with previous text for SDDCF strength equations, this shear stiffness equation will be referred to as the DDM04 shear stiffness equation, G'_{DDM04}.

$$G'_{DDM04} = \frac{Et}{2(1+\upsilon)\frac{s}{d} + C} + K_3, \text{ kip/in.} \qquad \text{(Eq. 5.20)}$$

$K_3 = 3.5 d_c (f'_c)^{0.7}$, kip/in.

f'_c, d_c as described in (Eq. 5.12)

$t, s, and\ d$ as described in (Eq. 5.5), in.

E elastic modulus of steel deck, ksi

υ, C as described in (Eq. 5.15)

The steel deck term (first term of summation in (Eq. 5.20)) is identical to the shear stiffness equation for steel deck diaphragms without concrete fill (Eq. 5.15), except that the warping coefficient, D_n, no longer applies, since the concrete placed on top of the deck restrains out of plane deck deformations. The concrete's shear stiffness contribution is reflected by the K_3 term in (Eq. 5.20). In (Eq. 5.20), K_3 only considers the stiffness contribution of the concrete above the flute of the steel panels with thickness d_c. The concrete term follows classical mechanics stiffness derivations for concrete material in shear and is a semi-empirical expression adjusted to fit test data, hence the exponent value of 0.7 and the coefficient value of 3.5 (Mattingly, 2017).

5.4.2 Proposed Shear Stiffness Equation

A few proposed modifications to the current *G'* equation are discussed here. There are several sources of flexibility that may contribute to an SDDCF's shear stiffness. First, flexural stiffness of the diaphragm chords and parallel structural members may contribute to *G'*, but the effects are often considered negligible. In experiments, support movement of the test frame may also contribute to flexibility, but published load-deformation data is often corrected to account for these movements. The most significant contribution to *G'* is due to the composite deck/concrete system. There is also the potential for slip between the deck and the supporting steel frame due to the structural fasteners' flexibility, as captured in the fastener slip term, *C*. This effect may be more prevalent for SDDCFs utilizing a light structural fastening configuration (not studs). The sidelap fastener flexibility, however, will not contribute to slip between the deck and steel supports, assuming adequate mechanical and chemical bonds of the deck to concrete. As such, a modification to *C* to exclude sidelap flexibility term is suggested, as shown in (Eq. 5.21). A less usual source of flexibility may occur from the deck-concrete interface de-bonding at a diaphragm's 'edge zone'. This behavior is only observed for diaphragms with an unusually large amount of structural fasteners, not including shear studs as common to most SDDCFs, and is therefore not considered further.

The concrete term in the DDM04 equation, K_3, only considers the concrete cover, d_c. Instead, an average concrete thickness including a transformed thickness for the steel deck contribution, t_e, as previously defined for the recommended SDDCF strength equation, is used to account for the shear stiffness contribution of the concrete and steel deck. The coefficient and exponent in the modified concrete term, K_4, is calibrated to give best fit predictions to experimental results from the ISU testing program. Because the steel deck contribution is now considered in K_4,

it is no longer considered in the first term on the right hand side of the shear stiffness prediction equation. The resulting proposed shear stiffness expression, $G'_{Proposed}$, is shown below.

$$G'_{Propsed} = \frac{Et}{C_2} + K_4 \quad \text{(Eq. 5.21)}$$

$$C_2 = \left(\frac{Et}{w}\right)\left(\frac{2L}{2\alpha_1 + \mathrm{n_p}\alpha_2}\right)S_f$$

$K_4 = 4.8t_e(f'_c)^{0.5}$, kip/in

$E, t, w, L, \alpha_1, \mathrm{n_p}, \alpha_1, S_f$ as defined in (Eq. 5.19)

t_e, f'_c as defined in (Eq. 5.20)

5.4.3 Test to Predicted Comparisons

Shear stiffness test and predicted values for all 32 SDDCF specimens tested in the ISU program, regardless of failure mode or test setup configuration, are presented in Table 5-2. Prediction values are reported using both the DDM04 and proposed equations and are graphically presented in Figure 5-6. The coefficient and exponent in the concrete term was calibrated to give best fit predictions to experimental results, as shown in Table 5-2, by an average test/predicted ratio of 1.02 for all 32 specimens, in comparison to DDM04's average value of 0.46, giving a 52% more accurate prediction.

Table 5-2 Test and Predicted Shear Stiffness for ISU SDDCF Specimens

Spec. ID	G' Test[1] (kip/in.)	Predicted (kip/in.)		Test / Predicted	
		G'_{DDM04}	$G'_{Proposed}$	G'_{DDM04}	$G'_{Proposed}$
1	1520	3663	1547	0.42	0.98
2	1961	3662	1540	0.54	1.27
3	1131	3282	1505	0.34	0.75
4	1348	2745	1360	0.49	0.99
5	1708	2125	927	0.80	1.84
6	1891	7797	2452	0.24	0.77
7	1336	3706	1711	0.36	0.78
8	674	2665	1200	0.25	0.56
9	1345	3811	1877	0.35	0.72
10	1609	2525	1412	0.64	1.14
11	1770	3108	1490	0.57	1.19
12	1712	2636	1445	0.65	1.18
13	2021	4240	1993	0.48	1.01
14	1838	5647	2252	0.33	0.82
15	1132	2677	1123	0.42	1.01
16	921	2714	1131	0.34	0.81
17	1595	7458	2383	0.21	0.67
18	1582	2418	1374	0.65	1.15
19	930	2674	1400	0.35	0.66
20	1302	3678	1463	0.35	0.89
21	868	2776	1331	0.31	0.65
22	1654	2701	1509	0.61	1.10
23	1368	3569	1404	0.38	0.97
24	1657	3353	1585	0.49	1.05
25	1726	3323	1507	0.52	1.15
26	1592	3178	1295	0.50	1.23
27	1751	3051	1263	0.57	1.39
28	1582	3485	1382	0.45	1.15
29	1887	2509	1162	0.75	1.62
30	1535	3024	1316	0.51	1.17
31	1347	2944	1300	0.46	1.04
32	917	2325	1115	0.39	0.82
Avg.	1475	3421	1492	0.46	1.02
Std. Dev.	343	1274	350	0.14	0.28

[1] *Taken as the secant stiffness at 40% of the maximum strength (see Figure 4-4)*

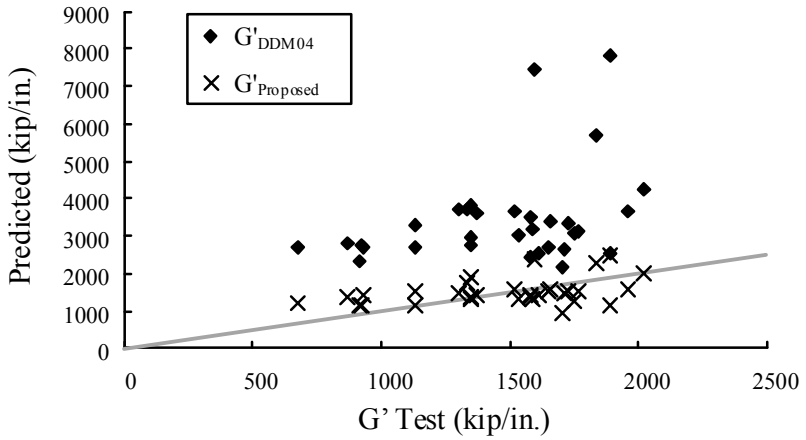

Figure 5-6 Test and Predicted Shear Stiffness for ISU SDDCF Specimens

Tested shear stiffness values ranged from approximately 600 to 2000 kip/in, with an average value for all specimens equal to 1475 kip/in. The standard deviation for this group was 343 kip/in. When using the shear stiffness equation as prescribed by DDM04, the average standard deviation more than doubles. Using the DDM04 shear stiffness equation for SDDCFs may then understate in-plane diaphragm deflections when used in design. Using the proposed equation gives more accurate test-to-predicted shear stiffness values, as shown by an average value of 1.02. However, both the DDM04 and proposed equations give significant scatter for test to predicted ratios. This may be due to the difficulty of taking reliable measurement readings at small displacements during testing.

Tested shear stiffness values are taken as the secant stiffness of the strength vs. shear angle curve through a shear angle corresponding to 40% of the ultimate strength (see Figure 4-4). This method, as prescribed by AISI testing procedures (AISI, 2013a), assumes that tested stiffness value obtained falls within the elastic range of an experimental diaphragm specimen. As such, measurement readings typically fall within very small displacements where readings may be less reliable due to noise, instrumentation reliability, and more. It is common to see considerable

variation in the test values for shear stiffness, making calibration of stiffness equations challenging. Further testing of SDDCFs to investigate shear stiffness predictions equations is recommended.

5.5 Resistance Factors

Resistance factors for diaphragm design are presented in this section. The methodology used to derive resistance factors and assumptions made are briefly discussed. This methodology, outlined in AISI S310 and AISI S100, is followed to calculate resistance factors for the proposed SDDCF strength equation for the diagonal tension cracking failure mode using both prescribed calibration factors and test data available from the ISU program. These calibration factors are discussed and in many cases, concluded to be conservative. As such, they are slightly modified and a second resistance factor for this failure mode is calculated.

5.5.1 Current Resistance Factors

Resistance factors, ϕ, for steel deck diaphragms are specified in AISI S310, as summarized in Table 5-3. Note that the recently published AISI S310 (AISI, 2016b) includes updated resistance factors to those found in DDM04. Resistance factors are prescribed dependent on loading type, diaphragm type (concrete fill vs. no concrete fill) and fastener type. For diaphragms without concrete fill, the governing resistance factor is further subcategorized as connection related, as described by limit states S_{ne}, S_{ni} and S_{nc}, or stability related, as described by limit state S_{nb} (discussion of these limit states is provided in Section 5.1.1). For diaphragms utilizing multiple types of fasteners, the lower resistance factor for the different fastener types is to be used. Table 5-3 does not specify factors for mechanical fasteners other than screws. Instead, AISI S310 allows

the resistance factor for PAFs and other mechanical fasteners to be no greater than that of screws. Due to this note and the reliability of shear strength prediction equations for PAFs, an upper limit of ϕ = 0.70 for steel deck diaphragm strength limited by PAF failure is used. For SDDCFs, a resistance factor of 0.50 is set, regardless of loading type, connection type or governing limit state. Other types of concrete fill (e.g. insulating fill) are outside the scope of this work.

Table 5-3 AISI S310 Resistance Factors for Steel Deck Diaphragms (LRFD)

Load Type	Connection Type	ϕ, No Concrete S_{ne}, S_{ni}, S_{nc}	ϕ, No Concrete S_{nb}	ϕ, Concrete Fill
Earthquake and Others	Weld	0.55	0.80	0.50
	Screw	0.70		
Wind	Weld	0.75	0.80	0.50
	Screw	0.80		

Resistance factors for Load and Resistance Factored Design (LRFD) are traditionally specified for the failure mode of a specific structural component (e.g. ϕ = 0.9 for tension yielding on gross sections of structural steel members per AISC 360). A limitation when prescribing diaphragm ϕ dependent solely on fastener type and load type is that it does not distinguish between the different failure modes that a fastener may fail in. For example, AISI S100, *North American Specification for the Design of Cold-Formed Steel Structural Members*, gives ϕ = 0.60 for a welded structural fastener controlled by failure of the weld, as is common for thicker decks with smaller sized welds (AISI, 2016a). Conversely, a welded structural fastener with a thinner deck and larger weld area may have steel deck buckling or tearing as the controlling failure mode, in which case ϕ = 0.70 or 0.55 is used. Furthermore, several resistance factors for different weld types can be employed in steel deck diaphragms, such as welds with washers or seam welds as

structural fasteners, fillet welds or top seam welds as sidelap fasteners, and more. This emphasizes that the generalized diaphragm resistance factors in Table 5-3 may be conservative.

The resistance factors presented in Table 5-3 are derived using (Eq. 5.22). The calibration factors used in determining diaphragm resistance factors are available in Table 5-4. The professional factor, P_m, is calibrated to full scale diaphragm test data available from Luttrell (1967), Luttrell (1981), Ellifritt and Luttrell (1971), Luttrell (2004) and Bagwell (2008) (AISI, 2016b). The calibration factor, C_Φ, and the coefficient of variation of load effect, V_Q, are dependent on dead load (D) to live load (L) ratios assumed for a specific load case.

$$\emptyset = C_\phi (M_m F_m P_m) e^{-\beta_0 \sqrt{V_M^2 + V_F^2 + C_P V_P^2 + V_Q^2}} \quad \text{(Eq. 5.22)}$$

$$P_m = \sum_{i=1}^{n} \frac{R_{t,i}}{R_{n,i}} / n \quad \text{(Eq. 5.23)}$$

$R_{t,i}$ = tested diaphragm strength

$R_{n,i}$ = predicted diaphragm strength

$V_P = {}^{s_c}/_{P_m}$ where s_c is the standard deviation of $R_{t,i}$ divided by $R_{n,i}$ for all the test results

$C_P = (1+1/n)m/(m\text{-}2)$ for $n \geq 4$, with $m = n - 1$

Table 5-4 AISI S310 Calibration Factors for Steel Deck Diaphragms (LRFD)

Diaphragm Condition[1]	C_Φ	V_Q	M_m	V_M	F_m	V_F	V_P	n	C_P	P_m
Welds	1.6	0.25	1.10	0.10	1	0.10	0.188	88	1.035	1.008
Screws				0.08		0.05	0.145	61	1.051	1.162
SDDCF				0.10	0.90	0.10	U/A[2]	U/A[2]	U/A[2]	U/A[2]

[1] *Welds, screws refer to fastener type for diaphragms without concrete fill*
[2] *U/A = unavailable*

The mean value of material factor, M_m, and coefficient of variation of material factor, V_M, represent uncertainties and variations for materials used in construction. The mean value of fabrication factor, F_m, and coefficient of variation of fabrication factor, V_F, are analogous to M_m and V_m and correspond to uncertainties in the construction process in contrast to the 'as-designed' condition. Note that $F_m < 1.0$ is unusual, and suggests that SDDCFs are systematically constructed in a manner that does not meet specified design requirements (Schafer, 2017). The correction factor, C_p, amplifies the coefficient of variation of test results, V_P, and serves to encourage manufacturers to increase number of tests.

The target reliability index, $\beta_0 = 3.5$, is used for all resistance factors in Table 5-3 except for diaphragm conditions controlled by connections subject to wind loading, in which case $\beta_0 = 2.5$ was used (AISI, 2013b). $\beta_0 = 3.5$ is typically used for cold-formed steel connections, giving lower ϕ values than if $\beta_0 = 2.5$, typical to cold-formed steel structural members, were used. AISI S310-16 commentary describes the derivation of resistance factors to be controlled by the dominant limit state which is connection related (with the exception being the buckling, or stability limit state, S_{nb}, for steel diaphragms without concrete fill). This implies that procedures to develop ϕ factors for diaphragm strength, and subsequently the calibration factors, treat the diaphragm as a connection (Schafer, 2017). This is conservative in nature, as the redundancy from multiple connections and the potential for load redistribution for ductile diaphragm behavior may allow for a load-sharing network.

Chatterrjee (2016) investigates the contrasts between single component reliability (e.g. single fastener in a diaphragm) and network level reliability (e.g. diaphragm system composed of several fasteners), and emphasizes the conservative nature of resistance factor derivations as embodied in high target reliability indices. Capturing whether a system will fail due to component failure, as often idealized as a 'weak-link' system, or if the system has adequate redundancy,

ductility and redistribution capabilities for multiple load paths, can be difficult to capture in design, especially for larger diaphragms with several components (Chatterrjee, 2016). Galambos (1990) gives several reasons as to why the current approach for calculating resistance factors may be conservative, including:

1. Connection reliability may be an order of magnitude larger than for members
2. Added strength of non-structural components contribute to system
3. Overdesign as a consequence of material availability, conservative modeling, conservative load assignments, and more

As such, reliability studies accounting for conservative design considerations and the redundancy of multiple connections in steel deck diaphragms are recommended, similar to Chatterjee's (2016) investigation of an oriented strand board (OSB) sheathed diaphragm.

5.5.2 Resistance Factor for Steel Deck Diaphragms with Concrete Fill

AISI S310 allows for calibration of safety factors in accordance with AISI S100, either through small scale individual fastener tests or full scale diaphragm tests, as described in the previous section, providing sufficient data is considered. These procedures were followed to calculate a resistance factor for SDDCFs controlled by diagonal tension cracking using the proposed equation, $S_{n\_Proposed}$, and the ISU test data for the 15 test specimens failing in the diagonal tension failure mode. Note that if a diaphragm is controlled by the perimeter fastener limit state, an appropriate resistance factor for the shear strength of the connection should be used (e.g. SDDCFs limited by perimeter fastener failure of steel headed stud anchors subjected to shear in should use $\phi = 0.65$, as specified in ASIC 360, Eq. (I8-3) (AISC, 2010). A few calibration factors

are modified from those given in AISI S310, and an 'adapted' resistance factor is calculated, as shown in Table 5-5.

Because calibration factors considered for SDDCFs are limited by both the fasteners and the concrete slab, a worst case target reliability index, $\beta_0 = 3.5$, is assigned to the current resistance factor in AISI S310. However, for the proposed shear strength equation constrained to the diagonal tension failure mode, concrete failure will be the limiting condition. Therefore, $\beta_0 = 3.5$ may no longer be appropriate. Instead, diagonal tension failure is treated as a member limit state rather than a connection limit state. As such, AISI S100 specifies a $\beta_0 = 2.5$ (AISI, 2016a).

Table 5-5 SDDCF Calibration and Resistance Factors for Diagonal Tension Cracking Failure Limit State (LRFD)

Calibration Method	C_Φ	V_Q	M_m	V_M	F_m	V_F	V_P[1]	n[1]	C_P[1]	P_m[1, 2]	β_0	Φ
AISI S310	1.6	0.25	1.10	0.10	0.90	0.10	0.095	15	1.24	1.08	3.5	0.58
Adapted											2.5	0.79

[1] *Using ISU test data*
[2] *Using* $S_{n\_Proposed}$ *for predicted diaphragm strength*

The resulting calculated resistance factors using ISU test data for the AISI S310 and adapted AISI S310 method yields values of 0.58 and 0.79 respectively. The corresponding safety factors are $\Omega = 2.74$ and $\Omega = 2.01$, respectively. This is considerably higher than the generalized $\phi = 0.50$ for all SDDCFs (AISI, 2016b). It is worth noting that AISI S310 limits calculated resistance factors to ACI 318 values, where $\phi = 0.75$ and $\phi = 0.60$ for concrete diaphragms with and without supplemental reinforcement, respectively. Considering this limitation and assuming concrete diagonal tension cracking failure to be a member limit state (i.e. $\beta_0 = 2.5$), tentative resistance factors for SDDCFs are selected as given in Table 5-6. Further reliability studies are recommended

to evaluate whether calibration factors as given by AISI S310 are appropriate, before conclusively proposing resistance factors for SDDCFs.

Table 5-6 Resistance Factors for Diagonal Tension Cracking and Perimeter Fastener Limit States (LRFD)

Reference	Diaphragm Condition	Limit State[1]	Resistance Factor, ϕ
AISC 360 (AISC, 2010)	Shear studs at composite beams	P	0.65
ACI 318-14 (ACI, 2014)	Without supplemental reinforcement	DT	0.65
ACI 318-14 (ACI, 2014)	With supplemental reinforcement	DT	0.75

[1] *P = perimeter fastener limit state, DT = diagonal tension cracking limit state*

6 DIAPHRAGM BEHAVIOR CHARACTERIZATION AND R_S FACTORS

Diaphragm load-deformation behavior for several past experimental subassemblage tests is discussed in this chapter, with special attention to inelastic post-peak deformations. Available load-deformation plots from the literature were digitized to allow unification of units, comparison between groups of specimens, and further analysis. A subset of 108 cantilever tests for which post-peak data was available is presented in the following section. These subassemblage tests are indicative of diaphragm behavior, and provide key parameters necessary for system ductility calculations, and subsequently diaphragm design force reduction factors, R_s. Subassemblage diaphragm test results are presented, and the influence of certain test variables on the load-deformation behavior is discussed. Finally, diaphragm design force reduction factors, calculated using the procedure outlined in Chapter 4, are presented. Appendix A contains summary sheets with general information of test setups, calculated design strengths, and test results for all specimens used to calculate R_s factors.

6.1 Test Results of Subassemblage Tests

6.1.1 Specimens without Concrete Fill

While behavior of diaphragms can be influenced by a multitude of variables, four major groups were identified for diaphragm specimens without concrete fill, dependent on the combination of structural fastener type and sidelap fastener type used. Table 6-1 presents the results for steel deck diaphragm subassemblage tests subjected to monotonic loading as grouped by the structural fastener type / sidelap fastener type combination. Figure 6-1 shows plots of the associated data. Note that vertical lines towards toward maximum reported shear angles in the load-deformation curves correspond to unloading curves and not necessarily brittle failure.

Methods for determining test results reported for subassemblage tests were defined in Section 4.3.1 (see Figure 4-2).

The unit shear strength of the diaphragm specimens, S_{max}, were mostly in the range of 0.75 k/ft to 2.5 k/ft. Three research programs tested higher capacity diaphragms (Pinkham 1999; Martin 2002; and Beck 2008, 2013a, 2013b) which included specimens with unit shear capacity as large as 6.68 k/ft. Strength and stiffness of diaphragms is highly dependent on the fastener spacing and deck type. However, it is not the intent of this research to study strength and stiffness of steel deck diaphragms without concrete fill which have been previously characterized (Luttrell et al., 2015). Instead, this research focuses on quantifying the ductile behavior of these specimens.

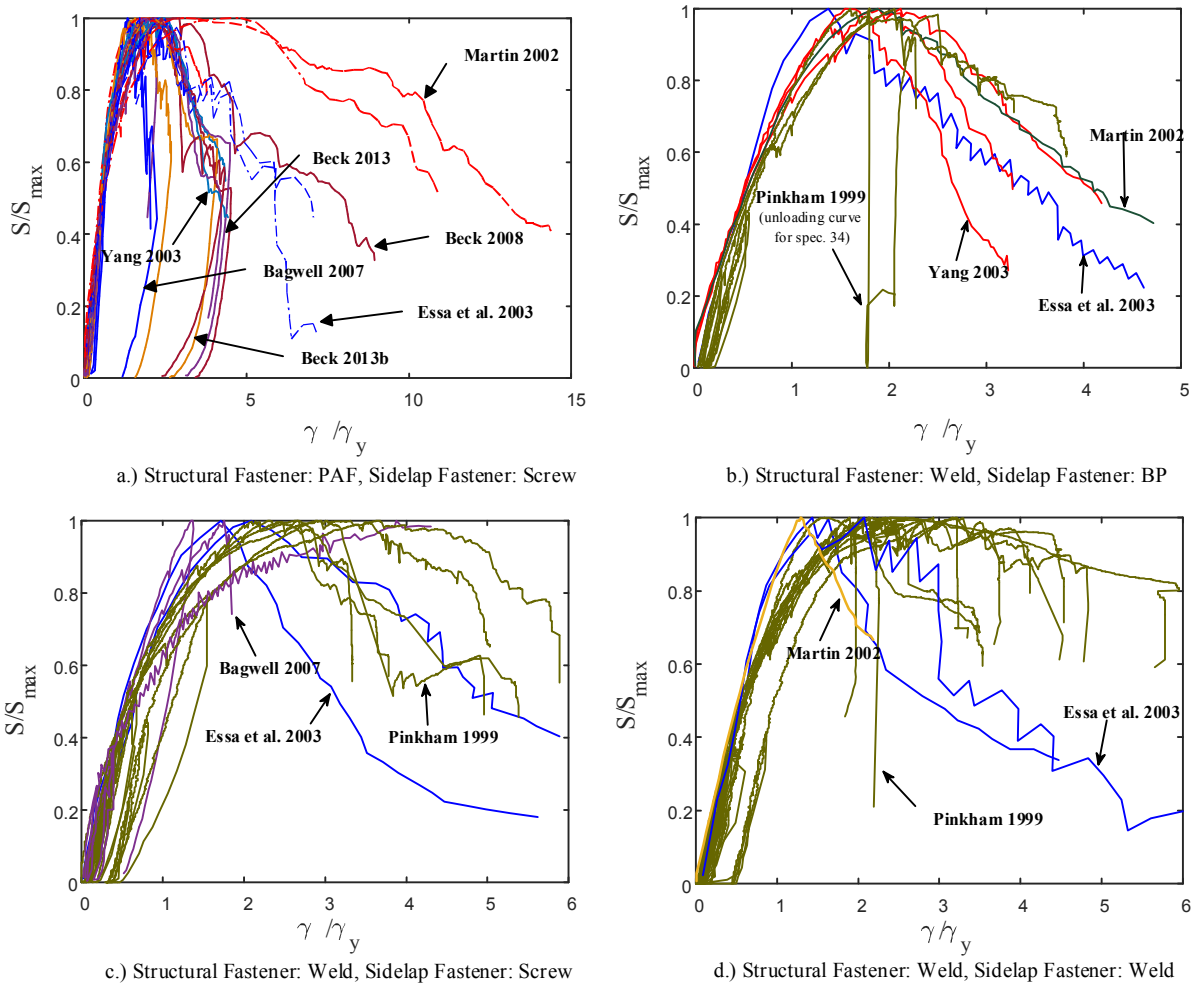

a.) Structural Fastener: PAF, Sidelap Fastener: Screw

b.) Structural Fastener: Weld, Sidelap Fastener: BP

c.) Structural Fastener: Weld, Sidelap Fastener: Screw

d.) Structural Fastener: Weld, Sidelap Fastener: Weld

Figure 6-1 Subassemblage Behavior of Monotonically Loaded Steel Deck Diaphragms

Table 6-1 Test Results for Specimens Tested Monotonically and Grouped by Structural Fastener Type / Sidelap Fastener Type

Reference	Spec. ID	G' k/in	S_{max} k/ft	γ_y Rad*1000	γ_{ult} Rad*1000	Subassemblage Ductility, μ_{sub}
PAF / Screw; n[1] = 22						
Martin 2002	19	24.2	1.14	3.93	14.8	3.76
Martin 2002	30	99.4	1.60	1.34	13.0	9.68
Martin 2002	32	130	2.36	1.51	10.7	7.12
Essa et al. 2003	5	15.7	0.76	4.02	12.5	3.11
Essa et al. 2003	17	22.9	0.99	3.61	11.6	3.22
Yang 2003	39	12.0	0.77	5.37	18.5	3.44
Yang 2003	43	15.4	0.92	4.94	15.8	3.20
Yang 2003	44	14.9	0.72	4.01	13.1	3.25
Bagwell 2007	7	12.0	0.49	3.42	10.2	2.98
Bagwell 2007	8	13.5	0.53	3.29	5.14	1.56
Bagwell 2007	9	3.05	0.40	10.8	33.2	3.06
Bagwell 2007	10	35.5	0.49	1.16	16.8	14.5
Bagwell 2007	11	44.7	0.45	0.83	12.3	14.8
Bagwell 2007	17	89.2	2.50	2.34	4.19	1.79
Beck 2008	63	60.7	2.04	2.80	12.3	4.39
Beck 2008	64	67.8	3.06	3.76	12.1	3.20
Beck 2008	65	85.2	3.95	3.87	11.3	2.93
Beck 2013a	M 01	70.1	4.05	4.81	15.2	3.16
Beck 2013a	M 02	70.4	3.81	4.51	14.4	3.20
Beck 2013a	M 03	54.9	6.07	9.21	20.5	2.22
Beck 2013b	S 02	61.1	3.45	4.70	13.7	2.91
Beck 2013b	S 03	51.4	4.05	6.57	14.8	2.25
Average		47.9	2.03	4.13	13.9	4.53
Std. dev.		33.5	1.58	2.35	5.52	3.62
Weld / BP[2]; n[1] = 8						
Pinkham 1999	32	75.7	3.15	3.47	10.3	2.96
Pinkham 1999	34	11.0	1.43	10.8	29.9	2.76
Pinkham 1999	36	16.4	2.45	12.4	28.3	2.28
Martin 2002	37	24.9	0.86	2.87	8.06	2.81
Essa et al. 2003	1	11.8	0.54	3.82	7.49	1.96
Yang 2003	41	10.5	0.63	4.96	15.0	3.02
Yang 2003	47	5.24	0.50	7.88	17.6	2.23
Yang 2003	49	7.07	0.58	6.89	17.8	2.58
Average		20.3	1.27	6.65	16.8	2.58
Std. dev.		21.7	0.94	3.31	8.02	0.36

[1] *n = number of tests in respective group*
[2] *"BP" for button punch*

Table 6-1 (b) Test Results for Specimens Tested Monotonically and Grouped by Structural Fastener Type / Sidelap Fastener Type

Reference	Spec. ID	G' k/in	S_{max} k/ft	γ_y rad*1000	γ_{ult} rad*1000	Subassemblage Ductility, μ_{sub}
Weld / Screw; n[1] = 11						
Pinkham 1999	50	167	6.19	3.09	10.7	3.46
Pinkham 1999	51	81.5	3.00	3.07	16.7	5.43
Pinkham 1999	52	12.4	0.95	6.40	21.1	3.30
Pinkham 1999	53	55.6	1.58	2.37	11.5	4.85
Pinkham 1999	54	48.6	1.90	3.25	11.2	3.43
Pinkham 1999	R54	34.9	2.12	5.06	16.0	3.16
Essa et al. 2003	11	19.1	1.23	5.35	12.4	2.33
Essa et al. 2003	15	22.0	1.30	4.93	18.8	3.81
Bagwell 2007	12	10.3	1.41	11.4	14.7	1.29
Bagwell 2007	13	57.4	1.05	1.52	N/A[2]	N/A[2]
Bagwell 2007	14	32.3	1.88	4.86	8.95	1.84
Average		49.2	2.05	4.66	14.2	3.29
Std. dev.		42.6	1.42	2.54	3.71	1.20
Weld / Weld; n[1] = 14						
Pinkham 1999	31	119	4.83	3.37	12.6	3.74
Pinkham 1999	33	120	4.82	3.34	15.2	4.54
Pinkham 1999	35	80.1	3.60	3.75	15.4	4.12
Pinkham 1999	37	127	2.82	1.85	10.5	5.70
Pinkham 1999	38	14.8	1.62	9.10	29.3	3.22
Pinkham 1999	39	81.4	3.32	3.40	9.54	2.81
Pinkham 1999	40	167	6.68	3.33	14.2	4.27
Pinkham 1999	41	80.5	3.22	3.33	16.1	4.83
Pinkham 1999	42	13.3	1.51	9.46	21.3	2.26
Pinkham 1999	43	70.0	2.42	2.88	7.04	2.45
Pinkham 1999	44	31.5	3.13	8.28	16.4	1.98
Martin 2002	22	27.0	2.20	6.79	12.2	1.79
Essa et al. 2003	9	13.1	0.81	5.16	15.5	2.99
Essa et al. 2003	10	13.1	0.98	6.27	12.6	2.01
Average		68.5	3.00	5.02	14.9	3.34
Std. dev.		49.3	1.57	2.42	5.22	1.17

[1] *n = number of tests in respective group*
[2] *Post peak-force deformations did not reach strength degradation 80% of S_{max}*

There is a marked difference in ductility between specimens with mechanical structural fasteners as compared to specimens with welds to the support. Figure 6-1a shows load-deformation behavior of diaphragm specimens with PAF structural fasteners. The average subassemblage ductility for this group was 4.53. Groups employing welded structural fasteners had lesser average subassemblage ductilities of 2.58, 3.29 and 3.34 for button punch, screw and

welded sidelap types, respectively. This suggests that the diaphragm ductility is considerably more sensitive to the type of structural fastener used (PAF vs. weld) than the type of sidelap fastener used. The variation was especially large for specimens with PAF structural fasteners, as demonstrated by the scatter in Figure 6-1a and a standard deviation of 3.62. There are several sources that may contribute to the highly variable subassemblage ductilities for these grouped specimens, including deck thickness, deck geometry, fastener failure mechanisms and more. These sources, their effect on diaphragm ductility and the associated diaphragm behavior are further examined in Section 6.2.

Figure 6-2 and Table 6-2 show data from similar specimens as the monotonically tested groups, but subjected to cyclic loading. The curves in Figure 6-2 represent the backbone curves specific to the quadrant of the hysteretic data where the peak strength was reached. Because cyclic degradation typically reduces the peak strength reached in the reversed cycle, backbone curves normally correspond to the first quadrant. The average ductility value for the PAF/Screw and Weld/BP groups reduced by 39% and 41% to 2.75 and 1.53, respectively. Strength degradation associated with cyclic loading causes a reduction in the available ductility of the diaphragm system. However, the trends described above are still applicable in that specimens with mechanical structural fasteners demonstrate more ductility than specimens with welds.

Table 6-2 Test Results for Specimens Tested Cyclically and Grouped by Structural Fastener Type/Sidelap Fastener Type

Reference	Spec. ID	G' kip/in	S_{max} kip/ft	γ_y Rad*1000	γ_{ult} Rad*1000	Subassemblage Ductility, μ_{sub}
PAF/Screw; n[1] = 21						
Martin 2002	28	12.1	0.96	6.62	13.1	1.97
Martin 2002	29	15.3	0.92	5.02	6.54	1.30
Martin 2002	31	65.3	1.81	2.31	10.1	4.37
Martin 2002	33	114	2.40	1.75	9.89	5.66
Martin 2002	34	24.7	1.16	3.90	11.9	3.04
Martin 2002	35	26.5	1.18	3.71	5.90	1.59
Essa et al. 2003	8	16.2	0.85	4.38	13.1	2.98
Essa et al. 2003	18	26.3	1.07	3.39	13.5	4.00
Yang 2003	38	23.1	1.03	3.73	13.1	3.50
Yang 2003	40	10.6	0.88	6.95	15.2	2.19
Beck 2008	S 03	72.3	3.96	4.56	14.6	3.20
Beck 2008	S 04	44.9	3.43	6.37	15.3	2.41
Beck 2008	S 05	46.1	3.48	6.29	14.2	2.26
Beck 2008	S 06	73.5	4.33	4.92	13.6	2.76
Beck 2008	S 07	59.6	2.08	2.90	11.0	3.79
Beck 2008	S 08	45.6	1.93	3.53	5.80	1.64
Beck 2013a	C 01	48.7	4.11	7.03	13.3	1.88
Beck 2013a	C 02	61.6	3.93	5.31	12.9	2.42
Beck 2013a	C 03	57.2	5.77	8.42	20.2	2.40
Beck 2013b	S 02C	58.4	3.47	4.95	12.4	2.50
Beck 2013b	S 03C	49.5	4.09	6.88	14.3	2.08
Average		45.3	2.52	4.90	12.4	2.76
Std. dev.		25.1	1.47	1.71	3.30	1.02
Weld/BP[2]; n[1] = 6						
Martin 2002	20	16.8	0.67	3.33	5.04	1.51
Martin 2002	21	15.2	0.93	5.11	6.51	1.27
Martin 2002	36	14.0	0.67	3.99	5.82	1.46
Essa et al. 2003	2	12.3	0.52	3.50	5.06	1.44
Yang 2003	42	11.2	0.70	5.18	12.2	2.36
Yang 2003	48	4.20	0.48	9.47	10.9	1.15
Average		12.3	0.66	5.10	7.60	1.53
Std. dev.		4.06	0.15	2.08	2.88	0.39
Weld/Screw n[1] = 2						
Essa et al. 2003	14	18.3	0.884	4.02	8.04	2.00
Essa et al. 2003	16	16.0	1.30	6.77	12.6	1.86
Weld/Weld; n[1] = 4						
Martin 2002	23	33.0	2.35	5.94	13.1	2.20
Martin 2002	24	26.7	2.27	7.09	10.0	1.40
Essa et al. 2003	12	14.0	0.71	4.25	11.1	2.62
Essa et al. 2003	13	11.2	0.89	6.58	13.1	2.00
Average		21.2	1.55	5.97	11.8	2.06
Std. dev.		8.94	0.76	1.07	1.35	0.44

[1] *n = number of tests in respective group*
[2] *"BP" for button punch*

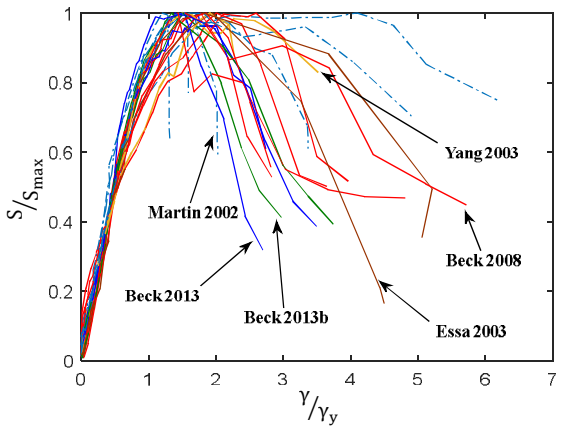

a.) Structural Fastener: PAF, Sidelap Fastener: Screw

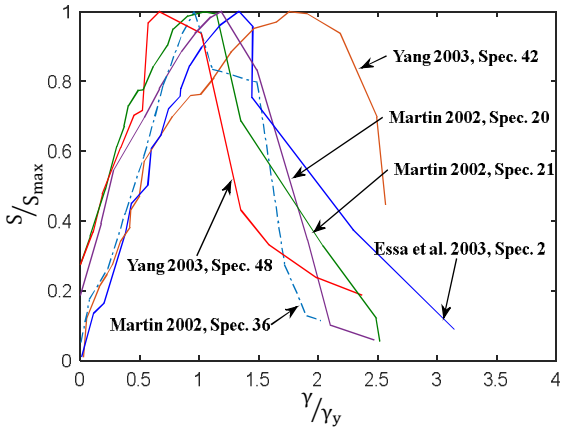

b.) Structural Fastener: Weld, Sidelap Fastener: BP

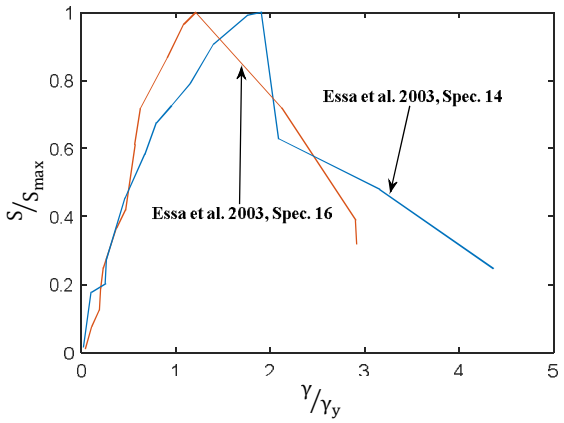

c.) Structural Fastener: Weld, Sidelap Fastener: Screw

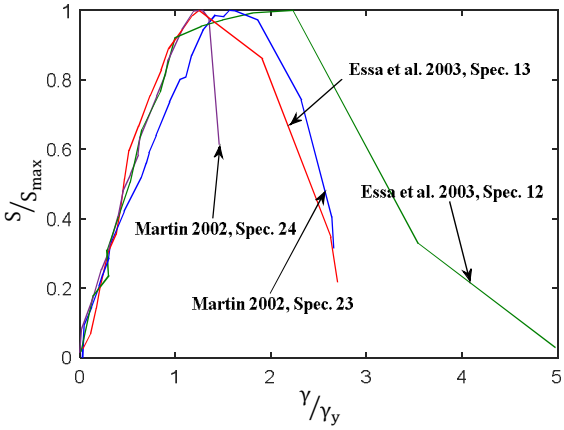

d.) Structural Fastener: Weld, Sidelap Fastener: Weld

Figure 6-2 Subassemblage Behavior of Cyclically Loaded Steel Deck Diaphragms

6.1.2 Specimens with Concrete Fill

A very limited amount of experimental research is available for SDDCFs, in comparison to specimens without concrete. Considering this research's interest in post-peak behavior, the data set of interest for SDDCFs is even more limited, as many programs only tested up to the ultimate diaphragm strength. The ISU research program includes 32 specimens with concrete fill subjected to post-peak deformations (Porter and Easterling, 1988), and is identified as the benchmark

program for this study on SDDCF ductility behavior characterization. Of the 32 tests, 20 complete load-deformation hystereses were obtained and digitized (specimens 11-30).

Note that the loading protocol for these specimens included large post-peak displacement steps (Porter and Easterling, 1988). A cyclic envelope rather than the traditional peak-to-peak backbone would better capture the shape and behavior of the hysteretic curve, and was therefore used. Figure 6-3 gives normalized cyclic envelopes corresponding to the quadrant in which peak strength was obtained, which was the 1st quadrant for all specimens analyzed. SDDCF specimens were grouped as to whether studs were used. If shear studs were not used, arc spot welds fastened the deck to support, often in a very heavy fastener configuration where up to four welded structural fasteners were in a single flute. This is atypical of construction practices and often resulted in the impractical shear transfer mechanism failure mode.

Table 6-3 and Figure 6-3 presents the test results. The three limit states as described in Section 5.2.1 are included in Table 6-3 for comparison. Specimens 11 through 24 shown below did not include headed shear studs and were reported to experience all three limit states. In several cases, this group reported multiple failure modes for a single specimen, usually a combination of the shear transfer failure and perimeter fastener failure modes. Slip between the deck and concrete, or 'interfacial' slip, characteristic of shear transfer failure is prevalent for both of these limit states. That is, specimens classified with perimeter fastener failure can have interfacial slip not limiting the maximum tested strength. Diaphragms without studs failing in the perimeter fastener mode were inspected post-test to observe the condition of the welds (Porter & Easterling, 1988). If no weld failure was observed, such as weld rupture or deck bearing on weld, then the shear transfer mechanism was conclusive. However, for specimens with a considerable amount of welds failing, a combination of perimeter fastener and shear transfer failure modes were determined. That is due to the possibility of welds failing in the post-peak deformation range where the shear transfer

Table 6-3 Subassemblage Steel Deck Diaphragms with Concrete Fill Grouped by Structural Fastener Type (Porter and Easterling, 1988)

Spec. ID	Failure Mod[1]	G' kip/in	S_{max} kip/ft	γ_y Rad*1000	γ_{ult} Rad*1000	Subassemblage Ductility, μ_{sub}
Welded; n[1] = 14						
11	S	1770	6.34	0.30	2.25	7.53
12	DT	1710	12.1	0.59	2.30	3.92
13	DT	2020	16.8	0.69	2.23	3.23
14	S	1840	14.0	0.64	5.64	8.85
15	S/DT	1130	6.84	0.50	2.41	4.78
16	DT	920	8.01	0.73	2.39	3.29
17	S	1600	9.70	0.51	5.61	11.1
18	DT	1580	10.7	0.56	2.27	4.03
19	DT	1820	16.5	0.76	1.06	1.40
20	S/P	1300	6.21	0.40	2.25	5.65
21	S/P	870	8.16	0.78	2.56	3.27
22	DT	1650	10.5	0.53	2.09	3.95
23	S/P	1370	7.09	0.43	5.29	12.3
24	DT	1330	11.2	0.71	2.96	4.20
Average		1490	10.3	0.58	2.95	5.53
Std. dev.		338	3.44	0.14	1.39	3.08
Welds with Headed Shear Studs; n[1] = 6						
25	DT	1730	12.0	0.58	2.26	3.92
26	DT	1590	5.80	0.30	1.35	4.45
27	P	1751	6.07	0.29	1.38	4.76
28	P	1580	7.98	0.42	1.41	3.37
29	DT	1890	9.00	0.40	1.24	3.13
30	P	1530	7.69	0.42	1.37	3.27
Average		1670	8.09	0.40	1.50	3.82
Std. dev		131	2.06	0.09	0.34	0.62

[1]*DT = Diagonal tension cracking, P = Perimeter fastener failure, S = Shear transfer mechanism failure*

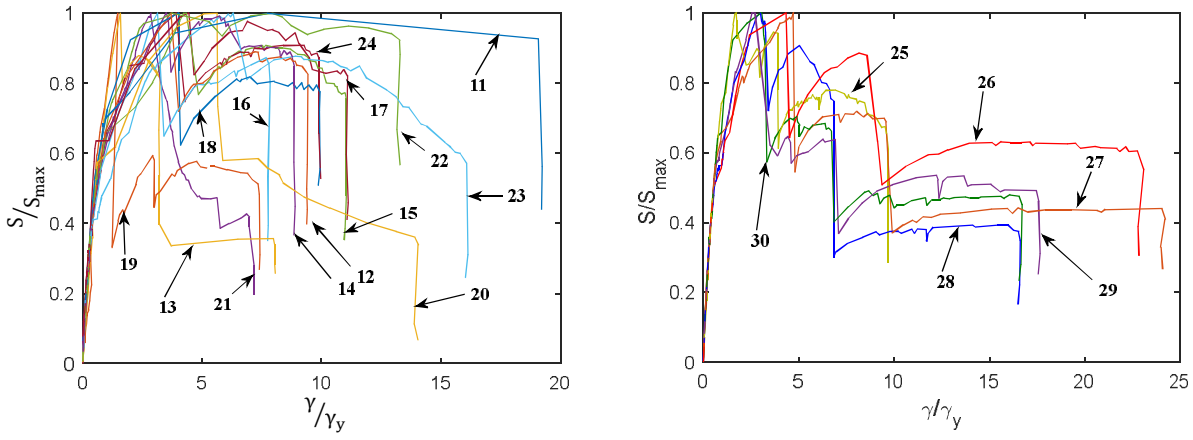

a.) Structural Fastener: Weld b.) Structural Fastener: Headed Shear Stud & Weld

Figure 6-3 Subassemblage Behavior of Cyclically Loaded Steel Deck Diaphragms with Concrete Fill

failure mode already limited the peak strength, proving assessment of a single failure mode to be not possible.

Shear studs ensure a strong composite connection between supporting steel frame and concrete fill which makes the shear transfer mechanism failure mode inapplicable. SDDCFs including shear studs (specimens 25, 26, 27, 28, 29, 30) failed either in diagonal tension cracking (specimens 25, 26, 29) or perimeter fastener failure (specimens 27, 28, 30), although the difference in terms of ductility was not substantial. Specimens reported as failing due to the shear transfer mode (e.g. 11, 14, 17) exhibited some of the largest ductilities. Conversely, specimens reported as experiencing diagonal tension cracking exhibited some of the smallest ductilities (e.g. 12, 13, 16, 18, 19, 24).

The average shear stiffness reported for SDDCFs with headed shear studs is 1670 kip/in. This marks an increase of approximately 7500% in shear stiffness compared to the weld/weld group cyclically tested without concrete fill, demonstrating the dramatic increase in shear stiffness due to the concrete fill. Average shear strengths and ductilities are also considerably larger for SDDCFs than their steel deck without concrete fill counterparts. For example, the SDDCFs with headed shear studs had an average ductility smaller than the specimens with no studs, but still exhibited an average subassemblage ductility of 3.82. This accounts for 38% increase in ductility from the group with the highest average ductility of the cyclically tested groups (i.e. PAF structural fasteners / screwed sidelap). A more in depth examination of the influence of several tests parameters on diaphragm behavior is available in the following section.

6.2 Effects of Certain Test Variables

General discussion on behavior was provided to compare the different classified groups to each other. While the combination of structural and sidelap fastener type was identified as the major classification for diaphragms without concrete fill, there are numerous variables that could have effected a specimen's behavior. This notion also applies to SDDCFs grouped on whether or not shear studs were used. This section intends to discuss the sources for such varied results of the previously classified groups, as shown by high standard deviations in Tables 6-1, 6-2 and 6-3. Variables identified to have a significant influence on a specimen's load-deformation results, with a focus on post-peak behavior and ductility, are specifically discussed here.

6.2.1 Power Actuated Fasteners and Arc Spot Welds

Two common deck to support fastener types include arc spot welds and power actuated fasteners. While PAFs typically offer less shear strength in comparison to an arc spot weld, the failure mechanisms for a PAF can allow for more ductile diaphragm behavior. Often, softening at sidelap connections allow for a redistribution of shear loads throughout the diaphragm, effectively increasing the demand on the structural fasteners. When PAFs are used, deck slotting can occur, especially for thinner deck. This will result in more ductile behavior than if the connections were to abruptly fracture, a failure mechanism more common to welded structural fasteners.

PAFs are commonly used in combination with sidelap screws, where screw tilting can occur. Sidelap screw tilting and deck slotting contribute to the ductile, yet pinched, hysteretic behavior for this type of system (for example, see Figure 6-4). For thicker decks, when tension pullout does not control, it is possible to see brittle fracture of the sidelap screws or PAFs control the ultimate strength, giving behavior with reduced ductility. For example, Beck (2008) Specimen 65 used 18 gauge deck and failed due to PAF shear fractures at endlaps (i.e. two overlapping

sheets, four at corners). However, at increasing post-peak shear angles, the activation of further sidelap screw tilting/opening and deck slotting still provided for a subassemblage ductility of μ_{sub} = 2.93 (Beck, 2008).

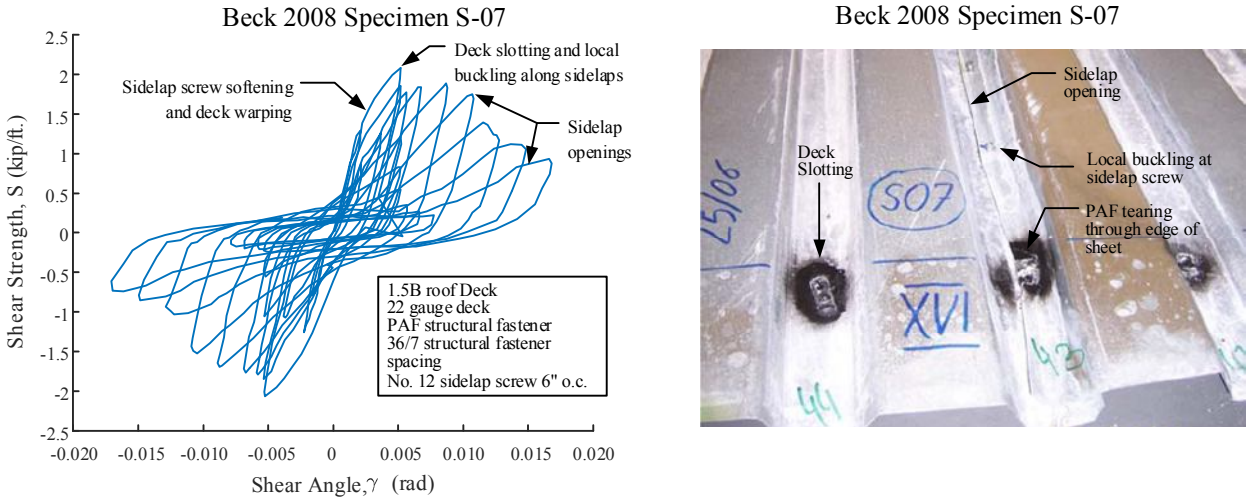

a.) Hysteretic data for PAF & Sidelap Screw Specimen

b.) PAF & Sidelap Screw Failure Mechanisms

Figure 6-4 PAF and Sidelap Screw Specimen [adapted from Beck (2008]

Figure 6-4a gives the load-deformation behavior for Beck 2008 Specimen S-07, where screw sidelap softening occurred prior to reaching the ultimate load limited by deck slotting of the 22 gauge deck against the PAF. Post-peak deformations were controlled mostly by excessive sidelap opening and PAF slotting, giving a subassemblage ductility μ_{sub} = 3.79 (Beck, 2008). Figure 6-4b shows deck slotting, sidelap opening, and even tearing of the PAF through the edge of the sheet at an overlapped structural fastener for the same specimen. When fastening multiple sheet overlaps into the steel support with a PAF, shear forces can cause edge tearing or tension pullout of fasteners.

Specimens with welds to the supports experienced limit states such as fracture and sheet tearing at welded connections, and slip at the sidelaps. Diaphragms with structural welds often used button punch sidelap connection that rely only on friction of the mechanical crimp. Due to the mechanical nature for this type of connection, there is no post-failure activation that may contribute towards ductile diaphragm behavior, contrasting diaphragms that use sidelap screws. Once failure of the structural welds occurred, often in rapid succession causing an 'unzipping' effect, there was a steep loss of load carrying capacity. It is shown, therefore, that ductility for welded diaphragms is not as sensitive to the type of sidelap fastener used. Although there are slight gains in ductility with mechanical sidelap fasteners, once failure occurs at support welds, sidelap fasteners are often not as relevant.

In an effort to isolate the effect of fastener type on ductility, a subset of 15 specimens was identified where the only major variable was the type of structural fastener used. All 15 specimens in this group included typical 1.5B roof deck with thicknesses of 20 or 22 gauge, deck span lengths between structural supports (L_v) of 5 ft, 36/4 structural fastener spacing configuration (i.e. 12 in. spacing o.c.), and monotonic loading. Table 6-4 gives the ductility for each specimen, grouped by structural fastener type (weld vs. PAF). Each specimen is given an index number, and the ductilities are graphically depicted in Figure 6-5.

Table 6-4 Ductility Comparison – Power Actuated Fasteners and Welds

Reference	Spec. ID	Index No.	Sub. Ductility, μ_{sub}	Reference	Spec. ID	Index No.	Subassemblage Ductility, μ_{sub}
Power Actuated Fastener[1]				**Arc Spot Weld**[1]			
Martin 2002	19	1	3.76	Pinkham 1999	36	7	2.28
Essa et al. 2003	5	2	3.11	Martin 2002	37	8	2.81
Essa et al. 2003	17	3	3.22	Essa et al. 2003	1	9	1.96
Yang 2003	39	4	3.44	Essa et al. 2003	9	10	2.99
Yang 2003	43	5	3.20	Essa et al. 2003	10	11	2.01
Yang 2003	44	6	3.25	Essa et al. 2003	11	12	2.33
				Yang 2003	41	13	3.02
				Yang 2003	47	14	2.23
				Yang 2003	49	15	2.58
Average			3.33				2.47
Std. Dev.			0.22				0.44

[1]*Structural fastener type*

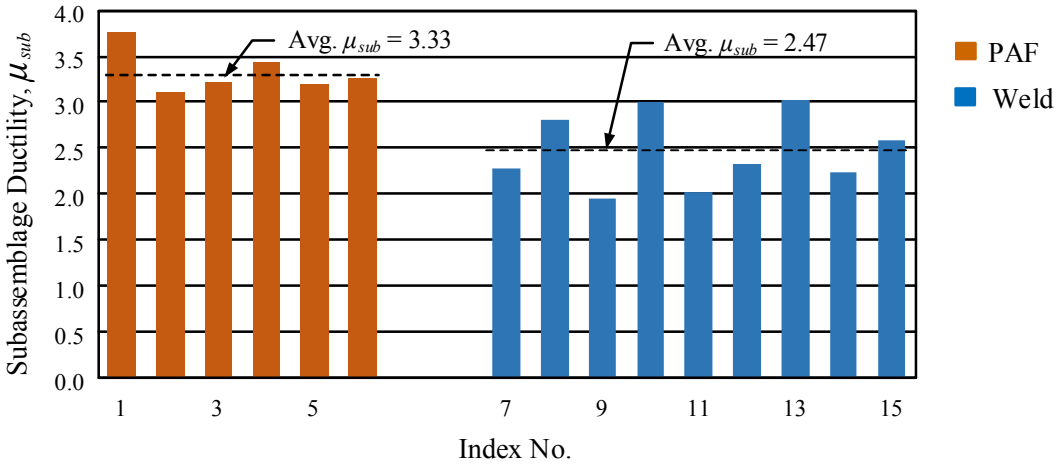

Figure 6-5 Ductility Comparison of Structural Fastener Types

The 9 specimens using arc spot welds as structural support fasteners had an average subassemblage ductility μ_{sub} = 2.47 with a standard deviation σ = 0.44. When PAF structural fasteners were used, ductility for the 6 grouped specimens increased by 35% to a value of μ_{sub} = 3.33. This is consistent with the trends observed in previous discussion, where ductility increases

when PAFs are used instead of welds. The low standard deviation for this group of σ = 0.22 reinforces the notion that diaphragms using mechanical fasteners result in consistent behavior.

6.2.2 Deck Thickness, Profile Geometry and Fastener Spacing

Selecting a thicker gauge steel will typically give higher shear strengths for steel deck diaphragms. Exceptions include diaphragms with fasteners that are not properly fastened through the thicker material at overlapping sheets. Welds through multiple sheets can have reduced effective weld diameters if the welding procedure is not adjusted to account for thicker sheets. This is especially true for endlaps, since the same welding procedure for a single sheet thickness is commonly used for the entire diaphragm. Similarly, for PAFs, fastener pullout may apply when multiple sheets are fastened by a single fastener.

For example, Pinkham (1999) Specimen 54 included 10 ft long panels, connected at endlaps to cover a length of 20 ft (Figure 6-6a). Thicker sheet material (t = 0.0480 in.) was used with structural weld fasteners that lacked proper penetration to the supports, most likely at the endlap, resulting in a steep drop in load at the peak strength and a subassemblage ductility of μ_{sub} = 3.43 (Martin, 2017). The same specimen was rewelded and tested as specimen R54, yielding a subassemblage ductility of 3.16. Because of adequate weld penetration, deck deformations allowed for more gradual post-peak strength degradation. Note that the decrease in ductility for specimen R54 with adequate weld penetration is a result of a smaller yield shear angle from the less stiff, retested specimen and is not necessarily characterized by the post-peak deformations alone, as shown in Figure 6-6b.

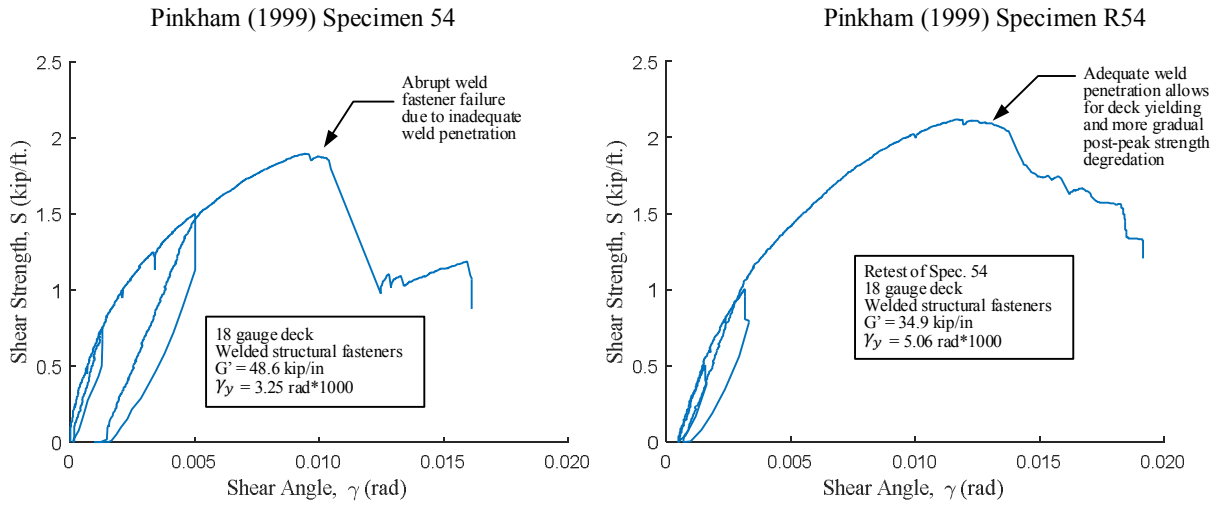

a.) Load-Deformation data for Pinkham 1999 Spec. 54 b.) Load-Deformation data for Pinkham 1999 Spec. R54

Figure 6-6 Effect of Inadequate Weld Penetration on Thicker Decks

The effects of different deck thicknesses and fastener spacings on ductility warrants a separate discussion. To isolate deck thickness as a variable, a group of specimens were identified with 1.5B deck, deck span length L_v = 5 ft, and monotonic loading as constants. To observe the influence of fastener spacing on ductility, this group was further subcategorized dependent on a 36/7 (10 specimens) or 36/4 (14 specimens) structural fastener spacing configurations. Whether welds or PAFs were used as structural fasteners is also noted. Deck thickness, fastener spacing and ductility for each of these specimens is reported in Table 6-5. Plots of the associated data are available in Figure 6-7.

Table 6-5 Ductility Comparison - Deck Thicknesses and Fastener Spacing

	Reference	Spec. ID	t^1 (in.)	μ_{sub}	Reference	Spec. ID	t^1 (in.)	μ_{sub}
36/7 Spacing[2]	**Power Actuated Fastener[3]**				**Arc Spot Weld[3]**			
	Martin 2002	30	0.0276	9.68	Pinkham 1999	35	0.031	4.12
	Martin 2002	32	0.0346	7.12	Pinkham 1999	51	0.031	5.43
	Beck 2013b	S-03	0.0350	2.25	Pinkham 1999	31	0.036	3.74
	Beck 2013	M-01	0.0465	3.16	Pinkham 1999	32	0.036	2.96
					Pinkham 1999	33	0.036	4.54
					Pinkham 1999	50	0.048	3.46
36/4 Spacing[2]	**Power Actuated Fastener[3]**				**Arc Spot Weld[3]**			
	Yang 2003	39	0.0276	3.44	Yang 2003	41	0.0280	3.02
	Yang 2003	43	0.0283	3.20	Yang 2003	47	0.0291	2.23
	Yang 2003	44	0.0283	3.25	Essa et al. 2003	1	0.0300	1.96
	Essa et al. 2003	5	0.0300	3.11	Essa et al. 2003	9	0.0300	2.99
	Martin 2002	19	0.0346	3.76	Essa et al. 2003	10	0.0300	2.01
	Essa et al. 2003	17	0.0360	3.22	Essa et al. 2003	11	0.0300	2.33
					Essa et al. 2003	15	0.0300	3.81
					Martin 2002	37	0.0339	2.81
					Yang 2003	49	0.0343	2.58
					Pinkham 1999	36	0.0360	2.28

[1] *Steel deck thickness; specimens arranged in order of increasing deck thickness for each group*
[2] *Structural fastener spacing configuration*
[3] *Structural fastener type*

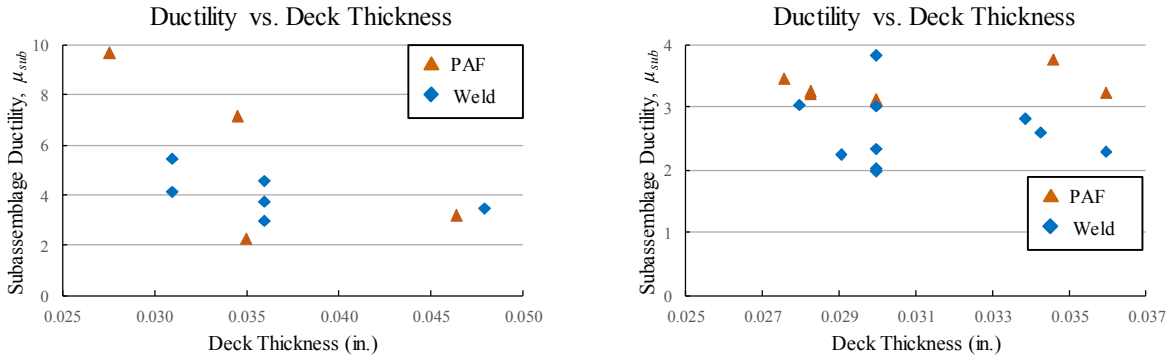

a.) Specimens with 36/7 structural fastener spacing

b.) Specimens with 36/4 structural fastener spacing

Figure 6-7 Ductility Comparison – Deck Thicknesses and Fastener Spacing

Specimens with thinner decks using a stronger fastener spacing configuration (e.g. 36/7 instead of 36/4) exhibited larger ductilities, likely due to ductile deck deformations contributing

more towards diaphragm behavior than fastener failure. This is especially true for specimens using PAFs. For example, Martin 2002 Specimens 30 and 32 used 20 and 22 gauge decks with a 36/7 PAF structural fastener configuration and experienced some of the largest ductilities (μ_{sub} = 9.68 and μ_{sub} = 7.12, respectively). Conversely, specimens in this group with thicker deck experienced lower ductilities.

When considering the lighter 36/4 fastener configuration, deck thickness did not noticeably influence diaphragm ductility, since fastener failure is more likely to contribute to diaphragm behavior than ductile deck deformations (Figure 6-7b). Because of this and the scatter of the limited data points, no conclusive relationship was determined between deck thickness and ductility for the lighter 36/4 fastener configuration. It is shown that a definitive range of ductilities between 1.96 and 3.81 is defined for 36/4 fastener spacings (Figure 6-7a). This range of subassemblage ductilities increases between 2.25 and 9.68 when considering the 36/7 fastener spacing suggesting increased ductility for diaphragms with smaller fastener spacings (this is most notable for thinner decks, as previously discussed and shown in Figure 6-7a). It is particularly noted that trends for higher ductilities when using PAF structural fasteners are consistent in these groups.

Deck profile geometry can also influence the warping of panels at panel ends. Deep deck profiles are used for the increased flexural resistance to gravity loads and often cover large spans. This increased flexural resistance often comes at a cost of in-plane shear stiffness, because deeper decks are more prone to lateral racking and shear distortions from in plane forces. The use of deep deck cellular profiles, where a flat sheet is attached to the bottom of the corrugated section, can increase the steel deck shear stiffness. Bagwell and Easterling (2008) studied deep deck and cellular deck wherein specimens 10 and 11 were 7.5 in. deep. Although these are not typical deck sections, they demonstrate that cellular deck can have large subassemblage ductility (μ_{sub} = 13.6

and 13.8) because they mitigate limit states associated with deck warping and buckling in favor of deformations at the support fasteners. In contrast, Bagwell and Easterling (2008) Specimen 9 used a similar deck without a flat sheet attached to the panel, resulting in a 77% decrease in ductility (μ_{sub} = 3.06).

6.2.3 Shear Studs

The inclusion of shear studs as a structural fastener for SDDCFs can dramatically influence diaphragm behavior. Shear studs provide a direct load path to and from the concrete and supporting steel frame and promote strong composite behavior. Perhaps the most influential aspect of using shear studs is the mitigation of the shear transfer failure mode, as previously discussed. SDDCFs with shear studs are therefore limited to perimeter fastener failure and diagonal tension cracking. Two distinct ranges of ductility are observed for SDDCFs dependent of failure mode and are depicted in Figure 6-8.

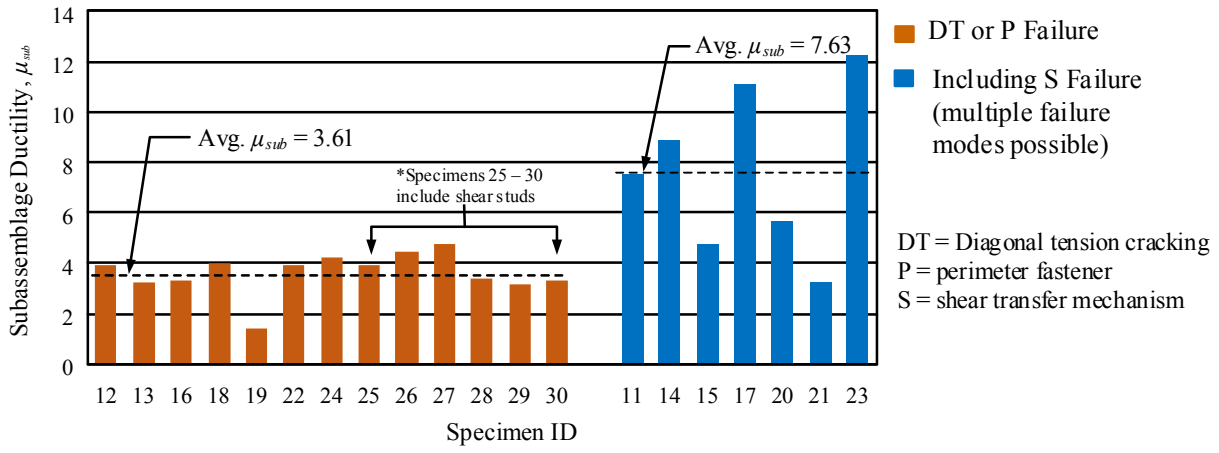

Figure 6-8 SDDCF Ductility Comparison – Failure Modes

Specimens failing in either diagonal tension (DT) cracking or perimeter fastener failure mode (P) had an average subassemblage ductility of 3.61 with a standard deviation of 0.80. Specimens 25 – 30 included shear studs. However, the influence of the shear studs on ductility is not clear, as ductility trends for specimens failing in either DT or P are consistent regardless if shear studs were used. For specimens failing in the shear transfer failure mode (S), there was a moderate drop in post-peak strength and subsequently higher ductilities. This is due to gradual deterioration and slip of the deck-concrete interfacial layer at increasing displacements, in contrast to sudden drops in load characteristic of diagonal tension cracking and perimeter fastener failure. Specimens reported to have failed only in the shear transfer failure mode (Specimens 11, 14, 17) experienced the largest subassemblage ductilities (7.53, 8.85, 11.1). As discussed earlier, this failure mode is not practical for design applications, and R_s values are calculated only for the specimens not failing in shear transfer.

Oher test variables are known to influence the strength and stiffness of SDDCFs, namely concrete compressive strength and concrete fill thickness. No conclusive trends between ductility and these variables were observed. Considering the shear transfer failure mode to be impractical, a well-defined range of subassemblage ductility between 3.13 and 4.76 is acknowledged for SDDCFs regardless of fastener types used. The sample size for SDDCFs that failed in diagonal tension that included headed studs is five specimens, only three of which were found to include complete load-deformation behavior. For this reason, further experimental research for this system utilizing studs is recommended.

6.3 Diaphragm Design Force Reduction Factors

Diaphragm design strengths are calculated in accordance with AISI S310 and DDM04, and allow for comparison to experimental strengths through the R_Ω factor needed for R_s calculations. Appendix A includes summary sheets of all the relevant input needed for the calculation of design strengths, as well as the corresponding subassemblage load-deformation data. The results in this section are grouped in the same manner as presented in Section 6.1. Note that the subset of 108 specimens with post-peak deformation data previously analyzed is reduced to 95 specimens. This reduction in data set is due to a number of specimens having irregularities not typical to conventional diaphragm construction. These irregular diaphragms include cellular deck diaphragms without concrete fill (Bagwell 2008, Specimens 10, 11, 13, 14, and 17), a retested specimen (Pinkham 1999, Specimen R54) and SDDCFs with failure modes including the shear transfer failure modes (Porter and Easterling 1988, Specimens 11, 14, 15, 17, 20, 21, and 23).

Table 6-6 and Table 6-7 present strength factors R_Ω, system ductilities μ, ductility factors R_μ and finally diaphragm design force reduction factors, R_s, for monotonic and cyclic loading respectively. The method used for calculating these variables is presented in Chapter 4. R_s calculations assume inelastic deformations concentrate at diaphragm ends equivalent to 10% of the span (i.e. $L_p / L = 0.10$) for steel deck diaphragms with and without concrete fill.

Essa et al. (2003) specimens 9, 10, 12 and 13 and Pinkham (1999) specimens 31-39 all include longitudinal standing seam sidelap welds that give relatively high sidelap fastener shear strength predictions with poor experimental diaphragm strength correlation; R_Ω for the majority of these specimens were comparatively low. There are a number of fabrication and construction considerations that draw to question the quality of these types of welds. Consider a welder standing over the standing seam of a sidelap connection. For this type of weld to reach its predicted values, a close interlock between the overlapping sheets is assumed. When the welder stands over the

sidelap seam, the interlocking panels undergo flexure and tend to separate, making quality assurance difficult. Deck fabrication widths must also be fabricated carefully such that the terminating, male edge of the deck profile is tall enough to properly fit within the interlocking, female edge of the adjacent deck to allow for a reliable weld (see dimension h_{st} in Figure 6-9). Martin (2002) specimens 22, 23 and 24 all include sidelap welds that utilize washers. This type of connection is now specified by AISI S310 to only be included in diaphragm construction as structural fasteners.

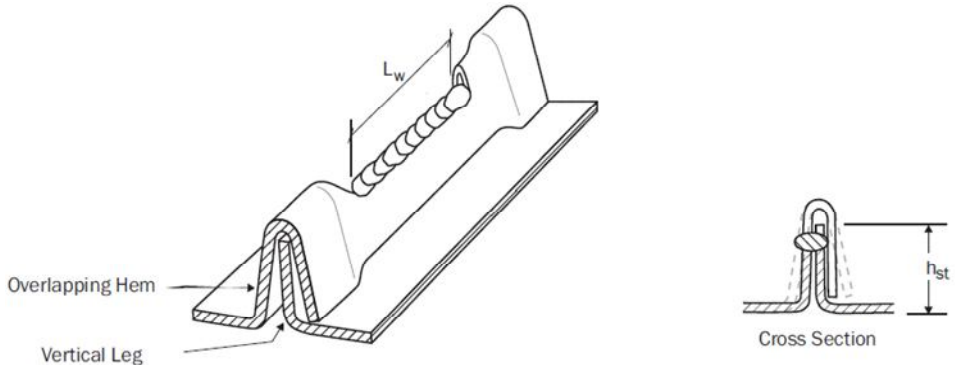

Figure 6-9 Standing Seam Sidelap Weld (AISI, 2016a)

Essa et al. (2003) specimens 15 and 16 included welds with washers as the structural fastener type. Specimens 11 and 14 included arc spot welds as structural fasteners. All four specimens had the same deck thickness, fastener spacings and sidelap connection types. R_Ω factors for specimens 15 and 16 were both 0.84, while specimens 11 and 14 were 1.36 and 0.98. This could suggest that the fastener nominal strengths for welds with washers are high or that the reliability of making a proper weld for this type of connection is low. Lower R_s values for weld with washer structural fasteners are consistent with lower R_Ω trends. R_s values for mechanically

fastened diaphragms trend in the same direction as previously discussed, with higher average values for ductility, ductility factor, and R_s then the remaining groups.

Table 6-6 System Ductilities, Strength Factors, Ductility Factors and R_s for Monotonically Loaded Steel Deck Diaphragm Specimens

Reference	Spec. ID	γ_y rad*1000	γ_{in} rad*1000	μ	R_Ω	R_μ Long T	R_μ Med. T	R_s Long T	R_s Med. T
PAF/Screw; n[1] = 19									
Martin 2002	19	3.93	10.9	2.10	1.15	2.10	1.79	2.42	2.06
Martin 2002	30	1.34	11.6	4.47	1.00	4.47	2.82	4.46	2.81
Martin 2002	32	1.51	9.22	3.45	1.23	3.45	2.43	4.25	2.99
Essa et al. 2003	5	4.02	8.48	1.84	0.95	1.84	1.64	1.74	1.55
Essa et al. 2003	17	3.61	8.00	1.89	1.01	1.89	1.67	1.90	1.68
Yang 2003	39	5.37	13.1	1.98	0.88	1.98	1.72	1.73	1.50
Yang 2003	43	4.94	10.8	1.88	1.10	1.88	1.66	2.06	1.82
Yang 2003	44	4.01	9.04	1.90	0.86	1.90	1.67	1.63	1.44
Bagwell 2007	7	3.42	6.79	1.79	1.34	1.79	1.61	2.41	2.16
Bagwell 2007	8	3.29	1.85	1.23	0.88	1.23	1.20	1.08	1.06
Bagwell 2007	9	10.8	22.3	1.82	0.82	1.82	1.63	1.50	1.33
Bagwell 2007	10	Cellular deck							
Bagwell 2007	11	Cellular deck							
Bagwell 2007	17	Cellular deck							
Beck 2008	63	2.80	9.49	2.36	1.33	2.36	1.93	3.13	2.56
Beck 2008	64	3.76	8.29	1.88	1.65	1.88	1.66	3.10	2.74
Beck 2008	65	3.87	7.45	1.77	1.61	1.77	1.59	2.85	2.56
Beck 2013a	M 01	4.81	10.4	1.86	1.47	1.86	1.65	2.74	2.43
Beck 2013a	M 02	4.51	9.93	1.88	1.34	1.88	1.66	2.53	2.23
Beck 2013a	M 03	9.21	11.2	1.49	0.99	1.49	1.41	1.48	1.40
Beck 2013b	S 02	4.70	8.98	1.76	1.13	1.76	1.59	1.99	1.79
Beck 2013b	S 03	6.57	8.20	1.50	1.41	1.50	1.41	2.12	2.00
Average		4.55	9.80	2.05	1.17	2.05	1.72	2.37	2.01
Std. dev.		2.23	3.73	0.72	0.25	0.72	0.35	0.87	0.55
Weld/BP[2]; n[1] = 8									
Pinkham 1999	32	3.47	6.81	1.78	1.35	1.78	1.60	2.42	2.17
Pinkham 1999	34	10.8	19.1	1.70	1.02	1.70	1.55	1.74	1.59
Pinkham 1999	36	12.4	15.9	1.51	1.43	1.51	1.42	2.16	2.04
Martin 2002	37	2.87	5.19	1.72	1.09	1.72	1.56	1.88	1.71
Essa et al. 2003	1	3.82	3.67	1.38	0.87	1.38	1.33	1.21	1.16
Yang 2003	41	4.96	10.1	1.81	0.90	1.81	1.62	1.62	1.45
Yang 2003	47	7.88	9.72	1.49	0.89	1.49	1.41	1.32	1.25
Yang 2003	49	6.89	10.9	1.63	0.83	1.63	1.51	1.35	1.25
Average		6.65	10.2	1.63	1.05	1.63	1.50	1.71	1.58
Std. dev.		3.31	4.89	0.14	0.22	0.14	0.10	0.40	0.35

[1] *n = number of tests in respective group*
[2] *"BP" for button punch*

Table 6-6 (b) System Ductilities, Strength Factors, Ductility Factors and R_s Factors for Monotonically Loaded Steel Deck Diaphragm Specimens

Reference	Spec. ID	γ_y rad*1000	γ_{in} rad*1000	μ	R_Ω	R_μ Long T	R_μ Med. T	R_s Long T	R_s Med. T
Weld/Screw; n[1] = 8									
Pinkham 1999	50	3.09	7.61	1.98	1.27	1.98	1.72	2.52	2.19
Pinkham 1999	51	3.07	13.6	2.77	0.94	2.77	2.13	2.61	2.01
Pinkham 1999	52	6.40	14.7	1.92	0.69	1.92	1.68	1.33	1.17
Pinkham 1999	53	2.37	9.13	2.54	0.89	2.54	2.02	2.27	1.80
Pinkham 1999	54	3.25	7.92	1.97	0.91	1.97	1.72	1.79	1.55
Pinkham 1999	54R	Retested specimen							
Essa et al. 2003	11	5.35	7.08	1.53	1.36	1.53	1.44	2.08	1.95
Essa et al. 2003	15	4.93	13.8	2.12	0.84	2.12	1.80	1.79	1.52
Bagwell 2007	12	11.4	3.27	1.11	0.99	1.11	1.11	1.10	1.10
Bagwell 2007	13	Cellular deck							
Bagwell 2007	14	Cellular deck							
Average		4.98	9.64	1.99	0.99	1.99	1.70	1.94	1.66
Std. dev.		2.94	4.03	0.52	0.22	0.52	0.32	0.54	0.40
Weld/Weld; n[1] = 14									
Pinkham 1999	31	3.37	9.24	2.10	1.01	2.10	1.79	2.13	1.81
Pinkham 1999	33	3.34	11.8	2.42	1.01	2.42	1.96	2.44	1.98
Pinkham 1999	35	3.75	11.7	2.25	0.89	2.25	1.87	2.01	1.67
Pinkham 1999	37	1.85	8.67	2.88	0.77	2.88	2.18	2.20	1.67
Pinkham 1999	38	9.10	20.2	1.89	0.65	1.89	1.67	1.23	1.09
Pinkham 1999	39	3.40	6.14	1.72	0.72	1.72	1.56	1.23	1.12
Pinkham 1999	40	3.33	10.9	2.31	1.36	2.31	1.90	3.13	2.58
Pinkham 1999	41	3.33	12.8	2.53	1.00	2.53	2.01	2.53	2.02
Pinkham 1999	42	9.46	11.9	1.50	0.83	1.50	1.42	1.25	1.17
Pinkham 1999	43	2.88	4.16	1.58	0.68	1.58	1.47	1.08	1.00
Pinkham 1999	44	8.28	8.08	1.39	1.12	1.39	1.33	1.56	1.50
Martin 2002	22	6.79	5.36	1.32	1.03	1.32	1.28	1.35	1.31
Essa et al. 2003	9	5.16	10.3	1.80	0.56	1.80	1.61	1.01	0.90
Essa et al. 2003	10	6.27	6.34	1.40	0.41	1.40	1.34	0.58	0.56
Average		5.02	9.83	1.93	0.86	1.93	1.67	1.70	1.46
Std. dev.		2.42	3.90	0.47	0.24	0.47	0.28	0.69	0.52

[1] *n = number of tests in respective group*

The average strength factor for the PAF/Screw monotonic group was 1.17, while the remaining groups with structural welds had lower values of 1.05, 0.99 and 0.86. This indicates that strength predictions for diaphragms using mechanical fasteners are conservative in comparison to diaphragms utilizing structural welds. The average strength factor value of 0.86 corresponds to diaphragms with welded sidelaps, where the sidelap predicted strengths may be overstated, as previously discussed.

Table 6-7 System Ductilities, Strength Factors, Ductility Factors and R_s Factors for Steel Deck Diaphragm Specimens – Cyclically Loaded

Reference	Spec. ID	γ_y rad*1000	γ_{in} rad*1000	μ	R_Ω	R_μ Long T	R_μ Med. T	R_s Long T	R_s Med. T
PAF/Screw; n[1] = 21									
Martin 2002	28	6.62	6.43	1.39	1.16	1.39	1.33	1.60	1.54
Martin 2002	29	5.02	1.52	1.12	1.11	1.12	1.11	1.25	1.24
Martin 2002	31	2.31	7.79	2.35	1.13	2.35	1.92	2.65	2.17
Martin 2002	33	1.75	8.14	2.86	1.26	2.86	2.17	3.61	2.74
Martin 2002	34	3.90	7.96	1.82	1.17	1.82	1.62	2.13	1.90
Martin 2002	35	3.71	2.18	1.24	1.19	1.24	1.21	1.47	1.45
Essa et al. 2003	8	4.38	8.67	1.79	1.01	1.79	1.61	1.81	1.63
Essa et al. 2003	18	3.39	10.2	2.20	1.14	2.20	1.84	2.50	2.10
Yang 2003	38	3.73	9.32	2.00	1.03	2.00	1.73	2.06	1.79
Yang 2003	40	6.95	8.30	1.48	0.98	1.48	1.40	1.45	1.38
Beck 2008	S 03	4.56	10.0	1.88	1.30	1.88	1.66	2.44	2.16
Beck 2008	S 04	6.37	8.97	1.56	1.48	1.56	1.46	2.32	2.16
Beck 2008	S 05	6.29	7.95	1.51	1.50	1.51	1.42	2.26	2.13
Beck 2008	S 06	4.92	8.64	1.70	1.41	1.70	1.55	2.41	2.19
Beck 2008	S 07	2.90	8.11	2.12	1.35	2.12	1.80	2.85	2.42
Beck 2008	S 08	3.53	2.27	1.26	1.26	1.26	1.23	1.58	1.55
Beck 2013a	C 01	7.03	6.22	1.35	1.49	1.35	1.31	2.02	1.95
Beck 2013a	C 02	5.31	7.55	1.57	1.39	1.57	1.46	2.18	2.03
Beck 2013a	C 03	8.42	11.8	1.56	0.94	1.56	1.46	1.47	1.37
Beck 2013b	S 02C	4.95	7.43	1.60	1.14	1.60	1.48	1.82	1.69
Beck 2013b	S 03C	6.88	7.40	1.43	1.43	1.43	1.36	2.04	1.95
Average		4.90	7.47	1.70	1.23	1.70	1.53	2.09	1.88
Std. dev.		1.71	2.54	0.41	0.17	0.41	0.25	0.54	0.38
Weld/BP[2]; n[1] = 6									
Martin 2002	20	3.33	1.71	1.21	1.06	1.21	1.19	1.28	1.26
Martin 2002	21	5.11	1.40	1.11	1.19	1.11	1.10	1.33	1.32
Martin 2002	36	3.99	1.82	1.18	0.63	1.18	1.17	0.74	0.73
Essa et al. 2003	2	3.50	1.56	1.18	0.82	1.18	1.16	0.96	0.95
Yang 2003	42	5.18	7.06	1.54	1.01	1.54	1.45	1.56	1.46
Yang 2003	48	9.47	1.46	1.06	0.86	1.06	1.06	0.91	0.91
Average		5.10	2.50	1.21	0.93	1.21	1.19	1.13	1.11
Std. dev.		2.08	2.04	0.16	0.18	0.16	0.12	0.28	0.26
Weld/Screw; n[1] = 2									
Essa et al. 2003	14	4.02	4.02	1.40	0.98	1.40	1.34	1.37	1.31
Essa et al. 2003	16	6.77	5.81	1.34	0.84	1.34	1.30	1.12	1.09
Weld/Weld; n[1] = 4									
Martin 2002	23	5.94	7.15	1.48	1.11	1.48	1.40	1.64	1.55
Martin 2002	24	7.09	2.87	1.16	1.06	1.16	1.15	1.23	1.22
Essa et al. 2003	12	4.25	6.89	1.65	0.53	1.65	1.52	0.87	0.80
Essa et al. 2003	13	6.58	6.56	1.40	0.37	1.40	1.34	0.52	0.50
Average		5.97	5.87	1.42	0.77	1.42	1.35	1.07	1.02
Std. dev.		1.07	1.74	0.18	0.32	0.18	0.13	0.42	0.40

[1] *n = number of tests in respective group*
[2] *"BP" for button punch*

Average R_s values (medium period) for cyclically tested diaphragms without concrete were 1.88, 1.11 and 1.02 for the PAF/Screw, Weld/BP and Weld/Weld groups respectively. This is consistent with monotonically tested diaphragms and further reiterates the positive influence on ductile diaphragm performance when mechanical fasteners are used.

Table 6-8 Strength, Ductility and R_s Factors for Specimens with Concrete Fill using DDM04 Strength Equation

Spec. ID	Failure Mode[1]	γ_y rad*1000	γ_{in} rad*1000	μ	R_Ω[2]	R_μ Long T	R_μ Med. T	R_s Long T	R_s Med. T
Welds; n[3] = 7									
12	DT	0.59	1.71	2.17	2.09	2.17	1.83	4.52	3.81
13	DT	0.69	1.54	1.89	2.55	1.89	1.67	4.82	4.25
16	DT	0.73	1.66	1.92	1.26	1.92	1.68	2.42	2.13
18	DT	0.56	1.71	2.21	1.87	2.21	1.85	4.13	3.45
19	DT	0.76	0.30	1.16	1.50	1.16	1.15	1.74	1.72
22	DT	0.53	1.56	2.18	1.96	2.18	1.83	4.27	3.59
24	DT	0.71	2.26	2.28	1.71	2.28	1.89	3.90	3.23
Average		0.65	1.53	1.97	1.85	1.97	1.70	3.69	3.17
Std. Dev.		0.08	0.55	0.36	0.39	0.36	0.238	1.07	0.85
Welds with Headed Shear Studs; n[3] = 6									
25	DT	0.58	1.69	2.17	2.09	2.17	1.83	4.52	3.81
26	DT	0.30	1.05	2.38	1.26	2.38	1.94	3.00	2.44
27	P	0.29	1.09	2.51	3.10	2.51	2.00	7.76	6.20
28	P	0.42	0.99	1.95	0.75	1.95	1.70	1.47	1.28
29	DT	0.40	0.85	1.85	1.40	1.85	1.64	2.58	2.29
30	P	0.42	0.95	1.91	0.62	1.91	1.68	1.19	1.05
Average		0.40	1.10	2.13	1.54	2.13	1.80	3.42	2.85
Std. Dev.		0.09	0.27	0.25	0.84	0.25	0.14	2.22	1.75
Total Average		0.54	1.33	2.04	1.70	2.04	1.75	3.56	3.02
Total Std. Dev.		0.15	0.49	0.32	0.66	0.32	0.20	1.71	1.35

[1] *DT = Diagonal Tension Cracking, P = Perimeter Fastener Failure*
[2] *Nominal compressive strength f'c = 3000 psi assumed*
[3] *n = number of tests in respective group*

Table 6-8 gives results for the SDDCF specimens tested in Porter and Easterling (1988) not failing in the shear transfer failure mode. Specimens are grouped according to whether headed shear studs were used. Note that strength factors in this table use the prescribed DDM04 design strength equations and not the recommended prediction equation as described in Section 5.2.3.

While there was considerable scatter in the concrete compressive strengths between specimens (2681 psi to 6187 psi), a nominal value of 3000 psi was assumed for the calculation of predicted nominal strengths. This caused higher standard deviations for R_Ω than if measured properties were used. Average R_Ω values of 1.85 and 1.54 and average R_s values (medium period) of 3.17 and 2.85 are given for SDDCFs without and with headed shear studs respectively. It is then observed that R_s factors for SDDCFs are considerably larger than diaphragms with no concrete fill from the strength factors alone.

Table 6-9 Strength, Ductility and R_s Factors for Specimens with Diagonal Tension Cracking Failure using Proposed Strength Equation

Spec. ID	Failure Mode[1]	γ_y rad*1000	γ_{in} rad*1000	μ	R_Ω[2]	R_μ Long T	R_μ Med. T	R_s Long T	R_s Med. T
Welds; n[3] = 7									
12	DT	0.59	1.71	2.17	1.34	2.17	1.83	2.90	2.44
13	DT	0.69	1.54	1.89	1.60	1.89	1.67	3.03	2.67
16	DT	0.73	1.66	1.92	1.10	1.92	1.68	2.10	1.85
18	DT	0.56	1.71	2.21	1.20	2.21	1.85	2.65	2.21
19	DT	0.76	0.30	1.16	1.05	1.16	1.15	1.22	1.21
22	DT	0.53	1.56	2.18	1.26	2.18	1.83	2.74	2.30
24	DT	0.71	2.26	2.28	1.20	2.28	1.89	2.74	2.27
Average		0.65	1.53	1.97	1.25	1.97	1.70	2.48	2.14
Std. Dev.		0.08	0.55	0.36	0.17	0.36	0.238	0.58	0.44
Welds with Headed Shear Studs; n[3] = 6									
25	DT	0.58	1.69	2.17	1.34	2.17	1.83	2.90	2.44
26[4]	DT	0.30	1.05	2.38	0.91	2.38	1.94	2.16	1.76
27	P	0.29	1.09	2.51	3.10	2.51	2.00	7.76	6.20
28	P	0.42	0.99	1.95	0.75	1.95	1.70	1.47	1.28
29	DT	0.40	0.85	1.85	1.02	1.85	1.64	1.90	1.68
30	P	0.42	0.95	1.91	0.62	1.91	1.68	1.19	1.05
Average		0.40	1.10	2.13	1.29	2.13	1.80	2.89	2.40
Std. Dev.		0.09	0.27	0.25	0.84	0.25	0.14	2.24	1.75
Total Average		0.54	1.33	2.04	1.27	2.04	1.75	2.67	2.26
Total Std. Dev.		0.15	0.49	0.32	0.58	0.32	0.20	1.59	1.24

[1] *DT = Diagonal Tension Cracking, P = Perimeter Fastener Failure*
[2] *Nominal compressive strength f'c = 3000 psi assumed*
[3] *n = number of tests in respective group*
[4] *Strength prediction calculated with lightweight factor λ = 0.75*

Table 6-9 provides alternative R_Ω values and subsequently R_s values for the same specimens designed with the recommended design equation that failed in the diagonal tension cracking mode. Note that diaphragms that failed in the perimeter fastener failure mode do not have alternative design equations; values for these specimens remain unaltered. Average R_Ω value of 1.20 (not shown in Table 6-9) for SDDCFs with diagonal tension cracking demonstrate much better agreement than the current SDI DDM04 designed specimens with R_Ω = 1.77 (not shown). While using more accurate prediction equations result in decreased R_s values, a more rational approach is gained and the resulting factors better represent the observed behavior of SDDCFs.

Table 6-10 provides a similar table as Table 6-8 and Table 6-9, except measured values for strength calculations are used. The primary difference in using measured values for prediction calculations is that measured concrete compressive strengths, rather than an assumed nominal 3000 psi concrete, is used. Measured fill thicknesses vs. nominal also contributed to this difference, but the effect is less. Because the yield shear angle, inelastic shear angle, and ductility do not change from previous tables, they are excluded in Table 6-10. Instead, Table 6-10 provides R_Ω, R_μ and R_s factors for SDDCFs using measured predicted strengths calculated per the DDM04 method and the recommended strength equation.

Table 6-10 Diaphragm Design Force Reduction Factors using Measured Input for Strength Calculations

Spec. ID	Failure Mode[1]	Using DDM04 Strength Equation					Using Proposed Strength Equation				
		R_Ω[2]	R_μ Long T	R_μ Med. T	R_s Long T	R_s Med. T	R_Ω[2]	R_μ Long T	R_μ Med. T	R_s Long T	R_s Med. T
Welds; n[3] = 7											
12	DT	1.88	2.17	1.83	4.07	3.43	1.24	2.17	1.83	2.68	2.26
13	DT	1.75	1.89	1.67	3.32	2.92	1.18	1.89	1.67	2.23	1.96
16	DT	1.19	1.92	1.68	2.28	2.00	1.05	1.92	1.68	2.02	1.77
18	DT	1.81	2.21	1.85	4.00	3.35	1.17	2.21	1.85	2.60	2.17
19	DT	1.44	1.16	1.15	1.67	1.66	1.05	1.16	1.15	1.22	1.20
22	DT	1.73	2.18	1.83	3.76	3.16	1.15	2.18	1.83	2.52	2.12
24	DT	1.40	2.28	1.89	3.19	2.64	1.02	2.28	1.89	2.32	1.92
Average		1.60	1.97	1.70	3.19	2.74	1.12	1.97	1.70	2.23	1.92
Std. Dev.		0.24	0.36	0.238	0.84	0.63	0.08	0.36	0.238	0.46	0.33
Welds with Headed Shear Studs; n[3] = 6											
25	DT	1.54	2.17	1.83	3.33	2.81	1.05	2.17	1.83	2.27	1.91
26[4]	DT	1.26	2.38	1.94	3.00	2.44	0.81	2.38	1.94	1.92	1.56
27	P	2.48	2.51	2.00	6.21	4.97	2.48	2.51	2.00	6.21	4.97
28	P	0.74	1.95	1.70	1.43	1.25	0.74	1.95	1.70	1.43	1.25
29	DT	1.40	1.85	1.64	2.58	2.29	1.03	1.85	1.64	1.91	1.69
30	P	0.61	1.91	1.68	1.16	1.02	0.61	1.91	1.68	1.16	1.02
Average		1.34	2.13	1.80	2.95	2.46	1.12	2.13	1.80	2.48	2.07
Std. Dev.		0.61	0.25	0.14	1.65	1.29	0.63	0.25	0.14	1.71	1.33
Total Average		1.48	2.04	1.75	3.08	2.61	1.12	2.04	1.75	2.34	1.99
Total Std. Dev.		0.47	0.32	0.20	1.29	1.00	0.43	0.32	0.20	1.21	0.94

[1] *DT = Diagonal Tension Cracking, P = Perimeter Fastener Failure*
[2] *Nominal compressive strength f'c = 3000 psi assumed*
[3] *n = number of tests in respective group*
[4] *Proposed strength prediction calculated with lightweight factor λ = 0.75*

Table 6-11 is a summary table for the 95 specimens with post-peak data and gives average R_s values for each group as reported in this section. Strength factors were calculated with and without resistance factors given in Section 5.5. Note that including the resistance factor in the design strength will increase R_Ω and subsequently R_s values. SDDCFs are further subcategorized on whether or not they were designed using the DDM04 or recommended strength equation, as well as if measured or nominal input was used for strength predictions. SDDCFs failing in shear transfer are not considered. Since only average values are reported and in an effort to avoid generalizing variable diaphragm behavior, only groups with four or more specimens are reported.

Table 6-11 Summary of Average R_s Values for all Groups

		Computed Rs values given as average values (std. dev.)									
		Not including resistance factors						Including resistance factors[1]			
		Monotonic Loading			Cyclic Loading			Monotonic Loading		Cyclic Loading	
	Diaphragm Condition	n[2]	Long T	Med T	n[2]	Long T	Med T	Long T	Med T	Long T	Med T
Without Concrete Fill	PAF/Screw	19	2.37 (0.87)	2.01 (0.55)	21	2.09 (0.54)	1.88 (0.38)	3.39 (1.25)	2.87 (0.78)	2.99 (0.78)	2.69 (0.54)
	Weld/BP	8	1.71 (0.40)	1.58 (0.35)	6	1.13 (0.28)	1.11 (0.26)	3.12 (0.72)	2.87 (0.64)	2.06 (0.51)	2.01 (0.47)
	Weld/Screw	8	1.94 (0.54)	1.66 (0.40)	U/A[6]			3.52 (0.98)	3.02 (0.72)	U/A[6]	
	Weld/Weld	14	1.70 (0.69)	1.46 (0.52)	4	1.07 (0.42)	1.02 (0.40)	3.08 (1.26)	2.65 (0.94)	1.94 (0.76)	1.85 (0.73)
With Concrete Fill[5]	DDM04 Nominal[3]	N/A[6]			13	3.56 (1.71)	3.02 (1.35)	N/A[6]		8.56 (2.39)	7.26 (1.77)
	DDM04 Measured[4]	N/A[6]				3.08 (1.29)	2.61 (1.00)	N/A[6]		7.26 (1.77)	6.17 (1.29)
	Proposed Nominal[3]	N/A[6]				2.67 (1.59)	2.26 (1.24)	N/A[6]		U/A[6]	
	Proposed Measured[4]	N/A[6]				2.34 (1.21)	1.99 (0.94)	N/A[6]		U/A[6]	

[1]*Resistance factors for PAF structural fasteners = 0.70, for welded structural fasteners = 0.55, for SDDCFs = 0.50*
[2]*Number of specimens in respective groups*
[3]*Predicted strengths calculated using nominal values*
[4]*Predicted strengths calculated using measured values*
[5]*SDDCF predicted strength calculated using either DDM04 strength equation or proposed strength equation*
[6]*"U/A" = unavailable, "N/A" = not applicable*

7 SUMMARY, CONCLUSIONS, AND RECOMMENDATIONS

7.1 Summary

The work described in this research is an important step toward characterizing inelastic behavior of steel deck diaphragms, with and without concrete fill. As our design methods evolve to better predict diaphragm demands during seismic events, it is increasingly important to understand the full load-deformation behavior of steel deck diaphragms. This understanding is also critical for accurate assessment of building behavior and associated performance based earthquake engineering. An alternate provision for diaphragm design in ASCE 7-16 permits inelastic deformations to occur in a building's diaphragm system through the use of a system specific diaphragm design force reduction factor, R_s. Yang (2003) notes that if diaphragms are designed as a ductile element of a LFRS (i.e. R_s values are used), then nonstructural components, especially gypsum boards for steel deck roof diaphragms, should be considered when determining forces transferred from the diaphragm.

In an effort to better understand steel deck diaphragm behavior, a database of 753 steel deck diaphragm test specimens was built. All information that may influence the load-deformation behavior of a test specimen, where available, was logged into the database. Furthermore, 108 of these specimens contained relevant post-peak load-deformation data to this study. As such, these curves were digitized and calculations were made to assess ductility and diaphragm behavior. Test result fields and calculated results are included in the database for the specimens with post-peak load-deformation behavior.

The current strength and stiffness prediction equations as available in DDM04 and AISI S310 were examined in Chapter 5. While predictions equations are well characterized for steel deck diaphragms without concrete fill, the more recent strength and stiffness equations for SDDCFs were closely examined. It was found that current strength predictions equations may be

overly conservative for SDDCFs failing in the diagonal tension mode, as given by a test-to-predicted ratio of 1.54. A strength equation for SDDCFs failing in diagonal tension cracking was proposed that more accurately represents the load resistance in a composite steel-deck diaphragm, and gave a test-to predicted ratio of 1.08. Test-to-predicted ratios are calculated for specimens failing in diagonal tension cracking from the landmark Iowa State Testing Program (Porter & Easterling, 1988). An alternative proposed stiffness equation to DDM04's stiffness equation was also derived. The proposed shear stiffness equation was calibrated to test results from all 32 ISU SDDCF specimens, as shown by an average test-to-predicted shear stiffness value of 1.02. Average shear stiffness test to predicted values using the DDM04/AISI S310 gave a value of 0.46. It is shown that the proposed equations result in a 46% and 52% improvement in predicting experimental strength and stiffness, respectively. Reduced variability when using the recommended prediction equations is noted. Resistance factors for the proposed strength equation for SDDCFs were also investigated.

A method was developed in Chapter 4 to use load-deformation behavior from the cantilever tested specimens with post-peak data to calculate diaphragm design force reduction factors, R_s. A system ductility expression was derived and was shown to be dependent on cantilever test data (S_{max}, G', γ_u) and the ratio of L_p / L (with L being the diaphragm span dimension). A simply supported diaphragm model, where diaphragm inelastic deformations concentrate at span ends over length L_p, was developed to convert diaphragm subassemblage ductility to diaphragm system ductility. After reviewing load-deformation data and considering experimental results that reported metrics for L_p / L (Cohen et al., 2004; Franquet, 2009; Massarelli, 2010), L_p / L was taken as 10% for diaphragms with and without concrete fill. System ductility was therefore completely defined, allowing for calculation of R_s factors.

Subassemblage test results, with a focus on ductility are presented and discussed in Chapter 6. Several test variables were discussed with respect to inelastic load-deformation behavior. Using results from subassemblage tests, R_s values were calculated. Of the 108 specimens identified with post-peak load-deformation behavior, 15 specimens were deemed impractical due to construction irregularities outside the scope of this research. As such, a subset of 95 specimens were used for the calculation of R_s factors.

7.2 Conclusions

A conclusive observation was that diaphragms without concrete fill using PAF structural fasteners in combination with sidelap screws resulted in consistently higher ductilities than if welded structural fasteners were used. This is especially true for diaphragms using thinner gauge decks with small fastener spacings, as ductile deck deformations (such as deck slotting) at the PAFs and sidelap softening (due to screw tilting) can contribute to higher ductilities. The effect of fastener spacing on ductility was less conclusive, although it was shown that fasteners with smaller spacings could have a larger range of ductility, dependent on the deck thinness used.

No correlation between structural fasteners and ductility was found for SDDCFs. Instead, the type of limit state exhibited by the SDDCF influenced ductility, with SDDCFs failing in diagonal tension cracking or perimeter fastener failure have average subassemblage ductility of 3.61. SDDCFs failing in the shear transfer limit state had higher ductilities (avg. μ_{sub} = 7.63). However, the shear transfer failure mode was deemed impractical, as a set of specific and highly atypical construction conditions must apply. It is noted, however, that shear studs will dismiss the possibility of shear transfer failure, and thus ensured subassemblage ductilities values conforming to ranges found from the perimeter and diagonal tension failure modes (μ_{sub} = 3.13 to 4.76).

Previously discussed trends were consistent with R_s calculations, in that diaphragms utilizing PAFs and screws exhibited the highest R_s values of 2.01 and 1.88 (medium period) for

the monotonically and cyclically tested groups, respectively. When using welded structural fasteners, these values dropped to as low as 1.02. This reiterates a diaphragm with mechanical fasteners can exhibit more ductile behavior than a welded diaphragm. Furthermore, when concrete fill was placed on top, R_s values mostly ranged from 2 to 4, dependent on the method used to calculate SDDCF design strength.

It is imperative to understand the ductile behavior of steel deck diaphragms to ensure efficient and safe seismic design for steel framed building. Diaphragm design force reduction factors offer key insight as to how a diaphragm may behave in a seismic event. R_s values for steel deck diaphragms with and without concrete fill larger than 1 demonstrate a diaphragm's ability to either exceed its design strength and exhibit ductile deformations, or both. This could be a very important factor as to why steel framed buildings with these types of diaphragms survived large earthquakes without the types of collapses observed in precast concrete diaphragms.

7.3 Recommendations

The following numbered items recommend future research to better understand the behavior of steel deck diaphragms, as mentioned throughout this research.

1.) Steel deck diaphragms with concrete fill literature is limited. Furthermore, several past experiments remain proprietary. While the Iowa State University testing program examined the effects of certain test variables on diaphragm strength and stiffness, a large amount of resources was spent on understanding the shear transfer limit state, which was later concluded to be impractical for the overwhelming majority of composite diaphragm systems in use today. Only 8 of the 32 specimens included headed shear studs, often implemented in irregular spacing patterns. It is therefore recommended that tests on SDDCFs utilizing regular fastener patterns including shear studs be further examined.

2.) In the past, the majority of diaphragm testing has used a cantilever set up. While this may be adequate for characterizing strength and stiffness, it presents its own challenges when examining ductile diaphragm behavior. Namely, cantilevered diaphragms will have inelastic deformations distributed throughout the field of the diaphragm. In a real diaphragm system, inelastic deformations localize at span ends. Cantilever diaphragm tests, therefore, make it difficult to determine the zone of inelasticity, characterized as L_p in this research, for realistic diaphragm systems. As such, further testing is recommended utilizing simply supported setups on either shake tables or with ground motion excitations applied at diaphragm ends. Adding mass to the system will results in dynamic loads characteristic of seismic demands and allow for better quantification for L_p / L. The effects of diaphragm geometry, such as varying aspect ratios and irregularities is also recommended to be studied, as this may have an impact on diaphragm ductility.

3.) A method was described in Section 4.3.2 using cantilever diaphragm load-deformation behavior to determine an L_p / L ratio. If this method is to be further pursued, an 'equal energy' calibration technique for the variable α is shown below in Figure 7-1, such that A_1 and A_2 are equal. This method can be repeated for all load-deformation curves in an attempt to define L_p / L. Note that using this method will redefine the yield shear angle and inelastic shear angle used in the system ductility equation (Eq. 4.16).

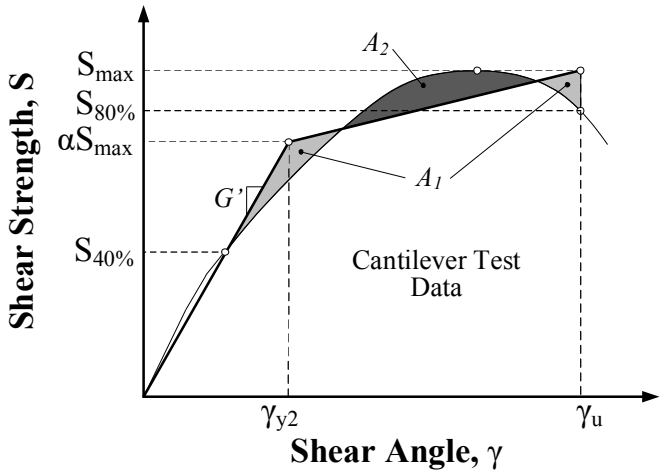

Figure 7-1 Calibration of α

4.) Welded sidelap connections, when constructed correctly, can offer significant strength in comparison other sidelap connection types. This may lead a designer to choose sidelap welds over sidelap screws or button punch connections. Test to predicted diaphragm shear strength for diaphragms using top seam welds as sidelap connections have considerably high variability. Often, the predicted strength is less than 50% of the tested strength. This may be due to improper contact between male and female edges of a standing seam deck, as discussed in Section 6.3. Therefore, connection tests simulating 'in the field' conditions and a reevaluation of prediction equations for this type of connection is recommended.

5.) AISI S310 offers a method to calculate resistance factors for diaphragms given adequate test data is available. For these calculations, AISI S310 prescribes calibration factors for SDDCFs that may be more appropriate to connection related limit states, rather than the proposed diagonal tensions cracking limit state which can be thought of as a member limit state. Reliability studies as discussed in Section 5.5.2 are recommended to evaluate whether these calibration values are appropriate for SDDCFs limited by failure of concrete in diagonal tension cracking.

8 REFERENCES

ABK, A Joint Venture. (1981). Methodology for mitigation of seismic hazards in existing unreinforced masonry buildings: diaphragm testing. *Report No. ABK-TR-03.*

ACI. (2014). Building code requirements for structural concrete *(ACI 318-14)* and commentary *(ACI 318R-14)*. American Concrete Institute.

AISC. (2010). Specification for structural steel buildings, *(AISC 360)*. American Iron and Steel Institute.

AISI. (2013a). Test standard for cantilever test method for cold-formed steel diaphragms*, (AISI S907)*. American Iron and Steel Institute.

AISI. (2013b). North American standard for the design of profiled steel diaphragm panels, *(AISI S310-13)*. American Iron and Steel Institute.

AISI. (2016a). North American specification for The design of cold-formed steel structural members, *(AISI S100).* American Iron and Steel Institute.

AISI. (2016b). North American standard for the design of profiled steel diaphragm panels*, (AISI S310-13).* American Iron and Steel Institute.

Ameen, A. (1989). Performance of cold-formed steel shear diaphragms with z-angle end closures. Master's thesis, West Virginia University.

Applied Technology Council. (1995). ATC-19: Structural response modification factors. Applied Technology Council, Redwood City, California.

Army, Navy and Air Force. (1982). Seismic design for buildings, *(Tri-services Manual)*. *Report No. Army TM 5-809-10*, Washington, D.C.: U.S. Government Printing Office.

ASCE. (2010). ASCE 7-10: Minimum design loads for buildings and other structures. American Society of Civil Engineers, Reston, Virginia.

ASCE. (2016). ASCE 7-16: Minimum design loads for buildings and other structures. American Society of Civil Engineers, Reston, Virginia.

Bagwell, J., and Easterling, W. (2008). Deep deck and cellular deck diaphragm strength and stiffness evaluation. *Report No. CEE/VPI-ST – 08/03*, Virginia Tech.

Beck, H. (2008). Inelastic cyclic diaphragm tests with Hilti powder-actuated fastener X-EDNK-22 THQ12M. *Report No. XE_08_10,* Technical Center of Hilti Corporation, Liechtenstein.

Beck, H. (2013a). Inelastic cyclic diaphragm tests with Hilti powder-actuated fastener X-ENP-19 L15. *Report No. XE_13_64,* Technical Center of Hilti Corporation, Liechtenstein.

Beck, H. (2013b). Inelastic cyclic diaphragm tests with hilti powder-actuated fastener X-HSN 24. Report No. *XE_13_162,* Technical Center of Hilti Corporation, Liechtenstein.

Bryan, E. (1975). Calculation of sheet steel diaphragms in the U.K. in research and developments in cold-formed steel design and construction. *International Specialty Conference on Cold-Formed Steel Structures*, pp. 491–533.

Cohen, G., Klingner, E., Hayes, J., and Sweeney, S. (2004). Seismic evaluation of low-rise reinforced masonry buildings with flexible diaphragms: I. *Seismic and quasi-static testing. Earthquake Spectra*, 20(3), pp. 779–802.

Chatterjee, A., (2016). Structural system reliability with application to light steel-framed buildings. Dissertation, Virginia Tech.

Davies, J., and Fisher, J. (1979). The diaphragm action of composite slabs. *Proceedings of the Institute of Civil Engineers*, 67(4), pp. 891–906.

Earls, C., and Murray, T. (1991). Cantilever Diaphragm Tests - Whirlwind Steel Buildings. *Report No. CE/VPI-ST-91/07*, Virginia Tech.

Easterling, W. S. (1987). Analysis and design of steel-deck-reinforced concrete diaphragms. Dissertation, Iowa State University.

Easterling, W. S., and Porter, M. (1988). Composite diaphragm behavior and strength. *9th International Specialty Conference on Cold-Formed Steel Structures*, pp. 387–404

Easterling, W. S., and Porter, M. (1994a). Steel-deck-reinforced concrete diaphragms. I. *Journal of Structural Engineering*, 120(2), pp. 560–576.

Easterling, W. S., and Porter, M. (1994b). Steel-Deck-Reinforced Concrete Diaphragms. II. *Journal of Structural Engineering*, 120(2), pp. 577–596.

EERI (1996). Northridge Earthquake Reconnaissance Report, Vol. 2 Earthquake Spectra - Supplement C to Volume 11 Earthquake Engineering Research Institute.

Ellifritt, S., and Luttrell, L. (1971). The Strength and stiffness of steel deck subjected to in-plane loading. *Report No. 2011*, West Virginia University.

Essa, H., Rogers, C., and Tremblay, R. (2003). Behavior of roof deck diaphragms under quasistatic cyclic loading. *Journal of Structural Engineering*, 129(12), pp. 1658–1666.

FEMA. (2009). Quantification of building seismic performance factors, *(FEMA P695)*. Applied Technology Council, Federal Emergency Management Agency.

Fleischman, R., and Farrow, K. (2001). Dynamic behavior of perimeter lateral-system structures with flexible diaphragms. *Earthquake Engineering & Structural Dynamics*, 30(5), pp. 745–763.

Fleischman, R., Naito, C., Restrepo, J., Sause, R., and Ghosh, S. (2005). Seismic design methodology for precast concrete diaphragms. Part 1: Design framework. *Precast Concrete Institute Journal*, 50(5), pp. 68–83.

Foster, T. (2008). Full scale tests of steel deck roof and floor diaphragms fastened with Hilti power actuated fasteners and self-drilling tapping screw fasteners. *Report No. STQA50098*, Hilti Inc.

Foster, T. (2013). Full scale tests of steel deck roof and floor diaphragms fastened with Hilti X-HSN 24 power-driven fasteners and Hilti S-SLC sidelap fasteners pursuant to ICC-ES AC43. *Report No. STQA50406*, Hilti Inc.

Foster, T. (2014). Full scale tests of steel deck roof and floor diaphragms fastened with Hilti X-HSN 24 power-driven fasteners and Hilti S-SLC sidelap fasteners pursuant to ICC-ES AC43. *Report No. STQA50406.3*, Hilti Inc.

Franquet, J. (2009). Seismic design repair and retrofit strategies for steel roof deck diaphragms. Master's thesis, McGill University.

Fukuda, Y., Watanabe, S., Togawa, T., Kami, H., Yoshimura, K., Kikuchi, K., and Yoshida, K. (1991). Seismic in-plane resistance of steel-deck concrete composite slabs with a bottomless trench duct. *Proceedings from the Third International Conference on Steel-Concrete Composite Structures*, pp. 473–478.

Galambos, T. (1990) System reliability and structural design. *Structural Safety*, 7(2-4), pp. 101–108.

Hankins, S., Easterling, W. S., and Murray, T. (1992). Vulcraft 1.5BI cantilever diaphragm tests. *Report No. CE/VPI-ST-92/01*, Virginia Tech.

Kircher, C., and Heintz, J. (2008). Overview and key concepts of the ATC-63 methodology. *Proceedings of 2008 ASCE-SEI Structures Congress*, Vancouver, B.C., pp. 1–10.

Lacap, D. A. (1971). Diaphragm test 3" V-32" deck with 2 ½ lightweight concrete. Inland Ryerson Construction Products Company Research Laboratory, Milwaukee, Wisconsin.

Liu, Y., Zhang, Q., and Qian, W. (2007). Testing and finite element modeling of stressed skin diaphragms. *Steel and Composite Structures*, 7(1), pp. 35–52.

Luttrell, L. (1967). Strength and behavior of light-gage steel shear diaphragms. Cornell University Engineering Research Bulletin 67-1, Ithaca, New York.

Luttrell, L. (1971). Shear diaphragms with lightweight concrete fill. *Presented at the 1st International Specialty Conference on Cold Formed Steel Structures*, pp. 111–117.

Luttrell, L. (1979a). Shear diaphragm tests using E.G. Smith Panels. Report, West Virginia University.

Luttrell, L. (1979b). Steel shear diaphragms using Ramset 55 B58 powder actuated fasteners. Report, West Virginia University.

Luttrell, L. (1981a). Steel Deck Institute diaphragm design manual , 1st Edition, *(DDM01)*.

Luttrell, L. (1981b). Steel shear diaphragms with Pneutek pin connections. *Report No. 2018-L*, West Virginia University.

Luttrell, L. (1984). Steel shear diaphragms using Ramset 26SD powder actuated fasteners. *Report No. 2046-L*, West Virginia University.

Luttrell, L. (1985). Steel shear diaphragms using Hilti ENP2-21L15 fasteners. *Report No. 2059-L*, West Virginia University.

Luttrell, L., and Winter, G. (1965). Structural performance of light gage steel diaphragms. *Report No. 319*, Cornell University.

Luttrell, L., Mattingly, J., Schultz, W., and Li, D., (2006). Steel Deck Institute diaphragm design manual, 3rd Edition, *(DDM03)*. Fox River Grove, Illinois.

Luttrell, L., Mattingly, J., Schultz, W., and Sputo, T., (2015). Steel Deck Institute diaphragm design manual - 4th Edition, *(DDM04)*. Glenshaw, Pennsylvania.

Martin, É. (2002). Inelastic response of steel roof deck diaphragms under simulated dynamically applied seismic loading. Master's thesis, Ecole Polytechnique de Montreal.

Martin, J. (2017). Personal communication, March 30, 2017.

Massarelli, R. (2010). Dynamic behavior and inelastic performance of steel roof deck diaphragms. Master's Thesis, McGill University.

Massarelli, R., Franquet, J., Shrestha, K., Tremblay, R., & Rogers, C. (2012). Seismic testing and retrofit of steel deck roof diaphragms for building structures. *Thin-Walled Structures*, *61*, pp. 239–247.

Mattingly, J. (2016). Personal communication, August 29, 2016.

NEHRP. (2015). Recommended seismic provisions for new buildings and other structures. *FEMA Report No. P-1050-1*, National Earthquake Hazards Reductions Program.

Neilsen, M. (1984). Effects of gravity load on composite floor diaphragm behavior. Master's thesis, Iowa State University.

Newmark, N., and Rosenblueth, E. (1971). Fundamentals of earthquake engineering. Englewood Cliffs, N.J: Prentice-Hall.

Nilson, A. (1960). Shear Diaphragms of Light Gage Steel. *Journal of the Structural Division*, 86(11), pp. 111–140.

Nilson, A. (1969). H.H. Robertson DC Deck used in shear diaphragms. Report, Cornell University.

Pinkham, C. (1997). Data from testing of Verco Decking, personal communication from Jeff Martin, Verco Manufacturing, obtained: March, 2017.

Pinkham, C. (1999). Data from testing of Wheeling High Strength Decking, personal communication from Jeff Martin, Verco Manufacturing, obtained: March, 2017.

Pinkham, C. (2008a). Data from testing of Wheeling High Strength Decking, personal communication from Jeff Martin, Verco Manufacturing, obtained: March, 2017.

Pinkham, C. (2008b). Data from testing of Wheeling High Strength Decking, personal communication from Jeff Martin, Verco Manufacturing, obtained: March, 2017.

Porter, M., and Easterling, W. (1988). Behavior, analysis, and design of steel-deck-reinforced concrete diaphragms. *Report No. ISU-ERI-Ames-88305 Project 1636*, Iowa State University.

Porter, M., and Greimann, L. (1980). Seismic resistance of composite floor diaphragms. *Report No. ISU-ERI-AMES-80133*, Iowa State University.

Porter, M., and Greimann, L. (1982). Composite steel deck diaphragm slabs - design modes. *6th International Specialty Conference on Cold-Formed Steel Structures*, pp. 467–484.

Prins, M. D. (1985). Elemental tests for the seismic resistance of composite floor diaphragms. Master's thesis, Iowa State University.

Pugh, A., and Murray, T. (1991). Cantilever diaphragm tests - Chief Industries CS Roof, AP and CS Wall Panels. *Report No. CE/VPI-ST-91/05*, Virginia Tech.

Rodkey, R., and Murray, T. (1993). Cantilever diaphragm tests - Steelox Systems TL-3. *Report No. CE/VPI-ST-93/02a*, Virginia Tech.

Rodriguez, M., Restrepo, J., and Blandón, J. (2007). Seismic design forces for rigid floor diaphragms in precast concrete building structures. *Journal of Structural Engineering*, 133(11), pp. 1604–1615.

Sabelli, R., Sabol, T., and Easterling, W. (2010). Steel deck and concrete-filled diaphragms; a guide for practicing engineers. *NEHRP Seismic Design Technical Brief No. 5.*

S. B. Barnes and Associates. (1957). Report on test program of Milcor steel floor and roof decks in horizontal diaphragm action.

S.B. Barnes and Associates. (1961). Report on Inland steel products company roof decks using a cover of lightweight concrete roof fill.

S. B. Barnes and Associates. (1962). Report on the analysis of tests of roof systems using Bethlehem slabform and lightweight insulating concrete to determine their adequacy as horizontal diaphragms.

S. B. Barnes and Associates. (1966). Report on concrete filled hi-bond steel deck diaphragms for the Inland Steel Products Company.

S. B. Barnes and Associates. (1967). Report on analysis of Inland Ribform Deck with lightweight concrete roof fills action as horizontal diaphragms.

Schafer, B. (2016). *What is the steel diaphragm innovation initiative?* Retrieved from http://steeli.org/?p=1

Schafer, B. (2017). Personal communication, April 26, 2017.

Schoettler, M., Belleri, A., Zhang, D., Restrepo, J., and Fleishman, R. (2009). Preliminary results of the shake-table testing for the development of a diaphragm seismic design methodology. *Precast Concrete Institute Journal*, 54(1), pp. 100–124.

Shimizu, N., Kanno, R., Ikarashi, K., Sato, K., and Hanya, K. (2013). Cyclic behavior of corrugated steel shear diaphragms with end failure. *Journal of Structural Engineering*, 139(5), pp. 796–806.

Tremblay, R., Martin, É., Yang, W., and Rogers, C. (2004). Analysis, testing and design of steel roof deck diaphragms for ductile earthquake resistance. *Journal of Earthquake Engineering*, 08(05), pp. 775–816.

Widjaja, B. (1993). Analytical investigation of composite diaphragms strength and behavior. Master's thesis, Virginia Tech.

Yang, W. (2003). Inelastic seismic response of steel roof deck diaphragms including effects of non-structural components and end laps. Master's thesis, Université de Montréal.

APPENDIX A – SUMMARY DATA SHEETS USED IN R_S CALCULATIONS

The following notes and assumptions are applicable to all following summary sheets, unless otherwise noted:

1. 60 ksi electrode classification is used for all weld strengths
2. Backbone curve extracted from hysteretic data corresponds to quadrant of load-deformation plot with the peak strength
    a. Load-deformation plots reaching peak strengths in the reversed cyclic direction are formatted so that backbone curves appear in the first quadrant
3. Hystereses with a large displacement step between consecutive cycles will use a backbone envelope instead of a traditional, peak-to-peak backbone curve
4. There are slight inaccuracies that result from digitized load-deformation curves, especially for references reported with low resolution figures or noisy data. For R_Ω calculations reported in Chapter 6, the published experimental peak strength from past literature was used. However, summary sheets in this appendix report experimental results from the digitized data
    a. Difference is noted for specimens where error between digitized vs. reported peak strengths are larger than 2.5%
5. AISI S310 and DDM04 both report methods for calculated predicted fastener shear strengths. When these two methods differ, unless otherwise noted, DDM04 expressions are used in prediction calculations
6. Endlaps shown are overlapped and not butted
7. Modulus of elasticity used for steel sheets is 29,500 ksi
8. Poisson's ratio for steel deck is 0.3

Easterling (1987) - Specimen 12

Input	Nominal	Measured
Structural Fastener Type	Arc Spot Weld	-
Sidelap Fastener Type	Seam Weld	-
Deck thickness, t (in.)	0.062	-
Panel Length, l (ft.)	15	-
Panel Span, l_v (ft.)	15	-
No. of sidelap connections per one edge of interior panel length, n_s	13	-
No. of structural fasteners along one edge panel	60	-
No. of structural fasteners along one depth perimeter member (b dimension)	60	-
No. of interior supports per panel length, n_p	0	-
Yield strength of deck, F_y (ksi)	33	40.4
Ultimate strength of deck, F_u (ksi)	45	53.2
Diamter of arc spot weld (in.)	0.75	-
Concrete compressive strength f'_c (psi)	3000	3412
Unit weight of concrete, w_c (pcf)	145	145
Slab thickness bottom steel flute to top of fill, (in.)	5.5	5.59

Fastener Strengths and Flexibilities	Nominal	Measured
Structural fastener strength, P_{nf} (kip)	4.22	4.99
Sidelap fastener strength, P_{ns} (kip)	5.75	6.48
Structural fastener flexibility, S_f (in/kip)	0.0046	-
Sidelap fastener flexibility, S_s (in/kip)	0.0045	-

Calculated Strength Equations Variables	Nominal	Measured
Structural concrete strength factor per DDM04, k	0.0030	-
Interior panel fastener contribution factor, β	16.4	16.0
Structural fastener distribution factor at panel ends, α_e^2	2.05	-
Transformed total thickness with deck contribution, t_e (in.)	4.27	4.33
Shear modular ratio of steel deck to concrete, n	9.35	8.76
Developed flute width, s (in.)	15.8	-
Fastener slip coefficient, C	3.59	-
Fastener slip coefficient w/o sidelap flexibility, C_2	7.92	-
DDM04 stiffness contribution of concrete fill, k_3 (kip/in)	2091	2382
Stiffness contribution of concrete fill for proposed eq., k_4 (kip/in)	1121	1214

Predicted Shear Strength and Stiffness	Nominal	Measured
Lesser shear strength of perimeter structural fasteners in either orthogonal direction, (kip/ft)	16.9	20.0
Shear strength of composite diaphragm excluding perimeter fastener limit per DDM04, S_n (kip/ft)	5.75	6.39
Shear strength of composite diaphragm using proposed strength eq., S_n (kip/ft)	8.97	9.71
Shear stiffness per DDM04, G' (kip/in.)	2345	2636
Shear stiffness per proposed eq., G' (kip/in.)	1352	1445

Notes

Six 1.50 in. seam welds assumed per panel length

Compressive strength f'_c = 3000 psi assumed

Four structural fasteners per rib across 36 in. wide panel

D_d (in.)	3.3
d (in.)	11.4

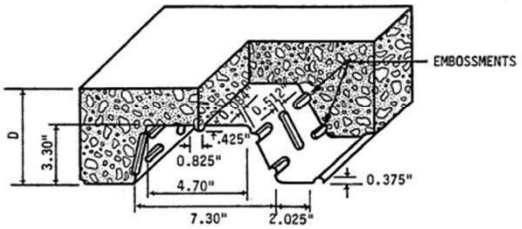

Figure from Porter and Easterling (1988)

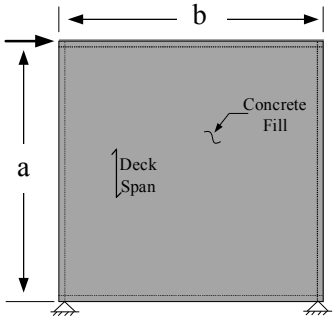

Loading Type: Cyclic

Load Rate: Static

a = 15'

b = 15'

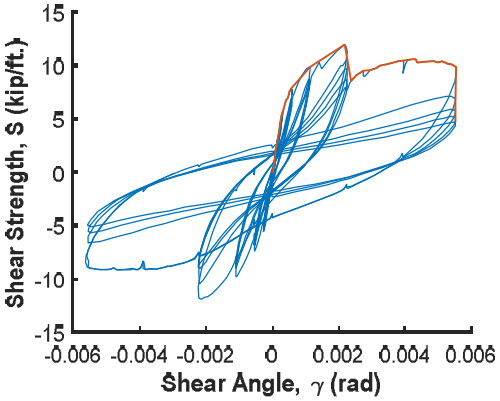

Eperimental Max Strength (kip/ft.)	12.1
Experimental Shear Stiffness (kip/in)	1710
Ultimate Shear Angle, $\gamma_{80\%}$ (rad*1000)	2.30
Failure Mode	Diag. Tension Cracking

Easterling (1987) - Specimen 13

Input	Nominal	Measured
Structural Fastener Type	Arc Spot Weld	-
Sidelap Fastener Type	Seam Weld	-
Deck thickness, t (in.)	0.058	-
Panel Length, l (ft.)	15	-
Panel Span, l_v (ft.)	15	-
No. of sidelap connections per one edge of interior panel length, n_s	6	-
No. of structural fasteners along one edge panel	60	-
No. of structural fasteners along one depth perimeter member (b dimension)	60	-
No. of interior supports per panel length, n_p	0	-
Yield strength of deck, F_y (ksi)	33	51.8
Ultimate strength of deck, F_u (ksi)	45	63.2
Diamter of arc spot weld (in.)	0.75	-
Concrete compressive strength f'_c (psi)	3000	6187
Unit weight of concrete, w_c (pcf)	145	145
Slab thickness bottom steel flute to top of fill, (in.)	5.5	5.53

Fastener Strengths and Flexibilities	Nominal	Measured
Structural fastener strength, P_{nf} (kip)	3.97	5.58
Sidelap fastener strength, P_{ns} (kip)	5.27	6.32
Structural fastener flexibility, S_f (in/kip)	0.0048	-
Sidelap fastener flexibility, S_s (in/kip)	0.0047	-

Calculated Strength Equations Variables	Nominal	Measured
Structural concrete strength factor per DDM04, k	0.0030	-
Interior panel fastener contribution factor, β	16.2	15.0
Structural fastener distribution factor at panel ends, α_e^2	2.05	-
Transformed total thickness with deck contribution, t_e (in.)	4.94	4.69
Shear modular ratio of steel deck to concrete, n	9.35	6.51
Developed flute width, s (in.)	16.2	-
Fastener slip coefficient, C	3.47	-
Fastener slip coefficient w/o sidelap flexibility, C_2	7.66	-
DDM04 stiffness contribution of concrete fill, k_3 (kip/in)	2377	3992
Stiffness contribution of concrete fill for proposed eq., k_4 (kip/in)	1523	1769

Predicted Shear Strength and Stiffness	Nominal	Measured
Lesser shear strength of perimeter structural fasteners in either orthogonal direction, (kip/ft)	15.9	22.3
Shear strength of composite diaphragm excluding perimeter fastener limit per DDM04, S_n (kip/ft)	6.54	9.50
Shear strength of composite diaphragm using proposed strength eq., S_n (kip/ft)	10.4	14.2
Shear stiffness per DDM04, G' (kip/in.)	2624	4240
Shear stiffness per proposed eq., G' (kip/in.)	1523	1993

Notes

Six 1.50 in. seam welds assumed per panel length

Compressive strength f'_c = 3000 psi assumed

Cellular deck used; 0.058" thick flat sheet with 0.057" thick corrugated sheet

Four structural fasteners per rib across 36 in. wide panel

D_d (in.)	3
d (in.)	12.2

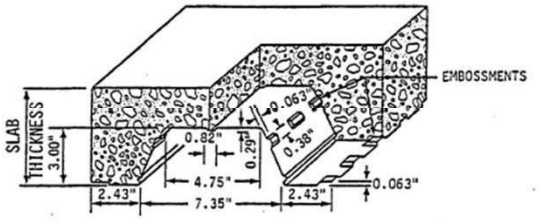

Figure from Porter and Easterling (1988)

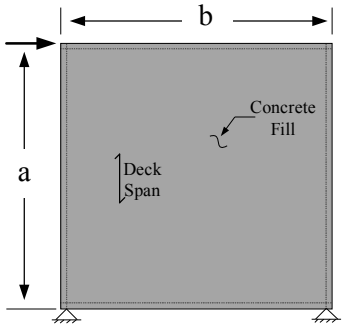

Loading Type: Cyclic

Load Rate: Static

a = 15'

b = 15'

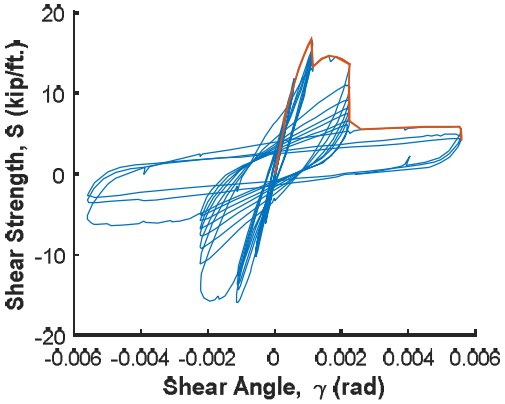

Eperimental Max Strength (kip/ft.)	16.8
Experimental Shear Stiffness (kip/in)	2021
Ultimate Shear Angle, $\gamma_{80\%}$ (rad*1000)	2.23
Failure Mode	Diag. Tension Cracking

Easterling (1987) - Specimen 16

Input	Nominal	Measured
Structural Fastener Type	Arc Spot Weld	-
Sidelap Fastener Type	Seam Weld	-
Deck thickness, t (in.)	0.047	-
Panel Length, l (ft.)	15	-
Panel Span, l_v (ft.)	15	-
No. of sidelap connections per one edge of interior panel length, n_s	6	-
No. of structural fasteners along one edge panel	60	-
No. of structural fasteners along one depth perimeter member (b dimension)	60	-
No. of interior supports per panel length, n_p	0	-
Yield strength of deck, F_y (ksi)	80	89.7
Ultimate strength of deck, F_u (ksi)	82	93.6
Diamter of arc spot weld (in.)	0.75	-
Concrete compressive strength f'_c (psi)	3000	2952
Unit weight of concrete, w_c (pcf)	145	145
Slab thickness bottom steel flute to top of fill, (in.)	4	4.18

Fastener Strengths and Flexibilities	Nominal	Measured
Structural fastener strength, P_{nf} (kip)	5.96	6.80
Sidelap fastener strength, P_{ns} (kip)	4.76	5.59
Structural fastener flexibility, S_f (in/kip)	0.0053	-
Sidelap fastener flexibility, S_s (in/kip)	0.0052	-

Calculated Strength Equations Variables	Nominal	Measured
Structural concrete strength factor per DDM04, k	0.0030	-
Interior panel fastener contribution factor, β	11.0	11.2
Structural fastener distribution factor at panel ends, α_e^2	1.56	-
Transformed total thickness with deck contribution, t_e (in.)	3.58	3.76
Shear modular ratio of steel deck to concrete, n	9.35	9.42
Developed flute width, s (in.)	8.05	-
Fastener slip coefficient, C	3.62	-
Fastener slip coefficient w/o sidelap flexibility, C_2	9.19	-
DDM04 stiffness contribution of concrete fill, k_3 (kip/in)	2377	2519
Stiffness contribution of concrete fill for proposed eq., k_4 (kip/in)	941	981

Predicted Shear Strength and Stiffness	Nominal	Measured
Lesser shear strength of perimeter structural fasteners in either orthogonal direction, (kip/ft)	23.8	27.2
Shear strength of composite diaphragm excluding perimeter fastener limit per DDM04, S_n (kip/ft)	6.54	6.95
Shear strength of composite diaphragm using proposed strength eq., S_n (kip/ft)	7.52	7.84
Shear stiffness per DDM04, G' (kip/in.)	2572	2714
Shear stiffness per proposed eq., G' (kip/in.)	1091	1131

Notes

Six 1.50 in. seam welds assumed per panel length

Compressive strength f'_c = 3000 psi assumed

Reported shear strength = 8.27 kip/ft (Porter and Easterling, 1980)

Two structural fasteners per rib across 36 in. wide panel

D_d (in.)	1.5
d (in.)	6

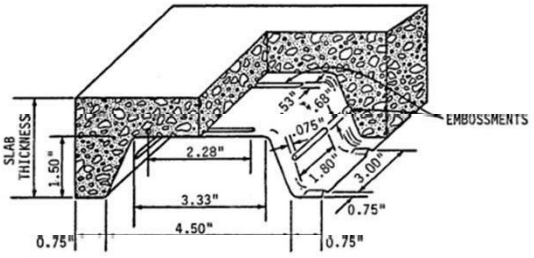

Figure from Porter and Easterling (1988)

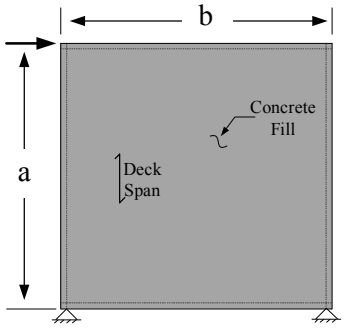

Loading Type: Cyclic

Load Rate: Static

a = 15'

b = 15'

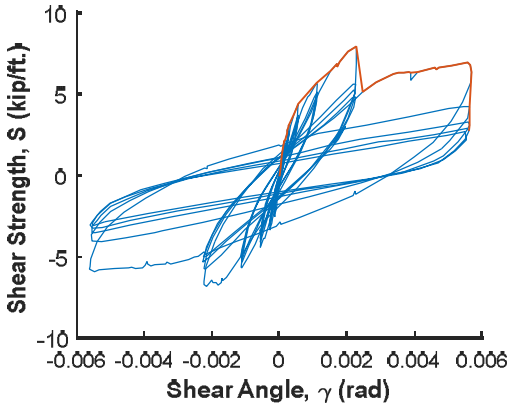

Eperimental Max Strength (kip/ft.)	8.01
Experimental Shear Stiffness (kip/in)	921
Ultimate Shear Angle, $\gamma_{80\%}$ (rad*1000)	2.39
Failure Mode	Diag. Tension Cracking

Easterling (1987) - Specimen 18

Input	Nominal	Measured
Structural Fastener Type	Arc Spot Weld	-
Sidelap Fastener Type	Seam Weld	-
Deck thickness, t (in.)	0.062	-
Panel Length, l (ft.)	15	-
Panel Span, l_v (ft.)	15	-
No. of sidelap connections per one edge of interior panel length, n_s	6	-
No. of structural fasteners along one edge panel	60	-
No. of structural fasteners along one depth perimeter member (b dimension)	60	-
No. of interior supports per panel length, n_p	0	-
Yield strength of deck, F_y (ksi)	33	40.4
Ultimate strength of deck, F_u (ksi)	45	53.4
Diamter of arc spot weld (in.)	0.75	-
Concrete compressive strength f'_c (psi)	3000	3052
Unit weight of concrete, w_c (pcf)	145	145
Slab thickness bottom steel flute to top of fill, (in.)	5.5	5.55

Fastener Strengths and Flexibilities	Nominal	Measured
Structural fastener strength, P_{nf} (kip)	4.22	5.01
Sidelap fastener strength, P_{ns} (kip)	5.75	6.54
Structural fastener flexibility, S_f (in/kip)	0.0046	-
Sidelap fastener flexibility, S_s (in/kip)	0.0045	-

Calculated Strength Equations Variables	Nominal	Measured
Structural concrete strength factor per DDM04, k	0.0030	-
Interior panel fastener contribution factor, β	16.4	16.0
Structural fastener distribution factor at panel ends, α_e^2	2.05	-
Transformed total thickness with deck contribution, t_e (in.)	4.27	4.31
Shear modular ratio of steel deck to concrete, n	9.35	9.27
Developed flute width, s (in.)	15.8	-
Fastener slip coefficient, C	3.59	-
Fastener slip coefficient w/o sidelap flexibility, C_2	7.92	-
DDM04 stiffness contribution of concrete fill, k_3 (kip/in)	2092	2165
Stiffness contribution of concrete fill for proposed eq., k_4 (kip/in)	1121	1143

Predicted Shear Strength and Stiffness	Nominal	Measured
Lesser shear strength of perimeter structural fasteners in either orthogonal direction, (kip/ft)	16.9	20.0
Shear strength of composite diaphragm excluding perimeter fastener limit per DDM04, S_n (kip/ft)	5.75	5.94
Shear strength of composite diaphragm using proposed strength eq., S_n (kip/ft)	8.97	9.15
Shear stiffness per DDM04, G' (kip/in.)	2345	2418
Shear stiffness per proposed eq., G' (kip/in.)	1352	1374

Notes

Six 1.50 in. seam welds assumed per panel length

Compressive strength f'_c = 3000 psi assumed

Four structural fasteners per rib across 36 in. wide panel

D_d (in.)	3.3
d (in.)	11.4

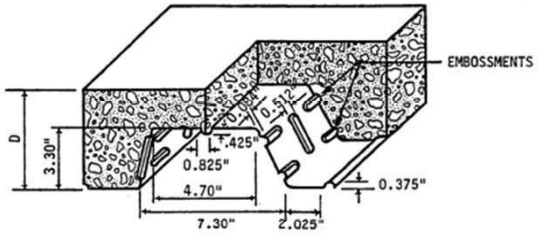

Figure from Porter and Easterling (1988)

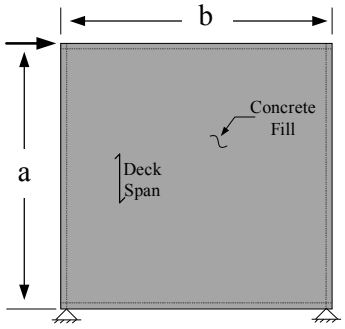

Loading Type: Cyclic

Load Rate: Static

a = 15'

b = 15'

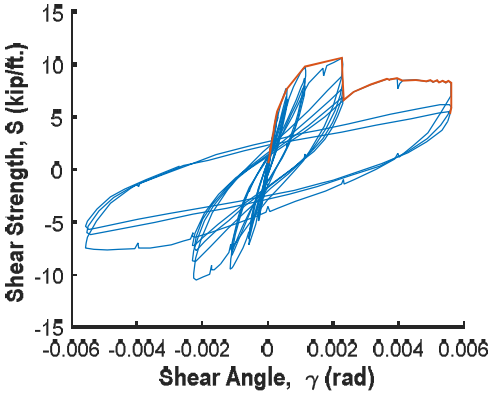

Eperimental Max Strength (kip/ft.)	10.7
Experimental Shear Stiffness (kip/in)	1582
Ultimate Shear Angle, $\gamma_{80\%}$ (rad*1000)	2.27
Failure Mode	Diag. Tension Cracking

Easterling (1987) - Specimen 19

Input	Nominal	Measured
Structural Fastener Type	Arc Spot Weld	-
Sidelap Fastener Type	Seam Weld	-
Deck thickness, t (in.)	0.062	-
Panel Length, l (ft.)	15	-
Panel Span, l_v (ft.)	15	-
No. of sidelap connections per one edge of interior panel length, n_s	6	-
No. of structural fasteners along one edge panel	60	-
No. of structural fasteners along one depth perimeter member (b dimension)	60	-
No. of interior supports per panel length, n_p	0	-
Yield strength of deck, F_y (ksi)	33	49.4
Ultimate strength of deck, F_u (ksi)	45	55.5
Diamter of arc spot weld (in.)	0.75	-
Concrete compressive strength f'_c (psi)	3000	2681
Unit weight of concrete, w_c (pcf)	145	145
Slab thickness bottom steel flute to top of fill, (in.)	5.5	5.75

Fastener Strengths and Flexibilities	Nominal	Measured
Structural fastener strength, P_{nf} (kip)	5.21	5.21
Sidelap fastener strength, P_{ns} (kip)	5.36	5.36
Structural fastener flexibility, S_f (in/kip)	0.0046	-
Sidelap fastener flexibility, S_s (in/kip)	0.0045	-

Calculated Strength Equations Variables	Nominal	Measured
Structural concrete strength factor per DDM04, k	0.0030	-
Interior panel fastener contribution factor, β	16.3	14.3
Structural fastener distribution factor at panel ends, α_e^2	2.04	-
Transformed total thickness with deck contribution, t_e (in.)	4.43	4.70
Shear modular ratio of steel deck to concrete, n	9.35	9.89
Developed flute width, s (in.)	16.3	-
Fastener slip coefficient, C	3.59	-
Fastener slip coefficient w/o sidelap flexibility, C_2	7.92	-
DDM04 stiffness contribution of concrete fill, k_3 (kip/in)	2377	2416
Stiffness contribution of concrete fill for proposed eq., k_4 (kip/in)	1164	1169

Predicted Shear Strength and Stiffness	Nominal	Measured
Lesser shear strength of perimeter structural fasteners in either orthogonal direction, (kip/ft)	16.9	20.8
Shear strength of composite diaphragm excluding perimeter fastener limit per DDM04, S_n (kip/ft)	6.54	6.80
Shear strength of composite diaphragm using proposed strength eq., S_n (kip/ft)	9.31	9.35
Shear stiffness per DDM04, G' (kip/in.)	2634	2674
Shear stiffness per proposed eq., G' (kip/in.)	1395	1400

Notes

Six 1.50 in. seam welds assumed per panel length

Compressive strength f'_c = 3000 psi assumed

Four structural fasteners per rib across 36 in. wide panel

D_d (in.) 3

d (in.) 12

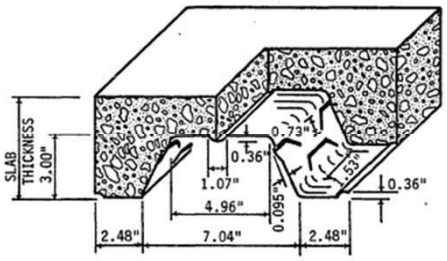

Figure from Porter and Easterling (1988)

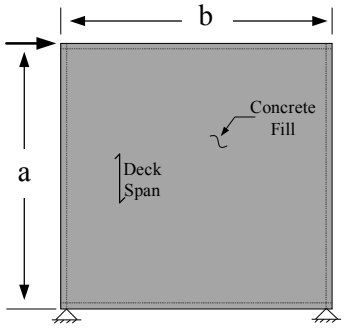

Loading Type: Cyclic

Load Rate: Static

a = 15'

b = 15'

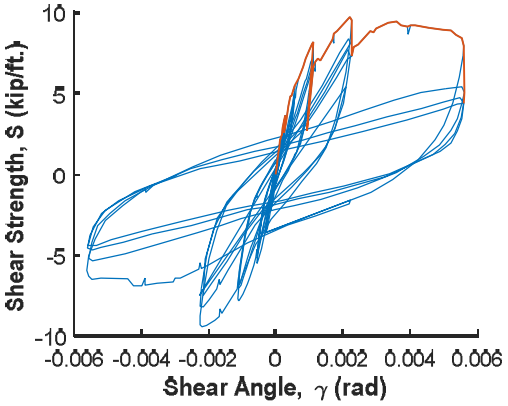

Eperimental Max Strength (kip/ft.)	9.79
Experimental Shear Stiffness (kip/in)	930
Ultimate Shear Angle, $\gamma_{80\%}$ (rad*1000)	2.26
Failure Mode	Diag. Tension Cracking

Easterling (1987) - Specimen 22

Input	Nominal	Measured
Structural Fastener Type	Arc Spot Weld	-
Sidelap Fastener Type	Seam Weld	-
Deck thickness, t (in.)	0.062	-
Panel Length, l (ft.)	12	-
Panel Span, l_v (ft.)	15	-
No. of sidelap connections per one edge of interior panel length, n_s	6	-
No. of structural fasteners along one edge panel	60	-
No. of structural fasteners along one depth perimeter member (b dimension)	48	-
No. of interior supports per panel length, n_p	0	-
Yield strength of deck, F_y (ksi)	33	40.4
Ultimate strength of deck, F_u (ksi)	45	53.4
Diamter of arc spot weld (in.)	0.75	-
Concrete compressive strength f'_c (psi)	3000	3301
Unit weight of concrete, w_c (pcf)	145	145
Slab thickness bottom steel flute to top of fill, (in.)	5.5	5.68

Fastener Strengths and Flexibilities	Nominal	Measured
Structural fastener strength, P_{nf} (kip)	4.22	5.01
Sidelap fastener strength, P_{ns} (kip)	5.75	6.54
Structural fastener flexibility, S_f (in/kip)	0.0046	-
Sidelap fastener flexibility, S_s (in/kip)	0.0045	-

Calculated Strength Equations Variables	Nominal	Measured
Structural concrete strength factor per DDM04, k	0.0030	-
Interior panel fastener contribution factor, β	16.4	16.0
Structural fastener distribution factor at panel ends, α_e^2	2.05	-
Transformed total thickness with deck contribution, t_e (in.)	4.27	4.43
Shear modular ratio of steel deck to concrete, n	9.35	8.91
Developed flute width, s (in.)	15.8	-
Fastener slip coefficient, C	2.87	-
Fastener slip coefficient w/o sidelap flexibility, C_2	6.34	-
DDM04 stiffness contribution of concrete fill, k_3 (kip/in)	2092	2419
Stiffness contribution of concrete fill for proposed eq., k_4 (kip/in)	1121	1221

Predicted Shear Strength and Stiffness	Nominal	Measured
Lesser shear strength of perimeter structural fasteners in either orthogonal direction, (kip/ft)	16.9	20.0
Shear strength of composite diaphragm excluding perimeter fastener limit per DDM04, S_n (kip/ft)	5.75	6.53
Shear strength of composite diaphragm using proposed strength eq., S_n (kip/ft)	8.97	9.76
Shear stiffness per DDM04, G' (kip/in.)	2373	2701
Shear stiffness per proposed eq., G' (kip/in.)	1410	1509

Notes

Six 1.50 in. seam welds assumed per panel length

Compressive strength f'_c = 3000 psi assumed

Reported shear strength = 11.3 kip/ft (Porter and Easterling, 1980)

Four structural fasteners per rib across 36 in. wide panel

D_d (in.)	3.3
d (in.)	11.4

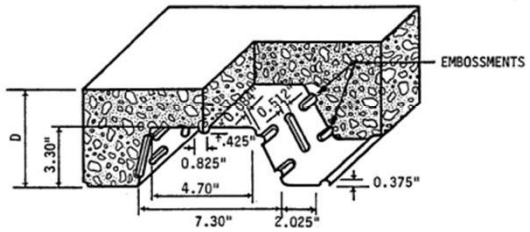

Figure from Porter and Easterling (1988)

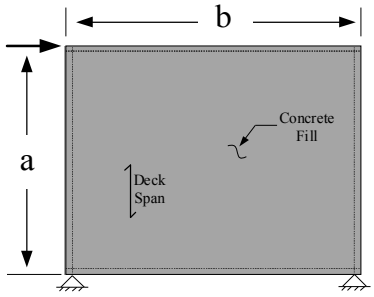

Loading Type: Cyclic

Load Rate: Static

a = 12'

b = 15'

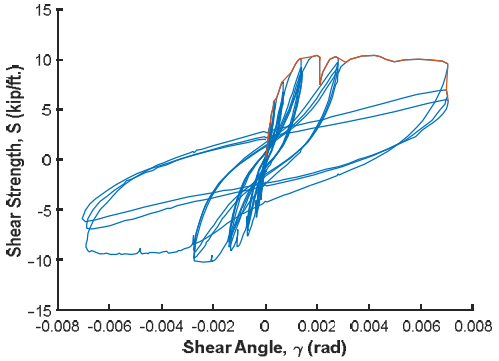

Eperimental Max Strength (kip/ft.)	10.5
Experimental Shear Stiffness (kip/in)	1654
Ultimate Shear Angle, $\gamma_{80\%}$ (rad*1000)	2.09
Failure Mode	Diag. Tension Cracking

Easterling (1987) - Specimen 24

Input	Nominal	Measured
Structural Fastener Type	Arc Spot Weld	-
Sidelap Fastener Type	Seam Weld	-
Deck thickness, t (in.)	0.062	-
Panel Length, l (ft.)	12	-
Panel Span, l_v (ft.)	15	-
No. of sidelap connections per one edge of interior panel length, n_s	6	-
No. of structural fasteners along one edge panel	48	-
No. of structural fasteners along one depth perimeter member (b dimension)	48	-
No. of interior supports per panel length, n_p	0	-
Yield strength of deck, F_y (ksi)	33	49.4
Ultimate strength of deck, F_u (ksi)	45	55.5
Diamter of arc spot weld (in.)	0.75	-
Concrete compressive strength f'_c (psi)	3000	4047
Unit weight of concrete, w_c (pcf)	145	145
Slab thickness bottom steel flute to top of fill, (in.)	5.5	5.63

Fastener Strengths and Flexibilities	Nominal	Measured
Structural fastener strength, P_{nf} (kip)	4.22	5.21
Sidelap fastener strength, P_{ns} (kip)	5.75	5.40
Structural fastener flexibility, S_f (in/kip)	0.0046	-
Sidelap fastener flexibility, S_s (in/kip)	0.0045	-

Calculated Strength Equations Variables	Nominal	Measured
Structural concrete strength factor per DDM04, k	0.0030	-
Interior panel fastener contribution factor, β	14.1	12.1
Structural fastener distribution factor at panel ends, α_e^2	1.47	-
Transformed total thickness with deck contribution, t_e (in.)	4.43	4.50
Shear modular ratio of steel deck to concrete, n	9.35	8.05
Developed flute width, s (in.)	16.3	-
Fastener slip coefficient, C	3.26	-
Fastener slip coefficient w/o sidelap flexibility, C_2	8.65	-
DDM04 stiffness contribution of concrete fill, k_3 (kip/in)	2377	3083
Stiffness contribution of concrete fill for proposed eq., k_4 (kip/in)	1164	1374

Predicted Shear Strength and Stiffness	Nominal	Measured
Lesser shear strength of perimeter structural fasteners in either orthogonal direction, (kip/ft)	13.5	16.7
Shear strength of composite diaphragm excluding perimeter fastener limit per DDM04, S_n (kip/ft)	6.54	7.99
Shear strength of composite diaphragm using proposed strength eq., S_n (kip/ft)	9.31	11.0
Shear stiffness per DDM04, G' (kip/in.)	2646	3353
Shear stiffness per proposed eq., G' (kip/in.)	1376	1585

Notes

Six 1.50 in. seam welds assumed per panel length

Compressive strength f'_c = 3000 psi assumed

Three structural fasteners per rib across 36 in. wide panel assumed

D_d (in.) 3

d (in.) 12

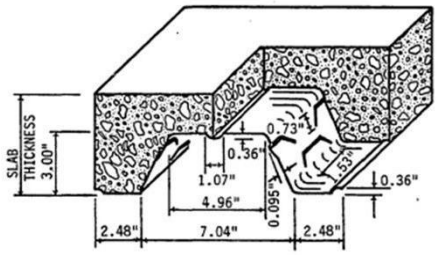

Figure from Porter and Easterling (1988)

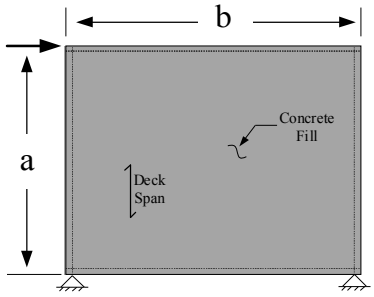

Loading Type: Cyclic

Load Rate: Static

a = 12'

b = 15'

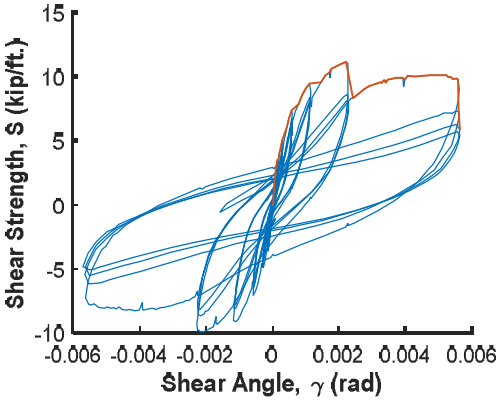

Eperimental Max Strength (kip/ft.)	11.2
Experimental Shear Stiffness (kip/in)	1657
Ultimate Shear Angle, $\gamma_{80\%}$ (rad*1000)	2.37
Failure Mode	Diag. Tension Cracking

Easterling (1987) - Specimen 25

Input	Nominal	Measured
Structural Fastener Type	Mix	-
Sidelap Fastener Type	Seam Weld	-
Deck thickness, t (in.)	0.062	-
Panel Length, l (ft.)	12	-
Panel Span, l_v (ft.)	15	-
No. of sidelap connections per one edge of interior panel length, n_s	6	-
No. of structural fasteners along one edge panel	8 Studs	-
No. of structural fasteners along one depth perimeter member (b dimension)	16 Welds	-
No. of interior supports per panel length, n_p	0	-
Yield strength of deck, F_y (ksi)	33	40.4
Ultimate strength of deck, F_u (ksi)	45	53.4
Diameter of arc spot weld and shear stud (in.)	0.75	-
Concrete compressive strength f'_c (psi)	3000	4672
Unit weight of concrete, w_c (pcf)	145	145
Slab thickness bottom steel flute to top of fill, (in.)	5.5	5.69

Fastener Strengths and Flexibilities	Nominal	Measured
Structural fastener strength, P_{nf} (kip)	4.22	5.01
Sidelap fastener strength, P_{ns} (kip)	5.75	6.54
Structural fastener flexibility, S_f (in/kip)	0.0046	-
Sidelap fastener flexibility, S_s (in/kip)	0.0045	-

Calculated Strength Equations Variables	Nominal	Measured
Structural concrete strength factor per DDM04, k	0.0030	-
Interior panel fastener contribution factor, β	10.4	10.1
Structural fastener distribution factor at panel ends, α_e^2	0.56	-
Transformed total thickness with deck contribution, t_e (in.)	4.27	4.37
Shear modular ratio of steel deck to concrete, n	9.35	7.49
Developed flute width, s (in.)	15.8	-
Fastener slip coefficient, C	4.51	-
Fastener slip coefficient w/o sidelap flexibility, C_2	25.3	-
DDM04 stiffness contribution of concrete fill, k_3 (kip/in)	2092	3098
Stiffness contribution of concrete fill for proposed eq., k_4 (kip/in)	1121	1435

Predicted Shear Strength and Stiffness	Nominal	Measured
Lesser shear strength of perimeter structural fasteners in either orthogonal direction, (kip/ft)	4.50	5.3
Shear strength of composite diaphragm excluding perimeter fastener limit per DDM04, S_n (kip/ft)	5.75	7.80
Shear strength of composite diaphragm using proposed strength eq., S_n (kip/ft)	8.97	11.5
Shear stiffness per DDM04, G' (kip/in.)	2316	3323
Shear stiffness per proposed eq., G' (kip/in.)	1194	1507

Notes

Six 1.50 in. seam welds assumed per panel length

Compressive strength f'_c = 3000 psi assumed

Studs treated as 1.00 in. diameter spot welds for application into DDM04 equation

36 in. wide panel

D_d (in.)	3.3
d (in.)	11.4

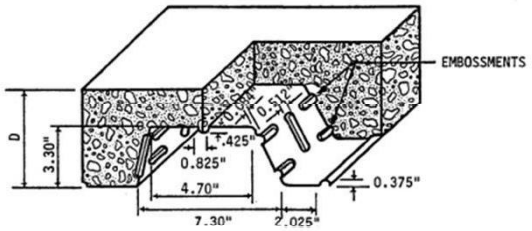

Figure from Porter and Easterling (1988)

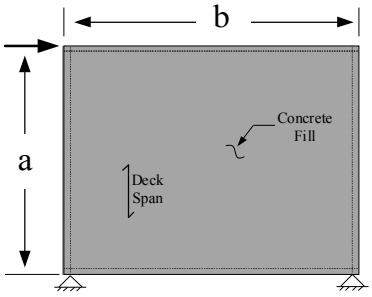

Loading Type: Cyclic

Load Rate: Static

a = 12'

b = 15'

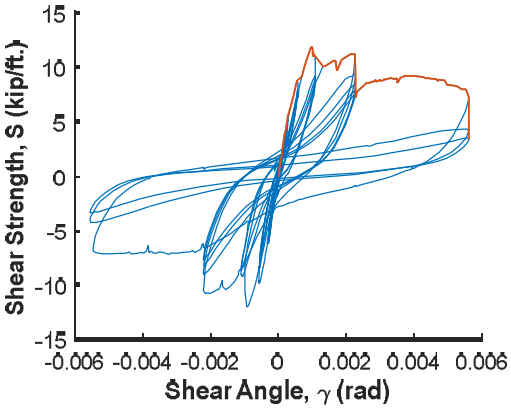

Eperimental Max Strength (kip/ft.)	12.0
Experimental Shear Stiffness (kip/in)	1726
Ultimate Shear Angle, $\gamma_{80\%}$ (rad*1000)	2.26
Failure Mode	Diag. Tension Cracking

P_{nf} reported refers to 0.75 in. arc spot weld

Easterling (1987) - Specimen 26

Input	Nominal	Measured
Structural Fastener Type	Mix	-
Sidelap Fastener Type	Seam Weld	-
Deck thickness, t (in.)	0.036	-
Panel Length, l (ft.)	12	-
Panel Span, l_v (ft.)	15	-
No. of sidelap connections per one edge of interior panel length, n_s	6	-
No. of structural fasteners along one edge panel	7 Welds	-
No. of structural fasteners along one depth perimeter member (b dimension)	8 Studs +15Welds	-
No. of interior supports per panel length, n_p	0	-
Yield strength of deck, F_y (ksi)	80	92.8
Ultimate strength of deck, F_u (ksi)	82	93.6
Diameter of arc spot weld and shear stud (in.)	0.75	-
Concrete compressive strength f'_c (psi)	3000	3462
Unit weight of concrete, w_c (pcf)	100	100
Slab thickness bottom steel flute to top of fill, (in.)	4.5	4.72

Fastener Strengths and Flexibilities	Nominal	Measured
Structural fastener strength, P_{nf} (kip)	4.64	5.29
Sidelap fastener strength, P_{ns} (kip)	3.34	3.71
Structural fastener flexibility, S_f (in/kip)	0.0061	-
Sidelap fastener flexibility, S_s (in/kip)	0.0059	-

Calculated Strength Equations Variables	Nominal	Measured
Structural concrete strength factor per DDM04, k	0.0017	-
Interior panel fastener contribution factor, β	9.25	9.12
Structural fastener distribution factor at panel ends, α_e^2	1.06	-
Transformed total thickness with deck contribution, t_e (in.)	4.06	4.24
Shear modular ratio of steel deck to concrete, n	16.3	15.2
Developed flute width, s (in.)	14.4	-
Fastener slip coefficient, C	3.03	-
Fastener slip coefficient w/o sidelap flexibility, C_2	11.0	-
DDM04 stiffness contribution of concrete fill, k_3 (kip/in)	2510	3006
Stiffness contribution of concrete fill for proposed eq., k_4 (kip/in)	1067	1199

Predicted Shear Strength and Stiffness	Nominal	Measured
Lesser shear strength of perimeter structural fasteners in either orthogonal direction, (kip/ft)	2.70	3.09
Shear strength of composite diaphragm excluding perimeter fastener limit per DDM04, S_n (kip/ft)	3.95	4.60
Shear strength of composite diaphragm using proposed strength eq., S_n (kip/ft)	6.40	7.19
Shear stiffness per DDM04, G' (kip/in.)	2682	3178
Shear stiffness per proposed eq., G' (kip/in.)	1163	1295

36 in. wide panel

D_d (in.) 1.86

d (in.) 12

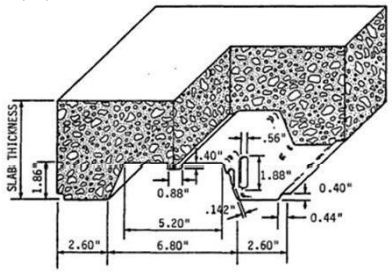

Figure from Porter and Easterling (1988)

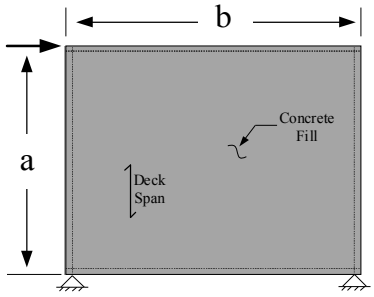

Loading Type: Cyclic

Load Rate: Static

a = 12'

b = 15'

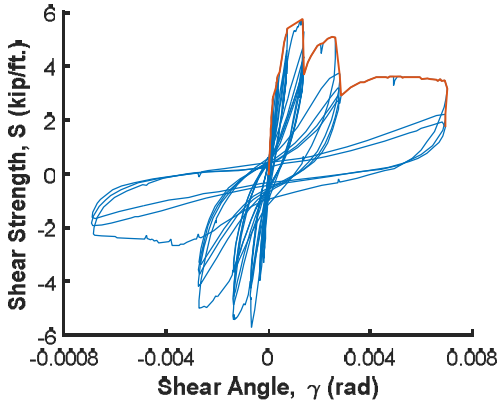

Eperimental Max Strength (kip/ft.)	5.80
Experimental Shear Stiffness (kip/in)	1592
Ultimate Shear Angle, $\gamma_{80\%}$ (rad*1000)	1.35
Failure Mode	Diag. Tension Cracking

Notes

Six 1.50 in. seam welds assumed per panel length

Compressive strength f'_c = 3000 psi assumed

Studs treated as 1.00 in. diameter spot welds for application into DDM04 equation

λ = 0.75 lightweigth factor used for proposed strength equation

P_{nf} reported refers to 0.75 in. arc spot weld

Fastener type and frequency changes on span (a) perimeter beam, controlling fastener type is reported

Easterling (1987) - Specimen 27

Input	Nominal	Measured
Structural Fastener Type	Mix	-
Sidelap Fastener Type	Seam Weld	-
Deck thickness, t (in.)	0.037	-
Panel Length, l (ft.)	12	-
Panel Span, l_v (ft.)	15	-
No. of sidelap connections per one edge of interior panel length, n_s	6	-
No. of structural fasteners along one edge panel	9 Welds	-
No. of structural fasteners along one depth perimeter member (b dimension)	8 Studs +15Welds	-
No. of interior supports per panel length, n_p	0	-
Yield strength of deck, F_y (ksi)	33	48.6
Ultimate strength of deck, F_u (ksi)	45	56.2
Diameter of arc spot weld and shear stud (in.)	0.75	-
Concrete compressive strength f'_c (psi)	3000	2883
Unit weight of concrete, w_c (pcf)	145	145
Slab thickness bottom steel flute to top of fill, (in.)	5.5	5.66

Fastener Strengths and Flexibilities	Nominal	Measured
Structural fastener strength, P_{nf} (kip)	2.61	3.26
Sidelap fastener strength, P_{ns} (kip)	2.90	2.85
Structural fastener flexibility, S_f (in/kip)	0.0060	-
Sidelap fastener flexibility, S_s (in/kip)	0.0058	-

Calculated Strength Equations Variables	Nominal	Measured
Structural concrete strength factor per DDM04, k	0.0030	-
Interior panel fastener contribution factor, β	10.9	9.47
Structural fastener distribution factor at panel ends, α_e^2	1.06	-
Transformed total thickness with deck contribution, t_e (in.)	4.49	4.65
Shear modular ratio of steel deck to concrete, n	9.35	9.54
Developed flute width, s (in.)	11.8	-
Fastener slip coefficient, C	4.61	-
Fastener slip coefficient w/o sidelap flexibility, C_2	16.8	-
DDM04 stiffness contribution of concrete fill, k_3 (kip/in)	2852	2922
Stiffness contribution of concrete fill for proposed eq., k_4 (kip/in)	1179	1198

Predicted Shear Strength and Stiffness	Nominal	Measured
Lesser shear strength of perimeter structural fasteners in either orthogonal direction, (kip/ft)	1.96	2.45
Shear strength of composite diaphragm excluding perimeter fastener limit per DDM04, S_n (kip/ft)	7.85	8.10
Shear strength of composite diaphragm using proposed strength eq., S_n (kip/ft)	N/A	N/A
Shear stiffness per DDM04, G' (kip/in.)	2982	3051
Shear stiffness per proposed eq., G' (kip/in.)	1244	1263

24 in. wide panel (assumed)

D_d (in.) 2.5

d (in.) 8.00

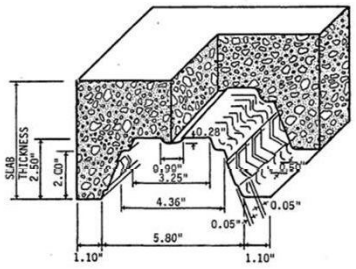

Figure from Porter and Easterling (1988)

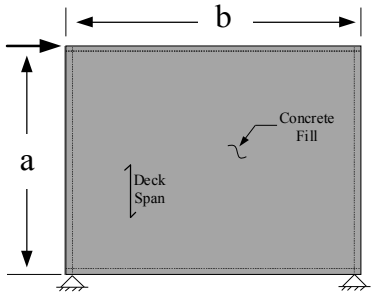

Loading Type: Cyclic

Load Rate: Static

a = 12'

b = 15'

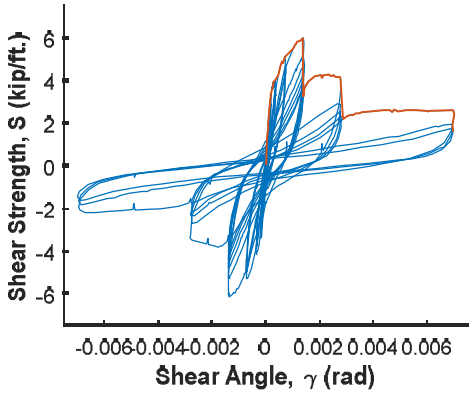

Eperimental Max Strength (kip/ft.)	6.07
Experimental Shear Stiffness (kip/in)	1751
Ultimate Shear Angle, $\gamma_{80\%}$ (rad*1000)	1.38
Failure Mode	Perimeter Fastener

Notes

Six 1.50 in. seam welds assumed per panel length

Compressive strength f'_c = 3000 psi assumed

Studs treated as 1.00 in. diameter spot welds for application into DDM04 equation

P_{nf} reported refers to 0.75 in. arc spot weld

Proposed equation not applicable to perimter fastener failure

Easterling (1987) - Specimen 28

Input	Nominal	Measured
Structural Fastener Type	Mix	-
Sidelap Fastener Type	Seam Weld	-
Deck thickness, t (in.)	0.037	-
Panel Length, l (ft.)	12	-
Panel Span, l_v (ft.)	15	-
No. of sidelap connections per one edge of interior panel length, n_s	6	-
No. of structural fasteners along one edge panel	6 Studs	-
No. of structural fasteners along one depth perimeter member (b dimension)	8 Studs +15Welds	-
No. of interior supports per panel length, n_p	0	-
Yield strength of deck, F_y (ksi)	33	48.6
Ultimate strength of deck, F_u (ksi)	45	56.2
Diameter of arc spot weld and shear stud (in.)	0.75	-
Concrete compressive strength f'_c (psi)	3000	3611
Unit weight of concrete, w_c (pcf)	145	145
Slab thickness bottom steel flute to top of fill, (in.)	5.5	5.60

Fastener Strengths and Flexibilities	Nominal	Measured
Structural fastener strength, P_{nf} (kip)	2.61	3.26
Sidelap fastener strength, P_{ns} (kip)	2.90	2.85
Structural fastener flexibility, S_f (in/kip)	0.0060	-
Sidelap fastener flexibility, S_s (in/kip)	0.0058	-

Calculated Strength Equations Variables	Nominal	Measured
Structural concrete strength factor per DDM04, k	0.0030	-
Interior panel fastener contribution factor, β	10.9	9.47
Structural fastener distribution factor at panel ends, α_e^2	1.06	-
Transformed total thickness with deck contribution, t_e (in.)	4.49	4.56
Shear modular ratio of steel deck to concrete, n	9.35	8.52
Developed flute width, s (in.)	11.8	-
Fastener slip coefficient, C	4.61	-
Fastener slip coefficient w/o sidelap flexibility, C_2	16.8	-
DDM04 stiffness contribution of concrete fill, k_3 (kip/in)	2852	3356
Stiffness contribution of concrete fill for proposed eq., k_4 (kip/in)	1179	1317

Predicted Shear Strength and Stiffness	Nominal	Measured
Lesser shear strength of perimeter structural fasteners in either orthogonal direction, (kip/ft)	10.5	10.8
Shear strength of composite diaphragm excluding perimeter fastener limit per DDM04, S_n (kip/ft)	7.85	8.90
Shear strength of composite diaphragm using proposed strength eq., S_n (kip/ft)	N/A	N/A
Shear stiffness per DDM04, G' (kip/in.)	2982	3485
Shear stiffness per proposed eq., G' (kip/in.)	1244	1382

24 in. wide panel (assumed)

D_d (in.) 2.5

d (in.) 8.00

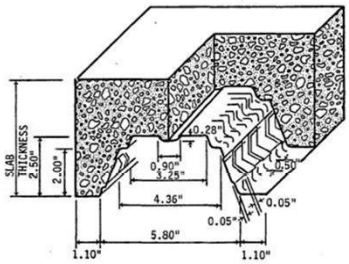

Figure from Porter and Easterling (1988)

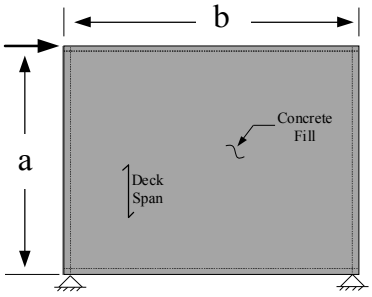

Loading Type: Cyclic

Load Rate: Static

a = 12'

b = 15'

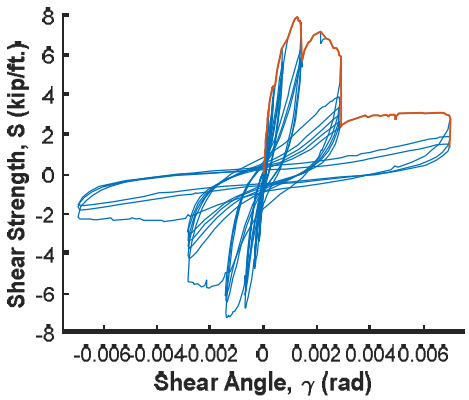

Eperimental Max Strength (kip/ft.)	7.98
Experimental Shear Stiffness (kip/in)	1582
Ultimate Shear Angle, $\gamma_{80\%}$ (rad*1000)	1.41
Failure Mode	Perimeter Fastener

Notes

Six 1.50 in. seam welds assumed per panel length

Compressive strength f'_c = 3000 psi assumed

Studs treated as 1.00 in. diameter spot welds for application into DDM04 equation

P_{nf} reported refers to 0.75 in. arc spot weld

Proposed equation not applicable to perimeter fastener failure

Easterling (1987) - Specimen 29

Input	Nominal	Measured
Structural Fastener Type	Shear Studs	-
Sidelap Fastener Type	Seam Weld	-
Deck thickness, t (in.)	0.035	-
Panel Length, l (ft.)	12	-
Panel Span, l_v (ft.)	15	-
No. of sidelap connections per one edge of interior panel length, n_s	6	-
No. of structural fasteners along one edge panel	16	-
No. of structural fasteners along one depth perimeter member (b dimension)	11	-
No. of interior supports per panel length, n_p	0	-
Yield strength of deck, F_y (ksi)	80	86.9
Ultimate strength of deck, F_u (ksi)	82	89.8
Diameter of arc spot weld and shear stud (in.)	0.75	-
Concrete compressive strength f'_c (psi)	3000	2887
Unit weight of concrete, w_c (pcf)	145	145
Slab thickness bottom steel flute to top of fill, (in.)	5.5	5.55

Fastener Strengths and Flexibilities	Nominal	Measured
Structural fastener strength, P_{nf} (kip)	3.88	4.67
Sidelap fastener strength, P_{ns} (kip)	3.21	4.54
Structural fastener flexibility, S_f (in/kip)	0.0061	-
Sidelap fastener flexibility, S_s (in/kip)	0.0060	-

Calculated Strength Equations Variables	Nominal	Measured
Structural concrete strength factor per DDM04, k	0.0030	-
Interior panel fastener contribution factor, β	7.20	8.06
Structural fastener distribution factor at panel ends, α_e^2	0.56	-
Transformed total thickness with deck contribution, t_e (in.)	4.24	4.30
Shear modular ratio of steel deck to concrete, n	9.35	9.53
Developed flute width, s (in.)	16.3	-
Fastener slip coefficient, C	3.39	-
Fastener slip coefficient w/o sidelap flexibility, C_2	19.0	-
DDM04 stiffness contribution of concrete fill, k_3 (kip/in)	2377	2360
Stiffness contribution of concrete fill for proposed eq., k_4 (kip/in)	1115	1162

Predicted Shear Strength and Stiffness	Nominal	Measured
Lesser shear strength of perimeter structural fasteners in either orthogonal direction, (kip/ft)	18.4	18.4
Shear strength of composite diaphragm excluding perimeter fastener limit per DDM04, S_n (kip/ft)	6.54	6.54
Shear strength of composite diaphragm using proposed strength eq., S_n (kip/ft)	8.92	8.86
Shear stiffness per DDM04, G' (kip/in.)	2526	2509
Shear stiffness per proposed eq., G' (kip/in.)	1169	1162

36 in. wide panel

D_d (in.) 3

d (in.) 12.00

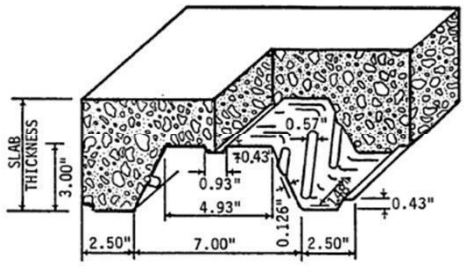

Figure from Porter and Easterling (1988)

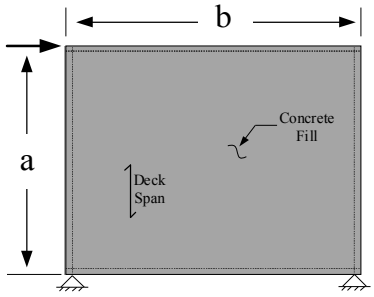

Loading Type: Cyclic

Load Rate: Static

a = 12'

b = 15'

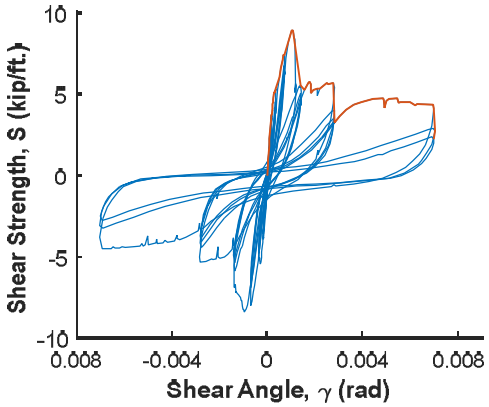

Eperimental Max Strength (kip/ft.)	9.00
Experimental Shear Stiffness (kip/in)	1887
Ultimate Shear Angle, $\gamma_{80\%}$ (rad*1000)	1.24
Failure Mode	Diag. Tension Cracking

Notes

Six 1.50 in. seam welds assumed per panel length

Compressive strength f'_c = 3000 psi assumed

Studs treated as 1.00 in. diameter spot welds for application into DDM04 equation

P_{nf} reported refers to 1.00 in. arc spot weld

Easterling (1987) - Specimen 30

Input	Nominal	Measured
Structural Fastener Type	Mix	-
Sidelap Fastener Type	Seam Weld	-
Deck thickness, t (in.)	0.035	-
Panel Length, l (ft.)	12	-
Panel Span, l_v (ft.)	15	-
No. of sidelap connections per one edge of interior panel length, n_s	6	-
No. of structural fasteners along one edge panel	7 Studs	-
No. of structural fasteners along one depth perimeter member (b dimension)	12Studs + 4Welds	-
No. of interior supports per panel length, n_p	0	-
Yield strength of deck, F_y (ksi)	80	86.9
Ultimate strength of deck, F_u (ksi)	82	89.8
Diameter of arc spot weld and shear stud (in.)	0.75	-
Concrete compressive strength f'_c (psi)	3000	3565
Unit weight of concrete, w_c (pcf)	145	145
Slab thickness bottom steel flute to top of fill, (in.)	5.5	5.68

Fastener Strengths and Flexibilities	Nominal	Measured
Structural fastener strength, P_{nf} (kip)	4.51	4.94
Sidelap fastener strength, P_{ns} (kip)	3.21	3.57
Structural fastener flexibility, S_f (in/kip)	0.0061	-
Sidelap fastener flexibility, S_s (in/kip)	0.0060	-

Calculated Strength Equations Variables	Nominal	Measured
Structural concrete strength factor per DDM04, k	0.0030	-
Interior panel fastener contribution factor, β	7.20	7.26
Structural fastener distribution factor at panel ends, α_e^2	0.56	-
Transformed total thickness with deck contribution, t_e (in.)	4.24	4.40
Shear modular ratio of steel deck to concrete, n	9.35	8.57
Developed flute width, s (in.)	16.3	-
Fastener slip coefficient, C	3.39	-
Fastener slip coefficient w/o sidelap flexibility, C_2	19.0	-
DDM04 stiffness contribution of concrete fill, k_3 (kip/in)	2377	2875
Stiffness contribution of concrete fill for proposed eq., k_4 (kip/in)	1115	1261

Predicted Shear Strength and Stiffness	Nominal	Measured
Lesser shear strength of perimeter structural fasteners in either orthogonal direction, (kip/ft)	12.3	12.6
Shear strength of composite diaphragm excluding perimeter fastener limit per DDM04, S_n (kip/ft)	6.54	7.64
Shear strength of composite diaphragm using proposed strength eq., S_n (kip/ft)	N/A	N/A
Shear stiffness per DDM04, G' (kip/in.)	2526	3024
Shear stiffness per proposed eq., G' (kip/in.)	1169	1316

36 in. wide panel

D_d (in.) 3

d (in.) 12.00

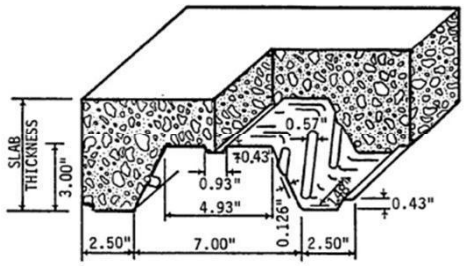

Figure from Porter and Easterling (1988)

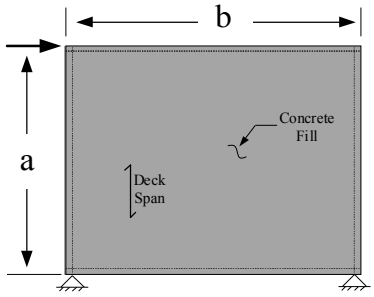

Loading Type: Cyclic

Load Rate: Static

a = 12'

b = 15'

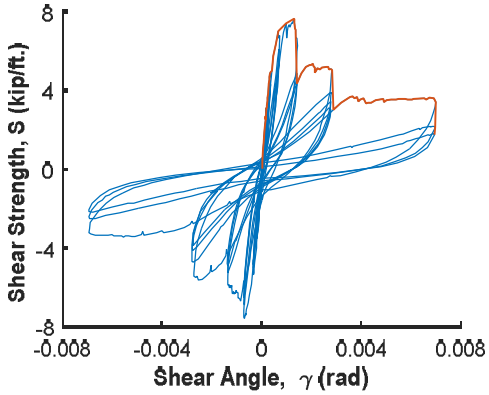

Eperimental Max Strength (kip/ft.)	7.69
Experimental Shear Stiffness (kip/in)	1535
Ultimate Shear Angle, $\gamma_{80\%}$ (rad*1000)	1.37
Failure Mode	Perimeter Fastener

Notes

Six 1.50 in. seam welds assumed per panel length

Compressive strength f'_c = 3000 psi assumed

Studs treated as 1.00 in. diameter spot welds for application into DDM04 equation

P_{nf} reported refers to 1.00 in. arc spot weld

Proposed equation not applicable to perimeter fastener failure

Pinkham (1999) - Specimen 31

Input	
Structural Fastener Type	Arc Spot Weld
Sidelap Fastener Type	Top Seam Weld
Deck thickness, t (in.)	0.0360
Panel Length, l (ft.)	10
Panel Span, l_v (ft.)	5
No. of sidelap connections per one edge of interior panel length, n_s	12
No. of edge structural connections not in line with int. or ext. supports, n_e	16
No. of interior supports per panel length, n_p	2
Yield strength of deck, F_y (ksi)	38
Ultimate strength of deck, F_u (ksi)	55
Length of sidelap weld, L_w (in.)	1.5
Moment of inertia of fully effective panel per unit width, I_x (in^4)	0.1865
Diameter of structural weld, (in.)	0.875

Fastener Strengths and Flexibilities	
Structural fastener strength, P_{nf} (kip)	3.65
Sidelap fastener strength, P_{ns} (kip)	3.70
Structural fastener flexibility, S_f (in/kip)	0.0061
Sidelap fastener flexibility, S_s (in/kip)	0.0059

Calculated Strength Equations Variables	
Corner fastener reduction factor, λ	0.835
Interior panel fastener contribution factor, β	18.4
Structural fastener distribution factor at panel ends, α_e^2	0.778
Structural fastener distribution factor at interior supports, α_p^2	0.778
Number of structural fasteners at panel ends per unit width, N	2.33
Fastener slip coefficient, C	1.31
Warping factor, D_n (in.)	4.64
Warping support factor, ρ	0.90

Predicted Shear Strength and Stiffness	
Interior panel shear strength, S_{ni} (kip/ft.)	6.60
Edge panel shear strength, S_{ne} (kip/ft.)	8.77
Panel shear strength limited by corner fastener, S_{nc} (kip/ft.)	5.28
Panel buckling shear strength, S_{nb} (kip/ft.)	6.92
Shear stiffness, G' (kip/in)	119

36/7 fastener pattern at interior and exterior supports

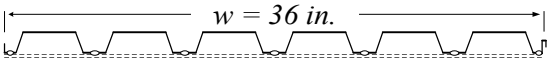

e (in.)	0.75
w_c (in.)	1.68
f (in.)	3.00
d (in.)	6.00
s (in.)	7.85
D_d (in.)	1.50

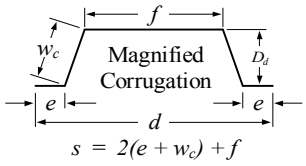

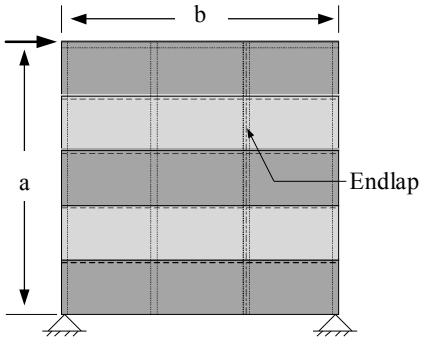

Loading Type: Monotonic

Load Rate: Static

a = 15'

b = 15'

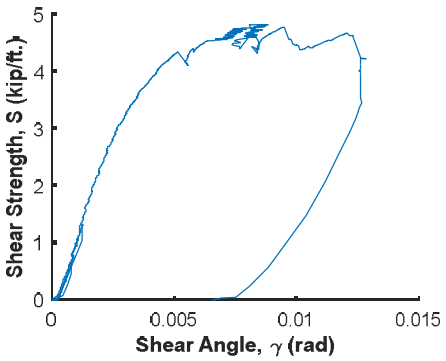

Eperimental Max Strength (kip/ft.)	4.83
Experimental Shear Stiffness (kip/in)	119
Ultimate Shear Angle, $\gamma_{80\%}$ (rad*1000)	12.6

Notes

Specimens 31 and 33 have identical test setups.

Pinkham (1999) - Specimen 32

Input	
Structural Fastener Type	Arc Spot Weld
Sidelap Fastener Type	Button Punch
Deck thickness, t (in.)	0.0360
Panel Length, l (ft.)	10
Panel Span, l_v (ft.)	5
No. of sidelap connections per one edge of interior panel length, n_s	12
No. of edge structural connections not in line with int. or ext. supports, n_e	11
No. of interior supports per panel length, n_p	2
Yield strength of deck, F_y (ksi)	38
Ultimate strength of deck, F_u (ksi)	55
Moment of inertia of fully effective panel per unit width, I_x (in^4)	0.1865
Diameter of structural weld, (in.)	0.875

Fastener Strengths and Flexibilities	
Structural fastener strength, P_{nf} (kip)	3.65
Sidelap fastener strength, P_{ns} (kip)	0.31
Structural fastener flexibility, S_f (in/kip)	0.0061
Sidelap fastener flexibility, S_s (in/kip)	0.0059

Calculated Strength Equations Variables	
Corner fastener reduction factor, λ	0.835
Interior panel fastener contribution factor, β	7.24
Structural fastener distribution factor at panel ends, α_e^2	0.778
Structural fastener distribution factor at interior supports, α_p^2	0.778
Number of structural fasteners at panel ends per unit width, N	2.33
Fastener slip coefficient, C	4.81
Warping factor, D_n (in.)	4.64
Warping support factor, ρ	0.90

Predicted Shear Strength and Stiffness	
Interior panel shear strength, S_{ni} (kip/ft.)	2.53
Edge panel shear strength, S_{ne} (kip/ft.)	6.94
Panel shear strength limited by corner fastener, S_{nc} (kip/ft.)	2.53
	6.92
Panel buckling shear strength, S_{nb} (kip/ft.)	
Shear stiffness, G' (kip/in)	85.7

36/7 fastener pattern at interior and exterior supports

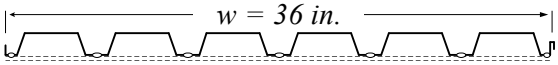

e (in.)	0.75
w_c (in.)	1.68
f (in.)	3.00
d (in.)	6.00
s (in.)	7.85
D_d (in.)	1.50

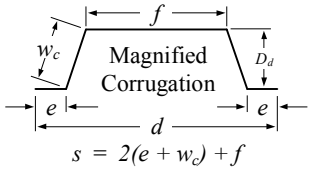

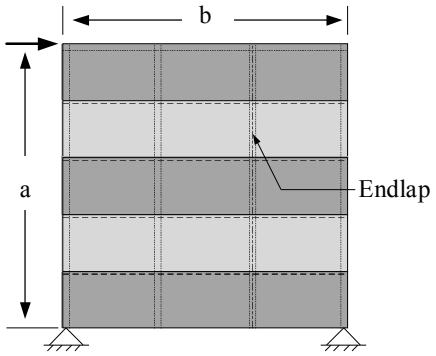

Loading Type: Monotonic

Load Rate: Static

a = 15'

b = 15'

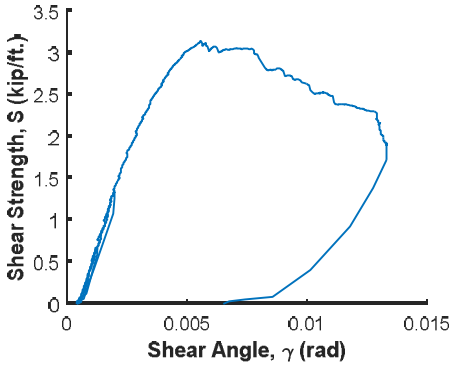

Eperimental Max Strength (kip/ft.)	3.15
Experimental Shear Stiffness (kip/in)	75.7
Ultimate Shear Angle, $\gamma_{80\%}$ (rad*1000)	10.3

Notes

Pinkham (1999) - Specimen 33

Input	
Structural Fastener Type	Arc Spot Weld
Sidelap Fastener Type	Top Seam Weld
Deck thickness, t (in.)	0.0360
Panel Length, l (ft.)	10
Panel Span, l_v (ft.)	5
No. of sidelap connections per one edge of interior panel length, n_s	12
No. of edge structural connections not in line with int. or ext. supports, n_e	16
No. of interior supports per panel length, n_p	2
Yield strength of deck, F_y (ksi)	38
Ultimate strength of deck, F_u (ksi)	55
Length of sidelap weld, L_w (in.)	1.5
Moment of inertia of fully effective panel per unit width, I_x (in^4)	0.1865
Diameter of structural weld, (in.)	0.875

Fastener Strengths and Flexibilities	
Structural fastener strength, P_{nf} (kip)	3.65
Sidelap fastener strength, P_{ns} (kip)	3.70
Structural fastener flexibility, S_f (in/kip)	0.0061
Sidelap fastener flexibility, S_s (in/kip)	0.0059

Calculated Strength Equations Variables	
Corner fastener reduction factor, λ	0.835
Interior panel fastener contribution factor, β	18.4
Structural fastener distribution factor at panel ends, α_e^2	0.778
Structural fastener distribution factor at interior supports, α_p^2	0.778
Number of structural fasteners at panel ends per unit width, N	2.33
Fastener slip coefficient, C	1.31
Warping factor, D_n (in.)	4.64
Warping support factor, ρ	0.90

Predicted Shear Strength and Stiffness	
Interior panel shear strength, S_{ni} (kip/ft.)	6.60
Edge panel shear strength, S_{ne} (kip/ft.)	8.77
Panel shear strength limited by corner fastener, S_{nc} (kip/ft.)	5.28
Panel buckling shear strength, S_{nb} (kip/ft.)	6.92
Shear stiffness, G' (kip/in)	119

36/7 fastener pattern at interior and exterior supports

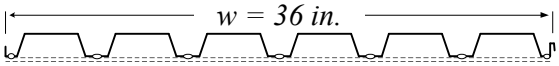

e (in.)	0.75
w_c (in.)	1.68
f (in.)	3.00
d (in.)	6.00
s (in.)	7.85
D_d (in.)	1.50

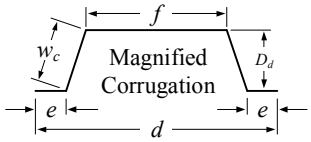

$s = 2(e + w_c) + f$

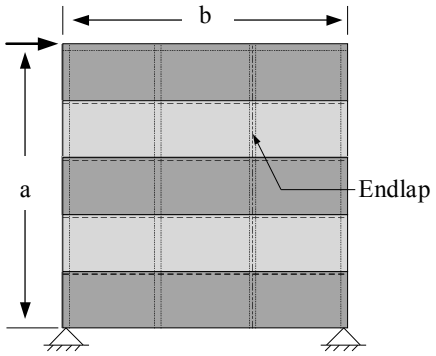

Loading Type: Monotonic

Load Rate: Static

a = 15'

b = 15'

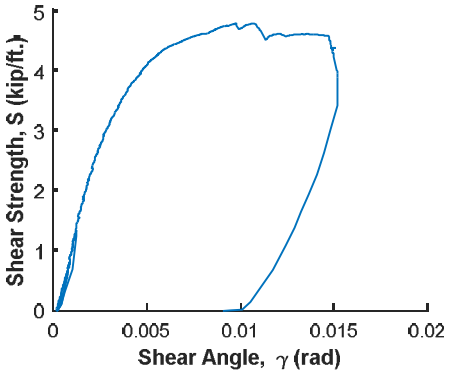

Eperimental Max Strength (kip/ft.)	4.81
Experimental Shear Stiffness (kip/in)	120
Ultimate Shear Angle, $\gamma_{80\%}$ (rad*1000)	15.2

Notes

Specimens 31 and 33 have identical test setups.

Pinkham (1999) - Specimen 34

Input	
Structural Fastener Type	Arc Spot Weld
Sidelap Fastener Type	Button Punch
Deck thickness, t (in.)	0.0310
Panel Length, l (ft.)	8
Panel Span, l_v (ft.)	8
No. of sidelap connections per one edge of interior panel length, n_s	14
No. of edge structural connections not in line with int. or ext. supports, n_e	14
No. of interior supports per panel length, n_p	1
Yield strength of deck, F_y (ksi)	38
Ultimate strength of deck, F_u (ksi)	55
Moment of inertia of fully effective panel per unit width, I_x (in^4)	0.1865
Diameter of structural weld, (in.)	0.875

Fastener Strengths and Flexibilities	
Structural fastener strength, P_{nf} (kip)	3.17
Sidelap fastener strength, P_{ns} (kip)	0.23
Structural fastener flexibility, S_f (in/kip)	0.0065
Sidelap fastener flexibility, S_s (in/kip)	0.1704

Calculated Strength Equations Variables	
Corner fastener reduction factor, λ	0.716
Interior panel fastener contribution factor, β	4.35
Structural fastener distribution factor at panel ends, α_e^2	0.556
Structural fastener distribution factor at interior supports, α_p^2	0.556
Number of structural fasteners at panel ends per unit width, N	1.33
Fastener slip coefficient, C	6.28
Warping factor, D_n (in.)	78.1
Warping support factor, ρ	1.00

Predicted Shear Strength and Stiffness	
Interior panel shear strength, S_{ni} (kip/ft.)	1.50
Edge panel shear strength, S_{ne} (kip/ft.)	7.12
Panel shear strength limited by corner fastener, S_{nc} (kip/ft.)	1.60
Panel buckling shear strength, S_{nb} (kip/ft.)	2.03
Shear stiffness, G' (kip/in)	10.4

36/4 fastener pattern at interior and exterior supports

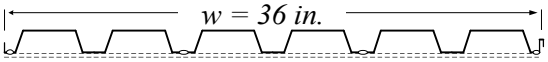

e (in.)	0.75
w_c (in.)	1.68
f (in.)	3.00
d (in.)	6.00
s (in.)	7.85
D_d (in.)	1.50

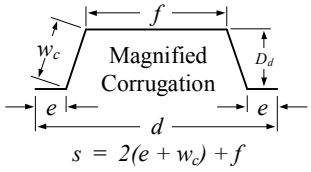

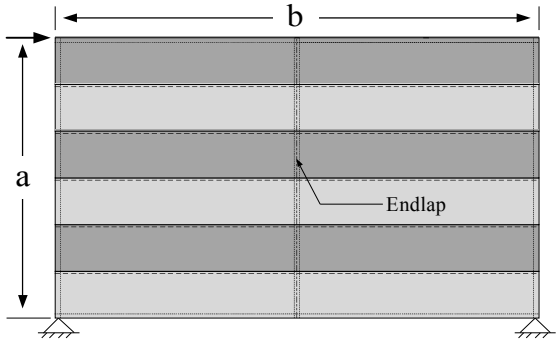

Loading Type: Monotonic

Load Rate: Static

a = 18'

b = 16'

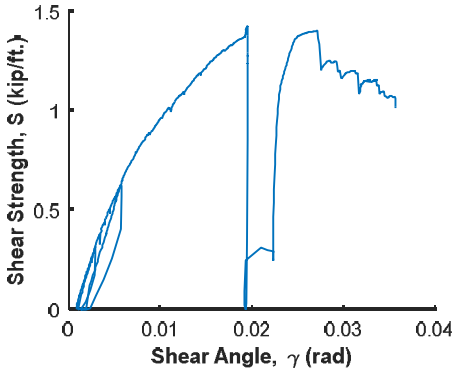

Eperimental Max Strength (kip/ft.)	1.43
Experimental Shear Stiffness (kip/in)	11.0
Ultimate Shear Angle, $\gamma_{80\%}$ (rad*1000)	19.5

Notes

Pinkham (1999) - Specimen 35

Input	
Structural Fastener Type	Arc Spot Weld
Sidelap Fastener Type	Top Seam Weld
Deck thickness, t (in.)	0.0310
Panel Length, l (ft.)	10
Panel Span, l_v (ft.)	5
No. of sidelap connections per one edge of interior panel length, n_s	12
No. of edge structural connections not in line with int. or ext. supports, n_e	16
No. of interior supports per panel length, n_p	2
Yield strength of deck, F_y (ksi)	38
Ultimate strength of deck, F_u (ksi)	55
Length of sidelap weld, L_w (in.)	1.50
Moment of inertia of fully effective panel per unit width, I_x (in^4)	0.1481
Diameter of structural weld, (in.)	0.875

Fastener Strengths and Flexibilities	
Structural fastener strength, P_{nf} (kip)	3.17
Sidelap fastener strength, P_{ns} (kip)	3.04
Structural fastener flexibility, S_f (in/kip)	0.0065
Sidelap fastener flexibility, S_s (in/kip)	0.0064

Calculated Strength Equations Variables	
Corner fastener reduction factor, λ	0.823
Interior panel fastener contribution factor, β	17.7
Structural fastener distribution factor at panel ends, α_e^2	0.778
Structural fastener distribution factor at interior supports, α_p^2	0.778
Number of structural fasteners at panel ends per unit width, N	2.33
Fastener slip coefficient, C	1.22
Warping factor, D_n (in.)	5.81
Warping support factor, ρ	0.90

Predicted Shear Strength and Stiffness	
Interior panel shear strength, S_{ni} (kip/ft.)	5.50
Edge panel shear strength, S_{ne} (kip/ft.)	7.60
Panel shear strength limited by corner fastener, S_{nc} (kip/ft.)	4.47
Panel buckling shear strength, S_{nb} (kip/ft.)	5.20
Shear stiffness, G' (kip/in)	92.8

36/7 fastener pattern at interior and exterior supports

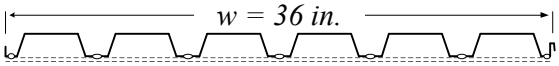

e (in.)	0.75
w_c (in.)	1.68
f (in.)	3.00
d (in.)	6.00
s (in.)	7.85
D_d (in.)	1.50

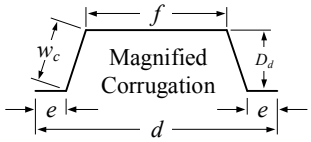

$s = 2(e + w_c) + f$

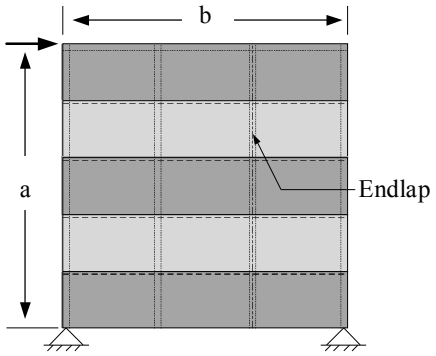

Loading Type: Monotonic

Load Rate: Static

a = 15'

b = 15'

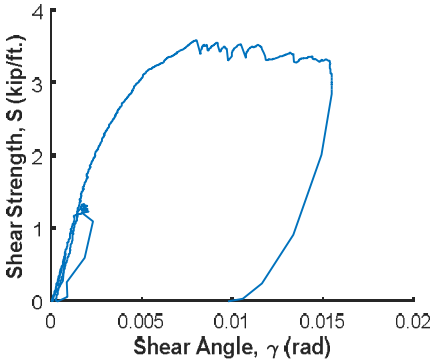

Eperimental Max Strength (kip/ft.)	3.60
Experimental Shear Stiffness (kip/in)	80.1
Ultimate Shear Angle, $\gamma_{80\%}$ (rad*1000)	15.4

Notes

Pinkham (1999) - Specimen 36

Input	
Structural Fastener Type	Arc Spot Weld
Sidelap Fastener Type	Button Punch
Deck thickness, t (in.)	0.0360
Panel Length, l (ft.)	10
Panel Span, l_v (ft.)	5
No. of sidelap connections per one edge of interior panel length, n_s	12
No. of edge structural connections not in line with int. or ext. supports, n_e	14
No. of interior supports per panel length, n_p	2
Yield strength of deck, F_y (ksi)	38
Ultimate strength of deck, F_u (ksi)	55
Moment of inertia of fully effective panel per unit width, I_x (in^4)	0.1865
Diameter of structural weld, (in.)	0.875

Fastener Strengths and Flexibilities	
Structural fastener strength, P_{nf} (kip)	3.65
Sidelap fastener strength, P_{ns} (kip)	0.31
Structural fastener flexibility, S_f (in/kip)	0.0061
Sidelap fastener flexibility, S_s (in/kip)	0.1581

Calculated Strength Equations Variables	
Corner fastener reduction factor, λ	0.835
Interior panel fastener contribution factor, β	5.47
Structural fastener distribution factor at panel ends, α_e^2	0.556
Structural fastener distribution factor at interior supports, α_p^2	0.556
Number of structural fasteners at panel ends per unit width, N	1.33
Fastener slip coefficient, C	6.86
Warping factor, D_n (in.)	50.1
Warping support factor, ρ	0.90

Predicted Shear Strength and Stiffness	
Interior panel shear strength, S_{ni} (kip/ft.)	1.88
Edge panel shear strength, S_{ne} (kip/ft.)	7.07
Panel shear strength limited by corner fastener, S_{nc} (kip/ft.)	1.85
Panel buckling shear strength, S_{nb} (kip/ft.)	6.92
Shear stiffness, G' (kip/in)	19.2

36/4 fastener pattern at interior and exterior supports

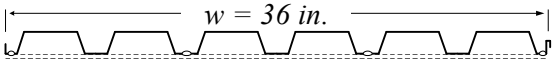

e (in.)	0.75
w_c (in.)	1.68
f (in.)	3.00
d (in.)	6.00
s (in.)	7.85
D_d (in.)	1.50

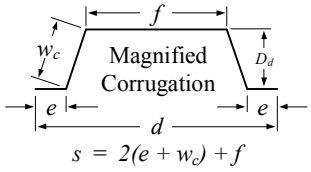

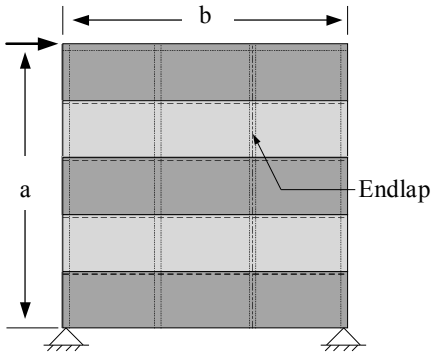

Loading Type: Monotonic

Load Rate: Static

a = 15'

b = 15'

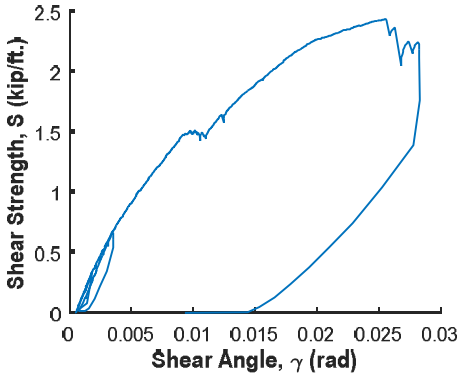

Eperimental Max Strength (kip/ft.)	2.45
Experimental Shear Stiffness (kip/in)	16.4
Ultimate Shear Angle, $\gamma_{80\%}$ (rad*1000)	28.3

Notes

Pinkham (1999) - Specimen 37

Input	
Structural Fastener Type	Arc Spot Weld
Sidelap Fastener Type	Top Seam Weld
Deck thickness, t (in.)	0.0360
Panel Length, l (ft.)	10
Panel Span, l_v (ft.)	10
No. of sidelap connections per one edge of interior panel length, n_s	8
No. of edge structural connections not in line with int. or ext. supports, n_e	12
No. of interior supports per panel length, n_p	1
Yield strength of deck, F_y (ksi)	38
Ultimate strength of deck, F_u (ksi)	55
Length of sidelap weld, L_w (in.)	1.50
Moment of inertia of fully effective panel per unit width, I_x (in^4)	0.1865
Diameter of structural weld, (in.)	0.875

Fastener Strengths and Flexibilities	
Structural fastener strength, P_{nf} (kip)	3.65
Sidelap fastener strength, P_{ns} (kip)	3.70
Structural fastener flexibility, S_f (in/kip)	0.0061
Sidelap fastener flexibility, S_s (in/kip)	0.0059

Calculated Strength Equations Variables	
Corner fastener reduction factor, λ	0.700
Interior panel fastener contribution factor, β	12.8
Structural fastener distribution factor at panel ends, α_e^2	0.778
Structural fastener distribution factor at interior supports, α_p^2	0.778
Number of structural fasteners at panel ends per unit width, N	2.33
Fastener slip coefficient, C	1.91
Warping factor, D_n (in.)	4.64
Warping support factor, ρ	1.00

Predicted Shear Strength and Stiffness	
Interior panel shear strength, S_{ni} (kip/ft.)	4.45
Edge panel shear strength, S_{ne} (kip/ft.)	8.77
Panel shear strength limited by corner fastener, S_{nc} (kip/ft.)	4.09
Panel buckling shear strength, S_{nb} (kip/ft.)	1.73
Shear stiffness, G' (kip/in)	107

36/7 fastener pattern at interior and exterior supports

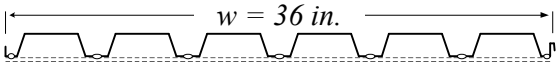

e (in.)	0.75
w_c (in.)	1.68
f (in.)	3.00
d (in.)	6.00
s (in.)	7.85
D_d (in.)	1.50

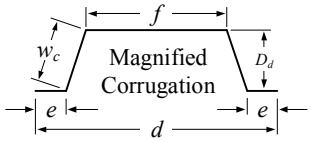

$s = 2(e + w_c) + f$

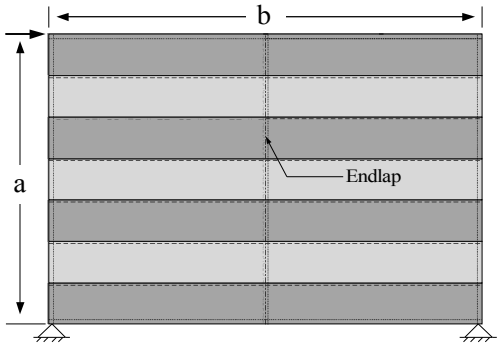

Loading Type: Monotonic

Load Rate: Static

a = 21'

b = 20'

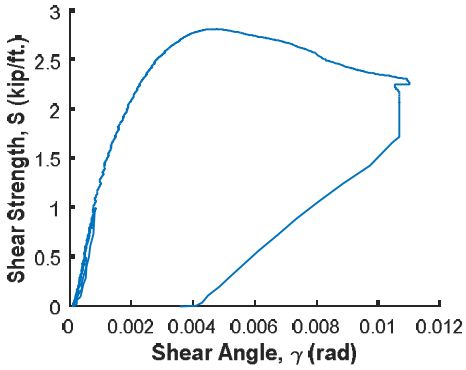

Eperimental Max Strength (kip/ft.)	2.82
Experimental Shear Stiffness (kip/in)	127
Ultimate Shear Angle, $\gamma_{80\%}$ (rad*1000)	10.5

Notes

Pinkham (1999) - Specimen 38

Input	
Structural Fastener Type	Arc Spot Weld
Sidelap Fastener Type	Top Seam Weld
Deck thickness, t (in.)	0.0360
Panel Length, l (ft.)	10
Panel Span, l_v (ft.)	10
No. of sidelap connections per one edge of interior panel length, n_s	8
No. of edge structural connections not in line with int. or ext. supports, n_e	18
No. of interior supports per panel length, n_p	1
Yield strength of deck, F_y (ksi)	38
Ultimate strength of deck, F_u (ksi)	55
Length of sidelap weld, L_w (in.)	1.50
Moment of inertia of fully effective panel per unit width, I_x (in^4)	0.1481
Diameter of structural weld, (in.)	0.875

Fastener Strengths and Flexibilities	
Structural fastener strength, P_{nf} (kip)	3.23
Sidelap fastener strength, P_{ns} (kip)	3.13
Structural fastener flexibility, S_f (in/kip)	0.0065
Sidelap fastener flexibility, S_s (in/kip)	0.0063

Calculated Strength Equations Variables	
Corner fastener reduction factor, λ	0.700
Interior panel fastener contribution factor, β	11.0
Structural fastener distribution factor at panel ends, α_e^2	0.556
Structural fastener distribution factor at interior supports, α_p^2	0.556
Number of structural fasteners at panel ends per unit width, N	1.33
Fastener slip coefficient, C	1.97
Warping factor, D_n (in.)	60.4
Warping support factor, ρ	1.00

Predicted Shear Strength and Stiffness	
Interior panel shear strength, S_{ni} (kip/ft.)	3.39
Edge panel shear strength, S_{ne} (kip/ft.)	7.12
Panel shear strength limited by corner fastener, S_{nc} (kip/ft.)	2.75
Panel buckling shear strength, S_{nb} (kip/ft.)	1.32
Shear stiffness, G' (kip/in)	14.2

36/4 fastener pattern at interior and exterior supports

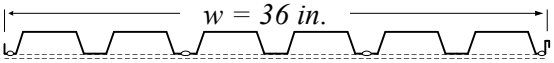

e (in.)	0.75
w_c (in.)	1.68
f (in.)	3.00
d (in.)	6.00
s (in.)	7.85
D_d (in.)	1.50

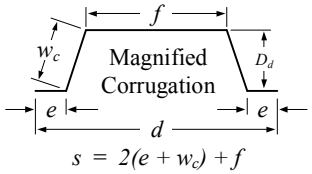

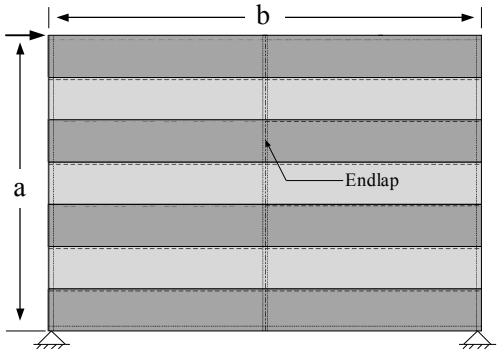

Loading Type: Monotonic

Load Rate: Static

a = 21'

b = 20'

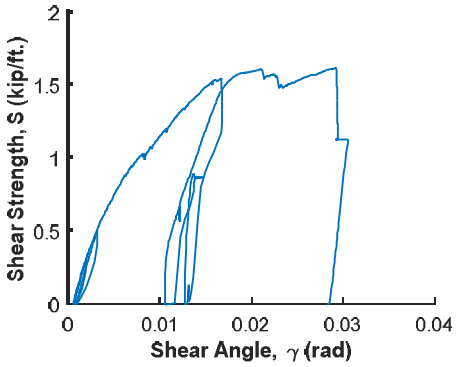

Eperimental Max Strength (kip/ft.)	1.62
Experimental Shear Stiffness (kip/in)	14.8
Ultimate Shear Angle, $\gamma_{80\%}$ (rad*1000)	29.3

Notes

Pinkham (1999) - Specimen 39

Input	
Structural Fastener Type	Arc Spot Weld
Sidelap Fastener Type	Top Seam Weld
Deck thickness, t (in.)	0.0310
Panel Length, l (ft.)	8
Panel Span, l_v (ft.)	8
No. of sidelap connections per one edge of interior panel length, n_s	14
No. of edge structural connections not in line with int. or ext. supports, n_e	18
No. of interior supports per panel length, n_p	1
Yield strength of deck, F_y (ksi)	38
Ultimate strength of deck, F_u (ksi)	55
Length of sidelap weld, L_w (in.)	1.50
Moment of inertia of fully effective panel per unit width, I_x (in^4)	0.1481
Diameter of structural weld, (in.)	0.875

Fastener Strengths and Flexibilities	
Structural fastener strength, P_{nf} (kip)	3.17
Sidelap fastener strength, P_{ns} (kip)	3.04
Structural fastener flexibility, S_f (in/kip)	0.0065
Sidelap fastener flexibility, S_s (in/kip)	0.0064

Calculated Strength Equations Variables	
Corner fastener reduction factor, λ	0.716
Interior panel fastener contribution factor, β	18.1
Structural fastener distribution factor at panel ends, α_e^2	0.778
Structural fastener distribution factor at interior supports, α_p^2	0.778
Number of structural fasteners at panel ends per unit width, N	2.33
Fastener slip coefficient, C	0.92
Warping factor, D_n (in.)	7.23
Warping support factor, ρ	1.00

Predicted Shear Strength and Stiffness	
Interior panel shear strength, S_{ni} (kip/ft.)	6.93
Edge panel shear strength, S_{ne} (kip/ft.)	9.50
Panel shear strength limited by corner fastener, S_{nc} (kip/ft.)	5.14
Panel buckling shear strength, S_{nb} (kip/ft.)	2.03
Shear stiffness, G' (kip/in)	79.0

36/7 fastener pattern at interior and exterior supports

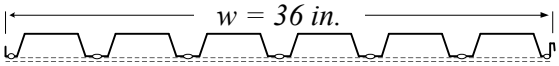

e (in.)	0.75
w_c (in.)	1.68
f (in.)	3.00
d (in.)	6.00
s (in.)	7.85
D_d (in.)	1.50

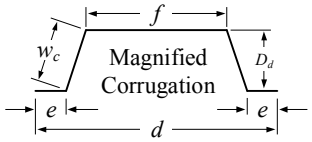

$s = 2(e + w_c) + f$

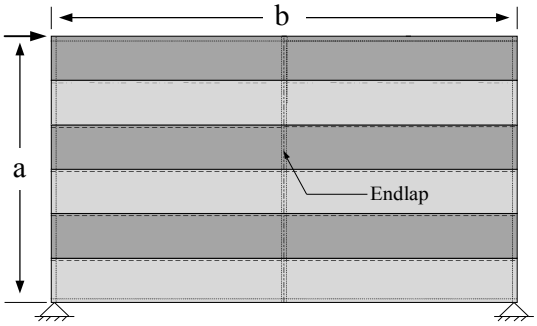

Loading Type: Monotonic

Load Rate: Static

a = 18'

b = 16'

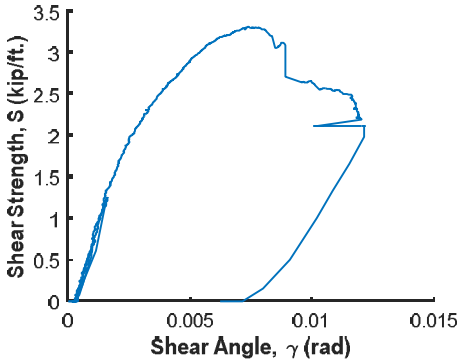

Eperimental Max Strength (kip/ft.)	3.32
Experimental Shear Stiffness (kip/in)	81.4
Ultimate Shear Angle, $\gamma_{80\%}$ (rad*1000)	9.54

Notes

Pinkham (1999) - Specimen 40

Input	
Structural Fastener Type	Arc Spot Weld
Sidelap Fastener Type	Fillet Weld
Deck thickness, t (in.)	0.0480
Panel Length, l (ft.)	10
Panel Span, l_v (ft.)	5
No. of sidelap connections per one edge of interior panel length, n_s	12
No. of edge structural connections not in line with int. or ext. supports, n_e	14
No. of interior supports per panel length, n_p	2
Yield strength of deck, F_y (ksi)	38
Ultimate strength of deck, F_u (ksi)	55
Length of sidelap weld, L_w (in.)	1.50
Moment of inertia of fully effective panel per unit width, I_x (in^4)	0.2920
Diameter of structural weld, (in.)	0.875

Fastener Strengths and Flexibilities	
Structural fastener strength, P_{nf} (kip)	4.80
Sidelap fastener strength, P_{ns} (kip)	2.97
Structural fastener flexibility, S_f (in/kip)	0.0052
Sidelap fastener flexibility, S_s (in/kip)	0.0057

Calculated Strength Equations Variables	
Corner fastener reduction factor, λ	0.857
Interior panel fastener contribution factor, β	13.6
Structural fastener distribution factor at panel ends, α_e^2	0.778
Structural fastener distribution factor at interior supports, α_p^2	0.778
Number of structural fasteners at panel ends per unit width, N	2.00
Fastener slip coefficient, C	1.65
Warping factor, D_n (in.)	3.02
Warping support factor, ρ	0.90

Predicted Shear Strength and Stiffness	
Interior panel shear strength, S_{ni} (kip/ft.)	6.42
Edge panel shear strength, S_{ne} (kip/ft.)	10.60
Panel shear strength limited by corner fastener, S_{nc} (kip/ft.)	5.41
Panel buckling shear strength, S_{nb} (kip/ft.)	12.0
Shear stiffness, G' (kip/in)	182

36/7 fastener pattern at interior and exterior supports

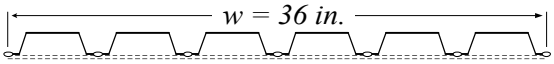

e (in.)	0.75
w_c (in.)	1.68
f (in.)	3.00
d (in.)	6.00
s (in.)	7.85
D_d (in.)	1.50

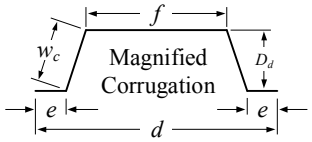

$s = 2(e + w_c) + f$

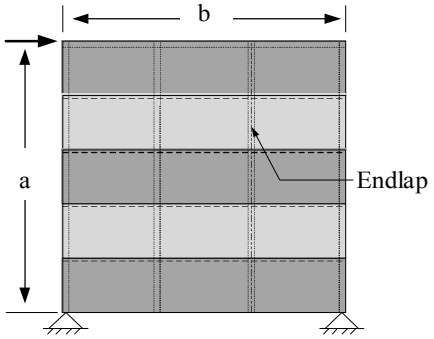

Loading Type: Monotonic

Load Rate: Static

a = 10'

b = 15'

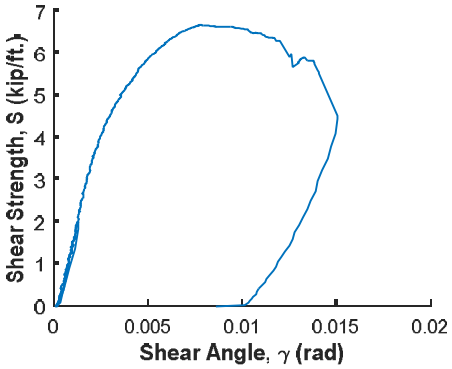

Eperimental Max Strength (kip/ft.)	6.68
Experimental Shear Stiffness (kip/in)	167
Ultimate Shear Angle, $\gamma_{80\%}$ (rad*1000)	14.2

Notes

Pinkham (1999) - Specimen 41

Input	
Structural Fastener Type	Arc Spot Weld
Sidelap Fastener Type	Fillet Weld
Deck thickness, t (in.)	0.0310
Panel Length, l (ft.)	10
Panel Span, l_v (ft.)	5
No. of sidelap connections per one edge of interior panel length, n_s	12
No. of edge structural connections not in line with int. or ext. supports, n_e	12
No. of interior supports per panel length, n_p	2
Yield strength of deck, F_y (ksi)	38
Ultimate strength of deck, F_u (ksi)	55
Length of sidelap weld, L_w (in.)	1.50
Moment of inertia of fully effective panel per unit width, I_x (in^4)	0.1481
Diameter of structural weld, (in.)	0.875

Fastener Strengths and Flexibilities	
Structural fastener strength, P_{nf} (kip)	3.17
Sidelap fastener strength, P_{ns} (kip)	1.92
Structural fastener flexibility, S_f (in/kip)	0.0065
Sidelap fastener flexibility, S_s (in/kip)	0.0071

Calculated Strength Equations Variables	
Corner fastener reduction factor, λ	0.823
Interior panel fastener contribution factor, β	13.5
Structural fastener distribution factor at panel ends, α_e^2	0.778
Structural fastener distribution factor at interior supports, α_p^2	0.778
Number of structural fasteners at panel ends per unit width, N	2.00
Fastener slip coefficient, C	1.32
Warping factor, D_n (in.)	3.02
Warping support factor, ρ	0.90

Predicted Shear Strength and Stiffness	
Interior panel shear strength, S_{ni} (kip/ft.)	4.16
Edge panel shear strength, S_{ne} (kip/ft.)	6.33
Panel shear strength limited by corner fastener, S_{nc} (kip/ft.)	3.54
Panel buckling shear strength, S_{nb} (kip/ft.)	5.20
Shear stiffness, G' (kip/in)	91.9

36/7 fastener pattern at interior and exterior supports

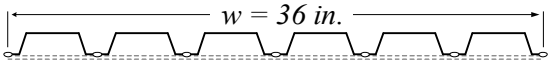

e (in.)	0.75
w_c (in.)	1.68
f (in.)	3.00
d (in.)	6.00
s (in.)	7.85
D_d (in.)	1.50

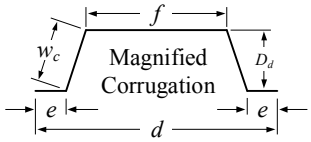

$s = 2(e + w_c) + f$

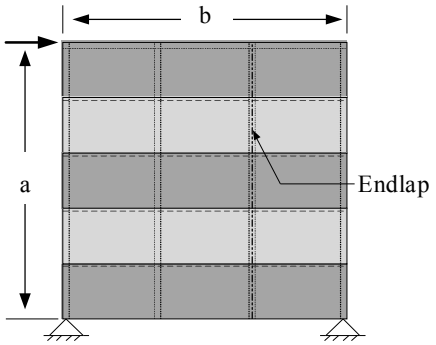

Loading Type: Monotonic

Load Rate: Static

a = 10'

b = 15'

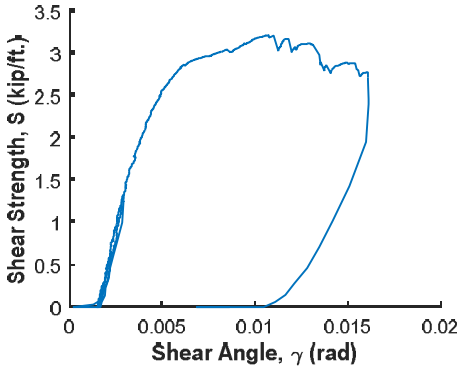

Eperimental Max Strength (kip/ft.)	3.22
Experimental Shear Stiffness (kip/in)	80.5
Ultimate Shear Angle, $\gamma_{80\%}$ (rad*1000)	16.1

Notes

Pinkham (1999) - Specimen 42

Input	
Structural Fastener Type	Arc Spot Weld
Sidelap Fastener Type	Fillet Weld
Deck thickness, t (in.)	0.0310
Panel Length, l (ft.)	10
Panel Span, l_v (ft.)	10
No. of sidelap connections per one edge of interior panel length, n_s	8
No. of edge structural connections not in line with int. or ext. supports, n_e	18
No. of interior supports per panel length, n_p	1
Yield strength of deck, F_y (ksi)	38
Ultimate strength of deck, F_u (ksi)	55
Length of sidelap weld, L_w (in.)	1.50
Moment of inertia of fully effective panel per unit width, I_x (in^4)	0.1481
Diameter of structural weld, (in.)	0.875

Fastener Strengths and Flexibilities	
Structural fastener strength, P_{nf} (kip)	3.17
Sidelap fastener strength, P_{ns} (kip)	1.92
Structural fastener flexibility, S_f (in/kip)	0.0065
Sidelap fastener flexibility, S_s (in/kip)	0.0071

Calculated Strength Equations Variables	
Corner fastener reduction factor, λ	0.700
Interior panel fastener contribution factor, β	8.18
Structural fastener distribution factor at panel ends, α_e^2	0.556
Structural fastener distribution factor at interior supports, α_p^2	0.556
Number of structural fasteners at panel ends per unit width, N	1.00
Fastener slip coefficient, C	2.13
Warping factor, D_n (in.)	62.5
Warping support factor, ρ	1.00

Predicted Shear Strength and Stiffness	
Interior panel shear strength, S_{ni} (kip/ft.)	2.40
Edge panel shear strength, S_{ne} (kip/ft.)	6.96
Panel shear strength limited by corner fastener, S_{nc} (kip/ft.)	2.00
Panel buckling shear strength, S_{nb} (kip/ft.)	1.30
Shear stiffness, G' (kip/in)	13.5

36/4 fastener pattern at interior and exterior supports

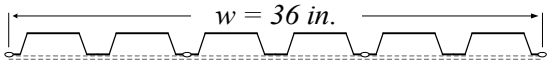

e (in.)	0.75
w_c (in.)	1.68
f (in.)	3.00
d (in.)	6.00
s (in.)	7.85
D_d (in.)	1.50

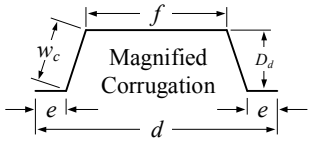

$s = 2(e + w_c) + f$

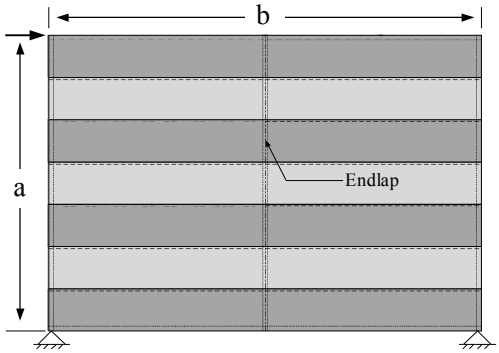

Loading Type: Monotonic

Load Rate: Static

a = 21'

b = 20'

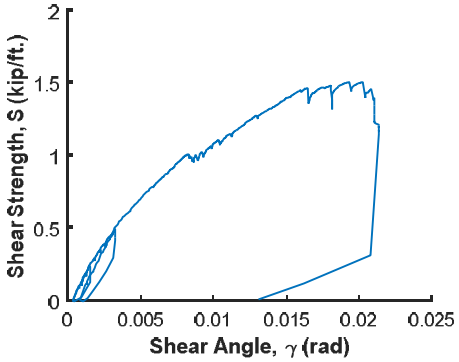

Eperimental Max Strength (kip/ft.)	1.51
Experimental Shear Stiffness (kip/in)	13.3
Ultimate Shear Angle, $\gamma_{80\%}$ (rad*1000)	21.3

Notes

Pinkham (1999) - Specimen 43

Input	
Structural Fastener Type	Arc Spot Weld
Sidelap Fastener Type	Fillet Weld
Deck thickness, t (in.)	0.0310
Panel Length, l (ft.)	10
Panel Span, l_v (ft.)	10
No. of sidelap connections per one edge of interior panel length, n_s	18
No. of edge structural connections not in line with int. or ext. supports, n_e	18
No. of interior supports per panel length, n_p	1
Yield strength of deck, F_y (ksi)	38
Ultimate strength of deck, F_u (ksi)	55
Length of sidelap weld, L_w (in.)	1.50
Moment of inertia of fully effective panel per unit width, I_x (in^4)	0.1481
Diameter of structural weld, (in.)	0.875

Fastener Strengths and Flexibilities	
Structural fastener strength, P_{nf} (kip)	3.17
Sidelap fastener strength, P_{ns} (kip)	1.92
Structural fastener flexibility, S_f (in/kip)	0.0065
Sidelap fastener flexibility, S_s (in/kip)	0.0071

Calculated Strength Equations Variables	
Corner fastener reduction factor, λ	0.700
Interior panel fastener contribution factor, β	15.6
Structural fastener distribution factor at panel ends, α_e^2	0.778
Structural fastener distribution factor at interior supports, α_p^2	0.778
Number of structural fasteners at panel ends per unit width, N	2.00
Fastener slip coefficient, C	1.02
Warping factor, D_n (in.)	5.81
Warping support factor, ρ	1.00

Predicted Shear Strength and Stiffness	
Interior panel shear strength, S_{ni} (kip/ft.)	4.74
Edge panel shear strength, S_{ne} (kip/ft.)	7.60
Panel shear strength limited by corner fastener, S_{nc} (kip/ft.)	3.89
Panel buckling shear strength, S_{nb} (kip/ft.)	1.30
Shear stiffness, G' (kip/in)	89.4

36/7 fastener pattern at interior and exterior supports

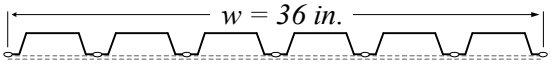

e (in.)	0.75
w_c (in.)	1.68
f (in.)	3.00
d (in.)	6.00
s (in.)	7.85
D_d (in.)	1.50

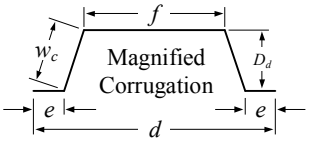

$s = 2(e + w_c) + f$

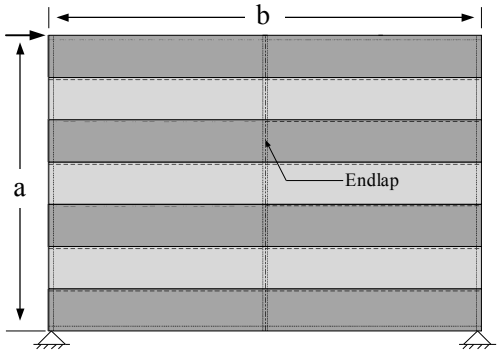

Loading Type: Monotonic

Load Rate: Static

a = 21'

b = 20'

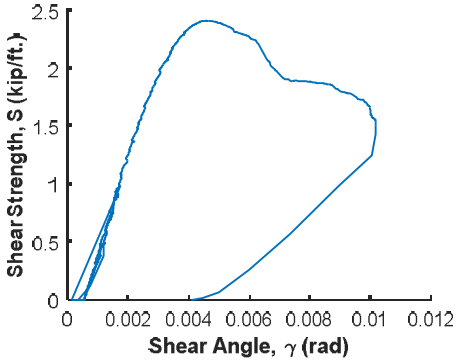

Eperimental Max Strength (kip/ft.)	2.42
Experimental Shear Stiffness (kip/in)	70
Ultimate Shear Angle, $\gamma_{80\%}$ (rad*1000)	7.04

Notes

Pinkham (1999) - Specimen 44

Input	
Structural Fastener Type	Arc Spot Weld
Sidelap Fastener Type	Fillet Weld
Deck thickness, t (in.)	0.0480
Panel Length, l (ft.)	10
Panel Span, l_v (ft.)	10
No. of sidelap connections per one edge of interior panel length, n_s	8
No. of edge structural connections not in line with int. or ext. supports, n_e	23
No. of interior supports per panel length, n_p	1
Yield strength of deck, F_y (ksi)	38
Ultimate strength of deck, F_u (ksi)	55
Length of sidelap weld, L_w (in.)	1.50
Moment of inertia of fully effective panel per unit width, I_x (in^4)	0.2920
Diameter of structural weld, (in.)	0.875

Fastener Strengths and Flexibilities	
Structural fastener strength, P_{nf} (kip)	4.80
Sidelap fastener strength, P_{ns} (kip)	2.97
Structural fastener flexibility, S_f (in/kip)	0.0052
Sidelap fastener flexibility, S_s (in/kip)	0.0057

Calculated Strength Equations Variables	
Corner fastener reduction factor, λ	0.715
Interior panel fastener contribution factor, β	8.28
Structural fastener distribution factor at panel ends, α_e^2	0.556
Structural fastener distribution factor at interior supports, α_p^2	0.556
Number of structural fasteners at panel ends per unit width, N	1.00
Fastener slip coefficient, C	2.65
Warping factor, D_n (in.)	32.4
Warping support factor, ρ	1.00

Predicted Shear Strength and Stiffness	
Interior panel shear strength, S_{ni} (kip/ft.)	3.70
Edge panel shear strength, S_{ne} (kip/ft.)	13.0
Panel shear strength limited by corner fastener, S_{nc} (kip/ft.)	3.06
Panel buckling shear strength, S_{nb} (kip/ft.)	3.00
Shear stiffness, G' (kip/in)	36.8

36/4 fastener pattern at interior and exterior supports

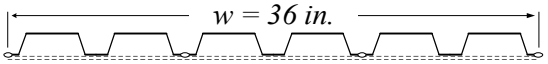

e (in.)	0.75
w_c (in.)	1.68
f (in.)	3.00
d (in.)	6.00
s (in.)	7.85
D_d (in.)	1.50

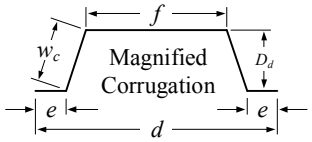

$s = 2(e + w_c) + f$

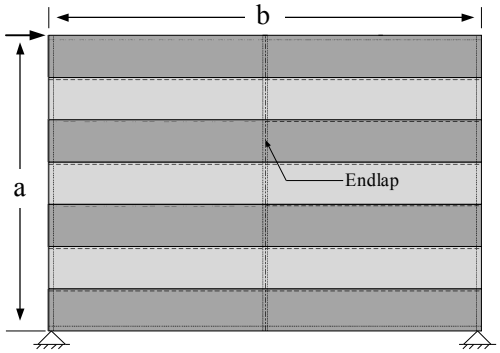

Loading Type: Monotonic

Load Rate: Static

a = 21'

b = 20'

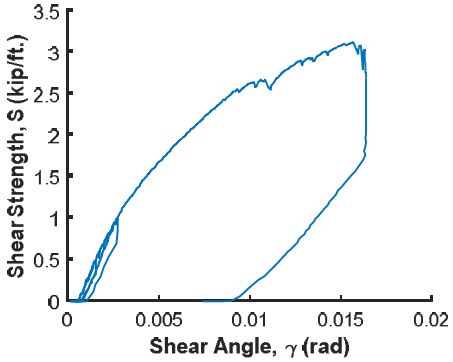

Eperimental Max Strength (kip/ft.)	3.13
Experimental Shear Stiffness (kip/in)	31.4
Ultimate Shear Angle, $\gamma_{80\%}$ (rad*1000)	16.4

Notes

Pinkham (1999) - Specimen 50

Input	
Structural Fastener Type	Arc Spot Weld
Sidelap Fastener Type	Screw
Deck thickness, t (in.)	0.0480
Panel Length, l (ft.)	10
Panel Span, l_v (ft.)	5
No. of sidelap connections per one edge of interior panel length, n_s	27
No. of edge structural connections not in line with int. or ext. supports, n_e	18
No. of interior supports per panel length, n_p	2
Yield strength of deck, F_y (ksi)	38
Ultimate strength of deck, F_u (ksi)	55
Diameter of sidelap screw (in.)	0.211
Moment of inertia of fully effective panel per unit width, I_x (in^4)	0.2920
Diameter of structural weld, (in.)	0.875

Fastener Strengths and Flexibilities	
Structural fastener strength, P_{nf} (kip)	4.80
Sidelap fastener strength, P_{ns} (kip)	1.17
Structural fastener flexibility, S_f (in/kip)	0.0052
Sidelap fastener flexibility, S_s (in/kip)	0.0137

Calculated Strength Equations Variables	
Corner fastener reduction factor, λ	0.857
Interior panel fastener contribution factor, β	12.8
Structural fastener distribution factor at panel ends, α_e^2	0.778
Structural fastener distribution factor at interior supports, α_p^2	0.778
Number of structural fasteners at panel ends per unit width, N	2.00
Fastener slip coefficient, C	1.73
Warping factor, D_n (in.)	3.02
Warping support factor, ρ	0.90

Predicted Shear Strength and Stiffness	
Interior panel shear strength, S_{ni} (kip/ft.)	6.00
Edge panel shear strength, S_{ne} (kip/ft.)	12.50
Panel shear strength limited by corner fastener, S_{nc} (kip/ft.)	5.17
Panel buckling shear strength, S_{nb} (kip/ft.)	12.0
Shear stiffness, G' (kip/in)	181

36/7 fastener pattern at interior and exterior supports

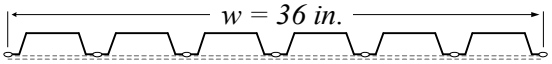

e (in.)	0.75
w_c (in.)	1.68
f (in.)	3.00
d (in.)	6.00
s (in.)	7.85
D_d (in.)	1.50

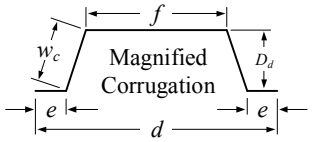

$s = 2(e + w_c) + f$

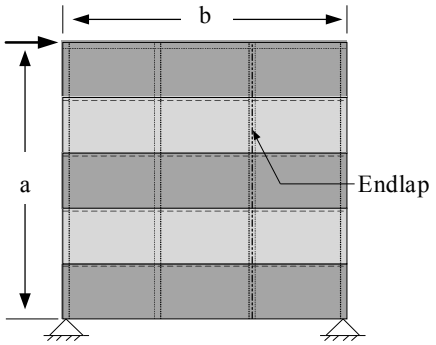

Loading Type: Monotonic

Load Rate: Static

a = 10'

b = 15'

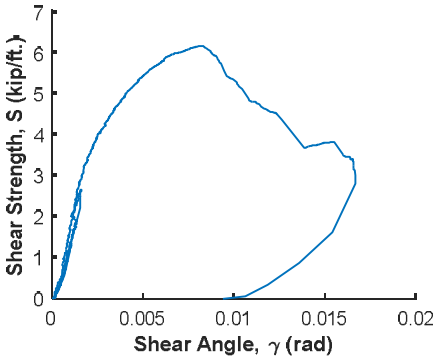

Eperimental Max Strength (kip/ft.)	6.19
Experimental Shear Stiffness (kip/in)	167
Ultimate Shear Angle, $\gamma_{80\%}$ (rad*1000)	10.7

Notes

Pinkham (1999) - Specimen 51

Input	
Structural Fastener Type	Arc Spot Weld
Sidelap Fastener Type	Screw
Deck thickness, t (in.)	0.0310
Panel Length, l (ft.)	10
Panel Span, l_v (ft.)	5
No. of sidelap connections per one edge of interior panel length, n_s	27
No. of edge structural connections not in line with int. or ext. supports, n_e	18
No. of interior supports per panel length, n_p	2
Yield strength of deck, F_y (ksi)	38
Ultimate strength of deck, F_u (ksi)	55
Diameter of sidelap screw (in.)	0.211
Moment of inertia of fully effective panel per unit width, I_x (in^4)	0.1481
Diameter of structural weld, (in.)	0.875

Fastener Strengths and Flexibilities	
Structural fastener strength, P_{nf} (kip)	3.17
Sidelap fastener strength, P_{ns} (kip)	0.75
Structural fastener flexibility, S_f (in/kip)	0.0065
Sidelap fastener flexibility, S_s (in/kip)	0.0170

Calculated Strength Equations Variables	
Corner fastener reduction factor, λ	0.823
Interior panel fastener contribution factor, β	12.6
Structural fastener distribution factor at panel ends, α_e^2	0.778
Structural fastener distribution factor at interior supports, α_p^2	0.778
Number of structural fasteners at panel ends per unit width, N	2.00
Fastener slip coefficient, C	1.39
Warping factor, D_n (in.)	5.81
Warping support factor, ρ	0.90

Predicted Shear Strength and Stiffness	
Interior panel shear strength, S_{ni} (kip/ft.)	3.89
Edge panel shear strength, S_{ne} (kip/ft.)	8.23
Panel shear strength limited by corner fastener, S_{nc} (kip/ft.)	3.38
Panel buckling shear strength, S_{nb} (kip/ft.)	5.20
Shear stiffness, G' (kip/in)	91.3

36/7 fastener pattern at interior and exterior supports

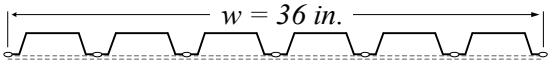

e (in.)	0.75
w_c (in.)	1.68
f (in.)	3.00
d (in.)	6.00
s (in.)	7.85
D_d (in.)	1.50

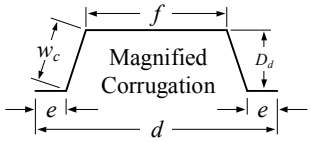

$s = 2(e + w_c) + f$

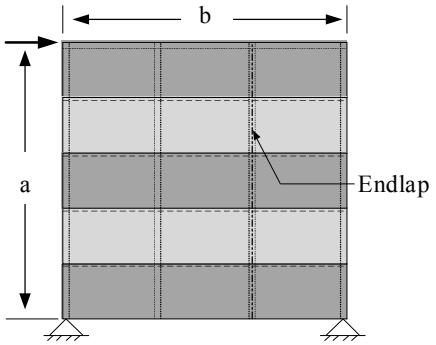

Loading Type: Monotonic

Load Rate: Static

a = 10'

b = 15'

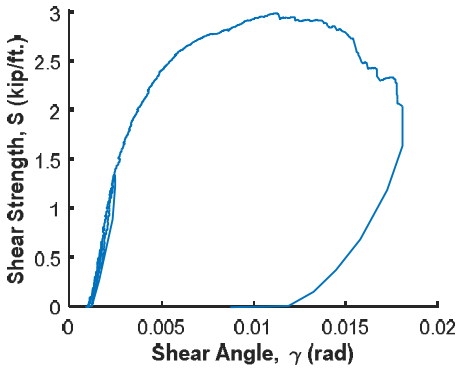

Eperimental Max Strength (kip/ft.)	3.00
Experimental Shear Stiffness (kip/in)	81.5
Ultimate Shear Angle, $\gamma_{80\%}$ (rad*1000)	16.7

Notes

Pinkham (1999) - Specimen 52

Input	
Structural Fastener Type	Arc Spot Weld
Sidelap Fastener Type	Screw
Deck thickness, t (in.)	0.0310
Panel Length, l (ft.)	10
Panel Span, l_v (ft.)	10
No. of sidelap connections per one edge of interior panel length, n_s	8
No. of edge structural connections not in line with int. or ext. supports, n_e	18
No. of interior supports per panel length, n_p	1
Yield strength of deck, F_y (ksi)	38
Ultimate strength of deck, F_u (ksi)	55
Diameter of sidelap screw (in.)	0.211
Moment of inertia of fully effective panel per unit width, I_x (in^4)	0.1481
Diameter of structural weld, (in.)	0.875

Fastener Strengths and Flexibilities	
Structural fastener strength, P_{nf} (kip)	3.17
Sidelap fastener strength, P_{ns} (kip)	0.75
Structural fastener flexibility, S_f (in/kip)	0.0065
Sidelap fastener flexibility, S_s (in/kip)	0.0170

Calculated Strength Equations Variables	
Corner fastener reduction factor, λ	0.700
Interior panel fastener contribution factor, β	5.24
Structural fastener distribution factor at panel ends, α_e^2	0.556
Structural fastener distribution factor at interior supports, α_p^2	0.556
Number of structural fasteners at panel ends per unit width, N	1.00
Fastener slip coefficient, C	3.93
Warping factor, D_n (in.)	62.5
Warping support factor, ρ	1.00

Predicted Shear Strength and Stiffness	
Interior panel shear strength, S_{ni} (kip/ft.)	1.47
Edge panel shear strength, S_{ne} (kip/ft.)	6.96
Panel shear strength limited by corner fastener, S_{nc} (kip/ft.)	1.47
Panel buckling shear strength, S_{nb} (kip/ft.)	1.30
Shear stiffness, G' (kip/in)	13.1

36/4 fastener pattern at interior and exterior supports

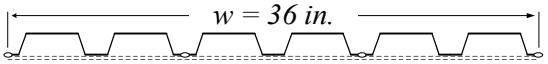

e (in.)	0.75
w_c (in.)	1.68
f (in.)	3.00
d (in.)	6.00
s (in.)	7.85
D_d (in.)	1.50

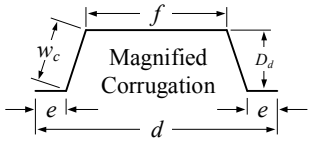

$s = 2(e + w_c) + f$

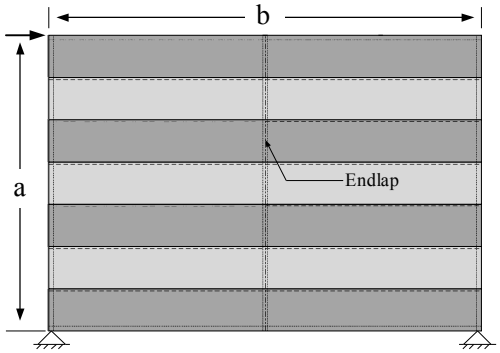

Loading Type: Monotonic

Load Rate: Static

a = 21'

b = 20'

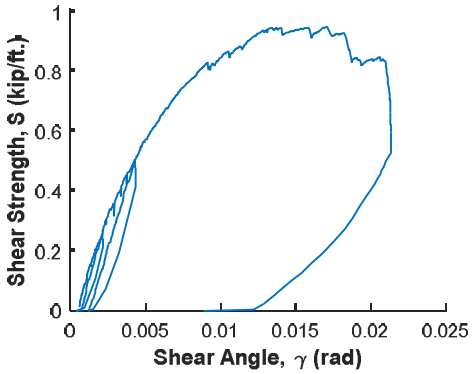

Eperimental Max Strength (kip/ft.)	0.951
Experimental Shear Stiffness (kip/in)	12.4
Ultimate Shear Angle, $\gamma_{80\%}$ (rad*1000)	21.2

Notes

Pinkham (1999) - Specimen 53

Input	
Structural Fastener Type	Arc Spot Weld
Sidelap Fastener Type	Screw
Deck thickness, t (in.)	0.0310
Panel Length, l (ft.)	10
Panel Span, l_v (ft.)	10
No. of sidelap connections per one edge of interior panel length, n_s	8
No. of edge structural connections not in line with int. or ext. supports, n_e	18
No. of interior supports per panel length, n_p	1
Yield strength of deck, F_y (ksi)	38
Ultimate strength of deck, F_u (ksi)	55
Diameter of sidelap screw (in.)	0.211
Moment of inertia of fully effective panel per unit width, I_x (in^4)	0.1481
Diameter of structural weld, (in.)	0.875

Fastener Strengths and Flexibilities	
Structural fastener strength, P_{nf} (kip)	3.17
Sidelap fastener strength, P_{ns} (kip)	0.75
Structural fastener flexibility, S_f (in/kip)	0.0065
Sidelap fastener flexibility, S_s (in/kip)	0.0170

Calculated Strength Equations Variables	
Corner fastener reduction factor, λ	0.700
Interior panel fastener contribution factor, β	6.57
Structural fastener distribution factor at panel ends, α_e^2	0.778
Structural fastener distribution factor at interior supports, α_p^2	0.778
Number of structural fasteners at panel ends per unit width, N	2.00
Fastener slip coefficient, C	3.28
Warping factor, D_n (in.)	5.81
Warping support factor, ρ	1.00

Predicted Shear Strength and Stiffness	
Interior panel shear strength, S_{ni} (kip/ft.)	1.89
Edge panel shear strength, S_{ne} (kip/ft.)	7.60
Panel shear strength limited by corner fastener, S_{nc} (kip/ft.)	1.98
Panel buckling shear strength, S_{nb} (kip/ft.)	1.30
Shear stiffness, G' (kip/in)	73.2

36/7 fastener pattern at interior and exterior supports

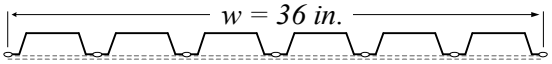

e (in.)	0.75
w_c (in.)	1.68
f (in.)	3.00
d (in.)	6.00
s (in.)	7.85
D_d (in.)	1.50

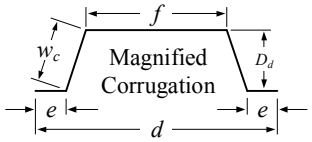

$s = 2(e + w_c) + f$

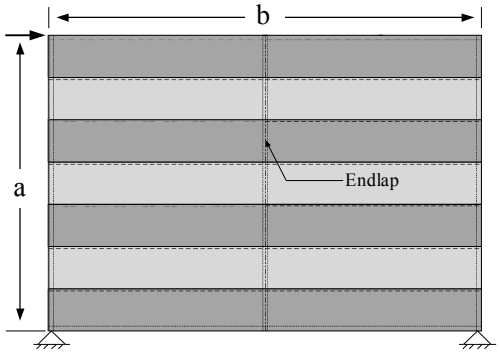

Loading Type: Monotonic

Load Rate: Static

a = 21'

b = 20'

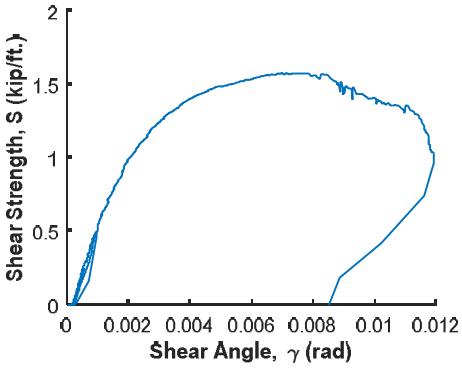

Eperimental Max Strength (kip/ft.)	1.58
Experimental Shear Stiffness (kip/in)	55.6
Ultimate Shear Angle, $\gamma_{80\%}$ (rad*1000)	11.5

Notes

Pinkham (1999) - Specimen 54

Input	
Structural Fastener Type	Arc Spot Weld
Sidelap Fastener Type	Screw
Deck thickness, t (in.)	0.0480
Panel Length, l (ft.)	10
Panel Span, l_v (ft.)	10
No. of sidelap connections per one edge of interior panel length, n_s	8
No. of edge structural connections not in line with int. or ext. supports, n_e	18
No. of interior supports per panel length, n_p	1
Yield strength of deck, F_y (ksi)	38
Ultimate strength of deck, F_u (ksi)	55
Diameter of sidelap screw (in.)	0.211
Moment of inertia of fully effective panel per unit width, I_x (in^4)	0.2920
Diameter of structural weld, (in.)	0.875

Fastener Strengths and Flexibilities	
Structural fastener strength, P_{nf} (kip)	4.80
Sidelap fastener strength, P_{ns} (kip)	1.17
Structural fastener flexibility, S_f (in/kip)	0.0052
Sidelap fastener flexibility, S_s (in/kip)	0.0137

Calculated Strength Equations Variables	
Corner fastener reduction factor, λ	0.715
Interior panel fastener contribution factor, β	5.27
Structural fastener distribution factor at panel ends, α_e^2	0.556
Structural fastener distribution factor at interior supports, α_p^2	0.556
Number of structural fasteners at panel ends per unit width, N	1.00
Fastener slip coefficient, C	4.89
Warping factor, D_n (in.)	32.4
Warping support factor, ρ	1.00

Predicted Shear Strength and Stiffness	
Interior panel shear strength, S_{ni} (kip/ft.)	2.26
Edge panel shear strength, S_{ne} (kip/ft.)	10.6
Panel shear strength limited by corner fastener, S_{nc} (kip/ft.)	2.24
Panel buckling shear strength, S_{nb} (kip/ft.)	3.00
Shear stiffness, G' (kip/in)	34.8

36/4 fastener pattern at interior and exterior supports

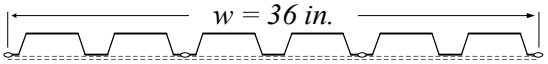

e (in.)	0.75
w_c (in.)	1.68
f (in.)	3.00
d (in.)	6.00
s (in.)	7.85
D_d (in.)	1.50

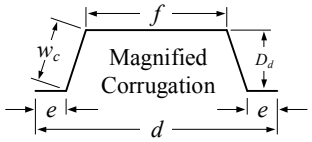

$s = 2(e + w_c) + f$

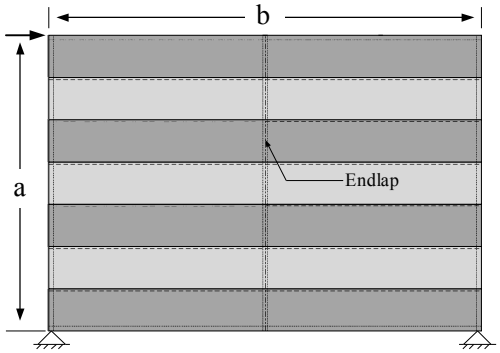

Loading Type: Monotonic

Load Rate: Static

a = 21'

b = 20'

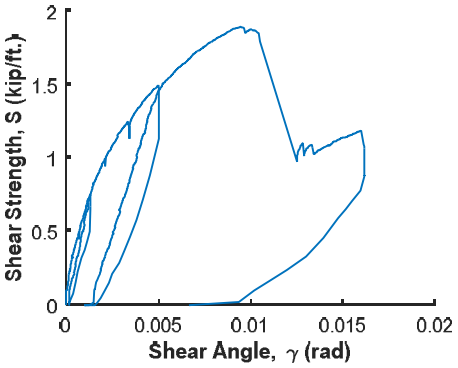

Eperimental Max Strength (kip/ft.)	1.90
Experimental Shear Stiffness (kip/in)	48.6
Ultimate Shear Angle, $\gamma_{80\%}$ (rad*1000)	11.1

Notes

Test 54 did not have adequate weld penetration. Retested as specimen 54R

Martin (2002) - Specimen 19

Input	
Structural Fastener Type	X-EDNK22
Sidelap Fastener Type	Screw
Deck thickness, t (in.)	0.0358
Panel Length, l (ft.)	20
Panel Span, l_v (ft.)	5
No. of sidelap connections per one edge of interior panel length, n_s	16
No. of edge structural connections not in line with int. or ext. supports, n_e	16
No. of interior supports per panel length, n_p	3
Yield strength of deck, F_y (ksi)	33
Ultimate strength of deck, F_u (ksi)	45
Sidelap screw diameter (in.)	0.2111
Moment of inertia of fully effective panel per unit width, I_x (in^4)	0.1865

Fastener Strengths and Flexibilities	
Structural fastener strength, P_{nf} (kip)	1.80
Sidelap fastener strength, P_{ns} (kip)	0.869
Structural fastener flexibility, S_f (in/kip)	0.0066
Sidelap fastener flexibility, S_s (in/kip)	0.0159

Calculated Strength Equations Variables	
Corner fastener reduction factor, λ	0.835
Interior panel fastener contribution factor, β	13.3
Structural fastener distribution factor at panel ends, α_e^2	0.556
Structural fastener distribution factor at interior supports, α_p^2	0.556
Number of structural fasteners at panel ends per unit width, N	1
Fastener slip coefficient, C	4.65
Warping factor, D_n (in.)	31.8
Warping support factor, ρ	0.8

Predicted Shear Strength and Stiffness	
Interior panel shear strength, S_{ni} (kip/ft.)	1.16
Edge panel shear strength, S_{ne} (kip/ft.)	2.03
Panel shear strength limited by corner fastener, S_{nc} (kip/ft.)	0.994
Panel buckling shear strength, S_{nb} (kip/ft.)	6.83
Shear stiffness, G' (kip/in)	31.4

36/4 fastener pattern at interior and exterior supports

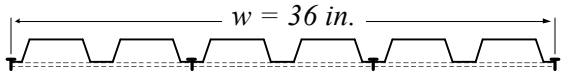

e (in.)	0.75
w_c (in.)	1.58
f (in.)	3.50
d (in.)	6.00
s (in.)	8.16
D_d (in.)	1.50

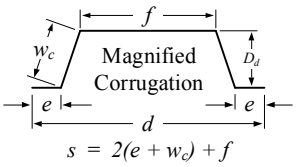

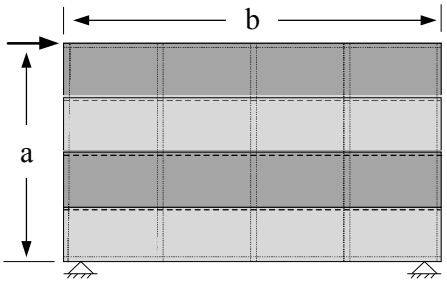

Loading Type: Monotonic
Load Rate: Static
a = 12'
b = 20'

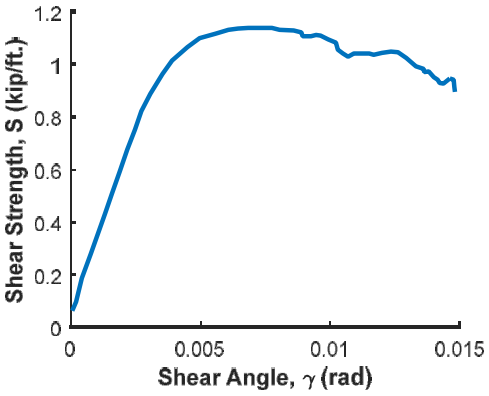

Eperimental Max Strength (kip/ft.)	1.15
Experimental Shear Stiffness (kip/in)	24.2
Ultimate Shear Angle, $\gamma_{80\%}$ (rad*1000)	14.8

Notes

Specimens 19, 34 and 35 have identical test setups with varying loading protocols.

Martin (2002) - Specimen 20

Input	
Structural Fastener Type	Arc Spot Weld
Sidelap Fastener Type	Button Punch
Deck thickness, t (in.)	0.0300
Panel Length, l (ft.)	20
Panel Span, l_v (ft.)	5
No. of sidelap connections per one edge of interior panel length, n_s	16
No. of edge structural connections not in line with int. or ext. supports, n_e	16
No. of interior supports per panel length, n_p	3
Yield strength of deck, F_y (ksi)	33
Ultimate strength of deck, F_u (ksi)	45
Arc Spot Weld diameter (in.)	0.625
Moment of inertia of fully effective panel per unit width, I_x (in^4)	0.1481

Fastener Strengths and Flexibilities	
Structural fastener strength, P_{nf} (kip)	1.77
Sidelap fastener strength, P_{ns} (kip)	0.216
Structural fastener flexibility, S_f (in/kip)	0.0066
Sidelap fastener flexibility, S_s (in/kip)	0.173

Calculated Strength Equations Variables	
Corner fastener reduction factor, λ	0.820
Interior panel fastener contribution factor, β	7.51
Structural fastener distribution factor at panel ends, α_e^2	0.556
Structural fastener distribution factor at interior supports, α_p^2	0.556
Number of structural fasteners at panel ends per unit width, N	1.33
Fastener slip coefficient, C	9.93
Warping factor, D_n (in.)	41.5
Warping support factor, ρ	0.8

Predicted Shear Strength and Stiffness	
Interior panel shear strength, S_{ni} (kip/ft.)	0.632
Edge panel shear strength, S_{ne} (kip/ft.)	2.00
Panel shear strength limited by corner fastener, S_{nc} (kip/ft.)	0.639
Panel buckling shear strength, S_{nb} (kip/ft.)	5.03
Shear stiffness, G' (kip/in)	19.0

36/4 fastener pattern at interior and exterior supports

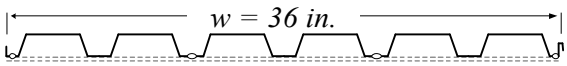

e (in.)	0.75
w_c (in.)	1.58
f (in.)	3.50
d (in.)	6.00
s (in.)	8.16
D_d (in.)	1.50

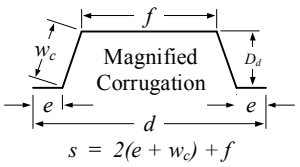

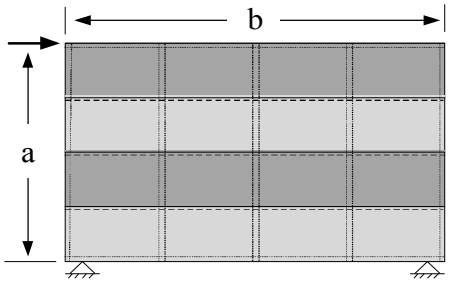

Loading Type: Cyclic
Load Rate: Fast-loading
a = 12'
b = 20'

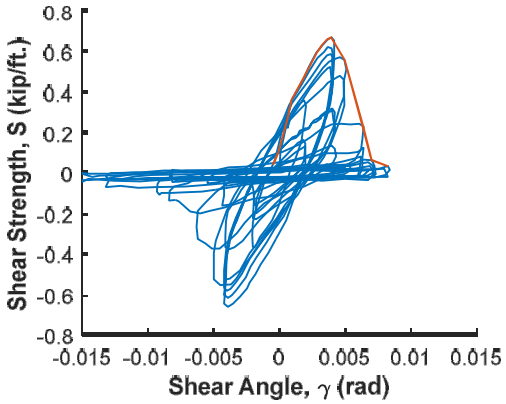

Eperimental Max Strength (kip/ft.)	0.672
Experimental Shear Stiffness (kip/in)	16.8
Ultimate Shear Angle, $\gamma_{80\%}$ (rad*1000)	5.04

Notes

No mass added to represent seismic weight for inertial forces for a truly dynamic test.

Specimens 20 and 36 have identical test setups with varying loading protocols.

Structural welds on both sides of interlocking sidelap seam.

Martin (2002) - Specimen 21

Input	
Structural Fastener Type	Arc Spot Weld
Sidelap Fastener Type	Button Punch
Deck thickness, t (in.)	0.0358
Panel Length, l (ft.)	20
Panel Span, l_v (ft.)	5
No. of sidelap connections per one edge of interior panel length, n_s	16
No. of edge structural connections not in line with int. or ext. supports, n_e	16
No. of interior supports per panel length, n_p	3
Yield strength of deck, F_y (ksi)	33
Ultimate strength of deck, F_u (ksi)	45
Arc Spot Weld diameter (in.)	0.625
Moment of inertia of fully effective panel per unit width, I_x (in^4)	0.1865

Fastener Strengths and Flexibilities	
Structural fastener strength, P_{nf} (kip)	2.09
Sidelap fastener strength, P_{ns} (kip)	0.308
Structural fastener flexibility, S_f (in/kip)	0.0061
Sidelap fastener flexibility, S_s (in/kip)	0.159

Calculated Strength Equations Variables	
Corner fastener reduction factor, λ	0.835
Interior panel fastener contribution factor, β	7.91
Structural fastener distribution factor at panel ends, α_e^2	0.556
Structural fastener distribution factor at interior supports, α_p^2	0.556
Number of structural fasteners at panel ends per unit width, N	1.33
Fastener slip coefficient, C	10.8
Warping factor, D_n (in.)	31.8
Warping support factor, ρ	0.8

Predicted Shear Strength and Stiffness	
Interior panel shear strength, S_{ni} (kip/ft.)	0.792
Edge panel shear strength, S_{ne} (kip/ft.)	2.37
Panel shear strength limited by corner fastener, S_{nc} (kip/ft.)	0.792
Panel buckling shear strength, S_{nb} (kip/ft.)	6.83
Shear stiffness, G' (kip/in)	26.5

36/4 fastener pattern at interior and exterior supports

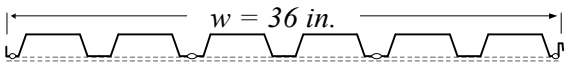

e (in.)	0.75
w_c (in.)	1.58
f (in.)	3.50
d (in.)	6.00
s (in.)	8.16
D_d (in.)	1.50

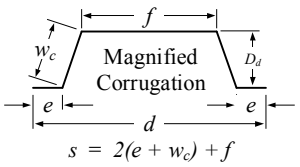

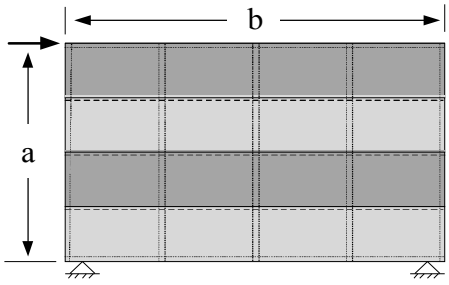

Loading Type: Cyclic
Load Rate: Fast-loading
a = 12'
b = 20'

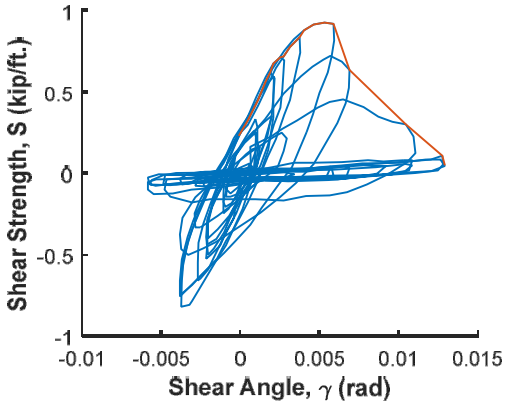

Eperimental Max Strength (kip/ft.)	0.932
Experimental Shear Stiffness (kip/in)	15.2
Ultimate Shear Angle, $\gamma_{80\%}$ (rad*1000)	6.51

Notes

No mass added to represent seismic weight for inertial forces for a truly dynamic test.

Specimens 21 and 37 have identical test setups with varying loading protocols.

Structural welds on both sides of interlocking sidelap seam.

Martin (2002) - Specimen 22

Input	
Structural Fastener Type	WWW
Sidelap Fastener Type	WWW
Deck thickness, t (in.)	0.0358
Panel Length, l (ft.)	20
Panel Span, l_v (ft.)	5
No. of sidelap connections per one edge of interior panel length, n_s	16
No. of edge structural connections not in line with int. or ext. supports, n_e	16
No. of interior supports per panel length, n_p	3
Yield strength of deck, F_y (ksi)	33
Ultimate strength of deck, F_u (ksi)	45
Inside (hole) diameter of weld washer (in.)	0.551
Moment of inertia of fully effective panel per unit width, I_x (in^4)	0.1865

Fastener Strengths and Flexibilities	
Structural fastener strength, P_{nf} (kip)	3.25
Sidelap fastener strength, P_{ns} (kip)	2.43
Structural fastener flexibility, S_f (in/kip)	0.0061
Sidelap fastener flexibility, S_s (in/kip)	0.0059

Calculated Strength Equations Variables	
Corner fastener reduction factor, λ	0.835
Interior panel fastener contribution factor, β	17.6
Structural fastener distribution factor at panel ends, α_e^2	0.556
Structural fastener distribution factor at interior supports, α_p^2	0.556
Number of structural fasteners at panel ends per unit width, N	1
Fastener slip coefficient, C	2.17
Warping factor, D_n (in.)	31.8
Warping support factor, ρ	0.8

Predicted Shear Strength and Stiffness	
Interior panel shear strength, S_{ni} (kip/ft.)	2.80
Edge panel shear strength, S_{ne} (kip/ft.)	3.68
Panel shear strength limited by corner fastener, S_{nc} (kip/ft.)	2.14
Panel buckling shear strength, S_{nb} (kip/ft.)	6.83
Shear stiffness, G' (kip/in)	33.9

36/4 fastener pattern at interior and exterior supports

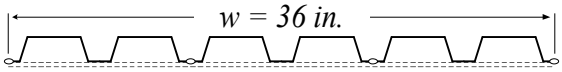

e (in.)	0.75
w_c (in.)	1.58
f (in.)	3.50
d (in.)	6.00
s (in.)	8.16
D_d (in.)	1.50

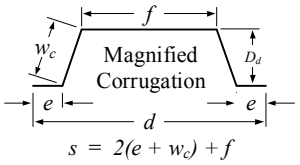

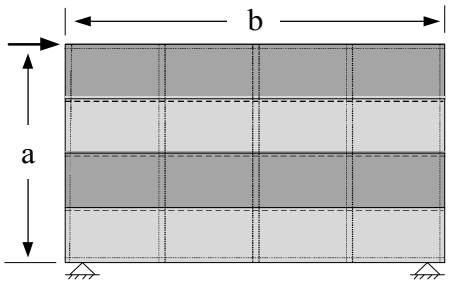

Loading Type: Monotonic
Load Rate: Static
a = 12'
b = 20'

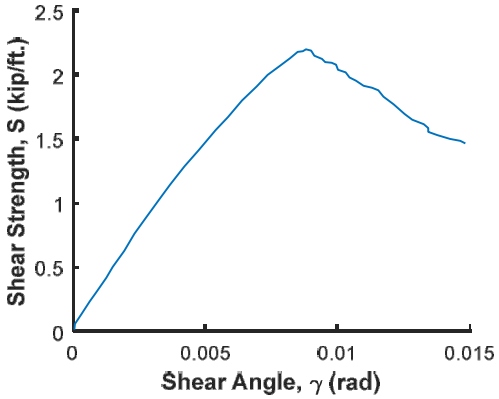

Eperimental Max Strength (kip/ft.)	2.20
Experimental Shear Stiffness (kip/in)	27.0
Ultimate Shear Angle, $\gamma_{80\%}$ (rad*1000)	12.2

Notes

WWW = weld with washer. Sidelap welds with washers prohibited in current design standards.

Specimens 22, 23 and 24 have identical test setups with varying loading protocols.

Martin (2002) - Specimen 23

Input	
Structural Fastener Type	WWW
Sidelap Fastener Type	WWW
Deck thickness, t (in.)	0.0358
Panel Length, l (ft.)	20
Panel Span, l_v (ft.)	5
No. of sidelap connections per one edge of interior panel length, n_s	16
No. of edge structural connections not in line with int. or ext. supports, n_e	16
No. of interior supports per panel length, n_p	3
Yield strength of deck, F_y (ksi)	33
Ultimate strength of deck, F_u (ksi)	45
Inside (hole) diameter of weld washer (in.)	0.551
Moment of inertia of fully effective panel per unit width, I_x (in^4)	0.1865

Fastener Strengths and Flexibilities	
Structural fastener strength, P_{nf} (kip)	3.25
Sidelap fastener strength, P_{ns} (kip)	2.43
Structural fastener flexibility, S_f (in/kip)	0.0061
Sidelap fastener flexibility, S_s (in/kip)	0.0059

Calculated Strength Equations Variables	
Corner fastener reduction factor, λ	0.835
Interior panel fastener contribution factor, β	17.6
Structural fastener distribution factor at panel ends, α_e^2	0.556
Structural fastener distribution factor at interior supports, α_p^2	0.556
Number of structural fasteners at panel ends per unit width, N	1
Fastener slip coefficient, C	2.17
Warping factor, D_n (in.)	31.8
Warping support factor, ρ	0.8

Predicted Shear Strength and Stiffness	
Interior panel shear strength, S_{ni} (kip/ft.)	2.80
Edge panel shear strength, S_{ne} (kip/ft.)	3.70
Panel shear strength limited by corner fastener, S_{nc} (kip/ft.)	2.14
Panel buckling shear strength, S_{nb} (kip/ft.)	6.83
Shear stiffness, G' (kip/in)	33.9

36/4 fastener pattern at interior and exterior supports

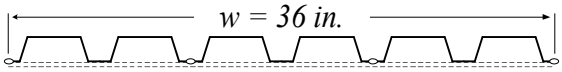

e (in.)	0.75
w_c (in.)	1.58
f (in.)	3.50
d (in.)	6.00
s (in.)	8.16
D_d (in.)	1.50

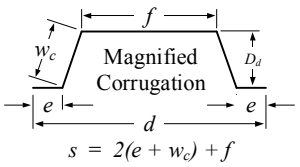

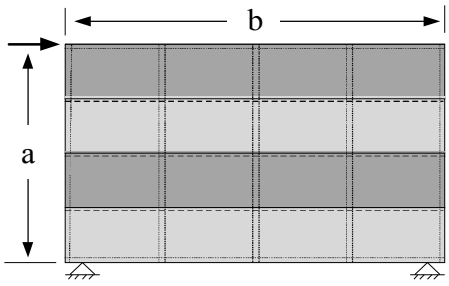

Loading Type: Cyclic
Load Rate: Fast-loading
a = 12'
b = 20'

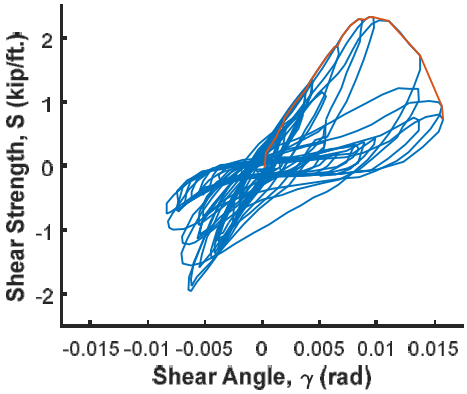

Eperimental Max Strength (kip/ft.)	2.35
Experimental Shear Stiffness (kip/in)	33.0
Ultimate Shear Angle, $\gamma_{80\%}$ (rad*1000)	13.1

Notes

WWW = weld with washer. Sidelap welds with washers prohibited in current design standards.

No mass added to represent seismic weight for inertial forces for a truly dynamic test.

Specimens 22, 23 and 24 have identical test setups with varying loading protocols.

Martin (2002) - Specimen 24

Input	
Structural Fastener Type	WWW
Sidelap Fastener Type	WWW
Deck thickness, t (in.)	0.0358
Panel Length, l (ft.)	20
Panel Span, l_v (ft.)	5
No. of sidelap connections per one edge of interior panel length, n_s	16
No. of edge structural connections not in line with int. or ext. supports, n_e	16
No. of interior supports per panel length, n_p	3
Yield strength of deck, F_y (ksi)	33
Ultimate strength of deck, F_u (ksi)	45
Inside (hole) diameter of weld washer (in.)	0.551
Moment of inertia of fully effective panel per unit width, I_x (in^4)	0.1865

Fastener Strengths and Flexibilities	
Structural fastener strength, P_{nf} (kip)	3.25
Sidelap fastener strength, P_{ns} (kip)	2.43
Structural fastener flexibility, S_f (in/kip)	0.0061
Sidelap fastener flexibility, S_s (in/kip)	0.0059

Calculated Strength Equations Variables	
Corner fastener reduction factor, λ	0.84
Interior panel fastener contribution factor, β	17.6
Structural fastener distribution factor at panel ends, α_e^2	0.556
Structural fastener distribution factor at interior supports, α_p^2	0.556
Number of structural fasteners at panel ends per unit width, N	1
Fastener slip coefficient, C	2.17
Warping factor, D_n (in.)	31.8
Warping support factor, ρ	0.8

Predicted Shear Strength and Stiffness	
Interior panel shear strength, S_{ni} (kip/ft.)	2.80
Edge panel shear strength, S_{ne} (kip/ft.)	3.70
Panel shear strength limited by corner fastener, S_{nc} (kip/ft.)	2.14
Panel buckling shear strength, S_{nb} (kip/ft.)	6.83
Shear stiffness, G' (kip/in)	33.9

36/4 fastener pattern at interior and exterior supports

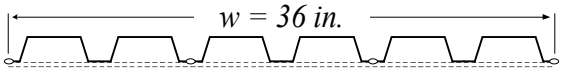

e (in.)	0.75
w_c (in.)	1.58
f (in.)	3.50
d (in.)	6.00
s (in.)	8.16
D_d (in.)	1.50

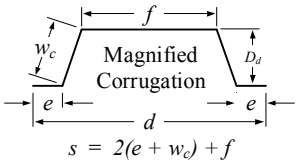

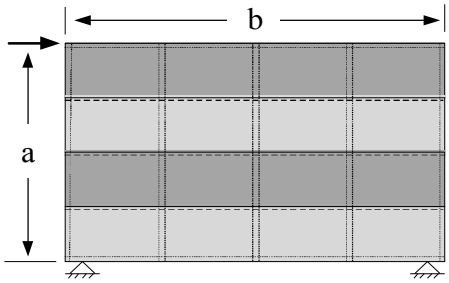

Loading Type: Cyclic
Load Rate: Fast-loading
a = 12'
b = 20'

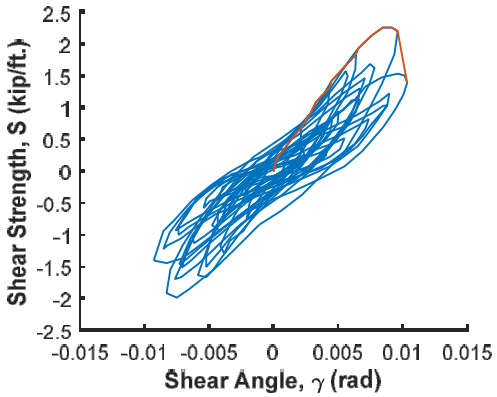

Eperimental Max Strength (kip/ft.)	2.27
Experimental Shear Stiffness (kip/in)	26.7
Ultimate Shear Angle, $\gamma_{80\%}$ (rad*1000)	9.96

Notes

WWW = weld with washer. Sidelap welds with washers prohibited in current design standards.

No mass added to represent seismic weight for inertial forces for a truly dynamic test.

Specimens 22, 23 and 24 have identical test setups with varying loading protocols.

Martin (2002) - Specimen 28

Input	
Structural Fastener Type	X-EDNK22
Sidelap Fastener Type	Screw
Deck thickness, t (in.)	0.0300
Panel Length, l (ft.)	20
Panel Span, l_v (ft.)	5
No. of sidelap connections per one edge of interior panel length, n_s	16
No. of edge structural connections not in line with int. or ext. supports, n_e	16
No. of interior supports per panel length, n_p	3
Yield strength of deck, F_y (ksi)	33
Ultimate strength of deck, F_u (ksi)	45
Sidelap screw diameter (in.)	0.2111
Moment of inertia of fully effective panel per unit width, I_x (in^4)	0.1481

Fastener Strengths and Flexibilities	
Structural fastener strength, P_{nf} (kip)	1.51
Sidelap fastener strength, P_{ns} (kip)	0.728
Structural fastener flexibility, S_f (in/kip)	0.0072
Sidelap fastener flexibility, S_s (in/kip)	0.0173

Calculated Strength Equations Variables	
Corner fastener reduction factor, λ	0.820
Interior panel fastener contribution factor, β	13.3
Structural fastener distribution factor at panel ends, α_e^2	0.556
Structural fastener distribution factor at interior supports, α_p^2	0.556
Number of structural fasteners at panel ends per unit width, N	1
Fastener slip coefficient, C	4.26
Warping factor, D_n (in.)	41.5
Warping support factor, ρ	0.8

Predicted Shear Strength and Stiffness	
Interior panel shear strength, S_{ni} (kip/ft.)	0.976
Edge panel shear strength, S_{ne} (kip/ft.)	1.72
Panel shear strength limited by corner fastener, S_{nc} (kip/ft.)	0.836
Panel buckling shear strength, S_{nb} (kip/ft.)	5.03
Shear stiffness, G' (kip/in)	21.6

36/4 fastener pattern at interior and exterior supports

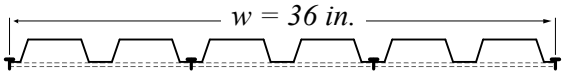

e (in.)	0.75
w_c (in.)	1.58
f (in.)	3.50
d (in.)	6.00
s (in.)	8.16
D_d (in.)	1.50

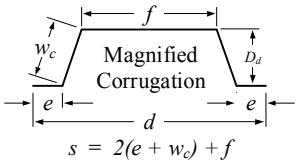

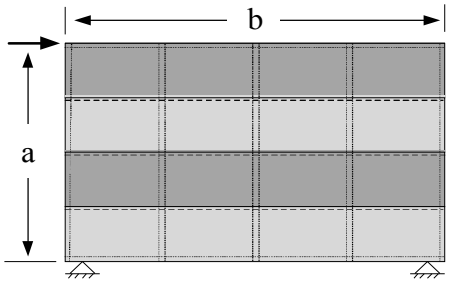

Loading Type: Cyclic
Load Rate: Fast-loading
a = 12'
b = 20'

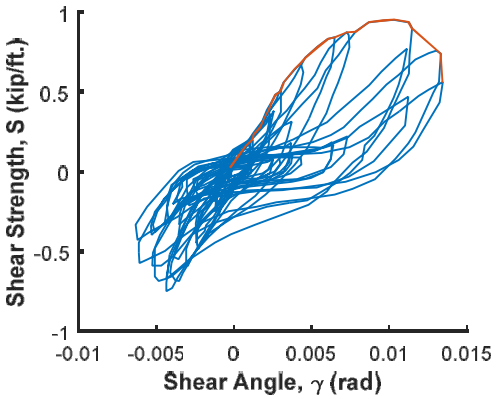

Eperimental Max Strength (kip/ft.)	0.959
Experimental Shear Stiffness (kip/in)	12.1
Ultimate Shear Angle, $\gamma_{80\%}$ (rad*1000)	13.1

Notes

Specimens 28 and 29 have identical test setups with varying loading protocols.

No mass added to represent seismic weight for inertial forces for a truly dynamic test.

Martin (2002) - Specimen 29

Input	
Structural Fastener Type	X-EDNK22
Sidelap Fastener Type	Screw
Deck thickness, t (in.)	0.0300
Panel Length, l (ft.)	20
Panel Span, l_v (ft.)	5
No. of sidelap connections per one edge of interior panel length, n_s	16
No. of edge structural connections not in line with int. or ext. supports, n_e	16
No. of interior supports per panel length, n_p	3
Yield strength of deck, F_y (ksi)	33
Ultimate strength of deck, F_u (ksi)	45
Sidelap screw diameter (in.)	0.2111
Moment of inertia of fully effective panel per unit width, I_x (in^4)	0.1481

Fastener Strengths and Flexibilities	
Structural fastener strength, P_{nf} (kip)	1.51
Sidelap fastener strength, P_{ns} (kip)	0.728
Structural fastener flexibility, S_f (in/kip)	0.0072
Sidelap fastener flexibility, S_s (in/kip)	0.0173

Calculated Strength Equations Variables	
Corner fastener reduction factor, λ	0.820
Interior panel fastener contribution factor, β	13.3
Structural fastener distribution factor at panel ends, α_e^2	0.556
Structural fastener distribution factor at interior supports, α_p^2	0.556
Number of structural fasteners at panel ends per unit width, N	1
Fastener slip coefficient, C	4.26
Warping factor, D_n (in.)	41.5
Warping support factor, ρ	0.8

Predicted Shear Strength and Stiffness	
Interior panel shear strength, S_{ni} (kip/ft.)	0.976
Edge panel shear strength, S_{ne} (kip/ft.)	1.72
Panel shear strength limited by corner fastener, S_{nc} (kip/ft.)	0.836
Panel buckling shear strength, S_{nb} (kip/ft.)	5.03
Shear stiffness, G' (kip/in)	21.6

36/4 fastener pattern at interior and exterior supports

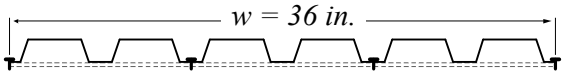

e (in.)	0.75
w_c (in.)	1.58
f (in.)	3.50
d (in.)	6.00
s (in.)	8.16
D_d (in.)	1.50

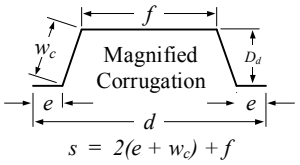

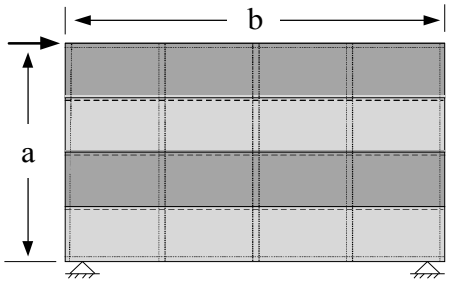

Loading Type: Cyclic
Load Rate: Fast-loading
a = 12'
b = 20'

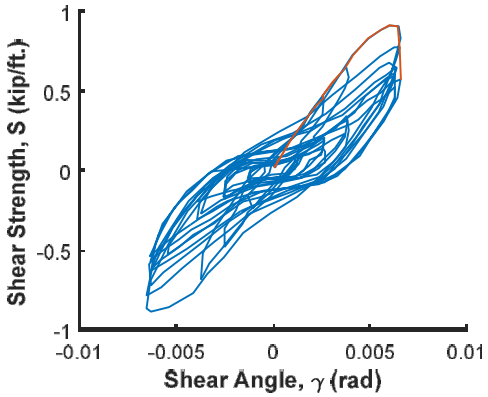

Eperimental Max Strength (kip/ft.)	0.919
Experimental Shear Stiffness (kip/in)	15.3
Ultimate Shear Angle, $\gamma_{80\%}$ (rad*1000)	6.54

Notes

Specimens 28 and 29 have identical test setups with varying loading protocols.

No mass added to represent seismic weight for inertial forces for a truly dynamic test.

Martin (2002) - Specimen 30

Input	
Structural Fastener Type	X-EDNK22
Sidelap Fastener Type	Screw
Deck thickness, t (in.)	0.0300
Panel Length, l (ft.)	20
Panel Span, l_v (ft.)	5
No. of sidelap connections per one edge of interior panel length, n_s	36
No. of edge structural connections not in line with int. or ext. supports, n_e	36
No. of interior supports per panel length, n_p	3
Yield strength of deck, F_y (ksi)	33
Ultimate strength of deck, F_u (ksi)	45
Sidelap screw diameter (in.)	0.2111
Moment of inertia of fully effective panel per unit width, I_x (in^4)	0.1481

Fastener Strengths and Flexibilities	
Structural fastener strength, P_{nf} (kip)	1.51
Sidelap fastener strength, P_{ns} (kip)	0.728
Structural fastener flexibility, S_f (in/kip)	0.0072
Sidelap fastener flexibility, S_s (in/kip)	0.0173

Calculated Strength Equations Variables	
Corner fastener reduction factor, λ	0.820
Interior panel fastener contribution factor, β	25.1
Structural fastener distribution factor at panel ends, α_e^2	0.778
Structural fastener distribution factor at interior supports, α_p^2	0.778
Number of structural fasteners at panel ends per unit width, N	2
Fastener slip coefficient, C	2.13
Warping factor, D_n (in.)	4.75
Warping support factor, ρ	0.8

Predicted Shear Strength and Stiffness	
Interior panel shear strength, S_{ni} (kip/ft.)	1.87
Edge panel shear strength, S_{ne} (kip/ft.)	3.48
Panel shear strength limited by corner fastener, S_{nc} (kip/ft.)	1.61
Panel buckling shear strength, S_{nb} (kip/ft.)	5.03
Shear stiffness, G' (kip/in)	93.5

36/7 fastener pattern at interior and exterior supports

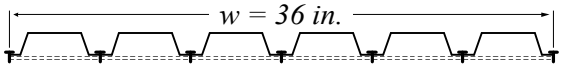

e (in.)	0.75
w_c (in.)	1.58
f (in.)	3.50
d (in.)	6.00
s (in.)	8.16
D_d (in.)	1.50

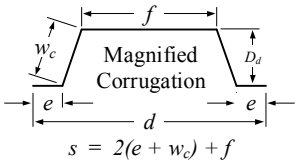

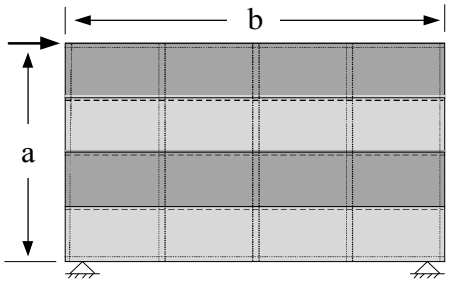

Loading Type: Monotonic
Load Rate: Static
a = 12'
b = 20'

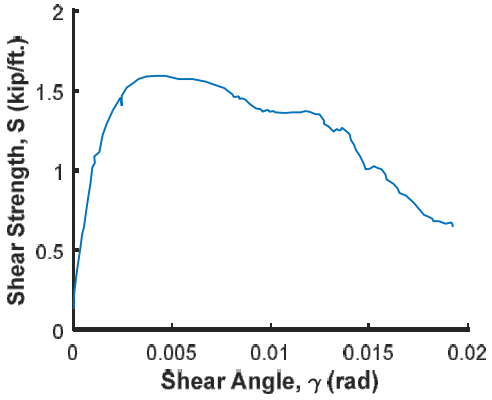

Eperimental Max Strength (kip/ft.)	1.60
Experimental Shear Stiffness (kip/in)	99.4
Ultimate Shear Angle, $\gamma_{80\%}$ (rad*1000)	13.00

Notes

Specimens 30 and 31 have identical test setups with varying loading protocols.

Martin (2002) - Specimen 31

Input	
Structural Fastener Type	X-EDNK22
Sidelap Fastener Type	Screw
Deck thickness, t (in.)	0.0300
Panel Length, l (ft.)	20
Panel Span, l_v (ft.)	5
No. of sidelap connections per one edge of interior panel length, n_s	36
No. of edge structural connections not in line with int. or ext. supports, n_e	36
No. of interior supports per panel length, n_p	3
Yield strength of deck, F_y (ksi)	33
Ultimate strength of deck, F_u (ksi)	45
Sidelap screw diameter (in.)	0.2111
Moment of inertia of fully effective panel per unit width, I_x (in^4)	0.1481

Fastener Strengths and Flexibilities	
Structural fastener strength, P_{nf} (kip)	1.51
Sidelap fastener strength, P_{ns} (kip)	0.728
Structural fastener flexibility, S_f (in/kip)	0.0072
Sidelap fastener flexibility, S_s (in/kip)	0.0173

Calculated Strength Equations Variables	
Corner fastener reduction factor, λ	0.820
Interior panel fastener contribution factor, β	25.1
Structural fastener distribution factor at panel ends, α_e^2	0.778
Structural fastener distribution factor at interior supports, α_p^2	0.778
Number of structural fasteners at panel ends per unit width, N	2
Fastener slip coefficient, C	2.13
Warping factor, D_n (in.)	4.75
Warping support factor, ρ	0.8

Predicted Shear Strength and Stiffness	
Interior panel shear strength, S_{ni} (kip/ft.)	1.87
Edge panel shear strength, S_{ne} (kip/ft.)	3.48
Panel shear strength limited by corner fastener, S_{nc} (kip/ft.)	1.61
Panel buckling shear strength, S_{nb} (kip/ft.)	5.03
Shear stiffness, G' (kip/in)	93.5

36/7 fastener pattern at interior and exterior supports

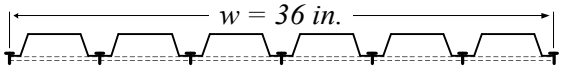

e (in.)	0.75
w_c (in.)	1.58
f (in.)	3.50
d (in.)	6.00
s (in.)	8.16
D_d (in.)	1.50

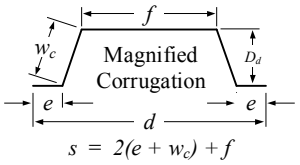

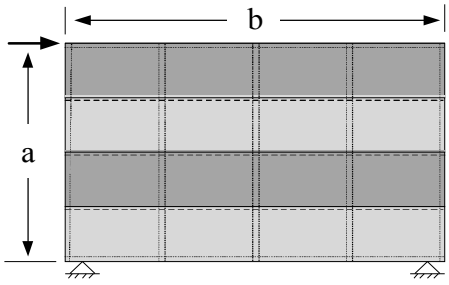

Loading Type: Cyclic
Load Rate: Fast-loading
a = 12'
b = 20'

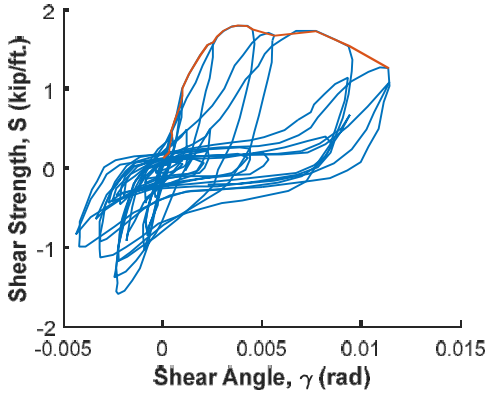

Eperimental Max Strength (kip/ft.)	1.81
Experimental Shear Stiffness (kip/in)	65.3
Ultimate Shear Angle, $\gamma_{80\%}$ (rad*1000)	10.10

Notes

Specimens 30 and 31 have identical test setups with varying loading protocols.

No mass added to represent seismic weight for inertial forces for a truly dynamic test.

Martin (2002) - Specimen 32

Input	
Structural Fastener Type	X-EDNK22
Sidelap Fastener Type	Screw
Deck thickness, t (in.)	0.0358
Panel Length, l (ft.)	20
Panel Span, l_v (ft.)	5
No. of sidelap connections per one edge of interior panel length, n_s	36
No. of edge structural connections not in line with int. or ext. supports, n_e	36
No. of interior supports per panel length, n_p	3
Yield strength of deck, F_y (ksi)	33
Ultimate strength of deck, F_u (ksi)	45
Sidelap screw diameter (in.)	0.2111
Moment of inertia of fully effective panel per unit width, I_x (in^4)	0.1865

Fastener Strengths and Flexibilities	
Structural fastener strength, P_{nf} (kip)	1.80
Sidelap fastener strength, P_{ns} (kip)	0.869
Structural fastener flexibility, S_f (in/kip)	0.0066
Sidelap fastener flexibility, S_s (in/kip)	0.0159

Calculated Strength Equations Variables	
Corner fastener reduction factor, λ	0.835
Interior panel fastener contribution factor, β	25.2
Structural fastener distribution factor at panel ends, α_e^2	0.778
Structural fastener distribution factor at interior supports, α_p^2	0.778
Number of structural fasteners at panel ends per unit width, N	2
Fastener slip coefficient, C	2.33
Warping factor, D_n (in.)	3.64
Warping support factor, ρ	0.8

Predicted Shear Strength and Stiffness	
Interior panel shear strength, S_{ni} (kip/ft.)	2.23
Edge panel shear strength, S_{ne} (kip/ft.)	4.13
Panel shear strength limited by corner fastener, S_{nc} (kip/ft.)	1.91
Panel buckling shear strength, S_{nb} (kip/ft.)	5.03
Shear stiffness, G' (kip/in)	120

36/7 fastener pattern at interior and exterior supports

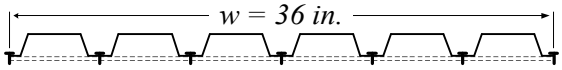

e (in.)	0.75
w_c (in.)	1.58
f (in.)	3.50
d (in.)	6.00
s (in.)	8.16
D_d (in.)	1.50

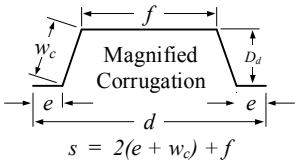

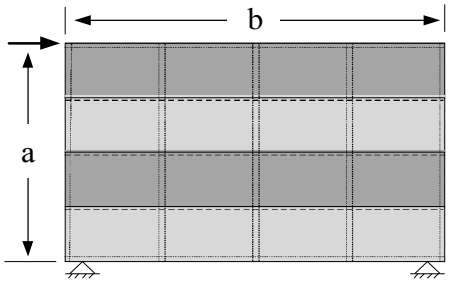

Loading Type: Monotonic
Load Rate: Static
a = 12'
b = 20'

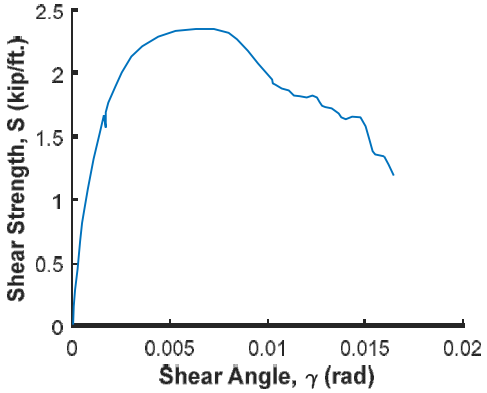

Eperimental Max Strength (kip/ft.)	2.36
Experimental Shear Stiffness (kip/in)	130
Ultimate Shear Angle, $\gamma_{80\%}$ (rad*1000)	10.7

Notes

Specimens 32 and 33 have identical test setups with varying loading protocols.

Martin (2002) - Specimen 33

Input	
Structural Fastener Type	X-EDNK22
Sidelap Fastener Type	Screw
Deck thickness, t (in.)	0.0358
Panel Length, l (ft.)	20
Panel Span, l_v (ft.)	5
No. of sidelap connections per one edge of interior panel length, n_s	36
No. of edge structural connections not in line with int. or ext. supports, n_e	36
No. of interior supports per panel length, n_p	3
Yield strength of deck, F_y (ksi)	33
Ultimate strength of deck, F_u (ksi)	45
Sidelap screw diameter (in.)	0.2111
Moment of inertia of fully effective panel per unit width, I_x (in^4)	0.1865

Fastener Strengths and Flexibilities	
Structural fastener strength, P_{nf} (kip)	1.80
Sidelap fastener strength, P_{ns} (kip)	0.869
Structural fastener flexibility, S_f (in/kip)	0.0066
Sidelap fastener flexibility, S_s (in/kip)	0.0159

Calculated Strength Equations Variables	
Corner fastener reduction factor, λ	0.835
Interior panel fastener contribution factor, β	25.2
Structural fastener distribution factor at panel ends, α_e^2	0.778
Structural fastener distribution factor at interior supports, α_p^2	0.778
Number of structural fasteners at panel ends per unit width, N	2
Fastener slip coefficient, C	2.33
Warping factor, D_n (in.)	3.64
Warping support factor, ρ	0.8

Predicted Shear Strength and Stiffness	
Interior panel shear strength, S_{ni} (kip/ft.)	2.23
Edge panel shear strength, S_{ne} (kip/ft.)	4.13
Panel shear strength limited by corner fastener, S_{nc} (kip/ft.)	1.91
Panel buckling shear strength, S_{nb} (kip/ft.)	5.03
Shear stiffness, G' (kip/in)	120

36/7 fastener pattern at interior and exterior supports

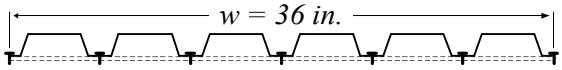

e (in.)	0.75
w_c (in.)	1.58
f (in.)	3.50
d (in.)	6.00
s (in.)	8.16
D_d (in.)	1.50

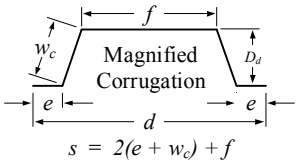

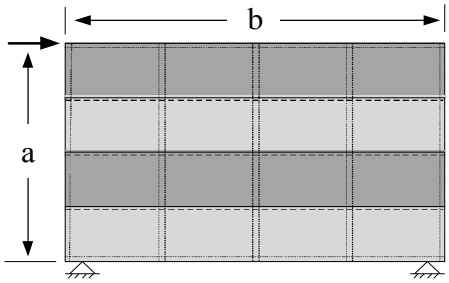

Loading Type: Cyclic
Load Rate: Fast-loading
a = 12'
b = 20'

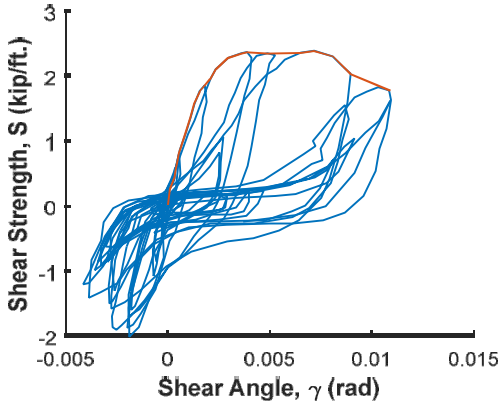

Eperimental Max Strength (kip/ft.)	2.40
Experimental Shear Stiffness (kip/in)	114
Ultimate Shear Angle, $\gamma_{80\%}$ (rad*1000)	9.89

Notes

Specimens 32 and 33 have identical test setups with varying loading protocols.

No mass added to represent seismic weight for inertial forces for a truly dynamic test.

Martin (2002) - Specimen 34

Input	
Structural Fastener Type	X-EDNK22
Sidelap Fastener Type	Screw
Deck thickness, t (in.)	0.0358
Panel Length, l (ft.)	20
Panel Span, l_v (ft.)	5
No. of sidelap connections per one edge of interior panel length, n_s	16
No. of edge structural connections not in line with int. or ext. supports, n_e	16
No. of interior supports per panel length, n_p	3
Yield strength of deck, F_y (ksi)	33
Ultimate strength of deck, F_u (ksi)	45
Sidelap screw diameter (in.)	0.2111
Moment of inertia of fully effective panel per unit width, I_x (in^4)	0.1865

Fastener Strengths and Flexibilities	
Structural fastener strength, P_{nf} (kip)	1.80
Sidelap fastener strength, P_{ns} (kip)	0.869
Structural fastener flexibility, S_f (in/kip)	0.0066
Sidelap fastener flexibility, S_s (in/kip)	0.0159

Calculated Strength Equations Variables	
Corner fastener reduction factor, λ	0.835
Interior panel fastener contribution factor, β	13.3
Structural fastener distribution factor at panel ends, α_e^2	0.556
Structural fastener distribution factor at interior supports, α_p^2	0.556
Number of structural fasteners at panel ends per unit width, N	1
Fastener slip coefficient, C	4.65
Warping factor, D_n (in.)	31.8
Warping support factor, ρ	0.8

Predicted Shear Strength and Stiffness	
Interior panel shear strength, S_{ni} (kip/ft.)	1.16
Edge panel shear strength, S_{ne} (kip/ft.)	2.03
Panel shear strength limited by corner fastener, S_{nc} (kip/ft.)	0.994
Panel buckling shear strength, S_{nb} (kip/ft.)	6.83
Shear stiffness, G' (kip/in)	31.4

36/4 fastener pattern at interior and exterior supports

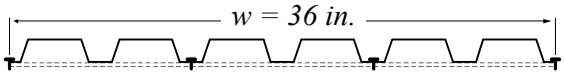

e (in.)	0.75
w_c (in.)	1.58
f (in.)	3.50
d (in.)	6.00
s (in.)	8.16
D_d (in.)	1.50

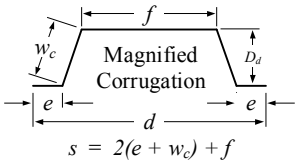

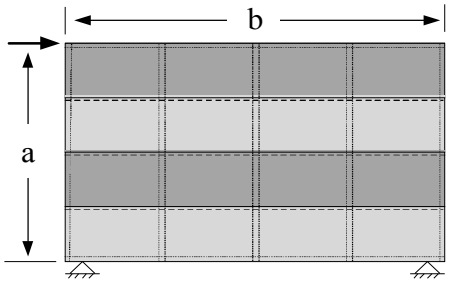

Loading Type: Cyclic
Load Rate: Fast-loading
a = 12'
b = 20'

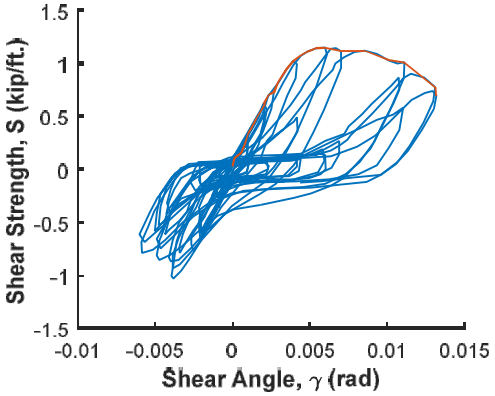

Eperimental Max Strength (kip/ft.)	1.16
Experimental Shear Stiffness (kip/in)	24.7
Ultimate Shear Angle, $\gamma_{80\%}$ (rad*1000)	11.9

Notes

Specimens 19, 34 and 35 have identical test setups with varying loading protocols.
No mass added to represent seismic weight for inertial forces for a truly dynamic test.

Martin (2002) - Specimen 35

Input	
Structural Fastener Type	X-EDNK22
Sidelap Fastener Type	Screw
Deck thickness, t (in.)	0.0358
Panel Length, l (ft.)	20
Panel Span, l_v (ft.)	5
No. of sidelap connections per one edge of interior panel length, n_s	16
No. of edge structural connections not in line with int. or ext. supports, n_e	16
No. of interior supports per panel length, n_p	3
Yield strength of deck, F_y (ksi)	33
Ultimate strength of deck, F_u (ksi)	45
Sidelap screw diameter (in.)	0.2111
Moment of inertia of fully effective panel per unit width, I_x (in^4)	0.1865

Fastener Strengths and Flexibilities	
Structural fastener strength, P_{nf} (kip)	1.80
Sidelap fastener strength, P_{ns} (kip)	0.869
Structural fastener flexibility, S_f (in/kip)	0.0066
Sidelap fastener flexibility, S_s (in/kip)	0.0159

Calculated Strength Equations Variables	
Corner fastener reduction factor, λ	0.835
Interior panel fastener contribution factor, β	13.3
Structural fastener distribution factor at panel ends, α_e^2	0.556
Structural fastener distribution factor at interior supports, α_p^2	0.556
Number of structural fasteners at panel ends per unit width, N	1
Fastener slip coefficient, C	4.65
Warping factor, D_n (in.)	31.8
Warping support factor, ρ	0.8

Predicted Shear Strength and Stiffness	
Interior panel shear strength, S_{ni} (kip/ft.)	1.16
Edge panel shear strength, S_{ne} (kip/ft.)	2.03
Panel shear strength limited by corner fastener, S_{nc} (kip/ft.)	0.994
Panel buckling shear strength, S_{nb} (kip/ft.)	6.83
Shear stiffness, G' (kip/in)	31.4

36/4 fastener pattern at interior and exterior supports

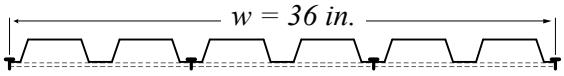

e (in.)	0.75
w_c (in.)	1.58
f (in.)	3.50
d (in.)	6.00
s (in.)	8.16
D_d (in.)	1.50

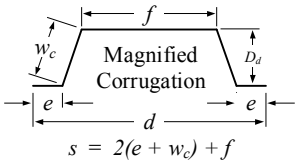

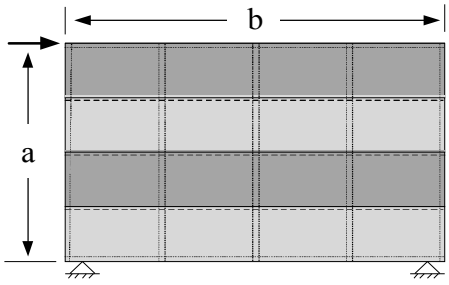

Loading Type: Cyclic
Load Rate: Fast-loading
a = 12'
b = 20'

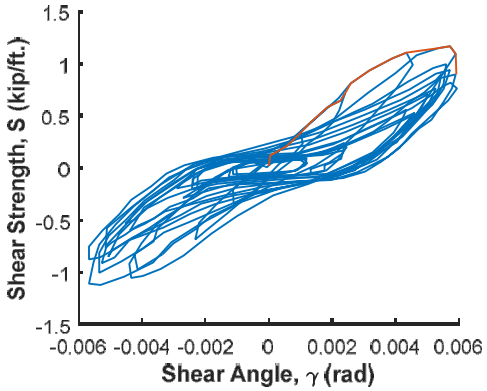

Eperimental Max Strength (kip/ft.)	1.18
Experimental Shear Stiffness (kip/in)	26.5
Ultimate Shear Angle, $\gamma_{80\%}$ (rad*1000)	5.90

Notes

Specimens 19, 34 and 35 have identical test setups with varying loading protocols.
No mass added to represent seismic weight for inertial forces for a truly dynamic test.

Martin (2002) - Specimen 36

Input	
Structural Fastener Type	Arc Spot Weld
Sidelap Fastener Type	Button Punch
Deck thickness, t (in.)	0.0300
Panel Length, l (ft.)	20
Panel Span, l_v (ft.)	5
No. of sidelap connections per one edge of interior panel length, n_s	16
No. of edge structural connections not in line with int. or ext. supports, n_e	16
No. of interior supports per panel length, n_p	3
Yield strength of deck, F_y (ksi)	33
Ultimate strength of deck, F_u (ksi)	45
Arc Spot Weld diameter (in.)	0.625
Moment of inertia of fully effective panel per unit width, I_x (in^4)	0.1481

Fastener Strengths and Flexibilities	
Structural fastener strength, P_{nf} (kip)	1.77
Sidelap fastener strength, P_{ns} (kip)	0.216
Structural fastener flexibility, S_f (in/kip)	0.0066
Sidelap fastener flexibility, S_s (in/kip)	0.173

Calculated Strength Equations Variables	
Corner fastener reduction factor, λ	0.820
Interior panel fastener contribution factor, β	7.51
Structural fastener distribution factor at panel ends, α_e^2	0.556
Structural fastener distribution factor at interior supports, α_p^2	0.556
Number of structural fasteners at panel ends per unit width, N	1.33
Fastener slip coefficient, C	9.93
Warping factor, D_n (in.)	41.5
Warping support factor, ρ	0.8

Predicted Shear Strength and Stiffness	
Interior panel shear strength, S_{ni} (kip/ft.)	0.632
Edge panel shear strength, S_{ne} (kip/ft.)	2.00
Panel shear strength limited by corner fastener, S_{nc} (kip/ft.)	0.639
Panel buckling shear strength, S_{nb} (kip/ft.)	5.03
Shear stiffness, G' (kip/in)	19.0

36/4 fastener pattern at interior and exterior supports

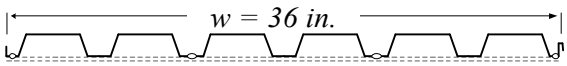

e (in.)	0.75
w_c (in.)	1.58
f (in.)	3.50
d (in.)	6.00
s (in.)	8.16
D_d (in.)	1.50

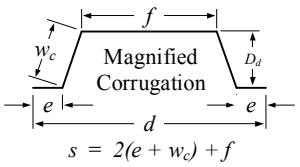

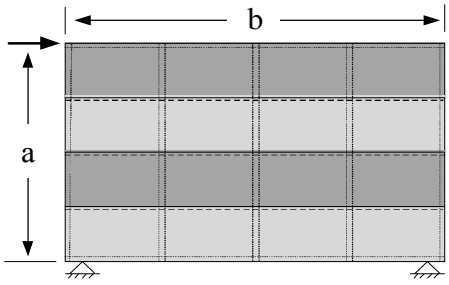

Loading Type: Cyclic
Load Rate: Fast-loading
a = 12'
b = 20'

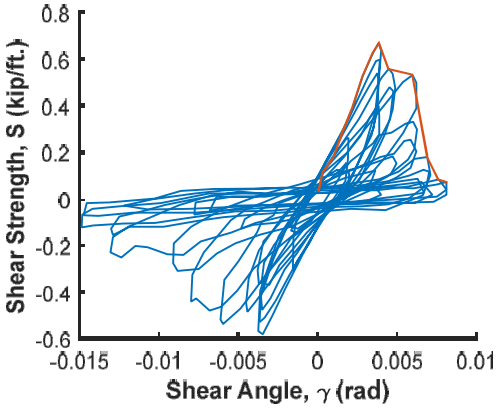

Eperimental Max Strength (kip/ft.)	0.672
Experimental Shear Stiffness (kip/in)	14.0
Ultimate Shear Angle, $\gamma_{80\%}$ (rad*1000)	5.82

Notes

No mass added to represent seismic weight for inertial forces for a truly dynamic test.

Specimens 20 and 36 have identical test setups with varying loading protocols.

202 static cycles at lower displacment displacement step before fast-loaded displacement history is applied. 202 cycles are meant to simulate wind fatigue at service loads.

Structural welds on both sides of interlocking sidelap seam.

Martin (2002) - Specimen 37

Input	
Structural Fastener Type	Arc Spot Weld
Sidelap Fastener Type	Button Punch
Deck thickness, t (in.)	0.0358
Panel Length, l (ft.)	20
Panel Span, l_v (ft.)	5
No. of sidelap connections per one edge of interior panel length, n_s	16
No. of edge structural connections not in line with int. or ext. supports, n_e	16
No. of interior supports per panel length, n_p	3
Yield strength of deck, F_y (ksi)	33
Ultimate strength of deck, F_u (ksi)	45
Arc Spot Weld diameter (in.)	0.625
Moment of inertia of fully effective panel per unit width, I_x (in^4)	0.1865

Fastener Strengths and Flexibilities	
Structural fastener strength, P_{nf} (kip)	2.09
Sidelap fastener strength, P_{ns} (kip)	0.308
Structural fastener flexibility, S_f (in/kip)	0.0061
Sidelap fastener flexibility, S_s (in/kip)	0.159

Calculated Strength Equations Variables	
Corner fastener reduction factor, λ	0.835
Interior panel fastener contribution factor, β	7.91
Structural fastener distribution factor at panel ends, α_e^2	0.556
Structural fastener distribution factor at interior supports, α_p^2	0.556
Number of structural fasteners at panel ends per unit width, N	1.33
Fastener slip coefficient, C	10.8
Warping factor, D_n (in.)	31.8
Warping support factor, ρ	0.8

Predicted Shear Strength and Stiffness	
Interior panel shear strength, S_{ni} (kip/ft.)	0.792
Edge panel shear strength, S_{ne} (kip/ft.)	2.37
Panel shear strength limited by corner fastener, S_{nc} (kip/ft.)	0.792
Panel buckling shear strength, S_{nb} (kip/ft.)	6.83
Shear stiffness, G' (kip/in)	26.5

36/4 fastener pattern at interior and exterior supports

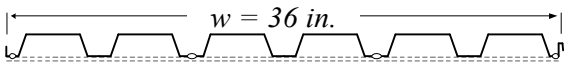

e (in.)	0.75
w_c (in.)	1.58
f (in.)	3.50
d (in.)	6.00
s (in.)	8.16
D_d (in.)	1.50

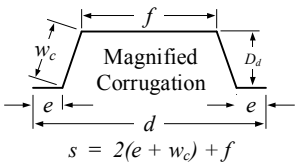

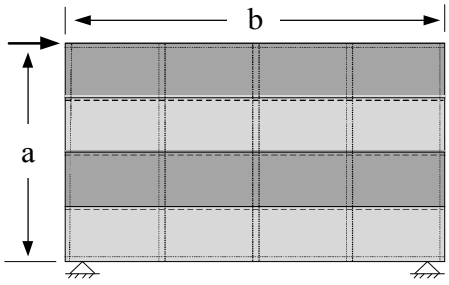

Loading Type: Monotonic
Load Rate: Static
a = 12'
b = 20'

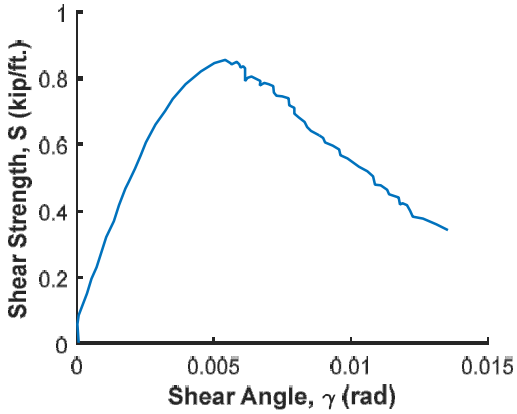

Eperimental Max Strength (kip/ft.)	0.858
Experimental Shear Stiffness (kip/in)	24.9
Ultimate Shear Angle, $\gamma_{80\%}$ (rad*1000)	8.06

Notes

Specimens 21 and 37 have identical test setups with varying loading protocols.

Structural welds on both sides of interlocking sidelap seam.

Essa (2003) - Specimen 1

Input	
Structural Fastener Type	Arc Spot Weld
Sidelap Fastener Type	Button Punch
Deck thickness, t (in.)	0.0300
Panel Length, l (ft.)	20
Panel Span, l_v (ft.)	5
No. of sidelap connections per one edge of interior panel length, n_s	16
No. of edge structural connections not in line with int. or ext. supports, n_e	16
No. of interior supports per panel length, n_p	3
Yield strength of deck, F_y (ksi)	33
Ultimate strength of deck, F_u (ksi)	45
Arc spot weld diameter, (in)	0.625
Moment of inertia of fully effective panel per unit width, I_x (in^4)	0.1481

Fastener Strengths and Flexibilities	
Structural fastener strength, P_{nf} (kip)	1.77
Sidelap fastener strength, P_{ns} (kip)	0.216
Structural fastener flexibility, S_f (in/kip)	0.0066
Sidelap fastener flexibility, S_s (in/kip)	0.1732

Calculated Strength Equations Variables	
Corner fastener reduction factor, λ	0.820
Interior panel fastener contribution factor, β	7.51
Structural fastener distribution factor at panel ends, α_e^2	0.556
Structural fastener distribution factor at interior supports, α_p^2	0.556
Number of structural fasteners at panel ends per unit width, N	1.33
Fastener slip coefficient, C	9.93
Warping factor, D_n (in.)	41.5
Warping support factor, ρ	0.8

Predicted Shear Strength and Stiffness	
Interior panel shear strength, S_{ni} (kip/ft.)	0.632
Edge panel shear strength, S_{ne} (kip/ft.)	2.00
Panel shear strength limited by corner fastener, S_{nc} (kip/ft.)	0.639
Panel buckling shear strength, S_{nb} (kip/ft.)	5.03
Shear stiffness, G' (kip/in)	19.0

36/4 fastener pattern at interior and exterior supports

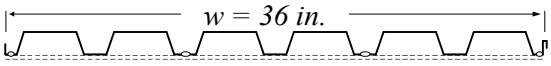

e (in.)	0.75
w_c (in.)	1.58
f (in.)	3.50
d (in.)	6.00
s (in.)	8.16
D_d (in.)	1.50

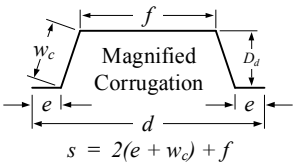

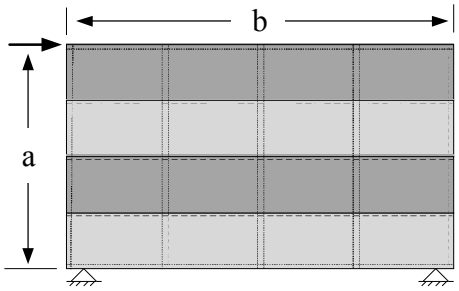

Loading Type: Monotonic
Load Rate: Static
a = 12'
b = 20'

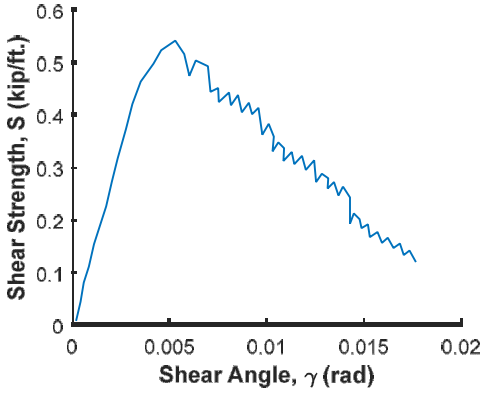

Eperimental Max Strength (kip/ft.)	0.542
Experimental Shear Stiffness (kip/in)	11.8
Ultimate Shear Angle, $\gamma_{80\%}$ (rad*1000)	7.49

Notes

Specimens 1 and 2 have identical test setups with varying loading protocols.
Structural welds on both sides of interlocking sidelap seam.

Essa (2003) - Specimen 2

Input	
Structural Fastener Type	Arc Spot Weld
Sidelap Fastener Type	Button Punch
Deck thickness, t (in.)	0.0300
Panel Length, l (ft.)	20
Panel Span, l_v (ft.)	5
No. of sidelap connections per one edge of interior panel length, n_s	16
No. of edge structural connections not in line with int. or ext. supports, n_e	16
No. of interior supports per panel length, n_p	3
Yield strength of deck, F_y (ksi)	33
Ultimate strength of deck, F_u (ksi)	45
Arc spot weld diameter, (in)	0.625
Moment of inertia of fully effective panel per unit width, I_x (in^4)	0.1481

Fastener Strengths and Flexibilities	
Structural fastener strength, P_{nf} (kip)	1.77
Sidelap fastener strength, P_{ns} (kip)	0.216
Structural fastener flexibility, S_f (in/kip)	0.0066
Sidelap fastener flexibility, S_s (in/kip)	0.1732

Calculated Strength Equations Variables	
Corner fastener reduction factor, λ	0.820
Interior panel fastener contribution factor, β	7.51
Structural fastener distribution factor at panel ends, α_e^2	0.556
Structural fastener distribution factor at interior supports, α_p^2	0.556
Number of structural fasteners at panel ends per unit width, N	1.33
Fastener slip coefficient, C	9.93
Warping factor, D_n (in.)	41.5
Warping support factor, ρ	0.8

Predicted Shear Strength and Stiffness	
Interior panel shear strength, S_{ni} (kip/ft.)	0.632
Edge panel shear strength, S_{ne} (kip/ft.)	2.00
Panel shear strength limited by corner fastener, S_{nc} (kip/ft.)	0.639
Panel buckling shear strength, S_{nb} (kip/ft.)	5.03
Shear stiffness, G' (kip/in)	19.0

36/4 fastener pattern at interior and exterior supports

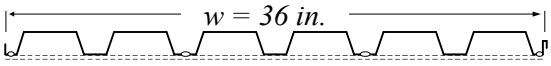

e (in.)	0.75
w_c (in.)	1.58
f (in.)	3.50
d (in.)	6.00
s (in.)	8.16
D_d (in.)	1.50

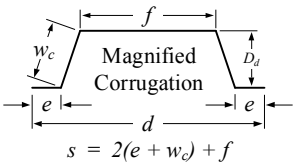

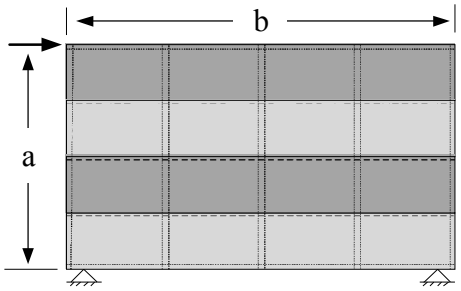

Loading Type: Cyclic
Load Rate: Quasistatic
a = 12'
b = 20'

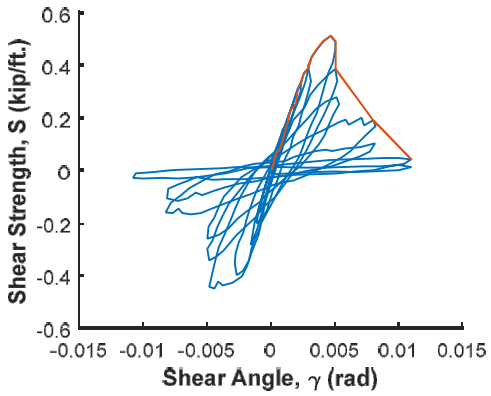

Eperimental Max Strength (kip/ft.)	0.517
Experimental Shear Stiffness (kip/in)	12.3
Ultimate Shear Angle, $\gamma_{80\%}$ (rad*1000)	5.06

Notes

Specimens 1 and 2 have identical test setups with varying loading protocols.
Structural welds on both sides of interlocking sidelap seam.

Essa (2003) - Specimen 5

Input	
Structural Fastener Type	Buildex BX-12
Sidelap Fastener Type	Screw
Deck thickness, t (in.)	0.0300
Panel Length, l (ft.)	20
Panel Span, l_v (ft.)	5
No. of sidelap connections per one edge of interior panel length, n_s	16
No. of edge structural connections not in line with int. or ext. supports, n_e	16
No. of interior supports per panel length, n_p	3
Yield strength of deck, F_y (ksi)	33
Ultimate strength of deck, F_u (ksi)	45
Sidelap screw diamete (in.)	0.2111
Moment of inertia of fully effective panel per unit width, I_x (in^4)	0.1481

Fastener Strengths and Flexibilities	
Structural fastener strength, P_{nf} (kip)	1.51
Sidelap fastener strength, P_{ns} (kip)	0.728
Structural fastener flexibility, S_f (in/kip)	0.0144
Sidelap fastener flexibility, S_s (in/kip)	0.0173

Calculated Strength Equations Variables	
Corner fastener reduction factor, λ	0.820
Interior panel fastener contribution factor, β	13.3
Structural fastener distribution factor at panel ends, α_e^2	0.556
Structural fastener distribution factor at interior supports, α_p^2	0.556
Number of structural fasteners at panel ends per unit width, N	1
Fastener slip coefficient, C	5.11
Warping factor, D_n (in.)	41.5
Warping support factor, ρ	0.8

Predicted Shear Strength and Stiffness	
Interior panel shear strength, S_{ni} (kip/ft.)	0.973
Edge panel shear strength, S_{ne} (kip/ft.)	1.71
Panel shear strength limited by corner fastener, S_{nc} (kip/ft.)	0.833
Panel buckling shear strength, S_{nb} (kip/ft.)	5.03
Shear stiffness, G' (kip/in)	17.2

36/4 fastener pattern at interior and exterior supports

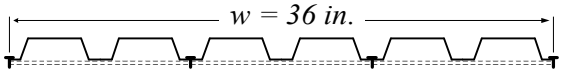

e (in.)	0.75
w_c (in.)	1.58
f (in.)	3.50
d (in.)	6.00
s (in.)	8.16
D_d (in.)	1.50

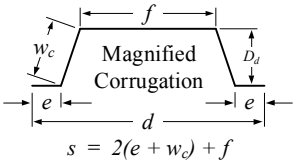

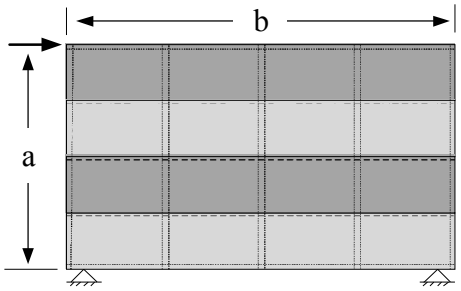

Loading Type: Monotonic
Load Rate: Static
a = 12'
b = 20'

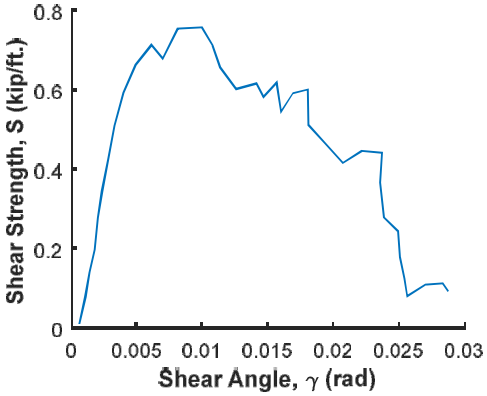

Eperimental Max Strength (kip/ft.)	0.759
Experimental Shear Stiffness (kip/in)	15.7
Ultimate Shear Angle, $\gamma_{80\%}$ (rad*1000)	12.5

Notes

Specimens 5 and 8 have identical test setups with varying loading protocols.

Essa (2003) - Specimen 8

Input	
Structural Fastener Type	Buildex BX-12
Sidelap Fastener Type	Screw
Deck thickness, t (in.)	0.0300
Panel Length, l (ft.)	20
Panel Span, l_v (ft.)	5
No. of sidelap connections per one edge of interior panel length, n_s	16
No. of edge structural connections not in line with int. or ext. supports, n_e	16
No. of interior supports per panel length, n_p	3
Yield strength of deck, F_y (ksi)	33
Ultimate strength of deck, F_u (ksi)	45
Sidelap screw diamete (in.)	0.2111
Moment of inertia of fully effective panel per unit width, I_x (in^4)	0.1481

Fastener Strengths and Flexibilities	
Structural fastener strength, P_{nf} (kip)	1.51
Sidelap fastener strength, P_{ns} (kip)	0.728
Structural fastener flexibility, S_f (in/kip)	0.0144
Sidelap fastener flexibility, S_s (in/kip)	0.0173

Calculated Strength Equations Variables	
Corner fastener reduction factor, λ	0.820
Interior panel fastener contribution factor, β	13.3
Structural fastener distribution factor at panel ends, α_e^2	0.556
Structural fastener distribution factor at interior supports, α_p^2	0.556
Number of structural fasteners at panel ends per unit width, N	1
Fastener slip coefficient, C	5.11
Warping factor, D_n (in.)	41.5
Warping support factor, ρ	0.8

Predicted Shear Strength and Stiffness	
Interior panel shear strength, S_{ni} (kip/ft.)	0.973
Edge panel shear strength, S_{ne} (kip/ft.)	1.71
Panel shear strength limited by corner fastener, S_{nc} (kip/ft.)	0.833
Panel buckling shear strength, S_{nb} (kip/ft.)	5.03
Shear stiffness, G' (kip/in)	17.2

36/4 fastener pattern at interior and exterior supports

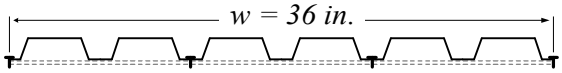

e (in.)	0.75
w_c (in.)	1.58
f (in.)	3.50
d (in.)	6.00
s (in.)	8.16
D_d (in.)	1.50

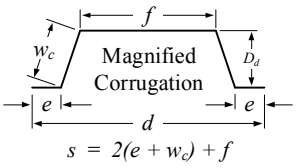

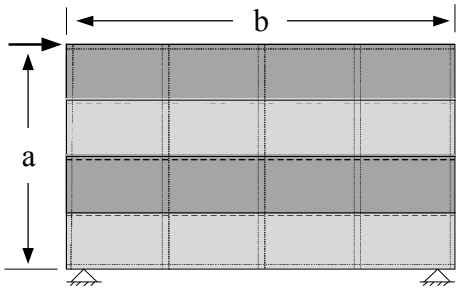

Loading Type: Cyclic
Load Rate: Quasistatic
a = 12'
b = 20'

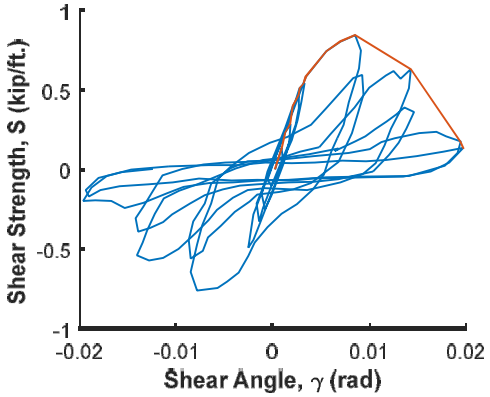

Eperimental Max Strength (kip/ft.)	0.850
Experimental Shear Stiffness (kip/in)	16.2
Ultimate Shear Angle, $\gamma_{80\%}$ (rad*1000)	13.1

Notes

Specimens 5 and 8 have identical test setups with varying loading protocols.

Essa (2003) - Specimen 9

Input	
Structural Fastener Type	Arc Spot Weld
Sidelap Fastener Type	Top Seam Weld
Deck thickness, t (in.)	0.0300
Panel Length, l (ft.)	20
Panel Span, l_v (ft.)	5
No. of sidelap connections per one edge of interior panel length, n_s	16
No. of edge structural connections not in line with int. or ext. supports, n_e	16
No. of interior supports per panel length, n_p	3
Yield strength of deck, F_y (ksi)	33
Ultimate strength of deck, F_u (ksi)	45
Arc spot weld diameter (in.)	0.625
Length of sidelap weld (in.)	1.38
Moment of inertia of fully effective panel per unit width, I_x (in^4)	0.1481

Fastener Strengths and Flexibilities	
Structural fastener strength, P_{nf} (kip)	1.77
Sidelap fastener strength, P_{ns} (kip)	2.07
Structural fastener flexibility, S_f (in/kip)	0.0066
Sidelap fastener flexibility, S_s (in/kip)	0.0063

Calculated Strength Equations Variables	
Corner fastener reduction factor, λ	0.820
Interior panel fastener contribution factor, β	24.3
Structural fastener distribution factor at panel ends, α_e^2	0.556
Structural fastener distribution factor at interior supports, α_p^2	0.556
Number of structural fasteners at panel ends per unit width, N	1.33
Fastener slip coefficient, C	1.95
Warping factor, D_n (in.)	41.5
Warping support factor, ρ	0.8

Predicted Shear Strength and Stiffness	
Interior panel shear strength, S_{ni} (kip/ft.)	1.87
Edge panel shear strength, S_{ne} (kip/ft.)	2.00
Panel shear strength limited by corner fastener, S_{nc} (kip/ft.)	1.48
Panel buckling shear strength, S_{nb} (kip/ft.)	5.03
Shear stiffness, G' (kip/in)	22.9

36/4 fastener pattern at interior and exterior supports

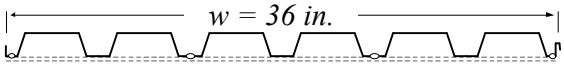

e (in.)	0.75
w_c (in.)	1.58
f (in.)	3.50
d (in.)	6.00
s (in.)	8.16
D_d (in.)	1.50

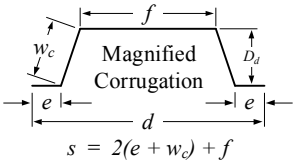

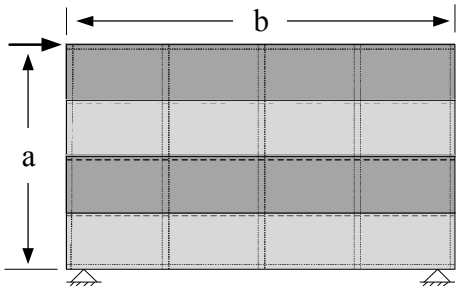

Loading Type: Monotonic
Load Rate: Static
a = 12'
b = 20'

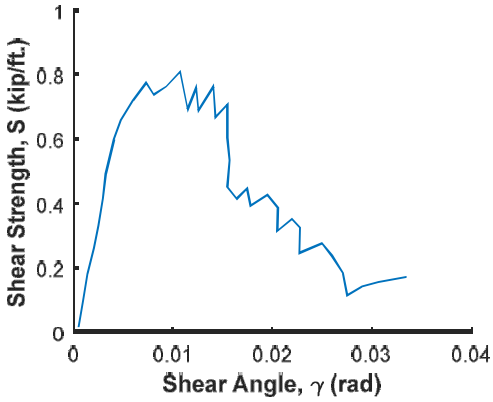

Eperimental Max Strength (kip/ft.)	0.811
Experimental Shear Stiffness (kip/in)	13.1
Ultimate Shear Angle, $\gamma_{80\%}$ (rad*1000)	15.5

Notes

Specimens 9 and 12 have identical test setups with varying loading protocols.

Sidelap fastener strength equations for longitudinal top seam welds may be non-conservative.

Structural welds on both sides of interlocking sidelap seam.

Essa (2003) - Specimen 10

Input	
Structural Fastener Type	Mix
Sidelap Fastener Type	Top Seam Weld
Deck thickness, t (in.)	0.0300
Panel Length, l (ft.)	20
Panel Span, l_v (ft.)	5
No. of sidelap connections per one edge of interior panel length, n_s	16
No. of edge structural connections not in line with int. or ext. supports, n_e	16
No. of interior supports per panel length, n_p	3
Yield strength of deck, F_y (ksi)	33
Ultimate strength of deck, F_u (ksi)	45
Inside (hole) diameter of washer (in.)	0.59
Length of sidelap weld (in.)	1.38
Moment of inertia of fully effective panel per unit width, I_x (in^4)	0.1481

Fastener Strengths and Flexibilities	
Structural fastener strength, P_{nf} (kip)	3.93
Sidelap fastener strength, P_{ns} (kip)	2.07
Structural fastener flexibility, S_f (in/kip)	0.0066
Sidelap fastener flexibility, S_s (in/kip)	0.0063

Calculated Strength Equations Variables	
Corner fastener reduction factor, λ	0.820
Interior panel fastener contribution factor, β	24.3
Structural fastener distribution factor at panel ends, α_e^2	0.556
Structural fastener distribution factor at interior supports, α_p^2	0.556
Number of structural fasteners at panel ends per unit width, N	1.33
Fastener slip coefficient, C	1.95
Warping factor, D_n (in.)	41.5
Warping support factor, ρ	0.8

Predicted Shear Strength and Stiffness	
Interior panel shear strength, S_{ni} (kip/ft.)	2.68
Edge panel shear strength, S_{ne} (kip/ft.)	4.46
Panel shear strength limited by corner fastener, S_{nc} (kip/ft.)	2.44
Panel buckling shear strength, S_{nb} (kip/ft.)	5.03
Shear stiffness, G' (kip/in)	22.9

36/4 fastener pattern at interior and exterior supports

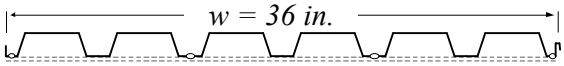

e (in.)	0.75
w_c (in.)	1.58
f (in.)	3.50
d (in.)	6.00
s (in.)	8.16
D_d (in.)	1.50

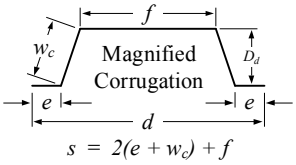

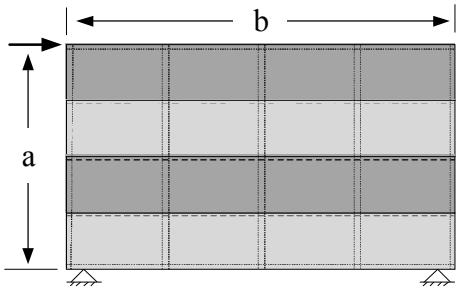

Loading Type: Monotonic
Load Rate: Static
a = 12'
b = 20'

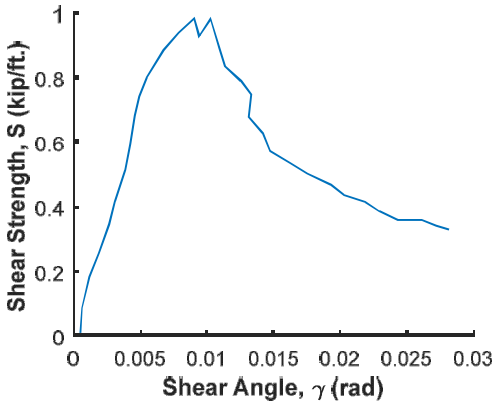

Eperimental Max Strength (kip/ft.)	0.985
Experimental Shear Stiffness (kip/in)	13.1
Ultimate Shear Angle, $\gamma_{80\%}$ (rad*1000)	12.6

Notes

Specimens 10 and 13 have identical test setups with varying loading protocols.

Mix of welds with and without washers as structural fasteners used. Standing seam at panel edge did not allow clearance to use welds with washers. For predicted strength, only weld with washer fastener strength used - gives overestimated diaphragm strength prediction.

Sidelap fastener strength equations for longitudinal top seam welds may be non-conservative.

Structural welds on both sides of interlocking sidelap seam.

Essa (2003) - Specimen 11

Input	
Structural Fastener Type	Arc Spot Weld
Sidelap Fastener Type	Screw
Deck thickness, t (in.)	0.0300
Panel Length, l (ft.)	20
Panel Span, l_v (ft.)	5
No. of sidelap connections per one edge of interior panel length, n_s	16
No. of edge structural connections not in line with int. or ext. supports, n_e	16
No. of interior supports per panel length, n_p	3
Yield strength of deck, F_y (ksi)	33
Ultimate strength of deck, F_u (ksi)	45
Arc spot weld diameter (in.)	0.625
Sidelap screw diameter (in.)	0.2111
Moment of inertia of fully effective panel per unit width, I_x (in^4)	0.1481

Fastener Strengths and Flexibilities	
Structural fastener strength, P_{nf} (kip)	1.77
Sidelap fastener strength, P_{ns} (kip)	0.728
Structural fastener flexibility, S_f (in/kip)	0.0066
Sidelap fastener flexibility, S_s (in/kip)	0.0173

Calculated Strength Equations Variables	
Corner fastener reduction factor, λ	0.820
Interior panel fastener contribution factor, β	12.2
Structural fastener distribution factor at panel ends, α_e^2	0.556
Structural fastener distribution factor at interior supports, α_p^2	0.556
Number of structural fasteners at panel ends per unit width, N	1
Fastener slip coefficient, C	4.14
Warping factor, D_n (in.)	41.5
Warping support factor, ρ	0.8

Predicted Shear Strength and Stiffness	
Interior panel shear strength, S_{ni} (kip/ft.)	1.04
Edge panel shear strength, S_{ne} (kip/ft.)	2.00
Panel shear strength limited by corner fastener, S_{nc} (kip/ft.)	0.917
Panel buckling shear strength, S_{nb} (kip/ft.)	5.03
Shear stiffness, G' (kip/in)	21.7

36/4 fastener pattern at interior and exterior supports

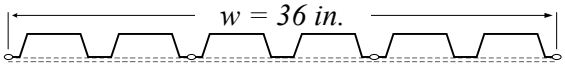

e (in.)	0.75
w_c (in.)	1.58
f (in.)	3.50
d (in.)	6.00
s (in.)	8.16
D_d (in.)	1.50

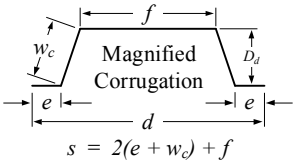

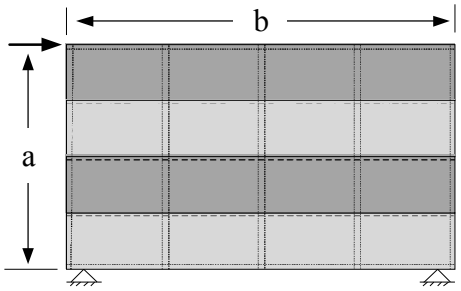

Loading Type: Monotonic
Load Rate: Static
a = 12'
b = 20'

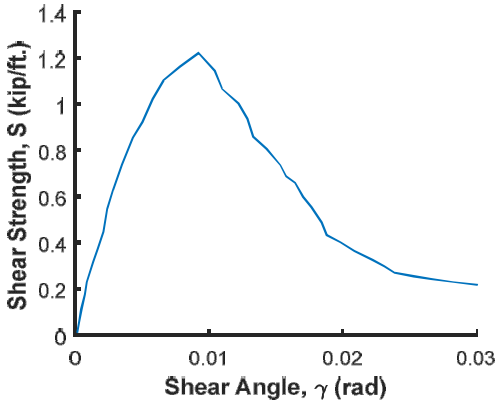

Eperimental Max Strength (kip/ft.)	1.23
Experimental Shear Stiffness (kip/in)	19.1
Ultimate Shear Angle, $\gamma_{80\%}$ (rad*1000)	12.4

Notes

Specimens 11 and 14 have identical test setups with varying loading protocols.

Essa (2003) - Specimen 12

Input	
Structural Fastener Type	Arc Spot Weld
Sidelap Fastener Type	Top Seam Weld
Deck thickness, t (in.)	0.0300
Panel Length, l (ft.)	20
Panel Span, l_v (ft.)	5
No. of sidelap connections per one edge of interior panel length, n_s	16
No. of edge structural connections not in line with int. or ext. supports, n_e	16
No. of interior supports per panel length, n_p	3
Yield strength of deck, F_y (ksi)	33
Ultimate strength of deck, F_u (ksi)	45
Arc spot weld diameter (in.)	0.625
Length of sidelap weld (in.)	1.38
Moment of inertia of fully effective panel per unit width, I_x (in^4)	0.1481

Fastener Strengths and Flexibilities	
Structural fastener strength, P_{nf} (kip)	1.77
Sidelap fastener strength, P_{ns} (kip)	2.07
Structural fastener flexibility, S_f (in/kip)	0.0066
Sidelap fastener flexibility, S_s (in/kip)	0.0063

Calculated Strength Equations Variables	
Corner fastener reduction factor, λ	0.820
Interior panel fastener contribution factor, β	24.3
Structural fastener distribution factor at panel ends, α_e^2	0.556
Structural fastener distribution factor at interior supports, α_p^2	0.556
Number of structural fasteners at panel ends per unit width, N	1.33
Fastener slip coefficient, C	1.95
Warping factor, D_n (in.)	41.5
Warping support factor, ρ	0.8

Predicted Shear Strength and Stiffness	
Interior panel shear strength, S_{ni} (kip/ft.)	1.87
Edge panel shear strength, S_{ne} (kip/ft.)	2.00
Panel shear strength limited by corner fastener, S_{nc} (kip/ft.)	1.48
Panel buckling shear strength, S_{nb} (kip/ft.)	5.03
Shear stiffness, G' (kip/in)	22.9

36/4 fastener pattern at interior and exterior supports

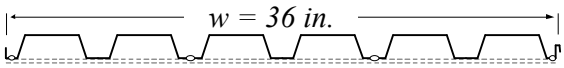

e (in.)	0.75
w_c (in.)	1.58
f (in.)	3.50
d (in.)	6.00
s (in.)	8.16
D_d (in.)	1.50

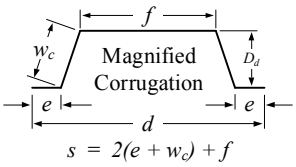

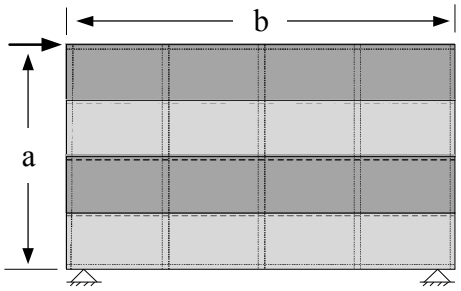

Loading Type: Cyclic
Load Rate: Quasistatic
a = 12'
b = 20'

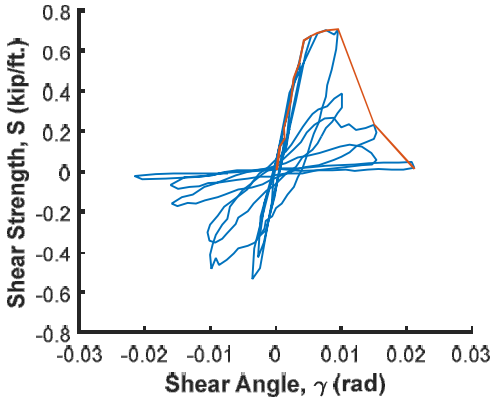

Eperimental Max Strength (kip/ft.)	0.712
Experimental Shear Stiffness (kip/in)	14.0
Ultimate Shear Angle, $\gamma_{80\%}$ (rad*1000)	11.1

Notes

Specimens 9 and 12 have identical test setups with varying loading protocols.

Sidelap fastener strength equations for longitudinal top seam welds may be non-conservative.

Peak strength varries from published value of Smax of 0.781 kip/ft to digitized Smax = 0.712 kip/ft.

Structural welds on both sides of interlocking sidelap seam.

Essa (2003) - Specimen 13

Input	
Structural Fastener Type	Mix
Sidelap Fastener Type	Top Seam Weld
Deck thickness, t (in.)	0.0300
Panel Length, l (ft.)	20
Panel Span, l_v (ft.)	5
No. of sidelap connections per one edge of interior panel length, n_s	16
No. of edge structural connections not in line with int. or ext. supports, n_e	16
No. of interior supports per panel length, n_p	3
Yield strength of deck, F_y (ksi)	33
Ultimate strength of deck, F_u (ksi)	45
Inside (hole) diameter of washer (in.)	0.59
Length of sidelap weld (in.)	1.38
Moment of inertia of fully effective panel per unit width, I_x (in^4)	0.1481

Fastener Strengths and Flexibilities	
Structural fastener strength, P_{nf} (kip)	3.93
Sidelap fastener strength, P_{ns} (kip)	2.07
Structural fastener flexibility, S_f (in/kip)	0.0066
Sidelap fastener flexibility, S_s (in/kip)	0.0063

Calculated Strength Equations Variables	
Corner fastener reduction factor, λ	0.820
Interior panel fastener contribution factor, β	24.3
Structural fastener distribution factor at panel ends, α_e^2	0.556
Structural fastener distribution factor at interior supports, α_p^2	0.556
Number of structural fasteners at panel ends per unit width, N	1.33
Fastener slip coefficient, C	1.95
Warping factor, D_n (in.)	41.5
Warping support factor, ρ	0.8

Predicted Shear Strength and Stiffness	
Interior panel shear strength, S_{ni} (kip/ft.)	2.68
Edge panel shear strength, S_{ne} (kip/ft.)	4.46
Panel shear strength limited by corner fastener, S_{nc} (kip/ft.)	2.43
Panel buckling shear strength, S_{nb} (kip/ft.)	5.03
Shear stiffness, G' (kip/in)	22.9

36/4 fastener pattern at interior and exterior supports

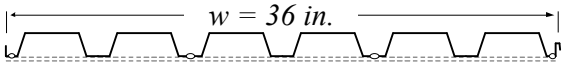

e (in.)	0.75
w_c (in.)	1.58
f (in.)	3.50
d (in.)	6.00
s (in.)	8.16
D_d (in.)	1.50

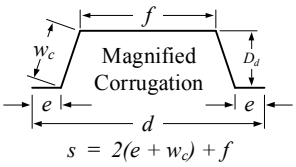

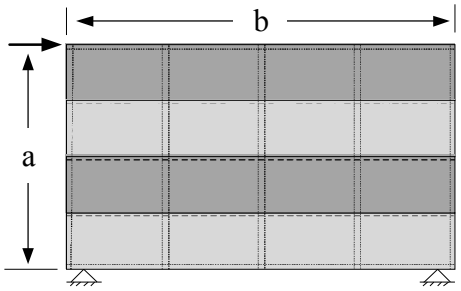

Loading Type: Cyclic
Load Rate: Quasitatic
a = 12'
b = 20'

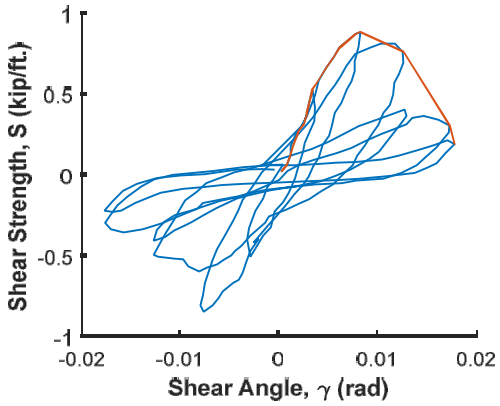

Eperimental Max Strength (kip/ft.)	0.881
Experimental Shear Stiffness (kip/in)	11.2
Ultimate Shear Angle, $\gamma_{80\%}$ (rad*1000)	13.1

Notes

Specimens 10 and 13 have identical test setups with varying loading protocols.

Mix of welds with and without washers as structural fasteners used. Standing seam at panel edge did not allow clearance to use welds with washers. For predicted strength, only weld with washer fastener strength used - gives overestimated diaphragm strength prediction.

Sidelap fastener strength equations for longitudinal top seam welds may be non-conservative.

Structural welds on both sides of interlocking sidelap seam.

Essa (2003) - Specimen 14

Input	
Structural Fastener Type	Arc Spot Weld
Sidelap Fastener Type	Screw
Deck thickness, t (in.)	0.0300
Panel Length, l (ft.)	20
Panel Span, l_v (ft.)	5
No. of sidelap connections per one edge of interior panel length, n_s	16
No. of edge structural connections not in line with int. or ext. supports, n_e	16
No. of interior supports per panel length, n_p	3
Yield strength of deck, F_y (ksi)	33
Ultimate strength of deck, F_u (ksi)	45
Arc spot weld diameter (in.)	0.625
Sidelap screw diameter (in.)	0.2111
Moment of inertia of fully effective panel per unit width, I_x (in^4)	0.1481

Fastener Strengths and Flexibilities	
Structural fastener strength, P_{nf} (kip)	1.77
Sidelap fastener strength, P_{ns} (kip)	0.728
Structural fastener flexibility, S_f (in/kip)	0.0066
Sidelap fastener flexibility, S_s (in/kip)	0.0173

Calculated Strength Equations Variables	
Corner fastener reduction factor, λ	0.820
Interior panel fastener contribution factor, β	12.2
Structural fastener distribution factor at panel ends, α_e^2	0.556
Structural fastener distribution factor at interior supports, α_p^2	0.556
Number of structural fasteners at panel ends per unit width, N	1
Fastener slip coefficient, C	4.14
Warping factor, D_n (in.)	41.5
Warping support factor, ρ	0.8

Predicted Shear Strength and Stiffness	
Interior panel shear strength, S_{ni} (kip/ft.)	1.04
Edge panel shear strength, S_{ne} (kip/ft.)	2.00
Panel shear strength limited by corner fastener, S_{nc} (kip/ft.)	0.917
Panel buckling shear strength, S_{nb} (kip/ft.)	5.03
Shear stiffness, G' (kip/in)	21.7

36/4 fastener pattern at interior and exterior supports

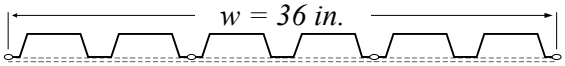

e (in.)	0.75
w_c (in.)	1.58
f (in.)	3.50
d (in.)	6.00
s (in.)	8.16
D_d (in.)	1.50

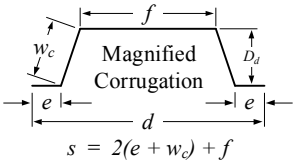

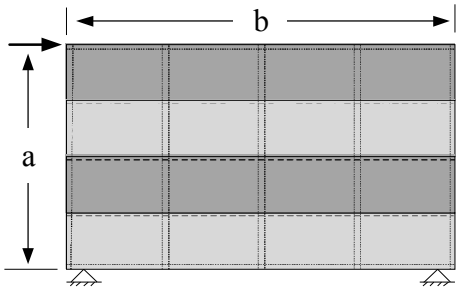

Loading Type: Cyclic
Load Rate: Quasistatic
a = 12'
b = 20'

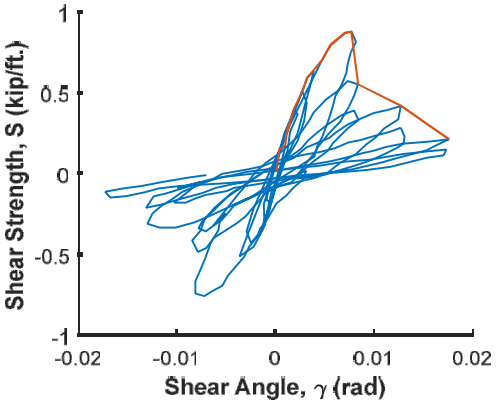

Eperimental Max Strength (kip/ft.)	0.884
Experimental Shear Stiffness (kip/in)	18.3
Ultimate Shear Angle, $\gamma_{80\%}$ (rad*1000)	8.04

Notes

Specimens 11 and 14 have identical test setups with varying loading protocols.

Essa (2003) - Specimen 15

Input	
Structural Fastener Type	WWW
Sidelap Fastener Type	Screw
Deck thickness, t (in.)	0.0300
Panel Length, l (ft.)	20
Panel Span, l_v (ft.)	5
No. of sidelap connections per one edge of interior panel length, n_s	16
No. of edge structural connections not in line with int. or ext. supports, n_e	16
No. of interior supports per panel length, n_p	3
Yield strength of deck, F_y (ksi)	33
Ultimate strength of deck, F_u (ksi)	45
Inside (hole) diameter of weld washer (in.)	0.59
Sidelap screw diameter (in.)	0.2111
Moment of inertia of fully effective panel per unit width, I_x (in^4)	0.1481

Fastener Strengths and Flexibilities	
Structural fastener strength, P_{nf} (kip)	3.93
Sidelap fastener strength, P_{ns} (kip)	0.728
Structural fastener flexibility, S_f (in/kip)	0.0066
Sidelap fastener flexibility, S_s (in/kip)	0.0173

Calculated Strength Equations Variables	
Corner fastener reduction factor, λ	0.820
Interior panel fastener contribution factor, β	8.52
Structural fastener distribution factor at panel ends, α_e^2	0.556
Structural fastener distribution factor at interior supports, α_p^2	0.556
Number of structural fasteners at panel ends per unit width, N	1
Fastener slip coefficient, C	4.14
Warping factor, D_n (in.)	41.5
Warping support factor, ρ	0.8

Predicted Shear Strength and Stiffness	
Interior panel shear strength, S_{ni} (kip/ft.)	1.60
Edge panel shear strength, S_{ne} (kip/ft.)	4.46
Panel shear strength limited by corner fastener, S_{nc} (kip/ft.)	1.54
Panel buckling shear strength, S_{nb} (kip/ft.)	5.03
Shear stiffness, G' (kip/in)	21.7

36/4 fastener pattern at interior and exterior supports

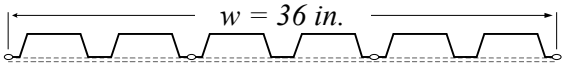

e (in.)	0.75
w_c (in.)	1.58
f (in.)	3.50
d (in.)	6.00
s (in.)	8.16
D_d (in.)	1.50

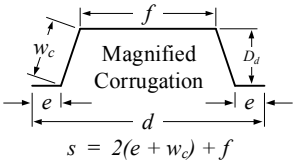

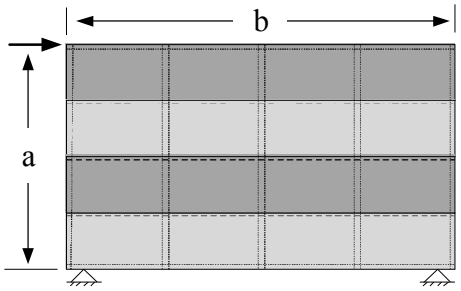

Loading Type: Monotonic
Load Rate: Static
a = 12'
b = 20'

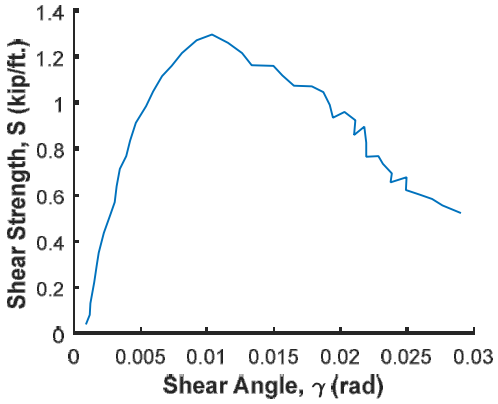

Eperimental Max Strength (kip/ft.)	1.30
Experimental Shear Stiffness (kip/in)	22.0
Ultimate Shear Angle, $\gamma_{80\%}$ (rad*1000)	18.8

Notes

Specimens 15 and 16 have identical test setups with varying loading protocols.

Essa (2003) - Specimen 16

Input	
Structural Fastener Type	WWW
Sidelap Fastener Type	Screw
Deck thickness, t (in.)	0.0300
Panel Length, l (ft.)	20
Panel Span, l_v (ft.)	5
No. of sidelap connections per one edge of interior panel length, n_s	16
No. of edge structural connections not in line with int. or ext. supports, n_e	16
No. of interior supports per panel length, n_p	3
Yield strength of deck, F_y (ksi)	33
Ultimate strength of deck, F_u (ksi)	45
Inside (hole) diameter of weld washer (in.)	0.59
Sidelap screw diameter (in.)	0.2111
Moment of inertia of fully effective panel per unit width, I_x (in^4)	0.1481

Fastener Strengths and Flexibilities	
Structural fastener strength, P_{nf} (kip)	3.93
Sidelap fastener strength, P_{ns} (kip)	0.728
Structural fastener flexibility, S_f (in/kip)	0.0066
Sidelap fastener flexibility, S_s (in/kip)	0.0173

Calculated Strength Equations Variables	
Corner fastener reduction factor, λ	0.820
Interior panel fastener contribution factor, β	8.52
Structural fastener distribution factor at panel ends, α_e^2	0.556
Structural fastener distribution factor at interior supports, α_p^2	0.556
Number of structural fasteners at panel ends per unit width, N	1
Fastener slip coefficient, C	4.14
Warping factor, D_n (in.)	41.5
Warping support factor, ρ	0.8

Predicted Shear Strength and Stiffness	
Interior panel shear strength, S_{ni} (kip/ft.)	1.60
Edge panel shear strength, S_{ne} (kip/ft.)	4.46
Panel shear strength limited by corner fastener, S_{nc} (kip/ft.)	1.54
Panel buckling shear strength, S_{nb} (kip/ft.)	5.03
Shear stiffness, G' (kip/in)	21.7

36/4 fastener pattern at interior and exterior supports

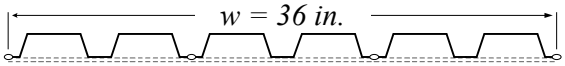

e (in.)	0.75
w_c (in.)	1.58
f (in.)	3.50
d (in.)	6.00
s (in.)	8.16
D_d (in.)	1.50

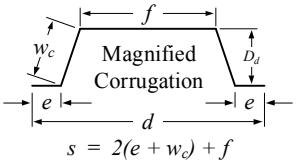

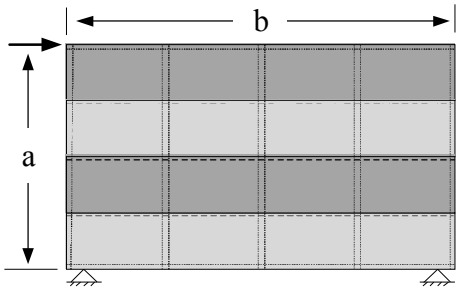

Loading Type: Cyclic
Load Rate: Quasistatic
a = 12'
b = 20'

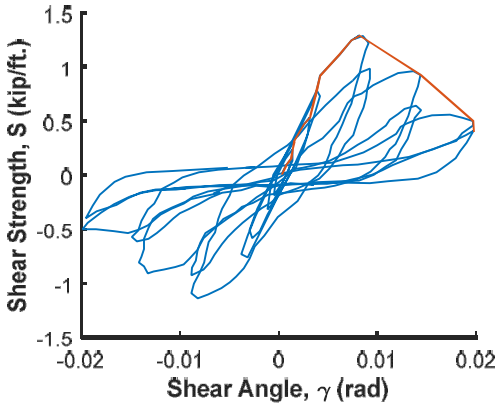

Eperimental Max Strength (kip/ft.)	1.30
Experimental Shear Stiffness (kip/in)	16.0
Ultimate Shear Angle, $\gamma_{80\%}$ (rad*1000)	12.6

Notes

Specimens 15 and 16 have identical test setups with varying loading protocols.

Essa (2003) - Specimen 17

Input	
Structural Fastener Type	X-EDNK22
Sidelap Fastener Type	Screw
Deck thickness, t (in.)	0.0358
Panel Length, l (ft.)	20
Panel Span, l_v (ft.)	5
No. of sidelap connections per one edge of interior panel length, n_s	16
No. of edge structural connections not in line with int. or ext. supports, n_e	16
No. of interior supports per panel length, n_p	3
Yield strength of deck, F_y (ksi)	33
Ultimate strength of deck, F_u (ksi)	45
Sidelap screw diamete (in.)	0.2111
Moment of inertia of fully effective panel per unit width, I_x (in^4)	0.1865

Fastener Strengths and Flexibilities	
Structural fastener strength, P_{nf} (kip)	1.80
Sidelap fastener strength, P_{ns} (kip)	0.869
Structural fastener flexibility, S_f (in/kip)	0.0066
Sidelap fastener flexibility, S_s (in/kip)	0.0159

Calculated Strength Equations Variables	
Corner fastener reduction factor, λ	0.835
Interior panel fastener contribution factor, β	13.3
Structural fastener distribution factor at panel ends, α_e^2	0.556
Structural fastener distribution factor at interior supports, α_p^2	0.556
Number of structural fasteners at panel ends per unit width, N	1
Fastener slip coefficient, C	4.65
Warping factor, D_n (in.)	31.8
Warping support factor, ρ	0.8

Predicted Shear Strength and Stiffness	
Interior panel shear strength, S_{ni} (kip/ft.)	1.16
Edge panel shear strength, S_{ne} (kip/ft.)	2.03
Panel shear strength limited by corner fastener, S_{nc} (kip/ft.)	0.994
Panel buckling shear strength, S_{nb} (kip/ft.)	6.83
Shear stiffness, G' (kip/in)	31.4

36/4 fastener pattern at interior and exterior supports

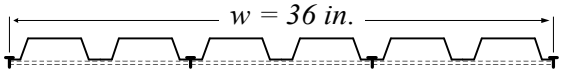

e (in.)	0.75
w_c (in.)	1.58
f (in.)	3.50
d (in.)	6.00
s (in.)	8.16
D_d (in.)	1.50

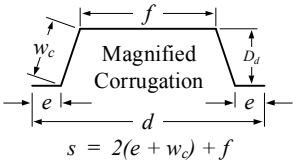

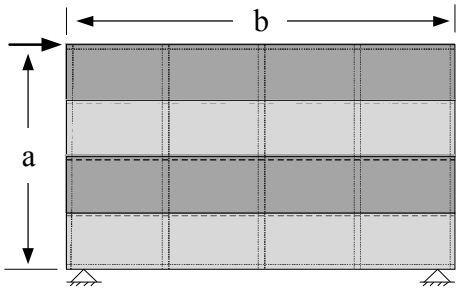

Loading Type: Monotonic
Load Rate: Static
a = 12'
b = 20'

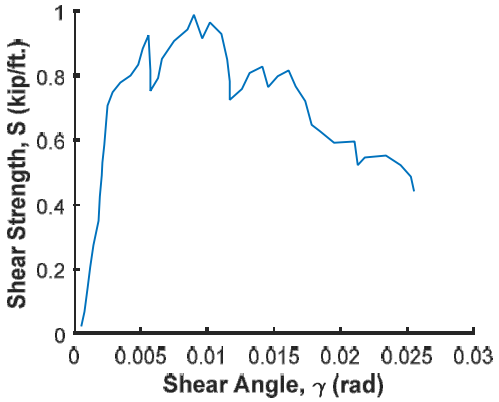

Eperimental Max Strength (kip/ft.)	0.991
Experimental Shear Stiffness (kip/in)	22.9
Ultimate Shear Angle, $\gamma_{80\%}$ (rad*1000)	11.6

Notes

Specimens 17 and 18 have identical test setups with varying loading protocols.

Essa (2003) - Specimen 18

Input	
Structural Fastener Type	X-EDNK22
Sidelap Fastener Type	Screw
Deck thickness, t (in.)	0.0358
Panel Length, l (ft.)	20
Panel Span, l_v (ft.)	5
No. of sidelap connections per one edge of interior panel length, n_s	16
No. of edge structural connections not in line with int. or ext. supports, n_e	16
No. of interior supports per panel length, n_p	3
Yield strength of deck, F_y (ksi)	33
Ultimate strength of deck, F_u (ksi)	45
Sidelap screw diamete (in.)	0.2111
Moment of inertia of fully effective panel per unit width, I_x (in^4)	0.1865

Fastener Strengths and Flexibilities	
Structural fastener strength, P_{nf} (kip)	1.80
Sidelap fastener strength, P_{ns} (kip)	0.869
Structural fastener flexibility, S_f (in/kip)	0.0066
Sidelap fastener flexibility, S_s (in/kip)	0.0159

Calculated Strength Equations Variables	
Corner fastener reduction factor, λ	0.835
Interior panel fastener contribution factor, β	13.3
Structural fastener distribution factor at panel ends, α_e^2	0.556
Structural fastener distribution factor at interior supports, α_p^2	0.556
Number of structural fasteners at panel ends per unit width, N	1
Fastener slip coefficient, C	4.65
Warping factor, D_n (in.)	31.8
Warping support factor, ρ	0.8

Predicted Shear Strength and Stiffness	
Interior panel shear strength, S_{ni} (kip/ft.)	1.16
Edge panel shear strength, S_{ne} (kip/ft.)	2.03
Panel shear strength limited by corner fastener, S_{nc} (kip/ft.)	0.994
Panel buckling shear strength, S_{nb} (kip/ft.)	6.83
Shear stiffness, G' (kip/in)	31.4

36/4 fastener pattern at interior and exterior supports

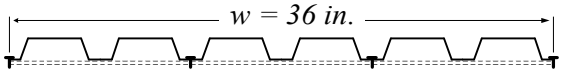

e (in.)	0.75
w_c (in.)	1.58
f (in.)	3.50
d (in.)	6.00
s (in.)	8.16
D_d (in.)	1.50

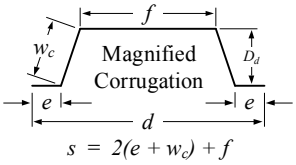

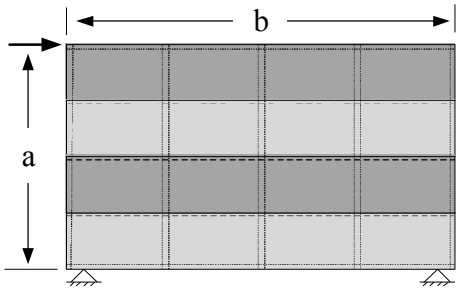

Loading Type: Cyclic
Load Rate: Qausistatic
a = 12'
b = 20'

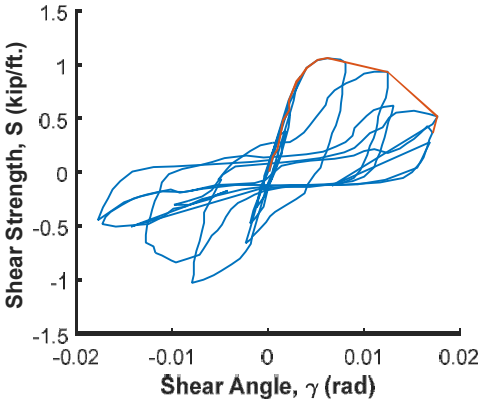

Eperimental Max Strength (kip/ft.)	1.07
Experimental Shear Stiffness (kip/in)	26.3
Ultimate Shear Angle, $\gamma_{80\%}$ (rad*1000)	13.5

Notes

Specimens 17 and 18 have identical test setups with varying loading protocols.
Peak strength varries from published value of Smax = 1.13 kip/ft to digitized Smax = 1.07 kip/ft.

Yang (2003) - Specimen 38

Input	
Structural Fastener Type	Buildex BX-14
Sidelap Fastener Type	Screw
Deck thickness, t (in.)	0.0360
Panel Length, l (ft.)	20
Panel Span, l_v (ft.)	5
No. of sidelap connections per one edge of interior panel length, n_s	16
No. of edge structural connections not in line with int. or ext. supports, n_e	16
No. of interior supports per panel length, n_p	3
Yield strength of deck, F_y (ksi)	33
Ultimate strength of deck, F_u (ksi)	45
Sidelap screw diameter (in.)	0.2111
Moment of inertia of fully effective panel per unit width, I_x (in^4)	0.1865

Fastener Strengths and Flexibilities	
Structural fastener strength, P_{nf} (kip)	1.85
Sidelap fastener strength, P_{ns} (kip)	0.874
Structural fastener flexibility, S_f (in/kip)	0.0132
Sidelap fastener flexibility, S_s (in/kip)	0.0158

Calculated Strength Equations Variables	
Corner fastener reduction factor, λ	0.835
Interior panel fastener contribution factor, β	13.1
Structural fastener distribution factor at panel ends, α_e^2	0.556
Structural fastener distribution factor at interior supports, α_p^2	0.556
Number of structural fasteners at panel ends per unit width, N	1.0
Fastener slip coefficient, C	5.60
Warping factor, D_n (in.)	31.5
Warping support factor, ρ	0.8

Predicted Shear Strength and Stiffness	
Interior panel shear strength, S_{ni} (kip/ft.)	1.18
Edge panel shear strength, S_{ne} (kip/ft.)	2.09
Panel shear strength limited by corner fastener, S_{nc} (kip/ft.)	1.01
Panel buckling shear strength, S_{nb} (kip/ft.)	6.85
Shear stiffness, G' (kip/in)	30.9

36/4 fastener pattern at interior and exterior supports

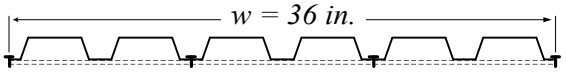

e (in.)	0.75
w_c (in.)	1.58
f (in.)	3.50
d (in.)	6.00
s (in.)	8.16
D_d (in.)	1.50

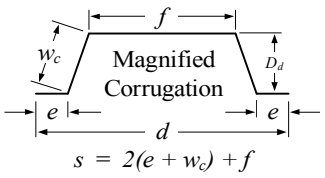

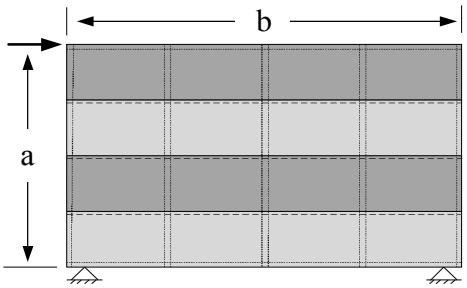

Loading Type: Cylic
Load Rate: Fast-loading
a = 12'
b = 20'

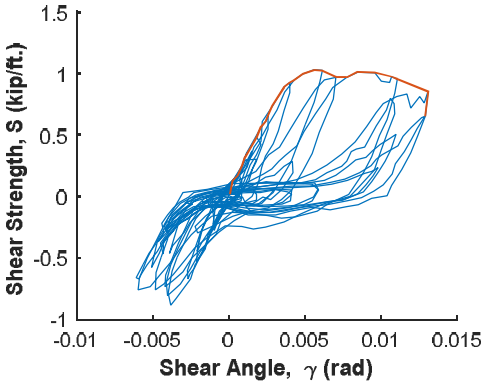

Eperimental Max Strength (kip/ft.)	1.03
Experimental Shear Stiffness (kip/in)	23.1
Ultimate Shear Angle, $\gamma_{80\%}$ (rad*1000)	13.1

Notes

Same load protocol as Martin (2002) - Specimen 34.

No mass added to represent seismic weight for inertial forces for a truly dynamic test.

Yang (2003) - Specimen 39

Input	
Structural Fastener Type	X-EDNK22
Sidelap Fastener Type	Screw
Deck thickness, t (in.)	0.0300
Panel Length, l (ft.)	10
Panel Span, l_v (ft.)	5
No. of sidelap connections per one edge of interior panel length, n_s	8
No. of edge structural connections not in line with int. or ext. supports, n_e	8
No. of interior supports per panel length, n_p	1
Yield strength of deck, F_y (ksi)	33
Ultimate strength of deck, F_u (ksi)	45
Sidelap screw diameter (in.)	0.2111
Moment of inertia of fully effective panel per unit width, I_x (in^4)	0.1481

Fastener Strengths and Flexibilities	
Structural fastener strength, P_{nf} (kip)	1.51
Sidelap fastener strength, P_{ns} (kip)	0.728
Structural fastener flexibility, S_f (in/kip)	0.0072
Sidelap fastener flexibility, S_s (in/kip)	0.0173

Calculated Strength Equations Variables	
Corner fastener reduction factor, λ	0.820
Interior panel fastener contribution factor, β	7.18
Structural fastener distribution factor at panel ends, α_e^2	0.556
Structural fastener distribution factor at interior supports, α_p^2	0.556
Number of structural fasteners at panel ends per unit width, N	1.0
Fastener slip coefficient, C	3.99
Warping factor, D_n (in.)	82.9
Warping support factor, ρ	1.0

Predicted Shear Strength and Stiffness	
Interior panel shear strength, S_{ni} (kip/ft.)	1.03
Edge panel shear strength, S_{ne} (kip/ft.)	1.74
Panel shear strength limited by corner fastener, S_{nc} (kip/ft.)	0.883
Panel buckling shear strength, S_{nb} (kip/ft.)	5.03
Shear stiffness, G' (kip/in)	9.78

36/4 fastener pattern at interior and exterior supports

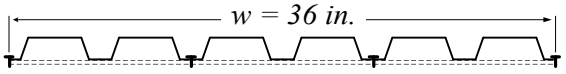

e (in.)	0.75
w_c (in.)	1.58
f (in.)	3.50
d (in.)	6.00
s (in.)	8.16
D_d (in.)	1.50

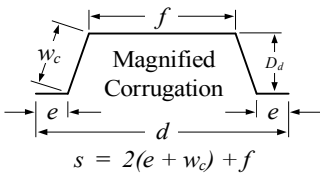

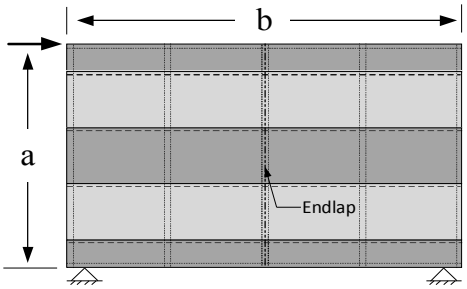

Loading Type: Monotonic
Load Rate: Static
a = 12'
b = 20'

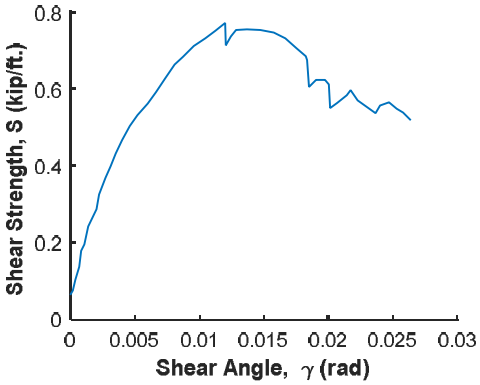

Eperimental Max Strength (kip/ft.)	0.774
Experimental Shear Stiffness (kip/in)	12.0
Ultimate Shear Angle, $\gamma_{80\%}$ (rad*1000)	18.5

Notes

Specimens 39 and 40 have identical test setups with varying loading protocols.
Half width panels at edge of diaphragm to minimize influence of test frame on sidelap slip. Drawback is possible decrease in strength and stiffness.
Edge panels do not control predictions.
Endlap at 10 ft.

Yang (2003) - Specimen 40

Input	
Structural Fastener Type	X-EDNK22
Sidelap Fastener Type	Screw
Deck thickness, t (in.)	0.0300
Panel Length, l (ft.)	10
Panel Span, l_v (ft.)	5
No. of sidelap connections per one edge of interior panel length, n_s	8
No. of edge structural connections not in line with int. or ext. supports, n_e	8
No. of interior supports per panel length, n_p	1
Yield strength of deck, F_y (ksi)	33
Ultimate strength of deck, F_u (ksi)	45
Sidelap screw diameter (in.)	0.2111
Moment of inertia of fully effective panel per unit width, I_x (in^4)	0.1481

Fastener Strengths and Flexibilities	
Structural fastener strength, P_{nf} (kip)	1.51
Sidelap fastener strength, P_{ns} (kip)	0.728
Structural fastener flexibility, S_f (in/kip)	0.0072
Sidelap fastener flexibility, S_s (in/kip)	0.0173

Calculated Strength Equations Variables	
Corner fastener reduction factor, λ	0.820
Interior panel fastener contribution factor, β	7.18
Structural fastener distribution factor at panel ends, α_e^2	0.556
Structural fastener distribution factor at interior supports, α_p^2	0.556
Number of structural fasteners at panel ends per unit width, N	1.0
Fastener slip coefficient, C	3.99
Warping factor, D_n (in.)	82.9
Warping support factor, ρ	1.0

Predicted Shear Strength and Stiffness	
Interior panel shear strength, S_{ni} (kip/ft.)	1.03
Edge panel shear strength, S_{ne} (kip/ft.)	1.74
Panel shear strength limited by corner fastener, S_{nc} (kip/ft.)	0.883
Panel buckling shear strength, S_{nb} (kip/ft.)	5.03
Shear stiffness, G' (kip/in)	9.78

36/4 fastener pattern at interior and exterior supports

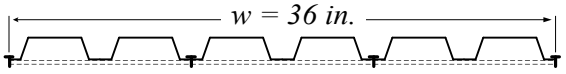

e (in.)	0.75
w_c (in.)	1.58
f (in.)	3.50
d (in.)	6.00
s (in.)	8.16
D_d (in.)	1.50

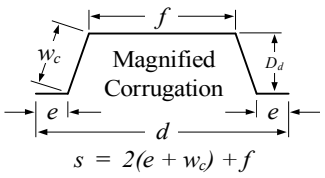

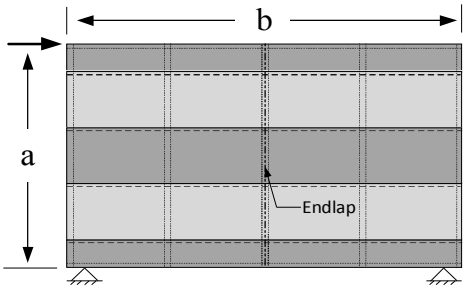

Loading Type: Cyclic

Load Rate: Fast-loading

a = 12'

b = 20'

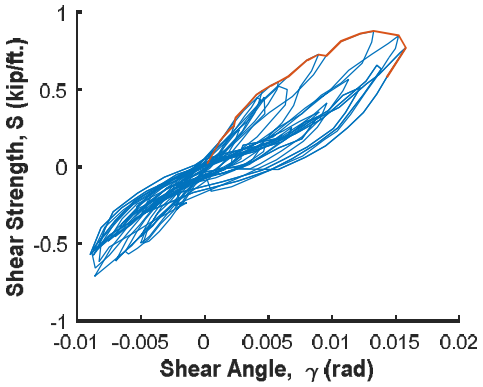

Eperimental Max Strength (kip/ft.)	0.884
Experimental Shear Stiffness (kip/in)	10.6
Ultimate Shear Angle, $\gamma_{80\%}$ (rad*1000)	15.2

Notes

Specimens 39 and 40 have identical test setups with varying loading protocols.

No mass added to represent seismic weight for inertial forces for a truly dynamic test.

Half width panels at edge of diaphragm to minimize influence of test frame on sidelap slip. Drawback is possible decrease in strength and stiffness.

Edge panels do not control predictions.

Endlap at 10 ft.

Unloading curve of last cycle partially traced for backbone in order to get shear angle at 80% strength degredation value.

Yang (2003) - Specimen 41

Input	
Structural Fastener Type	Arc Spot Weld
Sidelap Fastener Type	Button Punch
Deck thickness, t (in.)	0.0300
Panel Length, l (ft.)	10
Panel Span, l_v (ft.)	5
No. of sidelap connections per one edge of interior panel length, n_s	8
No. of edge structural connections not in line with int. or ext. supports, n_e	8
No. of interior supports per panel length, n_p	1
Yield strength of deck, F_y (ksi)	33
Ultimate strength of deck, F_u (ksi)	45
Arc spot weld diameter (in.)	0.625
Moment of inertia of fully effective panel per unit width, I_x (in^4)	0.1481

Fastener Strengths and Flexibilities	
Structural fastener strength, P_{nf} (kip)	1.77
Sidelap fastener strength, P_{ns} (kip)	0.216
Structural fastener flexibility, S_f (in/kip)	0.0066
Sidelap fastener flexibility, S_s (in/kip)	0.1732

Calculated Strength Equations Variables	
Corner fastener reduction factor, λ	0.820
Interior panel fastener contribution factor, β	4.31
Structural fastener distribution factor at panel ends, α_e^2	0.556
Structural fastener distribution factor at interior supports, α_p^2	0.556
Number of structural fasteners at panel ends per unit width, N	1.33
Fastener slip coefficient, C	8.49
Warping factor, D_n (in.)	82.9
Warping support factor, ρ	1.0

Predicted Shear Strength and Stiffness	
Interior panel shear strength, S_{ni} (kip/ft.)	0.698
Edge panel shear strength, S_{ne} (kip/ft.)	2.03
Panel shear strength limited by corner fastener, S_{nc} (kip/ft.)	0.725
Panel buckling shear strength, S_{nb} (kip/ft.)	5.03
Shear stiffness, G' (kip/in)	9.32

36/4 fastener pattern at interior and exterior supports

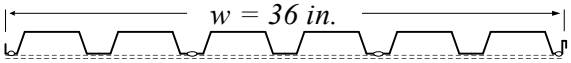

e (in.)	0.75
w_c (in.)	1.58
f (in.)	3.50
d (in.)	6.00
s (in.)	8.16
D_d (in.)	1.50

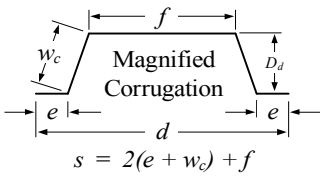

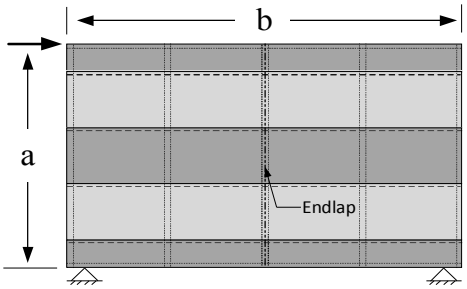

Loading Type: Monotonic
Load Rate: Static
a = 12'
b = 20'

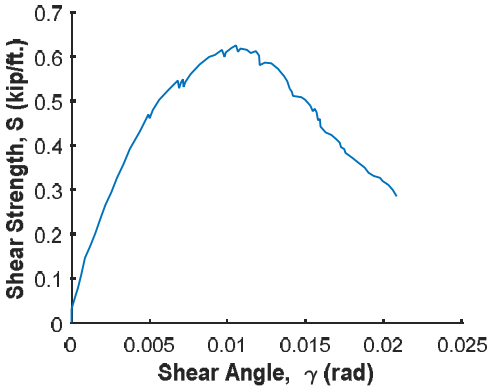

Eperimental Max Strength (kip/ft.)	0.627
Experimental Shear Stiffness (kip/in)	10.5
Ultimate Shear Angle, $\gamma_{80\%}$ (rad*1000)	8.06

Notes

Specimens 41 and 42 have identical test setups with varying loading protocols.
Half width panels at edge of diaphragm to minimize influence of test frame on sidelap slip. Drawback is possible decrease in strength and stiffness.
Structural welds on both sides of interlocking sidelap seam.
Edge panels do not control predictions.
Endlap at 10 ft.

Yang (2003) - Specimen 42

Input	
Structural Fastener Type	Arc Spot Weld
Sidelap Fastener Type	Button Punch
Deck thickness, t (in.)	0.0300
Panel Length, l (ft.)	10
Panel Span, l_v (ft.)	5
No. of sidelap connections per one edge of interior panel length, n_s	8
No. of edge structural connections not in line with int. or ext. supports, n_e	8
No. of interior supports per panel length, n_p	1
Yield strength of deck, F_y (ksi)	33
Ultimate strength of deck, F_u (ksi)	45
Arc spot weld diameter (in.)	0.625
Moment of inertia of fully effective panel per unit width, I_x (in^4)	0.1481

Fastener Strengths and Flexibilities	
Structural fastener strength, P_{nf} (kip)	1.77
Sidelap fastener strength, P_{ns} (kip)	0.216
Structural fastener flexibility, S_f (in/kip)	0.0066
Sidelap fastener flexibility, S_s (in/kip)	0.1732

Calculated Strength Equations Variables	
Corner fastener reduction factor, λ	0.820
Interior panel fastener contribution factor, β	4.31
Structural fastener distribution factor at panel ends, α_e^2	0.556
Structural fastener distribution factor at interior supports, α_p^2	0.556
Number of structural fasteners at panel ends per unit width, N	1.33
Fastener slip coefficient, C	8.49
Warping factor, D_n (in.)	82.9
Warping support factor, ρ	1.0

Predicted Shear Strength and Stiffness	
Interior panel shear strength, S_{ni} (kip/ft.)	0.698
Edge panel shear strength, S_{ne} (kip/ft.)	2.03
Panel shear strength limited by corner fastener, S_{nc} (kip/ft.)	0.725
Panel buckling shear strength, S_{nb} (kip/ft.)	5.03
Shear stiffness, G' (kip/in)	9.32

36/4 fastener pattern at interior and exterior supports

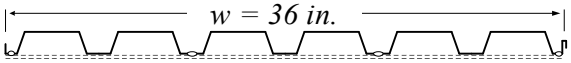

e (in.)	0.75
w_c (in.)	1.58
f (in.)	3.50
d (in.)	6.00
s (in.)	8.16
D_d (in.)	1.50

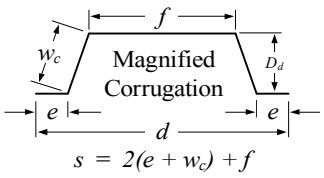

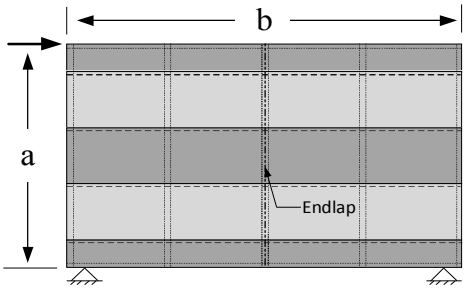

Loading Type: Cyclic

Load Rate: Fast-loading

a = 12'

b = 20'

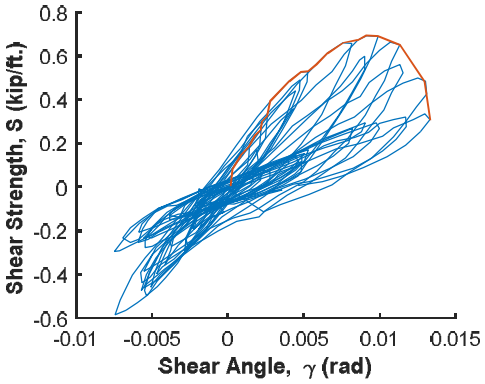

Eperimental Max Strength (kip/ft.)	0.696
Experimental Shear Stiffness (kip/in)	11.1
Ultimate Shear Angle, $\gamma_{80\%}$ (rad*1000)	12.2

Notes

Specimens 41 and 42 have identical test setups with varying loading protocols.

Half width panels at edge of diaphragm to minimize influence of test frame on sidelap slip. Drawback is possible decrease in strength and stiffness.

Structural welds on both sides of interlocking sidelap seam.

Edge panels do not control predictions.

Endlap at 10 ft.

No mass added to represent seismic weight for inertial forces for a truly dynamic test.

Yang (2003) - Specimen 43

Input	
Structural Fastener Type	X-EDNK22
Sidelap Fastener Type	Screw
Deck thickness, t (in.)	0.0300
Panel Length, l (ft.)	20
Panel Span, l_v (ft.)	5
No. of sidelap connections per one edge of interior panel length, n_s	16
No. of edge structural connections not in line with int. or ext. supports, n_e	16
No. of interior supports per panel length, n_p	3
Yield strength of deck, F_y (ksi)	33
Ultimate strength of deck, F_u (ksi)	45
Sidelap screw diameter (in.)	0.2111
Moment of inertia of fully effective panel per unit width, I_x (in^4)	0.1481

Fastener Strengths and Flexibilities	
Structural fastener strength, P_{nf} (kip)	1.51
Sidelap fastener strength, P_{ns} (kip)	0.728
Structural fastener flexibility, S_f (in/kip)	0.0072
Sidelap fastener flexibility, S_s (in/kip)	0.0173

Calculated Strength Equations Variables	
Corner fastener reduction factor, λ	0.820
Interior panel fastener contribution factor, β	13.3
Structural fastener distribution factor at panel ends, α_e^2	0.556
Structural fastener distribution factor at interior supports, α_p^2	0.556
Number of structural fasteners at panel ends per unit width, N	1.0
Fastener slip coefficient, C	4.26
Warping factor, D_n (in.)	41.5
Warping support factor, ρ	0.8

Predicted Shear Strength and Stiffness	
Interior panel shear strength, S_{ni} (kip/ft.)	0.975
Edge panel shear strength, S_{ne} (kip/ft.)	1.65
Panel shear strength limited by corner fastener, S_{nc} (kip/ft.)	0.836
Panel buckling shear strength, S_{nb} (kip/ft.)	5.03
Shear stiffness, G' (kip/in)	21.6

36/4 fastener pattern at interior and exterior supports

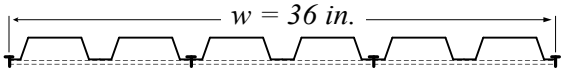

e (in.)	0.75
w_c (in.)	1.58
f (in.)	3.50
d (in.)	6.00
s (in.)	8.16
D_d (in.)	1.50

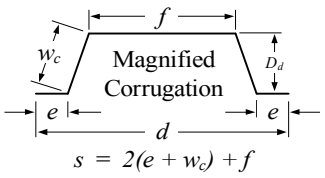

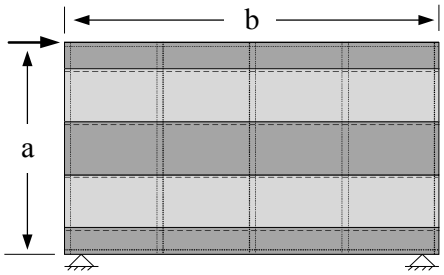

Loading Type: Monotonic
Load Rate: Static
a = 12'
b = 20'

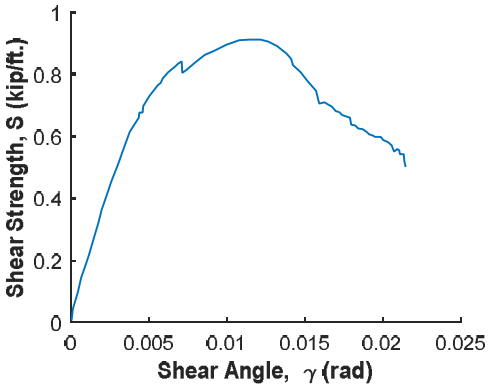

Eperimental Max Strength (kip/ft.)	0.915
Experimental Shear Stiffness (kip/in)	15.4
Ultimate Shear Angle, $\gamma_{80\%}$ (rad*1000)	15.8

Notes

Specimens 43 and 44 have identical test setups with varying loading protocols.
Half width panels at edge of diaphragm to minimize influence of test frame on sidelap slip. Drawback is possible decrease in strength and stiffness.
Edge panels do not control predictions.

Yang (2003) - Specimen 44

Input	
Structural Fastener Type	X-EDNK22
Sidelap Fastener Type	Screw
Deck thickness, t (in.)	0.0300
Panel Length, l (ft.)	20
Panel Span, l_v (ft.)	5
No. of sidelap connections per one edge of interior panel length, n_s	16
No. of edge structural connections not in line with int. or ext. supports, n_e	16
No. of interior supports per panel length, n_p	3
Yield strength of deck, F_y (ksi)	33
Ultimate strength of deck, F_u (ksi)	45
Sidelap screw diameter (in.)	0.2111
Moment of inertia of fully effective panel per unit width, I_x (in^4)	0.1481

Fastener Strengths and Flexibilities	
Structural fastener strength, P_{nf} (kip)	1.51
Sidelap fastener strength, P_{ns} (kip)	0.728
Structural fastener flexibility, S_f (in/kip)	0.0072
Sidelap fastener flexibility, S_s (in/kip)	0.0173

Calculated Strength Equations Variables	
Corner fastener reduction factor, λ	0.820
Interior panel fastener contribution factor, β	13.3
Structural fastener distribution factor at panel ends, α_e^2	0.556
Structural fastener distribution factor at interior supports, α_p^2	0.556
Number of structural fasteners at panel ends per unit width, N	1.0
Fastener slip coefficient, C	4.26
Warping factor, D_n (in.)	41.5
Warping support factor, ρ	0.8

Predicted Shear Strength and Stiffness	
Interior panel shear strength, S_{ni} (kip/ft.)	0.975
Edge panel shear strength, S_{ne} (kip/ft.)	1.65
Panel shear strength limited by corner fastener, S_{nc} (kip/ft.)	0.836
Panel buckling shear strength, S_{nb} (kip/ft.)	5.03
Shear stiffness, G' (kip/in)	21.6

36/4 fastener pattern at interior and exterior supports

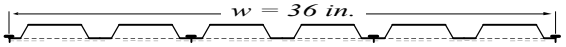

e (in.)	0.75
w_c (in.)	1.58
f (in.)	3.50
d (in.)	6.00
s (in.)	8.16
D_d (in.)	1.50

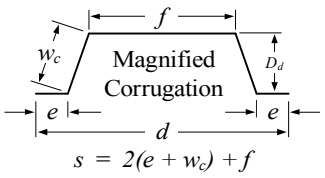

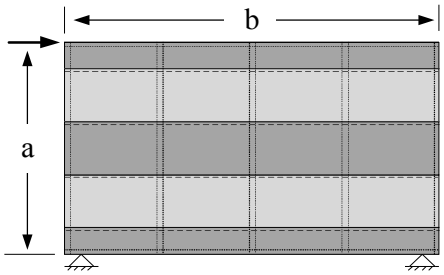

Loading Type: Cyclic + Monotonic
Load Rate: Static
a = 12'
b = 20'

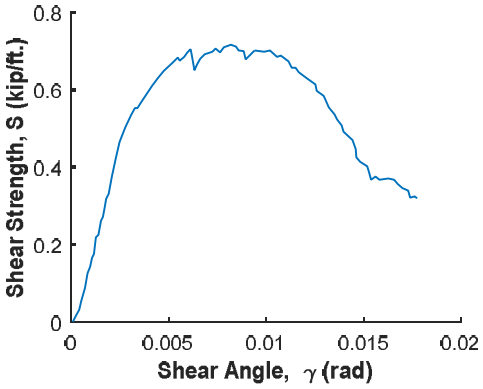

Eperimental Max Strength (kip/ft.)	0.718
Experimental Shear Stiffness (kip/in)	14.9
Ultimate Shear Angle, $\gamma_{80\%}$ (rad*1000)	13.1

Notes

Specimens 43 and 44 have identical test setups with varying loading protocols.
Half width panels at edge of diaphragm to minimize influence of test frame on sidelap slip. Drawback is possible decrease in strength and stiffness.
Edge panels do not control predictions.
200 cycles mostly in linear range (60% Smax) before pushed monotonically to failure.

Yang (2003) - Specimen 47

Input	
Structural Fastener Type	Arc Spot Weld
Sidelap Fastener Type	Button Punch
Deck thickness, t (in.)	0.0300
Panel Length, l (ft.)	20
Panel Span, l_v (ft.)	5
No. of sidelap connections per one edge of interior panel length, n_s	16
No. of edge structural connections not in line with int. or ext. supports, n_e	16
No. of interior supports per panel length, n_p	3
Yield strength of deck, F_y (ksi)	33
Ultimate strength of deck, F_u (ksi)	45
Arc spot weld diameter (in.)	0.625
Moment of inertia of fully effective panel per unit width, I_x (in^4)	0.7369

Fastener Strengths and Flexibilities	
Structural fastener strength, P_{nf} (kip)	1.77
Sidelap fastener strength, P_{ns} (kip)	0.216
Structural fastener flexibility, S_f (in/kip)	0.0066
Sidelap fastener flexibility, S_s (in/kip)	0.1732

Calculated Strength Equations Variables	
Corner fastener reduction factor, λ	0.700
Interior panel fastener contribution factor, β	6.96
Structural fastener distribution factor at panel ends, α_e^2	0.500
Structural fastener distribution factor at interior supports, α_p^2	0.500
Number of structural fasteners at panel ends per unit width, N	1.5
Fastener slip coefficient, C	18.9
Warping factor, D_n (in.)	127
Warping support factor, ρ	0.8

Predicted Shear Strength and Stiffness	
Interior panel shear strength, S_{ni} (kip/ft.)	0.562
Edge panel shear strength, S_{ne} (kip/ft.)	1.86
Panel shear strength limited by corner fastener, S_{nc} (kip/ft.)	0.599
Panel buckling shear strength, S_{nb} (kip/ft.)	15.5
Shear stiffness, G' (kip/in)	7.08

24/3 fastener pattern at interior and exterior supports

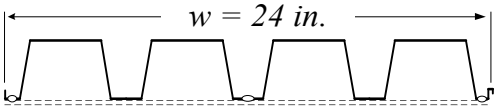

e (in.)	0.75
w_c (in.)	3.04
f (in.)	3.50
d (in.)	6.00
s (in.)	11.1
D_d (in.)	3.00

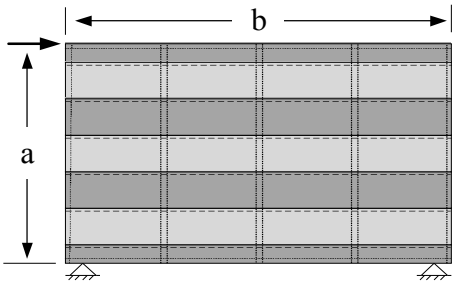

Loading Type: Monotonic
Load Rate: Static
a = 12'
b = 20'

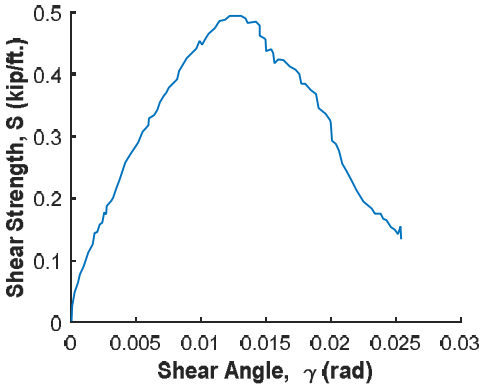

Eperimental Max Strength (kip/ft.)	0.496
Experimental Shear Stiffness (kip/in)	5.24
Ultimate Shear Angle, $\gamma_{80\%}$ (rad*1000)	17.6

Notes

Specimens 47 and 48 have identical test setups with varying loading protocols.
Half width panels at edge of diaphragm to minimize influence of test frame on sidelap slip. Drawback is possible decrease in strength and stiffness.
Structural welds on both sides of interlocking sidelap seam.
Edge panels do not control predictions.

Yang (2003) - Specimen 48

Input	
Structural Fastener Type	Arc Spot Weld
Sidelap Fastener Type	Button Punch
Deck thickness, t (in.)	0.0300
Panel Length, l (ft.)	20
Panel Span, l_v (ft.)	5
No. of sidelap connections per one edge of interior panel length, n_s	16
No. of edge structural connections not in line with int. or ext. supports, n_e	16
No. of interior supports per panel length, n_p	3
Yield strength of deck, F_y (ksi)	33
Ultimate strength of deck, F_u (ksi)	45
Arc spot weld diameter (in.)	0.625
Moment of inertia of fully effective panel per unit width, I_x (in^4)	0.7369

Fastener Strengths and Flexibilities	
Structural fastener strength, P_{nf} (kip)	1.77
Sidelap fastener strength, P_{ns} (kip)	0.216
Structural fastener flexibility, S_f (in/kip)	0.0066
Sidelap fastener flexibility, S_s (in/kip)	0.1732

Calculated Strength Equations Variables	
Corner fastener reduction factor, λ	0.700
Interior panel fastener contribution factor, β	6.96
Structural fastener distribution factor at panel ends, α_e^2	0.500
Structural fastener distribution factor at interior supports, α_p^2	0.500
Number of structural fasteners at panel ends per unit width, N	1.5
Fastener slip coefficient, C	18.9
Warping factor, D_n (in.)	127
Warping support factor, ρ	0.8

Predicted Shear Strength and Stiffness	
Interior panel shear strength, S_{ni} (kip/ft.)	0.562
Edge panel shear strength, S_{ne} (kip/ft.)	1.86
Panel shear strength limited by corner fastener, S_{nc} (kip/ft.)	0.599
Panel buckling shear strength, S_{nb} (kip/ft.)	15.5
Shear stiffness, G' (kip/in)	7.08

24/3 fastener pattern at interior and exterior supports

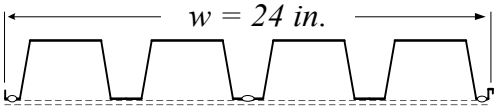

e (in.)	0.75
w_c (in.)	3.04
f (in.)	3.50
d (in.)	6.00
s (in.)	11.1
D_d (in.)	3.00

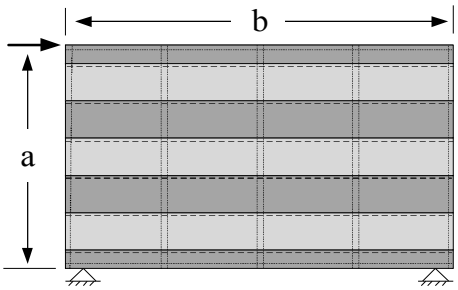

Loading Type: Cyclic
Load Rate: Fast-loading
a = 12'
b = 20'

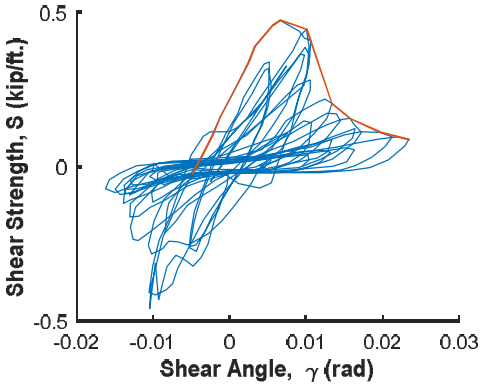

Eperimental Max Strength (kip/ft.)	0.477
Experimental Shear Stiffness (kip/in)	4.20
Ultimate Shear Angle, $\gamma_{80\%}$ (rad*1000)	10.9

Notes

Specimens 47 and 48 have identical test setups with varying loading protocols.
Half width panels at edge of diaphragm to minimize influence of test frame on sidelap slip. Drawback is possible decrease in strength and stiffness.
Structural welds on both sides of interlocking sidelap seam.
Edge panels do not control predictions.
No mass added to represent seismic weight for inertial forces for a truly dynamic test.

Yang (2003) - Specimen 49

Input	
Structural Fastener Type	Arc Spot Weld
Sidelap Fastener Type	Button Punch
Deck thickness, t (in.)	0.0360
Panel Length, l (ft.)	20
Panel Span, l_v (ft.)	5
No. of sidelap connections per one edge of interior panel length, n_s	16
No. of edge structural connections not in line with int. or ext. supports, n_e	16
No. of interior supports per panel length, n_p	3
Yield strength of deck, F_y (ksi)	33
Ultimate strength of deck, F_u (ksi)	45
Arc spot weld diameter (in.)	0.625
Moment of inertia of fully effective panel per unit width, I_x (in^4)	0.7369

Fastener Strengths and Flexibilities	
Structural fastener strength, P_{nf} (kip)	2.10
Sidelap fastener strength, P_{ns} (kip)	0.311
Structural fastener flexibility, S_f (in/kip)	0.0061
Sidelap fastener flexibility, S_s (in/kip)	0.1581

Calculated Strength Equations Variables	
Corner fastener reduction factor, λ	0.700
Interior panel fastener contribution factor, β	7.37
Structural fastener distribution factor at panel ends, α_e^2	0.500
Structural fastener distribution factor at interior supports, α_p^2	0.500
Number of structural fasteners at panel ends per unit width, N	1.5
Fastener slip coefficient, C	20.7
Warping factor, D_n (in.)	96.4
Warping support factor, ρ	0.8

Predicted Shear Strength and Stiffness	
Interior panel shear strength, S_{ni} (kip/ft.)	0.711
Edge panel shear strength, S_{ne} (kip/ft.)	2.20
Panel shear strength limited by corner fastener, S_{nc} (kip/ft.)	0.751
Panel buckling shear strength, S_{nb} (kip/ft.)	21.1
Shear stiffness, G' (kip/in)	10.40

24/3 fastener pattern at interior and exterior supports

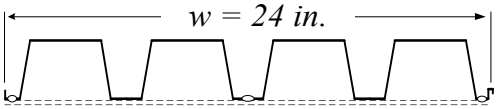

e (in.)	0.75
w_c (in.)	3.04
f (in.)	3.50
d (in.)	6.00
s (in.)	11.1
D_d (in.)	3.00

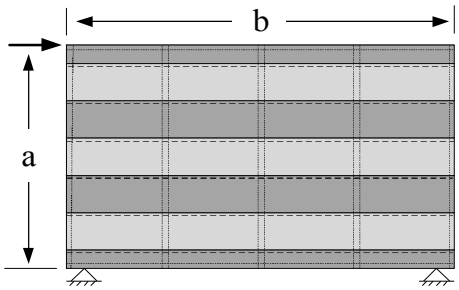

Loading Type: Monotonic
Load Rate: Static
a = 12'
b = 20'

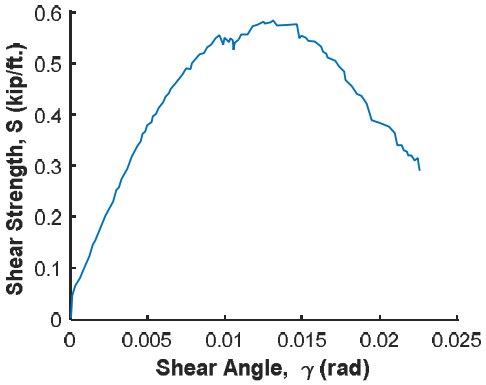

Eperimental Max Strength (kip/ft.)	0.585
Experimental Shear Stiffness (kip/in)	7.07
Ultimate Shear Angle, $\gamma_{80\%}$ (rad*1000)	17.8

Notes

Specimens 47 and 49 have identical test setups with varying deck thicknesses.
Half width panels at edge of diaphragm to minimize influence of test frame on sidelap slip. Drawback is possible decrease in strength and stiffness.
Structural welds on both sides of interlocking sidelap seam.
Edge panels do not control predictions.

Bagwell (2007) - Specimen 7

Input	
Structural Fastener Type	X-ENP19 L15
Sidelap Fastener Type	Screw
Deck thickness, t (in.)	0.0358
Panel Length, l (ft.)	24
Panel Span, l_v (ft.)	24
No. of sidelap connections per one edge of interior panel length, n_s	7
No. of edge structural connections not in line with int. or ext. supports, n_e	23
No. of interior supports per panel length, n_p	0
Yield strength of deck, F_y (ksi)	80
Ultimate strength of deck, F_u (ksi)	82
Sidelap screw diameter (in.)	0.2111

Fastener Strengths and Flexibilities	
Structural fastener strength, P_{nf} (kip)	1.933
Sidelap fastener strength, P_{ns} (kip)	0.869
Structural fastener flexibility, S_f (in/kip)	0.0066
Sidelap fastener flexibility, S_s (in/kip)	0.0159

Calculated Strength Equations Variables	
Corner fastener reduction factor, λ	0.700
Interior panel fastener contribution factor, β	5.15
Structural fastener distribution factor at panel ends, α_e^2	0.500
Structural fastener distribution factor at interior supports, α_p^2	0.500
Number of structural fasteners at panel ends per unit width, N	1.0
Fastener slip coefficient, C	21.40
Warping factor, D_n (in.)	79.8
Warping support factor, ρ	1.0

Predicted Shear Strength and Stiffness	
Interior panel shear strength, S_{ni} (kip/ft.)	0.366
Edge panel shear strength, S_{ne} (kip/ft.)	2.01
Panel shear strength limited by corner fastener, S_{nc} (kip/ft.)	0.405
Panel buckling shear strength, S_{nb} (kip/ft.)	Not Applicable
Shear stiffness, G' (kip/in)	9.99

24/3 fastener pattern at exterior supports

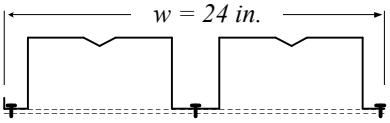

e (in.)	1.5
w_c (in.)	4.5
f (in.)	9.0
d (in.)	12.0
s (in.)	21.0
D_d (in.)	4.50

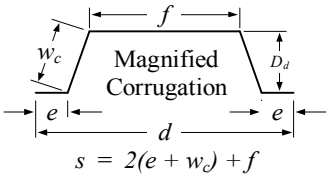

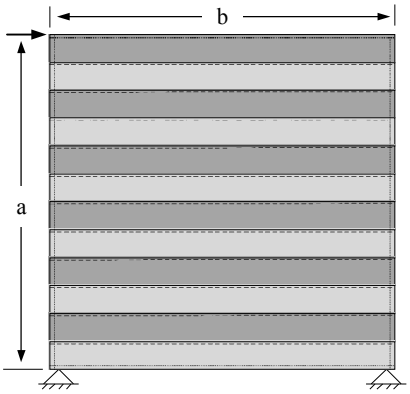

Loading Type: Monotonic

Load Rate: Static

a = 24'

b = 24'

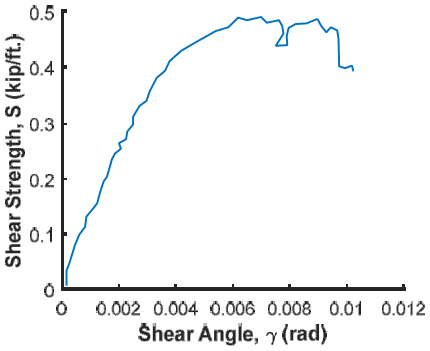

Eperimental Max Strength (kip/ft.)	0.492
Experimental Shear Stiffness (kip/in)	12.0
Ultimate Shear Angle, $\gamma_{80\%}$ (rad*1000)	10.2

Notes

Deck manufacturer information not available. $W_c = D_d$ assumed

Measured F_y = 108 ksi. Nominal F_y = 60 ksi assumed

Measured F_u = 110 ksi. Nominal F_u = 75 ksi assumed

Both diagonal and corner displacements measured. To stay consistent with this work, corner displacements are used in analysis

Specimens 7 and 8 had identical set ups with varying deck thickness.

Bagwell (2007) - Specimen 8

Input	
Structural Fastener Type	X-ENP19 L15
Sidelap Fastener Type	Screw
Deck thickness, t (in.)	0.0598
Panel Length, l (ft.)	24
Panel Span, l_v (ft.)	24
No. of sidelap connections per one edge of interior panel length, n_s	7
No. of edge structural connections not in line with int. or ext. supports, n_e	23
No. of interior supports per panel length, n_p	0
Yield strength of deck, F_y (ksi)	80
Ultimate strength of deck, F_u (ksi)	82
Sidelap screw diameter (in.)	0.2111

Fastener Strengths and Flexibilities	
Structural fastener strength, P_{nf} (kip)	3.15
Sidelap fastener strength, P_{ns} (kip)	1.45
Structural fastener flexibility, S_f (in/kip)	0.0051
Sidelap fastener flexibility, S_s (in/kip)	0.0123

Calculated Strength Equations Variables	
Corner fastener reduction factor, λ	0.700
Interior panel fastener contribution factor, β	5.23
Structural fastener distribution factor at panel ends, α_e^2	0.500
Structural fastener distribution factor at interior supports, α_p^2	0.500
Number of structural fasteners at panel ends per unit width, N	1.0
Fastener slip coefficient, C	27.6
Warping factor, D_n (in.)	37.0
Warping support factor, ρ	1.0

Predicted Shear Strength and Stiffness	
Interior panel shear strength, S_{ni} (kip/ft.)	0.607
Edge panel shear strength, S_{ne} (kip/ft.)	3.28
Panel shear strength limited by corner fastener, S_{nc} (kip/ft.)	0.670
Panel buckling shear strength, S_{nb} (kip/ft.)	Not Applicable
Shear stiffness, G' (kip/in)	25.5

24/3 fastener pattern at exterior supports

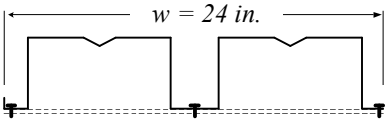

e (in.)	1.5
w_c (in.)	4.5
f (in.)	9.0
d (in.)	12.0
s (in.)	21.0
D_d (in.)	4.50

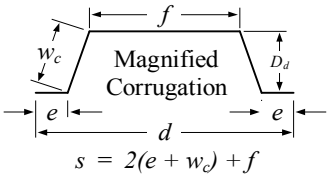

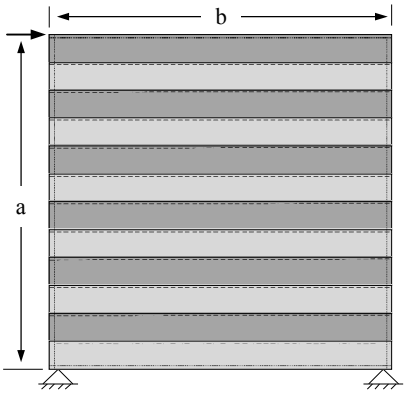

Loading Type: Monotonic

Load Rate: Static

a = 24'

b = 24'

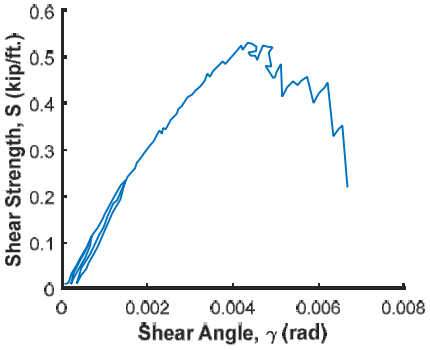

Eperimental Max Strength (kip/ft.)	0.533
Experimental Shear Stiffness (kip/in)	13.5
Ultimate Shear Angle, $\gamma_{80\%}$ (rad*1000)	5.14

Notes

Deck manufacturer information not available. $W_c = D_d$ assumed

Measured F_y = 108 ksi. Nominal F_y = 60 ksi assumed

Measured F_u = 110 ksi. Nominal F_u = 75 ksi assumed

Both diagonal and corner displacements measured. To stay consistent with this work, corner displacements are used in analysis

Specimens 7 and 8 had identical set ups with varying deck thickness.

Bagwell (2007) - Specimen 9

Input	
Structural Fastener Type	X-ENP19 L15
Sidelap Fastener Type	Screw
Deck thickness, t (in.)	0.0474
Panel Length, l (ft.)	24
Panel Span, l_v (ft.)	24
No. of sidelap connections per one edge of interior panel length, n_s	7
No. of edge structural connections not in line with int. or ext. supports, n_e	23
No. of interior supports per panel length, n_p	0
Yield strength of deck, F_y (ksi)	33
Ultimate strength of deck, F_u (ksi)	45
Sidelap screw diameter (in.)	0.2111

Fastener Strengths and Flexibilities	
Structural fastener strength, P_{nf} (kip)	2.53
Sidelap fastener strength, P_{ns} (kip)	1.15
Structural fastener flexibility, S_f (in/kip)	0.0057
Sidelap fastener flexibility, S_s (in/kip)	0.0138

Calculated Strength Equations Variables	
Corner fastener reduction factor, λ	0.700
Interior panel fastener contribution factor, β	5.19
Structural fastener distribution factor at panel ends, α_e^2	0.500
Structural fastener distribution factor at interior supports, α_p^2	0.500
Number of structural fasteners at panel ends per unit width, N	1.0
Fastener slip coefficient, C	49.20
Warping factor, D_n (in.)	52.4
Warping support factor, ρ	1.0

Predicted Shear Strength and Stiffness	
Interior panel shear strength, S_{ni} (kip/ft.)	0.483
Edge panel shear strength, S_{ne} (kip/ft.)	2.63
Panel shear strength limited by corner fastener, S_{nc} (kip/ft.)	0.534
Panel buckling shear strength, S_{nb} (kip/ft.)	Not Applicable
Shear stiffness, G' (kip/in)	7.58

12/2 fastener pattern at exterior supports

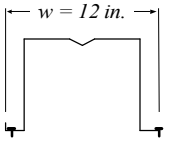

e (in.)	1.5
w_c (in.)	7.5
f (in.)	9.0
d (in.)	12.0
s (in.)	27.0
D_d (in.)	7.50

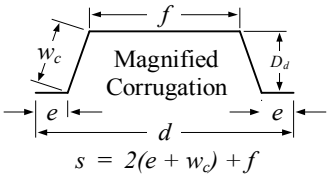

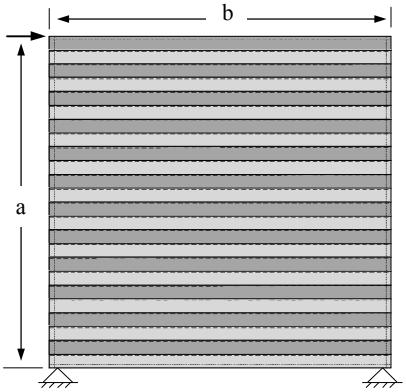

Loading Type: Monotonic

Load Rate: Static

a = 24'

b = 24'

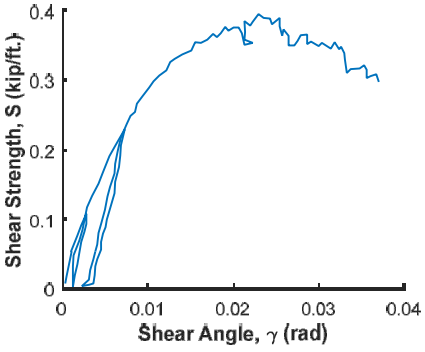

Eperimental Max Strength (kip/ft.)	0.396
Experimental Shear Stiffness (kip/in)	3.05
Ultimate Shear Angle, $\gamma_{80\%}$ (rad*1000)	33.2

Notes

Deck manufacturer information not available. $W_c = D_d$ assumed

Both diagonal and corner displacements measured. To stay consistent with this work, corner displacements are used in analysis

Bagwell (2007) - Specimen 12

Input	
Structural Fastener Type	Arc Spot Weld
Sidelap Fastener Type	Button Punch
Deck thickness, t (in.)	0.0474
Panel Length, l (ft.)	24
Panel Span, l_v (ft.)	24
No. of sidelap connections per one edge of interior panel length, n_s	23
No. of edge structural connections not in line with int. or ext. supports, n_e	23
No. of interior supports per panel length, n_p	0
Yield strength of deck, F_y (ksi)	80
Ultimate strength of deck, F_u (ksi)	82
Weld diameter (in.)	0.75

Fastener Strengths and Flexibilities	
Structural fastener strength, P_{nf} (kip)	5.50
Sidelap fastener strength, P_{ns} (kip)	1.15
Structural fastener flexibility, S_f (in/kip)	0.0053
Sidelap fastener flexibility, S_s (in/kip)	0.0138

Calculated Strength Equations Variables	
Corner fastener reduction factor, λ	0.700
Interior panel fastener contribution factor, β	6.82
Structural fastener distribution factor at panel ends, α_e^2	0.500
Structural fastener distribution factor at interior supports, α_p^2	0.500
Number of structural fasteners at panel ends per unit width, N	1.0
Fastener slip coefficient, C	9.03
Warping factor, D_n (in.)	52.4
Warping support factor, ρ	1.0

Predicted Shear Strength and Stiffness	
Interior panel shear strength, S_{ni} (kip/ft.)	1.42
Edge panel shear strength, S_{ne} (kip/ft.)	1.50
Panel shear strength limited by corner fastener, S_{nc} (kip/ft.)	5.720
Panel buckling shear strength, S_{nb} (kip/ft.)	Not Applicable
Shear stiffness, G' (kip/in)	21.2

24/3 fastener pattern at exterior supports

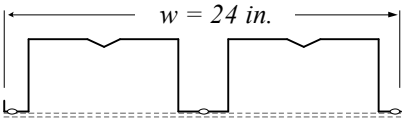

e (in.)	1.5
w_c (in.)	4.5
f (in.)	9.0
d (in.)	12.0
s (in.)	21.0
D_d (in.)	4.50

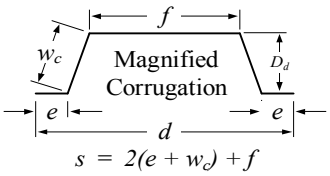

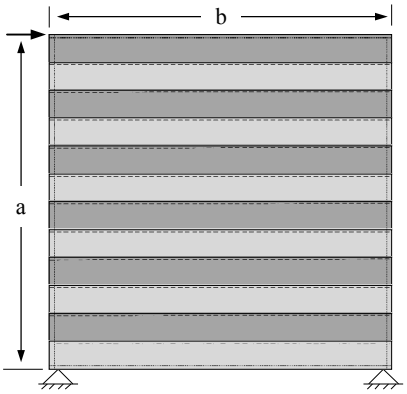

Loading Type: Monotonic

Load Rate: Static

a = 24'

b = 24'

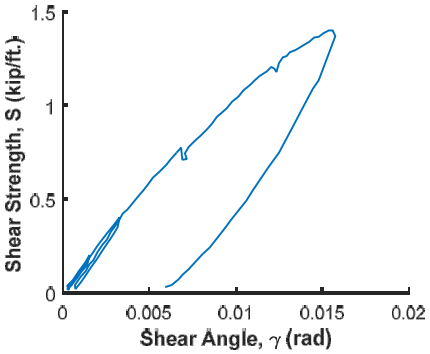

Eperimental Max Strength (kip/ft.)	1.41
Experimental Shear Stiffness (kip/in)	10.3
Ultimate Shear Angle, $\gamma_{80\%}$ (rad*1000)	14.7

Notes

Deck manufacturer information not available. $W_c = D_d$ assumed

Measured F_y = 108 ksi. Nominal F_y = 60 ksi assumed

Measured F_u = 110 ksi. Nominal F_u = 75 ksi assumed

Both diagonal and corner displacements measured. To stay consistent with this work, corner displacements are used in analysis

Actual sidelap strength for thicker gauge panels using button punches may not reach DDM04 predicted shear strength.

Beck (2008) - Specimen 63

Input	
Structural Fastener Type	X-EDNK22
Sidelap Fastener Type	Screw
Deck thickness, t (in.)	0.0295
Panel Length, l (ft.)	15
Panel Span, l_v (ft.)	7.5
No. of sidelap connections per one edge of interior panel length, n_s	28
No. of edge structural connections not in line with int. or ext. supports, n_e	28
No. of interior supports per panel length, n_p	1
Yield strength of deck, F_y (ksi)	33
Ultimate strength of deck, F_u (ksi)	45
Sidelap screw diameter (in.)	0.2111
Moment of inertia of fully effective panel per unit width, I_x (in^4)	0.169

Fastener Strengths and Flexibilities	
Structural fastener strength, P_{nf} (kip)	1.49
Sidelap fastener strength, P_{ns} (kip)	0.716
Structural fastener flexibility, S_f (in/kip)	0.0073
Sidelap fastener flexibility, S_s (in/kip)	0.0175

Calculated Strength Equations Variables	
Corner fastener reduction factor, λ	0.727
Interior panel fastener contribution factor, β	18.1
Structural fastener distribution factor at panel ends, α_e^2	0.778
Structural fastener distribution factor at interior supports, α_p^2	0.778
Number of structural fasteners at panel ends per unit width, N	2.0
Fastener slip coefficient, C	2.16
Warping factor, D_n (in.)	6.87
Warping support factor, ρ	1.0

Predicted Shear Strength and Stiffness	
Interior panel shear strength, S_{ni} (kip/ft.)	1.75
Edge panel shear strength, S_{ne} (kip/ft.)	3.37
Panel shear strength limited by corner fastener, S_{nc} (kip/ft.)	1.54
Panel buckling shear strength, S_{nb} (kip/ft.)	2.44
Shear stiffness, G' (kip/in)	68.8

36/7 fastener pattern at interior and exterior supports

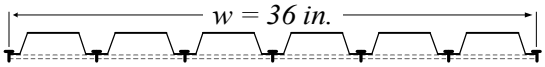

e (in.)	0.75
w_c (in.)	1.58
f (in.)	3.50
d (in.)	6.00
s (in.)	8.16
D_d (in.)	1.50

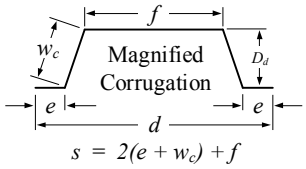

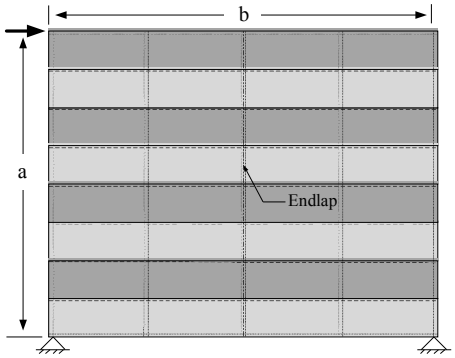

Loading Type: Monotonic

Load Rate: Static

a = 24'

b = 30'

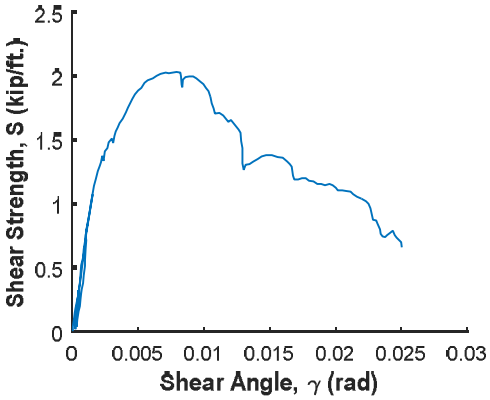

Eperimental Max Strength (kip/ft.)	2.04
Experimental Shear Stiffness (kip/in)	60.7
Ultimate Shear Angle, $\gamma_{80\%}$ (rad*1000)	12.3

Notes

Monotonic reference for specimens 7 and 8

Beck (2008) - Specimen 64

Input	
Structural Fastener Type	X-EDNK22
Sidelap Fastener Type	Screw
Deck thickness, t (in.)	0.0358
Panel Length, l (ft.)	15
Panel Span, l_v (ft.)	7.5
No. of sidelap connections per one edge of interior panel length, n_s	28
No. of edge structural connections not in line with int. or ext. supports, n_e	28
No. of interior supports per panel length, n_p	1
Yield strength of deck, F_y (ksi)	33
Ultimate strength of deck, F_u (ksi)	45
Sidelap screw diameter (in.)	0.2111
Moment of inertia of fully effective panel per unit width, I_x (in^4)	0.212

Fastener Strengths and Flexibilities	
Structural fastener strength, P_{nf} (kip)	1.80
Sidelap fastener strength, P_{ns} (kip)	0.869
Structural fastener flexibility, S_f (in/kip)	0.0066
Sidelap fastener flexibility, S_s (in/kip)	0.0159

Calculated Strength Equations Variables	
Corner fastener reduction factor, λ	0.752
Interior panel fastener contribution factor, β	18.2
Structural fastener distribution factor at panel ends, α_e^2	0.778
Structural fastener distribution factor at interior supports, α_p^2	0.778
Number of structural fasteners at panel ends per unit width, N	2.0
Fastener slip coefficient, C	2.34
Warping factor, D_n (in.)	5.14
Warping support factor, ρ	1.0

Predicted Shear Strength and Stiffness	
Interior panel shear strength, S_{ni} (kip/ft.)	2.12
Edge panel shear strength, S_{ne} (kip/ft.)	4.07
Panel shear strength limited by corner fastener, S_{nc} (kip/ft.)	1.86
Panel buckling shear strength, S_{nb} (kip/ft.)	3.34
Shear stiffness, G' (kip/in)	95.6

36/7 fastener pattern at interior and exterior supports

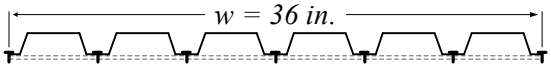

e (in.)	0.75
w_c (in.)	1.58
f (in.)	3.50
d (in.)	6.00
s (in.)	8.16
D_d (in.)	1.50

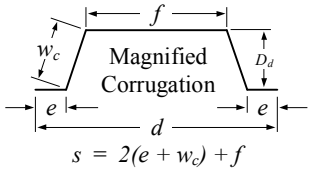

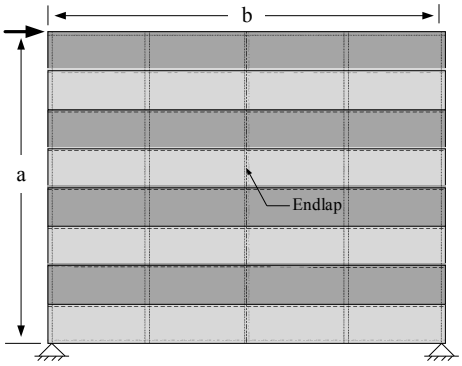

Loading Type: Monotonic

Load Rate: Static

a = 24'

b = 30'

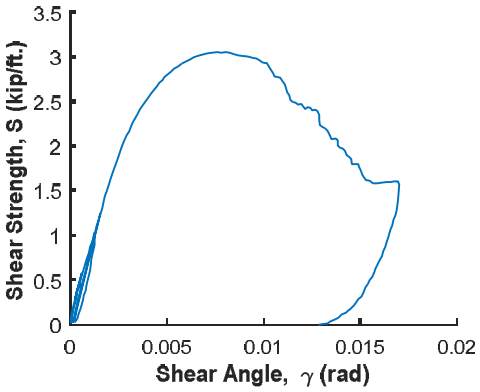

Eperimental Max Strength (kip/ft.)	3.06
Experimental Shear Stiffness (kip/in)	67.8
Ultimate Shear Angle, $\gamma_{80\%}$ (rad*1000)	12.1

Notes

Monotonic reference for specimens 4 and 5

Beck (2008) - Specimen 65

Input	
Structural Fastener Type	X-EDNK22
Sidelap Fastener Type	Screw
Deck thickness, t (in.)	0.0474
Panel Length, l (ft.)	15
Panel Span, l_v (ft.)	7.5
No. of sidelap connections per one edge of interior panel length, n_s	28
No. of edge structural connections not in line with int. or ext. supports, n_e	28
No. of interior supports per panel length, n_p	1
Yield strength of deck, F_y (ksi)	33
Ultimate strength of deck, F_u (ksi)	45
Sidelap screw diameter (in.)	0.2111
Moment of inertia of fully effective panel per unit width, I_x (in^4)	0.292

Fastener Strengths and Flexibilities	
Structural fastener strength, P_{nf} (kip)	2.35
Sidelap fastener strength, P_{ns} (kip)	1.15
Structural fastener flexibility, S_f (in/kip)	0.0057
Sidelap fastener flexibility, S_s (in/kip)	0.0138

Calculated Strength Equations Variables	
Corner fastener reduction factor, λ	0.785
Interior panel fastener contribution factor, β	18.4
Structural fastener distribution factor at panel ends, α_e^2	0.778
Structural fastener distribution factor at interior supports, α_p^2	0.778
Number of structural fasteners at panel ends per unit width, N	2.0
Fastener slip coefficient, C	2.74
Warping factor, D_n (in.)	3.37
Warping support factor, ρ	1.0

Predicted Shear Strength and Stiffness	
Interior panel shear strength, S_{ni} (kip/ft.)	2.81
Edge panel shear strength, S_{ne} (kip/ft.)	5.32
Panel shear strength limited by corner fastener, S_{nc} (kip/ft.)	2.45
Panel buckling shear strength, S_{nb} (kip/ft.)	5.24
Shear stiffness, G' (kip/in)	145.0

36/7 fastener pattern at interior and exterior supports

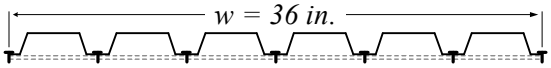

e (in.)	0.75
w_c (in.)	1.58
f (in.)	3.50
d (in.)	6.00
s (in.)	8.16
D_d (in.)	1.50

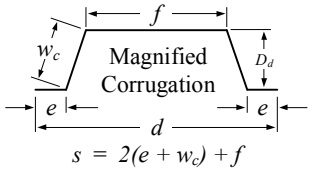

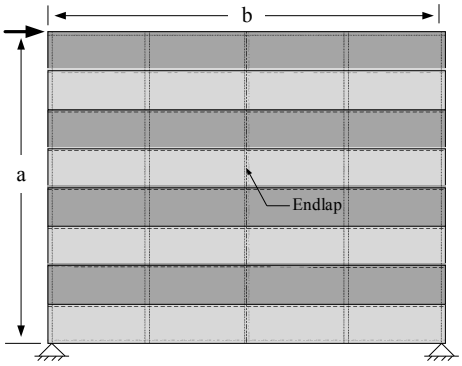

Loading Type: Monotonic

Load Rate: Static

a = 24'

b = 30'

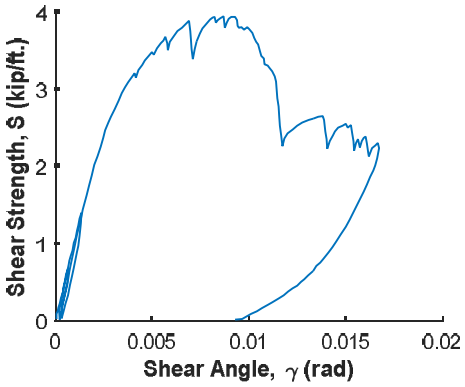

Eperimental Max Strength (kip/ft.)	3.95
Experimental Shear Stiffness (kip/in)	85.2
Ultimate Shear Angle, $\gamma_{80\%}$ (rad*1000)	11.3

Notes

Monotonic reference for specimens 3 and 6

Beck (2008) - Specimen 3

Input	
Structural Fastener Type	X-EDNK22
Sidelap Fastener Type	Screw
Deck thickness, t (in.)	0.0474
Panel Length, l (ft.)	15
Panel Span, l_v (ft.)	5.0
No. of sidelap connections per one edge of interior panel length, n_s	27
No. of edge structural connections not in line with int. or ext. supports, n_e	27
No. of interior supports per panel length, n_p	2
Yield strength of deck, F_y (ksi)	33
Ultimate strength of deck, F_u (ksi)	45
Sidelap screw diameter (in.)	0.2111
Moment of inertia of fully effective panel per unit width, I_x (in^4)	0.292

Fastener Strengths and Flexibilities	
Structural fastener strength, P_{nf} (kip)	2.35
Sidelap fastener strength, P_{ns} (kip)	1.15
Structural fastener flexibility, S_f (in/kip)	0.0057
Sidelap fastener flexibility, S_s (in/kip)	0.0138

Calculated Strength Equations Variables	
Corner fastener reduction factor, λ	0.785
Interior panel fastener contribution factor, β	18.4
Structural fastener distribution factor at panel ends, α_e^2	1.23
Structural fastener distribution factor at interior supports, α_p^2	1.23
Number of structural fasteners at panel ends per unit width, N	2.33
Fastener slip coefficient, C	2.74
Warping factor, D_n (in.)	3.37
Warping support factor, ρ	1.0

Predicted Shear Strength and Stiffness	
Interior panel shear strength, S_{ni} (kip/ft.)	3.58
Edge panel shear strength, S_{ne} (kip/ft.)	6.11
Panel shear strength limited by corner fastener, S_{nc} (kip/ft.)	3.05
Panel buckling shear strength, S_{nb} (kip/ft.)	11.8
Shear stiffness, G' (kip/in)	157

36/9 fastener pattern at interior and exterior supports

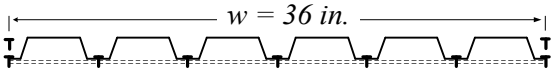

e (in.)	0.75
w_c (in.)	1.58
f (in.)	3.50
d (in.)	6.00
s (in.)	8.16
D_d (in.)	1.50

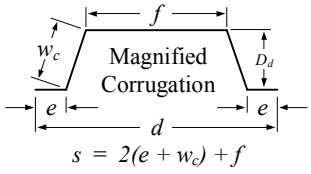

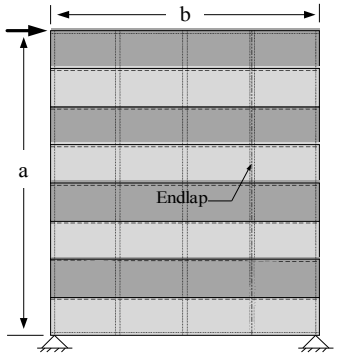

Loading Type: Cylic
Load Rate: Static
a = 24'
b = 20'

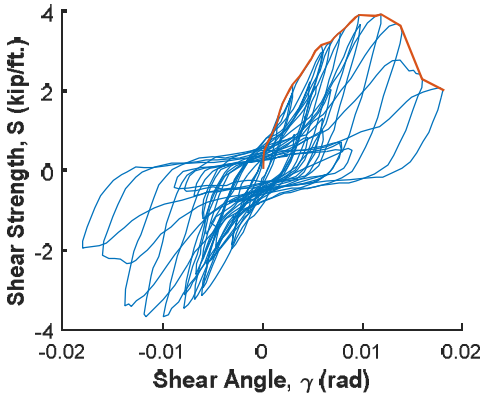

Eperimental Max Strength (kip/ft.)	3.96
Experimental Shear Stiffness (kip/in)	72.3
Ultimate Shear Angle, $\gamma_{80\%}$ (rad*1000)	14.6

Notes

Specimens 3 and 6 were identical, except specimen 6 used screw endlaps and specimen 3 used pinned endlap
Panel lengths were 5 ft or 15 ft.
Predictions use 3 span panel.
Hilti reported Smax does not match load-deformation data (Appendix 4 of Beck 2008). Smax from data is used in analysis
Hilti reported Smax = 4.49 kip/ft

Beck (2008) - Specimen 4

Input	
Structural Fastener Type	X-EDNK22
Sidelap Fastener Type	Screw
Deck thickness, t (in.)	0.0358
Panel Length, l (ft.)	15
Panel Span, l_v (ft.)	5.0
No. of sidelap connections per one edge of interior panel length, n_s	27
No. of edge structural connections not in line with int. or ext. supports, n_e	27
No. of interior supports per panel length, n_p	2
Yield strength of deck, F_y (ksi)	33
Ultimate strength of deck, F_u (ksi)	45
Sidelap screw diameter (in.)	0.2111
Moment of inertia of fully effective panel per unit width, I_x (in^4)	0.212

Fastener Strengths and Flexibilities	
Structural fastener strength, P_{nf} (kip)	1.80
Sidelap fastener strength, P_{ns} (kip)	0.869
Structural fastener flexibility, S_f (in/kip)	0.0066
Sidelap fastener flexibility, S_s (in/kip)	0.0159

Calculated Strength Equations Variables	
Corner fastener reduction factor, λ	0.835
Interior panel fastener contribution factor, β	23.3
Structural fastener distribution factor at panel ends, α_e^2	1.23
Structural fastener distribution factor at interior supports, α_p^2	1.23
Number of structural fasteners at panel ends per unit width, N	2.33
Fastener slip coefficient, C	2.02
Warping factor, D_n (in.)	5.14
Warping support factor, ρ	1.0

Predicted Shear Strength and Stiffness	
Interior panel shear strength, S_{ni} (kip/ft.)	2.71
Edge panel shear strength, S_{ne} (kip/ft.)	4.67
Panel shear strength limited by corner fastener, S_{nc} (kip/ft.)	2.32
Panel buckling shear strength, S_{nb} (kip/ft.)	7.51
Shear stiffness, G' (kip/in)	98.7

36/9 fastener pattern at interior and exterior supports

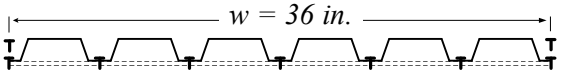

e (in.)	0.75
w_c (in.)	1.58
f (in.)	3.50
d (in.)	6.00
s (in.)	8.16
D_d (in.)	1.50

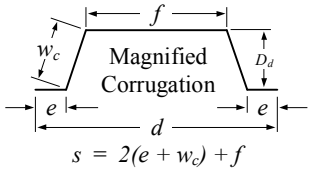

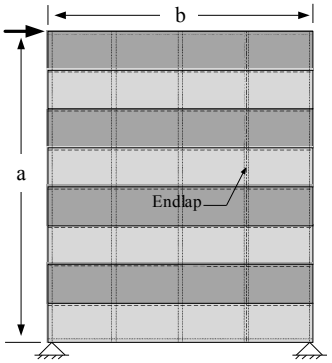

Loading Type: Cylic
Load Rate: Static
a = 24'
b = 20'

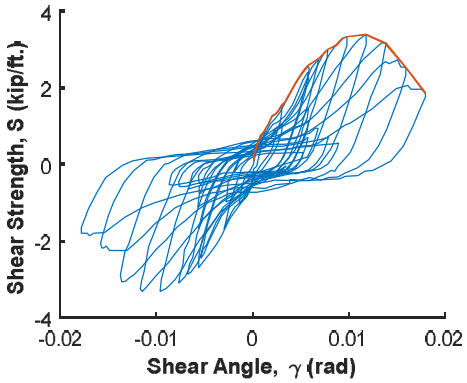

Eperimental Max Strength (kip/ft.)	3.43
Experimental Shear Stiffness (kip/in)	44.9
Ultimate Shear Angle, $\gamma_{80\%}$ (rad*1000)	15.3

Notes

Specimens 4 and 5 were identical, except specimen 4 used screw endlaps and specimen 5 used pinned endlap
Panel lengths were 5 ft or 15 ft.
Predictions use 3 span panel and Hilti pins at endlap.
S-MD 12-24x1 1/4" HWH #5 Screws used for endlap structural fasteners.

Beck (2008) - Specimen 5

Input	
Structural Fastener Type	X-EDNK22
Sidelap Fastener Type	Screw
Deck thickness, t (in.)	0.0358
Panel Length, l (ft.)	15
Panel Span, l_v (ft.)	5.0
No. of sidelap connections per one edge of interior panel length, n_s	27
No. of edge structural connections not in line with int. or ext. supports, n_e	27
No. of interior supports per panel length, n_p	2
Yield strength of deck, F_y (ksi)	33
Ultimate strength of deck, F_u (ksi)	45
Sidelap screw diameter (in.)	0.2111
Moment of inertia of fully effective panel per unit width, I_x (in^4)	0.212

Fastener Strengths and Flexibilities	
Structural fastener strength, P_{nf} (kip)	1.80
Sidelap fastener strength, P_{ns} (kip)	0.869
Structural fastener flexibility, S_f (in/kip)	0.0066
Sidelap fastener flexibility, S_s (in/kip)	0.0159

Calculated Strength Equations Variables	
Corner fastener reduction factor, λ	0.835
Interior panel fastener contribution factor, β	23.3
Structural fastener distribution factor at panel ends, α_e^2	1.23
Structural fastener distribution factor at interior supports, α_p^2	1.23
Number of structural fasteners at panel ends per unit width, N	2.33
Fastener slip coefficient, C	2.02
Warping factor, D_n (in.)	5.14
Warping support factor, ρ	1.0

Predicted Shear Strength and Stiffness	
Interior panel shear strength, S_{ni} (kip/ft.)	2.71
Edge panel shear strength, S_{ne} (kip/ft.)	4.67
Panel shear strength limited by corner fastener, S_{nc} (kip/ft.)	2.32
Panel buckling shear strength, S_{nb} (kip/ft.)	7.51
Shear stiffness, G' (kip/in)	98.7

36/9 fastener pattern at interior and exterior supports

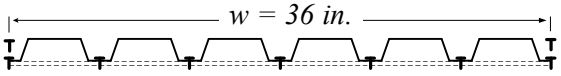

e (in.)	0.75
w_c (in.)	1.58
f (in.)	3.50
d (in.)	6.00
s (in.)	8.16
D_d (in.)	1.50

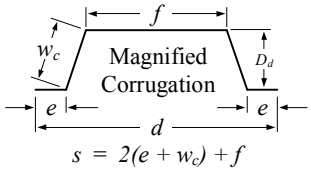

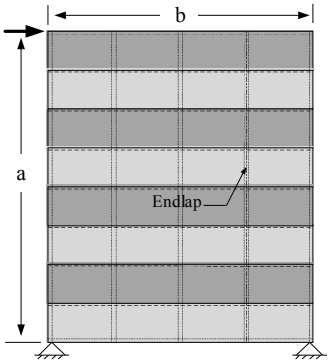

Loading Type: Cylic
Load Rate: Static
a = 24'
b = 20'

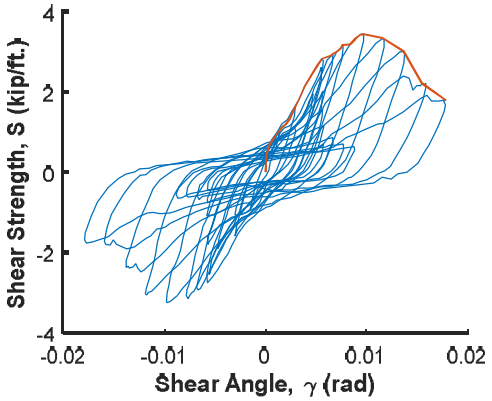

Eperimental Max Strength (kip/ft.)	3.48
Experimental Shear Stiffness (kip/in)	46.0
Ultimate Shear Angle, $\gamma_{80\%}$ (rad*1000)	14.2

Notes

Specimens 4 and 5 were identical, except specimen 4 used screw endlaps and specimen 5 used pinned endlap
Panel lengths were 5 ft or 15 ft.
Predictions use 3 span panel.

Beck (2008) - Specimen 6

Input	
Structural Fastener Type	X-EDNK22
Sidelap Fastener Type	Screw
Deck thickness, t (in.)	0.0474
Panel Length, l (ft.)	15
Panel Span, l_v (ft.)	5.0
No. of sidelap connections per one edge of interior panel length, n_s	27
No. of edge structural connections not in line with int. or ext. supports, n_e	27
No. of interior supports per panel length, n_p	2
Yield strength of deck, F_y (ksi)	33
Ultimate strength of deck, F_u (ksi)	45
Sidelap screw diameter (in.)	0.2111
Moment of inertia of fully effective panel per unit width, I_x (in^4)	0.292

Fastener Strengths and Flexibilities	
Structural fastener strength, P_{nf} (kip)	2.35
Sidelap fastener strength, P_{ns} (kip)	1.15
Structural fastener flexibility, S_f (in/kip)	0.0057
Sidelap fastener flexibility, S_s (in/kip)	0.0138

Calculated Strength Equations Variables	
Corner fastener reduction factor, λ	0.785
Interior panel fastener contribution factor, β	18.4
Structural fastener distribution factor at panel ends, α_e^2	1.23
Structural fastener distribution factor at interior supports, α_p^2	1.23
Number of structural fasteners at panel ends per unit width, N	2.33
Fastener slip coefficient, C	2.74
Warping factor, D_n (in.)	3.37
Warping support factor, ρ	1.0

Predicted Shear Strength and Stiffness	
Interior panel shear strength, S_{ni} (kip/ft.)	3.58
Edge panel shear strength, S_{ne} (kip/ft.)	6.11
Panel shear strength limited by corner fastener, S_{nc} (kip/ft.)	3.05
Panel buckling shear strength, S_{nb} (kip/ft.)	11.8
Shear stiffness, G' (kip/in)	157

36/9 fastener pattern at interior and exterior supports

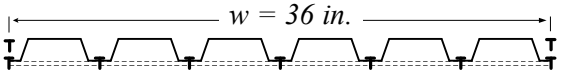

e (in.)	0.75
w_c (in.)	1.58
f (in.)	3.50
d (in.)	6.00
s (in.)	8.16
D_d (in.)	1.50

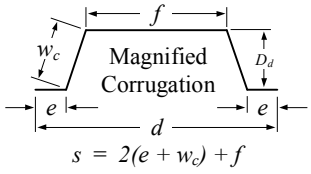

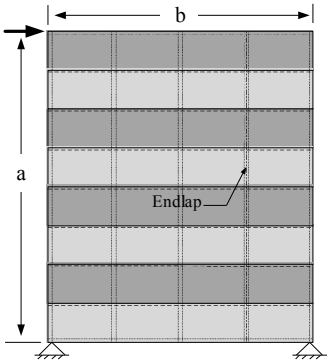

Loading Type: Cylic
Load Rate: Static
a = 24'
b = 20'

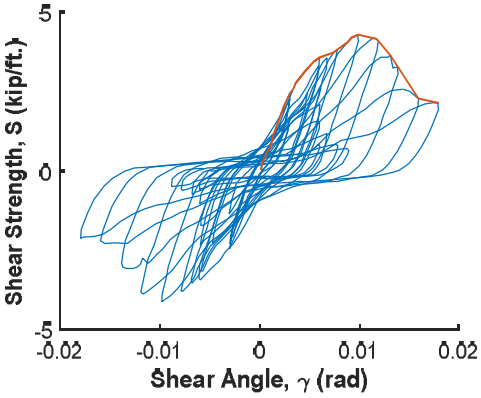

Eperimental Max Strength (kip/ft.)	4.33
Experimental Shear Stiffness (kip/in)	73.5
Ultimate Shear Angle, $\gamma_{80\%}$ (rad*1000)	13.6

Notes

Specimens 3 and 6 were identical, except specimen 6 used screw endlaps and specimen 3 used pinned endlap
Panel lengths were 5 ft or 15 ft.
Predictions use 3 span panel and Hilti pins at endlap.
S-MD 12-24x1 1/4" HWH #5 Screws used for endlap structural fasteners.

Beck (2008) - Specimen 7

Input	
Structural Fastener Type	X-EDNK22
Sidelap Fastener Type	Screw
Deck thickness, t (in.)	0.0295
Panel Length, l (ft.)	15
Panel Span, l_v (ft.)	7.5
No. of sidelap connections per one edge of interior panel length, n_s	28
No. of edge structural connections not in line with int. or ext. supports, n_e	28
No. of interior supports per panel length, n_p	1
Yield strength of deck, F_y (ksi)	33
Ultimate strength of deck, F_u (ksi)	45
Sidelap screw diameter (in.)	0.2111
Moment of inertia of fully effective panel per unit width, I_x (in^4)	0.169

Fastener Strengths and Flexibilities	
Structural fastener strength, P_{nf} (kip)	1.49
Sidelap fastener strength, P_{ns} (kip)	0.716
Structural fastener flexibility, S_f (in/kip)	0.0073
Sidelap fastener flexibility, S_s (in/kip)	0.0175

Calculated Strength Equations Variables	
Corner fastener reduction factor, λ	0.727
Interior panel fastener contribution factor, β	18.1
Structural fastener distribution factor at panel ends, α_e^2	0.778
Structural fastener distribution factor at interior supports, α_p^2	0.778
Number of structural fasteners at panel ends per unit width, N	2.0
Fastener slip coefficient, C	2.16
Warping factor, D_n (in.)	6.87
Warping support factor, ρ	1.0

Predicted Shear Strength and Stiffness	
Interior panel shear strength, S_{ni} (kip/ft.)	1.75
Edge panel shear strength, S_{ne} (kip/ft.)	3.37
Panel shear strength limited by corner fastener, S_{nc} (kip/ft.)	1.54
Panel buckling shear strength, S_{nb} (kip/ft.)	2.44
Shear stiffness, G' (kip/in)	68.8

36/7 fastener pattern at interior and exterior supports

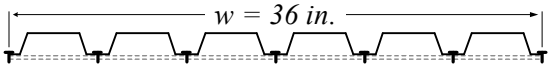

e (in.)	0.75
w_c (in.)	1.58
f (in.)	3.50
d (in.)	6.00
s (in.)	8.16
D_d (in.)	1.50

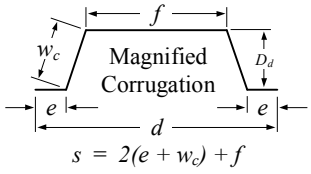

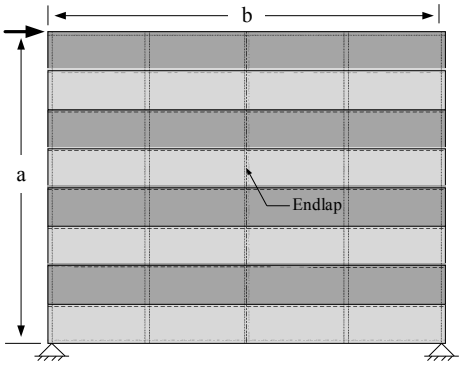

Loading Type: Cyclic

Load Rate: Static

a = 24'

b = 30'

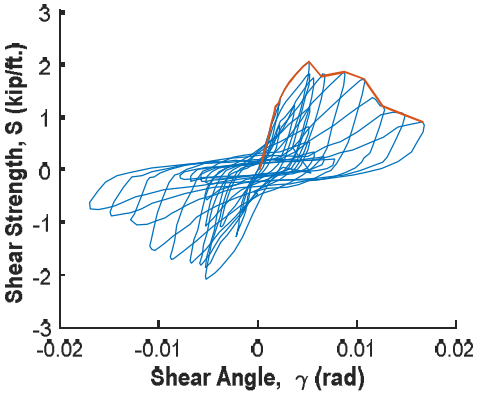

Eperimental Max Strength (kip/ft.)	2.08
Experimental Shear Stiffness (kip/in)	59.6
Ultimate Shear Angle, $\gamma_{80\%}$ (rad*1000)	11.0

Notes

Specimens 63, 7 and 8 had identical test setups with exception to endlap fastener type used.

Specimen 8 used screw endlaps.

Specimens 63 and 7 used pinned endlaps.

Beck (2008) - Specimen 8

Input	
Structural Fastener Type	X-EDNK22
Sidelap Fastener Type	Screw
Deck thickness, t (in.)	0.0295
Panel Length, l (ft.)	15
Panel Span, l_v (ft.)	7.5
No. of sidelap connections per one edge of interior panel length, n_s	28
No. of edge structural connections not in line with int. or ext. supports, n_e	28
No. of interior supports per panel length, n_p	1
Yield strength of deck, F_y (ksi)	33
Ultimate strength of deck, F_u (ksi)	45
Sidelap screw diameter (in.)	0.2111
Moment of inertia of fully effective panel per unit width, I_x (in^4)	0.169

Fastener Strengths and Flexibilities	
Structural fastener strength, P_{nf} (kip)	1.49
Sidelap fastener strength, P_{ns} (kip)	0.716
Structural fastener flexibility, S_f (in/kip)	0.0073
Sidelap fastener flexibility, S_s (in/kip)	0.0175

Calculated Strength Equations Variables	
Corner fastener reduction factor, λ	0.727
Interior panel fastener contribution factor, β	18.1
Structural fastener distribution factor at panel ends, α_e^2	0.778
Structural fastener distribution factor at interior supports, α_p^2	0.778
Number of structural fasteners at panel ends per unit width, N	2.0
Fastener slip coefficient, C	2.16
Warping factor, D_n (in.)	6.87
Warping support factor, ρ	1.0

Predicted Shear Strength and Stiffness	
Interior panel shear strength, S_{ni} (kip/ft.)	1.75
Edge panel shear strength, S_{ne} (kip/ft.)	3.37
Panel shear strength limited by corner fastener, S_{nc} (kip/ft.)	1.54
Panel buckling shear strength, S_{nb} (kip/ft.)	2.44
Shear stiffness, G' (kip/in)	68.8

36/7 fastener pattern at interior and exterior supports

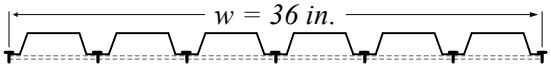

e (in.)	0.75
w_c (in.)	1.58
f (in.)	3.50
d (in.)	6.00
s (in.)	8.16
D_d (in.)	1.50

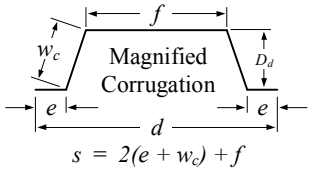

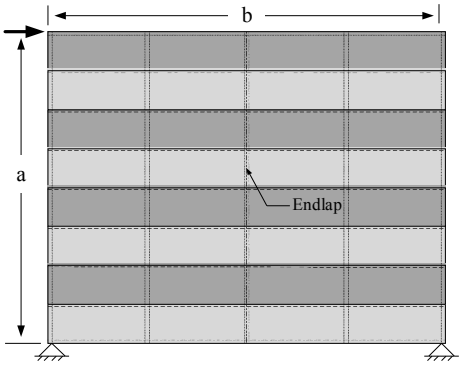

Loading Type: Cyclic

Load Rate: Static

a = 24'

b = 30'

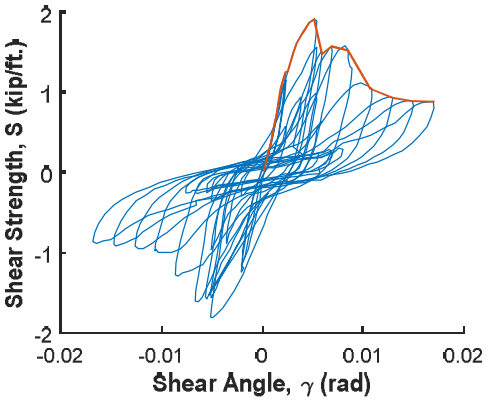

Eperimental Max Strength (kip/ft.)	1.93
Experimental Shear Stiffness (kip/in)	45.6
Ultimate Shear Angle, $\gamma_{80\%}$ (rad*1000)	5.80

Notes

Specimens 63, 7 and 8 had identical test setups with exception to endlap fastener type used.

Specimens 63 and 7 used pinned endlaps.

S-MD 12-24x1 1/4" HWH #5 Screws used for endlap structural fasteners.

Beck (2013) - Specimen M-1

Input	
Structural Fastener Type	X-ENP19 L15
Sidelap Fastener Type	Screw
Deck thickness, t (in.)	0.0474
Panel Length, l (ft.)	10
Panel Span, l_v (ft.)	5
No. of sidelap connections per one edge of interior panel length, n_s	18
No. of edge structural connections not in line with int. or ext. supports, n_e	18
No. of interior supports per panel length, n_p	1
Yield strength of deck, F_y (ksi)	33
Ultimate strength of deck, F_u (ksi)	45
Sidelap screw diameter (in.)	0.216
Moment of inertia of fully effective panel per unit width, I_x (in^4)	0.292

Fastener Strengths and Flexibilities	
Structural fastener strength, P_{nf} (kip)	2.53
Sidelap fastener strength, P_{ns} (kip)	1.18
Structural fastener flexibility, S_f (in/kip)	0.0034
Sidelap fastener flexibility, S_s (in/kip)	0.0138

Calculated Strength Equations Variables	
Corner fastener reduction factor, λ	0.856
Interior panel fastener contribution factor, β	13.1
Structural fastener distribution factor at panel ends, α_e^2	0.778
Structural fastener distribution factor at interior supports, α_p^2	0.778
Number of structural fasteners at panel ends per unit width, N	2.0
Fastener slip coefficient, C	2.14
Warping factor, D_n (in.)	5.06
Warping support factor, ρ	1.0

Predicted Shear Strength and Stiffness	
Interior panel shear strength, S_{ni} (kip/ft.)	3.23
Edge panel shear strength, S_{ne} (kip/ft.)	6.07
Panel shear strength limited by corner fastener, S_{nc} (kip/ft.)	2.76
Panel buckling shear strength, S_{nb} (kip/ft.)	11.8
Shear stiffness, G' (kip/in)	130

36/7 fastener pattern at interior and exterior supports

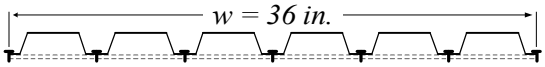

e (in.)	0.75
w_c (in.)	1.58
f (in.)	3.50
d (in.)	6.00
s (in.)	8.16
D_d (in.)	1.50

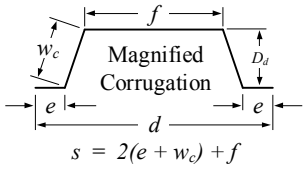

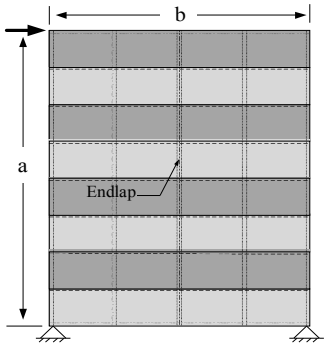

Loading Type: Monotonic
Load Rate: Static
a = 24'
b = 20'

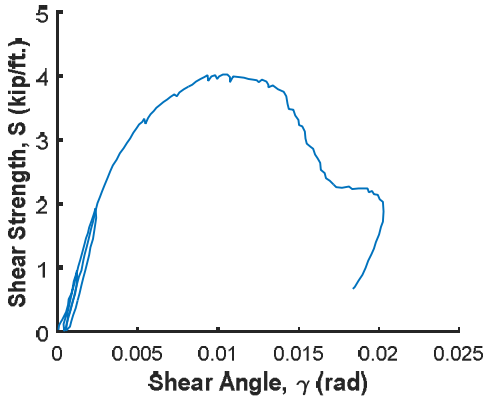

Eperimental Max Strength (kip/ft.)	4.05
Experimental Shear Stiffness (kip/in)	70.1
Ultimate Shear Angle, $\gamma_{80\%}$ (rad*1000)	15.2

Notes

Specimens M-01 and C-01 had identical test setups, with different load protocols.
S-SLC 02 M HWH 6 sidelap screws used

Beck (2013) - Specimen C-1

Input	
Structural Fastener Type	X-ENP19 L15
Sidelap Fastener Type	Screw
Deck thickness, t (in.)	0.0474
Panel Length, l (ft.)	10
Panel Span, l_v (ft.)	5
No. of sidelap connections per one edge of interior panel length, n_s	18
No. of edge structural connections not in line with int. or ext. supports, n_e	18
No. of interior supports per panel length, n_p	1
Yield strength of deck, F_y (ksi)	33
Ultimate strength of deck, F_u (ksi)	45
Sidelap screw diameter (in.)	0.216
Moment of inertia of fully effective panel per unit width, I_x (in^4)	0.292

Fastener Strengths and Flexibilities	
Structural fastener strength, P_{nf} (kip)	2.53
Sidelap fastener strength, P_{ns} (kip)	1.18
Structural fastener flexibility, S_f (in/kip)	0.0034
Sidelap fastener flexibility, S_s (in/kip)	0.0138

Calculated Strength Equations Variables	
Corner fastener reduction factor, λ	0.856
Interior panel fastener contribution factor, β	13.1
Structural fastener distribution factor at panel ends, α_e^2	0.778
Structural fastener distribution factor at interior supports, α_p^2	0.778
Number of structural fasteners at panel ends per unit width, N	2.0
Fastener slip coefficient, C	2.14
Warping factor, D_n (in.)	5.06
Warping support factor, ρ	1.0

Predicted Shear Strength and Stiffness	
Interior panel shear strength, S_{ni} (kip/ft.)	3.23
Edge panel shear strength, S_{ne} (kip/ft.)	6.07
Panel shear strength limited by corner fastener, S_{nc} (kip/ft.)	2.76
Panel buckling shear strength, S_{nb} (kip/ft.)	11.8
Shear stiffness, G' (kip/in)	130

36/7 fastener pattern at interior and exterior supports

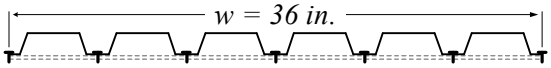

e (in.)	0.75
w_c (in.)	1.58
f (in.)	3.50
d (in.)	6.00
s (in.)	8.16
D_d (in.)	1.50

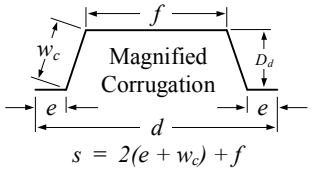

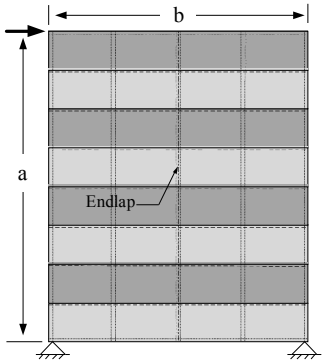

Loading Type: Cyclic

Load Rate: Static

a = 24'

b = 20'

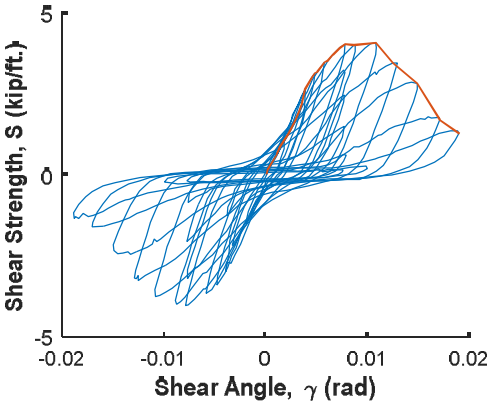

Eperimental Max Strength (kip/ft.)	4.11
Experimental Shear Stiffness (kip/in)	48.7
Ultimate Shear Angle, $\gamma_{80\%}$ (rad*1000)	13.3

Notes

Specimens M-01 and C-01 had identical test setups, with different load protocols.

S-SLC 02 M HWH 6 sidelap screws used

Beck (2013) - Specimen M-2

Input	
Structural Fastener Type	X-ENP19 L15
Sidelap Fastener Type	Screw
Deck thickness, t (in.)	0.0474
Panel Length, l (ft.)	10
Panel Span, l_v (ft.)	5
No. of sidelap connections per one edge of interior panel length, n_s	11
No. of edge structural connections not in line with int. or ext. supports, n_e	11
No. of interior supports per panel length, n_p	1
Yield strength of deck, F_y (ksi)	33
Ultimate strength of deck, F_u (ksi)	45
Sidelap screw diameter (in.)	0.216
Moment of inertia of fully effective panel per unit width, I_x (in^4)	0.292

Fastener Strengths and Flexibilities	
Structural fastener strength, P_{nf} (kip)	2.53
Sidelap fastener strength, P_{ns} (kip)	1.18
Structural fastener flexibility, S_f (in/kip)	0.0034
Sidelap fastener flexibility, S_s (in/kip)	0.0138

Calculated Strength Equations Variables	
Corner fastener reduction factor, λ	0.856
Interior panel fastener contribution factor, β	12.8
Structural fastener distribution factor at panel ends, α_e^2	1.23
Structural fastener distribution factor at interior supports, α_p^2	1.23
Number of structural fasteners at panel ends per unit width, N	2.33
Fastener slip coefficient, C	2.22
Warping factor, D_n (in.)	5.06
Warping support factor, ρ	1.0

Predicted Shear Strength and Stiffness	
Interior panel shear strength, S_{ni} (kip/ft.)	3.09
Edge panel shear strength, S_{ne} (kip/ft.)	5.06
Panel shear strength limited by corner fastener, S_{nc} (kip/ft.)	2.84
Panel buckling shear strength, S_{nb} (kip/ft.)	11.8
Shear stiffness, G' (kip/in)	129.0

36/9 fastener pattern at interior and exterior supports

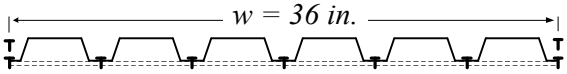

e (in.)	0.75
w_c (in.)	1.58
f (in.)	3.50
d (in.)	6.00
s (in.)	8.16
D_d (in.)	1.50

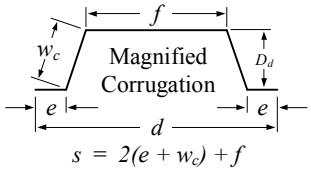

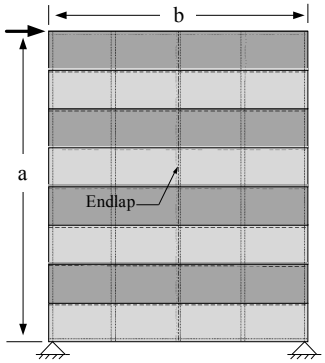

Loading Type: Monotonic

Load Rate: Static

a = 24'

b = 20'

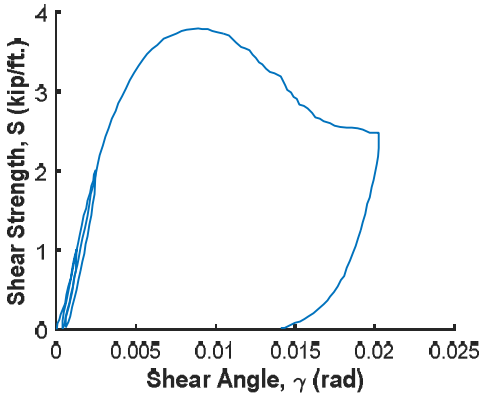

Eperimental Max Strength (kip/ft.)	3.81
Experimental Shear Stiffness (kip/in)	70.4
Ultimate Shear Angle, $\gamma_{80\%}$ (rad*1000)	14.4

Notes

Specimens M-02 and C-02 had identical test setups, with different load protocols.

S-SLC 02 M HWH 6 sidelap screws used

Beck (2013) - Specimen C-2

Input	
Structural Fastener Type	X-ENP19 L15
Sidelap Fastener Type	Screw
Deck thickness, t (in.)	0.0474
Panel Length, l (ft.)	10
Panel Span, l_v (ft.)	5
No. of sidelap connections per one edge of interior panel length, n_s	11
No. of edge structural connections not in line with int. or ext. supports, n_e	11
No. of interior supports per panel length, n_p	1
Yield strength of deck, F_y (ksi)	33
Ultimate strength of deck, F_u (ksi)	45
Sidelap screw diameter (in.)	0.216
Moment of inertia of fully effective panel per unit width, I_x (in^4)	0.292

Fastener Strengths and Flexibilities	
Structural fastener strength, P_{nf} (kip)	2.53
Sidelap fastener strength, P_{ns} (kip)	1.18
Structural fastener flexibility, S_f (in/kip)	0.0034
Sidelap fastener flexibility, S_s (in/kip)	0.0138

Calculated Strength Equations Variables	
Corner fastener reduction factor, λ	0.856
Interior panel fastener contribution factor, β	12.8
Structural fastener distribution factor at panel ends, α_e^2	1.23
Structural fastener distribution factor at interior supports, α_p^2	1.23
Number of structural fasteners at panel ends per unit width, N	2.33
Fastener slip coefficient, C	2.22
Warping factor, D_n (in.)	5.06
Warping support factor, ρ	1.0

Predicted Shear Strength and Stiffness	
Interior panel shear strength, S_{ni} (kip/ft.)	3.09
Edge panel shear strength, S_{ne} (kip/ft.)	5.06
Panel shear strength limited by corner fastener, S_{nc} (kip/ft.)	2.84
Panel buckling shear strength, S_{nb} (kip/ft.)	11.8
Shear stiffness, G' (kip/in)	129.0

36/9 fastener pattern at interior and exterior supports

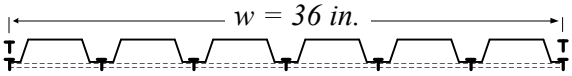

e (in.)	0.75
w_c (in.)	1.58
f (in.)	3.50
d (in.)	6.00
s (in.)	8.16
D_d (in.)	1.50

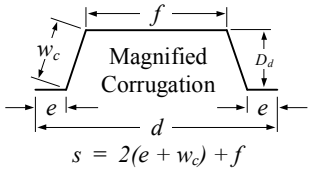

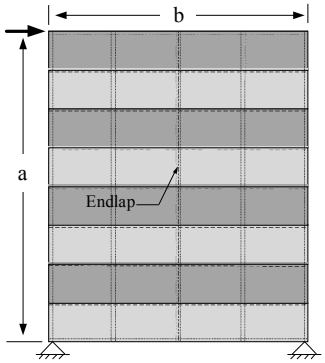

Loading Type: Cyclic

Load Rate: Static

a = 24'

b = 20'

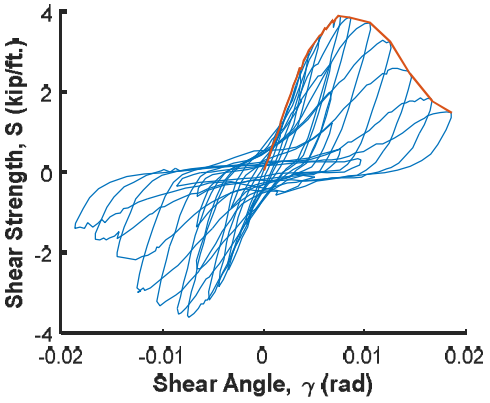

Eperimental Max Strength (kip/ft.)	3.93
Experimental Shear Stiffness (kip/in)	61.6
Ultimate Shear Angle, $\gamma_{80\%}$ (rad*1000)	12.9

Notes

Specimens M-02 and C-02 had identical test setups, with different load protocols.

S-SLC 02 M HWH 6 sidelap screws used

Beck (2013) - Specimen M-3

Input	
Structural Fastener Type	X-ENP19 L15
Sidelap Fastener Type	Screw
Deck thickness, t (in.)	0.0598
Panel Length, l (ft.)	10
Panel Span, l_v (ft.)	5
No. of sidelap connections per one edge of interior panel length, n_s	38
No. of edge structural connections not in line with int. or ext. supports, n_e	38
No. of interior supports per panel length, n_p	1
Yield strength of deck, F_y (ksi)	33
Ultimate strength of deck, F_u (ksi)	45
Sidelap screw diameter (in.)	0.216
Moment of inertia of fully effective panel per unit width, I_x (in^4)	0.373

Fastener Strengths and Flexibilities	
Structural fastener strength, P_{nf} (kip)	3.15
Sidelap fastener strength, P_{ns} (kip)	1.49
Structural fastener flexibility, S_f (in/kip)	0.0031
Sidelap fastener flexibility, S_s (in/kip)	0.0123

Calculated Strength Equations Variables	
Corner fastener reduction factor, λ	0.872
Interior panel fastener contribution factor, β	25.5
Structural fastener distribution factor at panel ends, α_e^2	1.50
Structural fastener distribution factor at interior supports, α_p^2 (at endlap)	0.778
Number of structural fasteners at panel ends per unit width, N	3.0
Fastener slip coefficient, C	1.27
Warping factor, D_n (in.)	3.58
Warping support factor, ρ	1.0

Predicted Shear Strength and Stiffness	
Interior panel shear strength, S_{ni} (kip/ft.)	7.86
Edge panel shear strength, S_{ne} (kip/ft.)	14.9
Panel shear strength limited by corner fastener, S_{nc} (kip/ft.)	6.12
Panel buckling shear strength, S_{nb} (kip/ft.)	16.9
Shear stiffness, G' (kip/in)	210

36/11 fastener pattern at exterior supports
36/7 fastener pattern at endlap

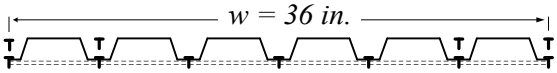

e (in.)	0.75
w_c (in.)	1.58
f (in.)	3.50
d (in.)	6.00
s (in.)	8.16
D_d (in.)	1.50

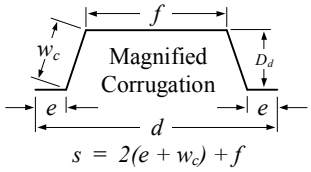

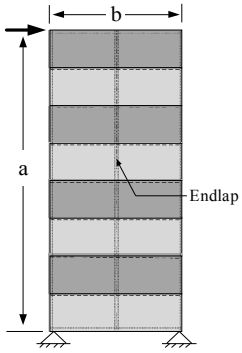

Loading Type: Monotonic
Load Rate: Static
a = 24'
b = 10'

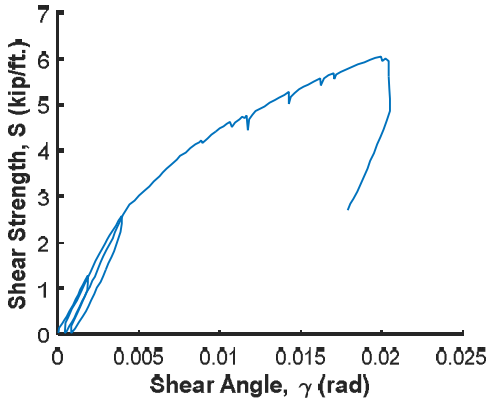

Eperimental Max Strength (kip/ft.)	6.07
Experimental Shear Stiffness (kip/in)	54.9
Ultimate Shear Angle, $\gamma_{80\%}$ (rad*1000)	20.5

Notes

Specimens M-01 and C-01 had identical test setups, with different load protocols.
S-SLC 02 M HWH 6 sidelap screws used
Strong structural fastener configurations (36/11) used in combination with a weaker endlap configuration (36/7).
Fastener configuration forced failure at endlap
Strength predictions made using 2 span condition.

Beck (2013) - Specimen C-3

Input	
Structural Fastener Type	X-ENP19 L15
Sidelap Fastener Type	Screw
Deck thickness, t (in.)	0.0598
Panel Length, l (ft.)	10
Panel Span, l_v (ft.)	5
No. of sidelap connections per one edge of interior panel length, n_s	38
No. of edge structural connections not in line with int. or ext. supports, n_e	38
No. of interior supports per panel length, n_p	1
Yield strength of deck, F_y (ksi)	33
Ultimate strength of deck, F_u (ksi)	45
Sidelap screw diameter (in.)	0.216
Moment of inertia of fully effective panel per unit width, I_x (in^4)	0.373

Fastener Strengths and Flexibilities	
Structural fastener strength, P_{nf} (kip)	3.15
Sidelap fastener strength, P_{ns} (kip)	1.49
Structural fastener flexibility, S_f (in/kip)	0.0031
Sidelap fastener flexibility, S_s (in/kip)	0.0123

Calculated Strength Equations Variables	
Corner fastener reduction factor, λ	0.872
Interior panel fastener contribution factor, β	25.5
Structural fastener distribution factor at panel ends, α_e^2	1.50
Structural fastener distribution factor at interior supports, α_p^2 (at endlap)	0.778
Number of structural fasteners at panel ends per unit width, N	3.0
Fastener slip coefficient, C	1.27
Warping factor, D_n (in.)	3.58
Warping support factor, ρ	1.0

Predicted Shear Strength and Stiffness	
Interior panel shear strength, S_{ni} (kip/ft.)	7.86
Edge panel shear strength, S_{ne} (kip/ft.)	14.9
Panel shear strength limited by corner fastener, S_{nc} (kip/ft.)	6.12
Panel buckling shear strength, S_{nb} (kip/ft.)	16.9
Shear stiffness, G' (kip/in)	210

36/11 fastener pattern at exterior supports
36/7 fastener pattern at endlap

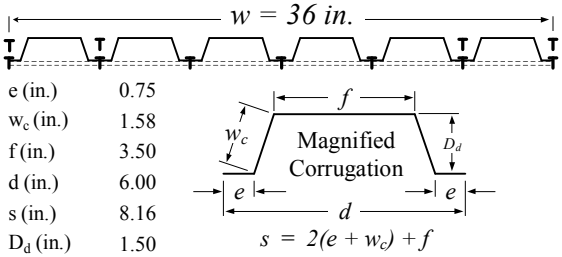

e (in.)	0.75
w_c (in.)	1.58
f (in.)	3.50
d (in.)	6.00
s (in.)	8.16
D_d (in.)	1.50

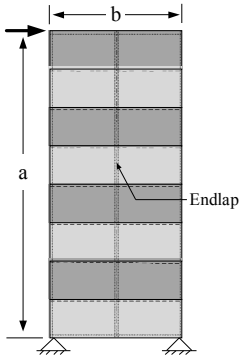

Loading Type: Cyclic
Load Rate: Static
a = 24'
b = 10'

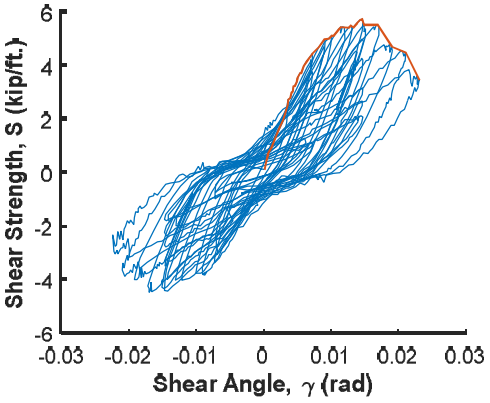

Eperimental Max Strength (kip/ft.)	5.77
Experimental Shear Stiffness (kip/in)	57.2
Ultimate Shear Angle, $\gamma_{80\%}$ (rad*1000)	20.2

Notes

Specimens M-01 and C-01 had identical test setups, with different load protocols.
S-SLC 02 M HWH 6 sidelap screws used
Strong structural fastener configurations (36/11) used in combination with a weaker endlap configuration (36/7).
Fastener configuration forced failure at endlap
Strength predictions made using 2 span condition.

Beck (2013b) - Specimen M-2

Input	
Structural Fastener Type	X-HSN24
Sidelap Fastener Type	Screw
Deck thickness, t (in.)	0.0474
Panel Length, l (ft.)	10
Panel Span, l_v (ft.)	5
No. of sidelap connections per one edge of interior panel length, n_s	14
No. of edge structural connections not in line with int. or ext. supports, n_e	14
No. of interior supports per panel length, n_p	1
Yield strength of deck, F_y (ksi)	33
Ultimate strength of deck, F_u (ksi)	45
Sidelap screw diameter (in.)	0.216
Moment of inertia of fully effective panel per unit width, I_x (in^4)	0.292

Fastener Strengths and Flexibilities	
Structural fastener strength, P_{nf} (kip)	2.53
Sidelap fastener strength, P_{ns} (kip)	1.18
Structural fastener flexibility, S_f (in/kip)	0.0057
Sidelap fastener flexibility, S_s (in/kip)	0.0138

Calculated Strength Equations Variables	
Corner fastener reduction factor, λ	0.856
Interior panel fastener contribution factor, β	14.2
Structural fastener distribution factor at panel ends, α_e^2	1.28
Structural fastener distribution factor at interior supports, α_p^2	1.28
Number of structural fasteners at panel ends per unit width, N	2.33
Fastener slip coefficient, C	2.59
Warping factor, D_n (in.)	5.06
Warping support factor, ρ	1.0

Predicted Shear Strength and Stiffness	
Interior panel shear strength, S_{ni} (kip/ft.)	3.44
Edge panel shear strength, S_{ne} (kip/ft.)	5.82
Panel shear strength limited by corner fastener, S_{nc} (kip/ft.)	3.07
Panel buckling shear strength, S_{nb} (kip/ft.)	11.7
Shear stiffness, G' (kip/in)	124

36/9 fastener pattern at interior and exterior supports

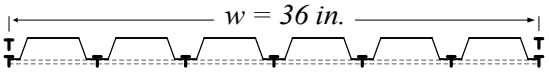

e (in.)	0.75
w_c (in.)	1.58
f (in.)	3.50
d (in.)	6.00
s (in.)	8.16
D_d (in.)	1.50

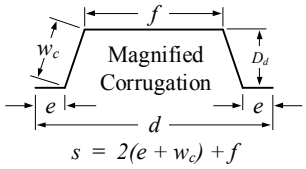

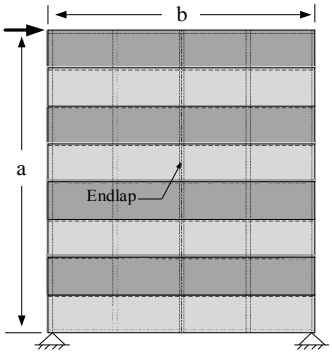

Loading Type: Monotonic
Load Rate: Static
a = 24'
b = 20'

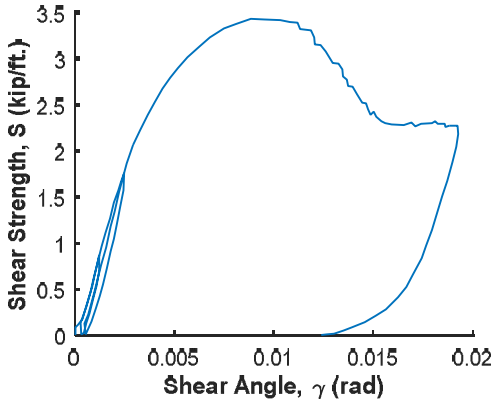

Eperimental Max Strength (kip/ft.)	3.45
Experimental Shear Stiffness (kip/in)	61.1
Ultimate Shear Angle, $\gamma_{80\%}$ (rad*1000)	13.7

Notes

Identical tes setup for specimens M-2 and C-2 with different loading protocols
S-SLC-02 M HWH sidelap screws used

Beck (2013b) - Specimen C-2

Input	
Structural Fastener Type	X-HSN24
Sidelap Fastener Type	Screw
Deck thickness, t (in.)	0.0474
Panel Length, l (ft.)	10
Panel Span, l_v (ft.)	5
No. of sidelap connections per one edge of interior panel length, n_s	14
No. of edge structural connections not in line with int. or ext. supports, n_e	14
No. of interior supports per panel length, n_p	1
Yield strength of deck, F_y (ksi)	33
Ultimate strength of deck, F_u (ksi)	45
Sidelap screw diameter (in.)	0.216
Moment of inertia of fully effective panel per unit width, I_x (in^4)	0.292

Fastener Strengths and Flexibilities	
Structural fastener strength, P_{nf} (kip)	2.53
Sidelap fastener strength, P_{ns} (kip)	1.18
Structural fastener flexibility, S_f (in/kip)	0.0057
Sidelap fastener flexibility, S_s (in/kip)	0.0138

Calculated Strength Equations Variables	
Corner fastener reduction factor, λ	0.856
Interior panel fastener contribution factor, β	14.2
Structural fastener distribution factor at panel ends, α_e^2	1.28
Structural fastener distribution factor at interior supports, α_p^2	1.28
Number of structural fasteners at panel ends per unit width, N	2.33
Fastener slip coefficient, C	2.59
Warping factor, D_n (in.)	5.06
Warping support factor, ρ	1.0

Predicted Shear Strength and Stiffness	
Interior panel shear strength, S_{ni} (kip/ft.)	3.44
Edge panel shear strength, S_{ne} (kip/ft.)	5.82
Panel shear strength limited by corner fastener, S_{nc} (kip/ft.)	3.07
Panel buckling shear strength, S_{nb} (kip/ft.)	11.7
Shear stiffness, G' (kip/in)	124

36/9 fastener pattern at interior and exterior supports

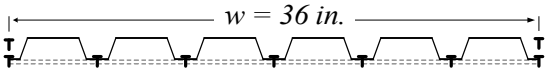

e (in.)	0.75
w_c (in.)	1.58
f (in.)	3.50
d (in.)	6.00
s (in.)	8.16
D_d (in.)	1.50

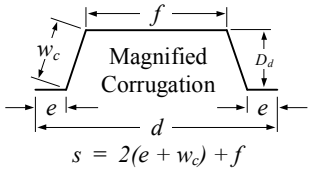

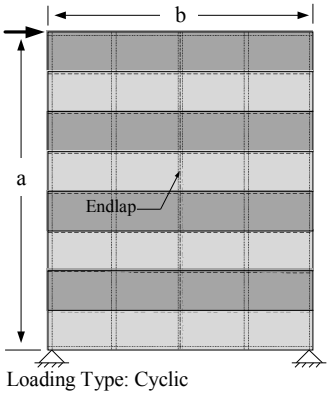

Loading Type: Cyclic
Load Rate: Static
a = 24'
b = 20'

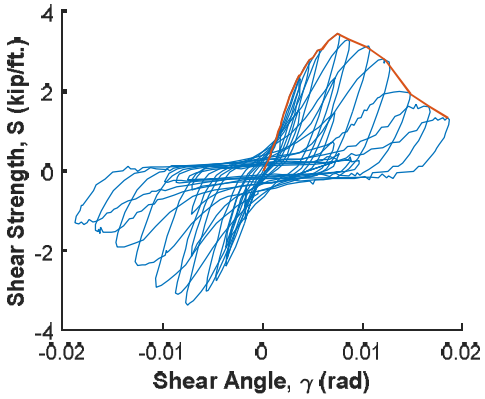

Eperimental Max Strength (kip/ft.)	3.47
Experimental Shear Stiffness (kip/in)	58.4
Ultimate Shear Angle, $\gamma_{80\%}$ (rad*1000)	12.4

Notes

Identical tes setup for specimens M-2 and C-2 with different loading protocols
S-SLC-02 M HWH sidelap screws used

Beck (2013b) - Specimen M-3

Input	
Structural Fastener Type	X-HSN24
Sidelap Fastener Type	Screw
Deck thickness, t (in.)	0.0358
Panel Length, l (ft.)	15
Panel Span, l_v (ft.)	5
No. of sidelap connections per one edge of interior panel length, n_s	38
No. of edge structural connections not in line with int. or ext. supports, n_e	38
No. of interior supports per panel length, n_p	1
Yield strength of deck, F_y (ksi)	80
Ultimate strength of deck, F_u (ksi)	82
Sidelap screw diameter (in.)	0.216
Moment of inertia of fully effective panel per unit width, I_x (in^4)	0.212

Fastener Strengths and Flexibilities	
Structural fastener strength, P_{nf} (kip)	1.93
Sidelap fastener strength, P_{ns} (kip)	0.889
Structural fastener flexibility, S_f (in/kip)	0.0066
Sidelap fastener flexibility, S_s (in/kip)	0.0159

Calculated Strength Equations Variables	
Corner fastener reduction factor, λ	0.835
Interior panel fastener contribution factor, β	22.2
Structural fastener distribution factor at panel ends, α_e^2	0.778
Structural fastener distribution factor at interior supports, α_p^2	0.778
Number of structural fasteners at panel ends per unit width, N	2.0
Fastener slip coefficient, C	1.24
Warping factor, D_n (in.)	7.71
Warping support factor, ρ	1.0

Predicted Shear Strength and Stiffness	
Interior panel shear strength, S_{ni} (kip/ft.)	4.22
Edge panel shear strength, S_{ne} (kip/ft.)	8.51
Panel shear strength limited by corner fastener, S_{nc} (kip/ft.)	2.87
Panel buckling shear strength, S_{nb} (kip/ft.)	7.47
Shear stiffness, G' (kip/in)	84.1

36/7 fastener pattern at interior and exterior supports

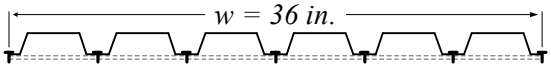

e (in.)	0.75
w_c (in.)	1.58
f (in.)	3.50
d (in.)	6.00
s (in.)	8.16
D_d (in.)	1.50

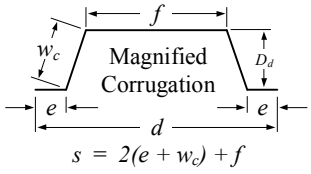

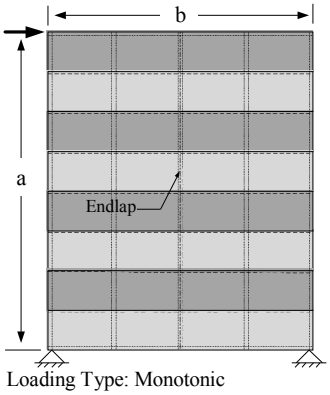

Loading Type: Monotonic

Load Rate: Static

a = 24'

b = 20'

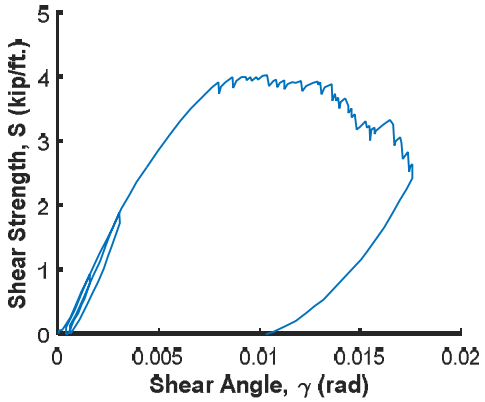

Eperimental Max Strength (kip/ft.)	4.05
Experimental Shear Stiffness (kip/in)	51.4
Ultimate Shear Angle, $\gamma_{80\%}$ (rad*1000)	14.8

Notes

Identical tes setup for specimens M-3 and C-3 with different loading protocols

S-SLC-01 M HWH sidelap screws used.

Beck (2013b) - Specimen C-3

Input	
Structural Fastener Type	X-HSN24
Sidelap Fastener Type	Screw
Deck thickness, t (in.)	0.0358
Panel Length, l (ft.)	15
Panel Span, l_v (ft.)	5
No. of sidelap connections per one edge of interior panel length, n_s	38
No. of edge structural connections not in line with int. or ext. supports, n_e	38
No. of interior supports per panel length, n_p	1
Yield strength of deck, F_y (ksi)	80
Ultimate strength of deck, F_u (ksi)	82
Sidelap screw diameter (in.)	0.216
Moment of inertia of fully effective panel per unit width, I_x (in^4)	0.212

Fastener Strengths and Flexibilities	
Structural fastener strength, P_{nf} (kip)	1.93
Sidelap fastener strength, P_{ns} (kip)	0.889
Structural fastener flexibility, S_f (in/kip)	0.0066
Sidelap fastener flexibility, S_s (in/kip)	0.0159

Calculated Strength Equations Variables	
Corner fastener reduction factor, λ	0.835
Interior panel fastener contribution factor, β	22.2
Structural fastener distribution factor at panel ends, α_e^2	0.778
Structural fastener distribution factor at interior supports, α_p^2	0.778
Number of structural fasteners at panel ends per unit width, N	2.0
Fastener slip coefficient, C	1.24
Warping factor, D_n (in.)	7.71
Warping support factor, ρ	1.0

Predicted Shear Strength and Stiffness	
Interior panel shear strength, S_{ni} (kip/ft.)	4.22
Edge panel shear strength, S_{ne} (kip/ft.)	8.51
Panel shear strength limited by corner fastener, S_{nc} (kip/ft.)	2.87
Panel buckling shear strength, S_{nb} (kip/ft.)	7.47
Shear stiffness, G' (kip/in)	84.1

36/7 fastener pattern at interior and exterior supports

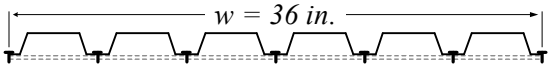

e (in.)	0.75
w_c (in.)	1.58
f (in.)	3.50
d (in.)	6.00
s (in.)	8.16
D_d (in.)	1.50

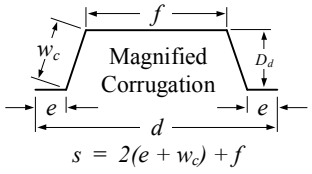

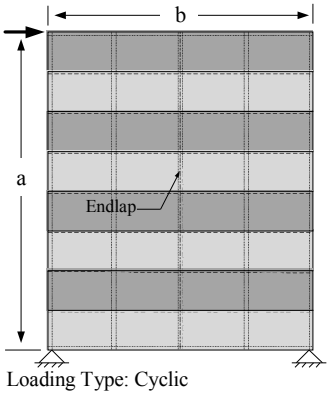

Loading Type: Cyclic

Load Rate: Static

a = 24'

b = 20'

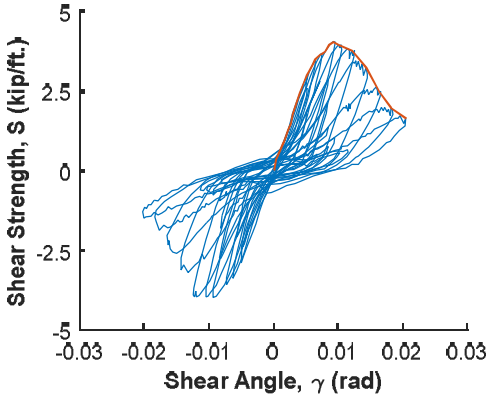

Eperimental Max Strength (kip/ft.)	4.09
Experimental Shear Stiffness (kip/in)	49.5
Ultimate Shear Angle, $\gamma_{80\%}$ (rad*1000)	14.3

Notes

Identical tes setup for specimens M-3 and C-3 with different loading protocols

S-SLC-01 M HWH sidelap screws used.